

ÉCOLE DOCTORALE DES SCIENCES CHIMIQUES

UMR7200 – Laboratoire d’Innovation Thérapeutique

THÈSE présentée par :

Shuang-Qi TANG

soutenue le : 20 septembre 2019

Pour obtenir le grade de : **Docteur de l’université de Strasbourg**

Discipline/ Spécialité : Chimie Organique

**Synthèse d’hétérocycles non planaires
à 6 ou 7 chaînons présentant une
liaison N-O**

THÈSE dirigée par :

M. BIHEL Frédéric

Mme SCHMITT Martine

CRCN, Université de Strasbourg

CRHC, Université de Strasbourg

RAPPORTEURS :

M. KNOCHÉL Paul

Mme GUILLOU Catherine

Pr, Université Ludwig-Maximilians de Munich

DR, Université Paris-Saclay

AUTRES MEMBRES DU JURY :

M. MESSAOUDI Samir

DR2, Université Paris-Sud

Acknowledgements

Upon the completion of the thesis, I would like to take this opportunity to express my sincere gratitude to my supervisor, Dr Frédéric Bihel and Dr Martine Schmitt, who has given me important guidance on the thesis. Besides their help with my thesis, they have also given me much advice on the methods of doing research, which is of great value to my future work. I am also grateful to Prof Paul Knochel, Dr Catherine Guillou and Dr Samir Messaoudi for their suggestions in my thesis.

Besides, I greatly appreciate all the members in my lab, especially Séverine Schneider, Jacques Bricard and Patrick Wagner who have provided me with help in experiments. I also thank Dr Mihaela Gulea and Dr Gaëlle Blond (SOMHet) for manuscript preparation; Dr Delphine Garnier and Dr Estefania Oliva (PACSI) for NMR and mass analyses; Dr Lydia Karmazin and Dr Corinne Bailly for X-ray analyses.

Furthermore, my gratitude extends to my family and friends, especially my girlfriend Xinyue Wang, who have been assisting, supporting and caring for my life in France.

Finally, I also thank China Scholarship Council (CSC) for the financial support of my PhD thesis.

RESUME

Synthèse d'hétérocycles non planaires à 6 ou 7 chaînons présentant une liaison N-O

Doctorant : Shuang-Qi Tang

Directeur de thèse : Dr Frédéric Bihel

Co-directeur de thèse : Dr Martine Schmitt

Laboratoire d'Innovation Thérapeutique, Labex MEDALIS, Faculté de Pharmacie, UMR7200 CNRS, Université de Strasbourg, 74 Route du Rhin, 67412 Illkirch, France.

1. Introduction

Les hétérocycles présentant 2 atomes d'azote adjacents sont très populaires en chimie médicinale. Ainsi, le cycle à 5 de type pyrazole, ainsi que les cycles à 6 de type pyridazine et 1,2,4-triazine ont été intensivement étudiés en *drug design*. En effet, la présence des atomes d'azote permet à ces systèmes hétérocycliques aromatiques de présenter 2 à 3 sites potentiels d'interactions de type accepteur de liaison hydrogène avec une cible protéique. De plus, la présence d'atomes d'azote permet de diminuer la lipophilie de ces systèmes aromatiques en comparaison avec le benzène. Toutefois, le caractère aromatique de ces hétérocycles leur confère une géométrie plane, ce qui constitue une limitation importante dans la recherche de structures moléculaires complexes. En 2009, Franck Lovering de Wyeth a proposé le concept "Escape from flatland", dans lequel il présente l'intérêt d'éviter les structures aromatiques pour privilégier des cycles saturés présentant des carbones sp^3 . Le rationnel de cette approche repose sur le fait que ces molécules non aromatiques sont plus proches des produits naturels, et que leur géométrie non-plane permet une plus grande exploration de l'espace chimique tridimensionnel, tout en améliorant les propriétés d'ADME (solubilité, sélectivité, lipophilie, etc.).

Dans ce projet de thèse, nous proposons de développer de nouveaux hétérocycles non aromatiques et non planaires présentant une liaison N-O. Si les cycles à 5 (isoxazole ou isoxazole) sont bien connus, les cycles à 6 ou 7 chaînons présentant un motif N-O sont particulièrement rares ou inexistant dans la littérature. Outre l'intérêt géométrique de ces hétérocycles, la présence de l'oxygène en alpha de l'azote permet de fortement diminuer la basicité de ce dernier, conférant à l'hétérocycle des propriétés physico-chimiques particulières. Par ailleurs, les oximes éthers (=N-O-) présentent une bonne résistance à la protonation, ce qui leur confère une stabilité intrinsèque à l'hydrolyse bien meilleure que celle observée avec les hydrazones ou les imines. Enfin, plusieurs

alkoxyamides sont actuellement en essai clinique. Durant cette thèse, nous avons focalisé nos travaux sur la synthèse de 3-amino-1,2,4-oxadiazine et benzo-2,3-oxazépine-4-one (Figure 1).



Figure 1 : Nouveaux châssis moléculaires

2. Résultats et discussions

2.1 Synthèse de 3-amino-1,2,4-oxadiazine

Les fonctions guanidines ont été extrêmement utilisées dans le développement d'outils pharmacologiques, tels que les antagonistes des récepteurs du NPPF, les inhibiteurs de FXa, de NOS ou encore d'urokinase. Toutefois, à cause de la basicité importante de la guanidine ($pK_a \approx 13$), ainsi que sa capacité à former de nombreuses liaisons hydrogène, il est difficile de développer des molécules présentant un bon profil pharmacocinétique, notamment en termes d'absorption orale, de distribution dans le CNS, ou encore de durée d'action. Le système iminoguanidine constitue un moyen intéressant de diminuer la basicité de la guanidine, comme le montre le développement thérapeutique du guanabenz (Wytensin[®]) contre l'hypertension. Néanmoins, cette molécule est entièrement plane et présente une certaine sensibilité à l'hydrolyse. Dans un précédent programme, l'équipe du Dr Bihel a développé une forme cyclique du guanabenz qui présente un effet inhibiteur sur le développement des prions, tout en étant moins sensible à l'hydrolyse.

Nous proposons de développer la synthèse de 3-amino-1,2,4-oxadiazines comme biomimétiques des fonctions guanidines et iminoguanidines. Alors que la synthèse des cycles à 6 chaînons 1,2-oxadiazines a été largement développée grâce à la réaction de cyclisation [4+2] de type nitroso-Diels Alder, les systèmes de type 3-amino-1,2,4-oxadiazines sont quasiment inconnus dans la littérature en termes de synthèse.

En partant de la Boc-Glycine, nous avons mis au point une synthèse multi-étape permettant d'accéder rapidement et avec d'excellents rendements au cycle 3-amino-1,2,4-oxadiazine sans contrôle du centre chiral en position 6 (Schéma 1). En utilisant la L-Proline, nous avons été capables de développer une synthèse énantiosélective permettant d'obtenir le cycle 4-amino ou 4-hydroxypyrrolo-[1,2-d]-1,2,4-oxadiazine avec un parfait contrôle des centres chiraux. La structure et la géométrie de ces nouveaux cycles ont été vérifiées par cristallographie aux rayons X. La mesure des pK_a a permis de confirmer une baisse importante de la basicité de ces alkoxyguanidines avec un $pK_a \approx 8$ à comparer avec les ≈ 10 de l'imino-guanidine et ≈ 13 pour une guanidine.

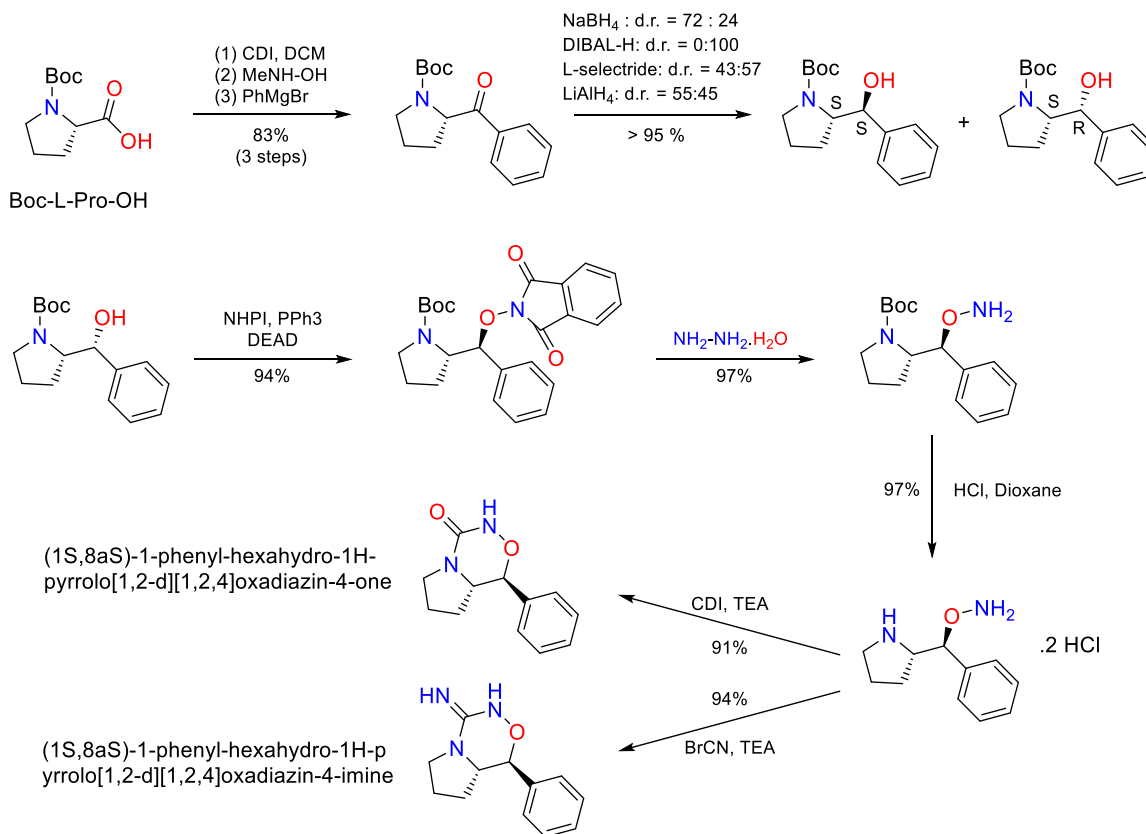


Schéma 1: Synthèse de 3-hydroxy- et 3-amino-1,2,4-oxadiazine

A ce jour, le seul produit naturel présentant un noyau 3-amino-1,2,4-oxadiazine est l'alchornédine, une molécule présentant des propriétés anti-parasitaires et extraites des feuilles d'alchornea glandulosa (Figure 2). Néanmoins, ce composé n'a jamais été synthétisé, et sa structure a été déduites d'analyses RMN. Nous avons mis au point une voie de synthèse permettant de synthétiser pour la première fois cet alcaloïde, et nous avons ainsi montré que la structure du produit décrit dans la littérature et nommé alchornédine était erronée. En effet, le cycle 3-amino-1,2,4-oxadiazine n'est pas présent, et nous pensons que l'alchornédine présente plutôt un cycle à 5 chaînons de type 2-amino-N-hydroxy-imidazole (Figure 2).

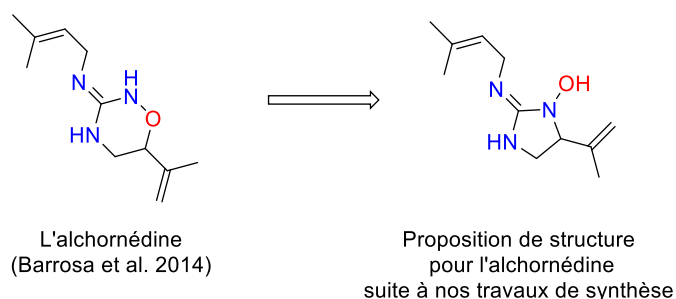


Figure 2: Structure publiée de l'alchornédine et notre contre-proposition

Au cours de ces travaux de synthèse, nous avons utilisé plusieurs voies de synthèse conduisant à l'insertion du motif N-O. L'une d'entre elles a consisté à insérer par réaction radicalaire en milieu

aqueux le motif N-hydroxyphthalimide en position bêta de dérivés de styrène, suivi d'une oxydation de la position alpha (Schéma 2). La mise au point de cette réaction a nécessité l'utilisation de tensio-actifs de type Triton X-100 permettant de réaliser la réaction en milieu micellaire. Cette méthodologie permet un meilleur respect des principes de la chimie verte, et a fait l'objet d'un article dans *Tetrahedron Letters* (Tang, S. Q.; Wang, A. P.; Schmitt, M.; Bihel, F. Dioxygenation of Styrenes with Molecular Oxygen in Water. *Tetrahedron Lett.* **2018**. <https://doi.org/10.1016/j.tetlet.2018.03.009>).

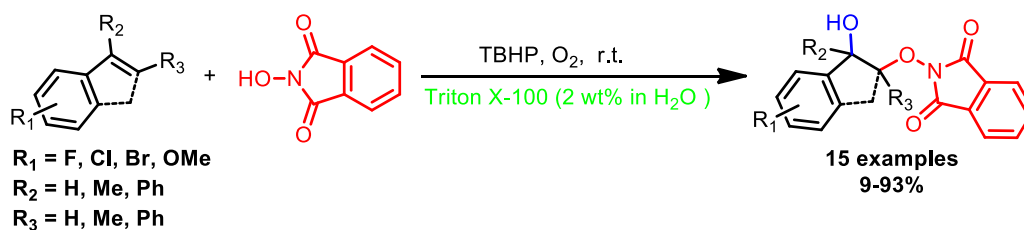


Schéma 2: Dioxygénation de styrènes avec de l'oxygène moléculaire dans l'eau

2.2 Synthèse de benzo-2,3-oxazépin-4-one

Dans notre approche de développer et caractériser de nouveaux châssis moléculaires innovants présentant une fonction N-O, nous avons choisi de construire le châssis benzo-2,3-oxazépin-4-one (Figure 1), en tant que bioisostère de 2,3-benzodiazépin-4-one. En effet, les benzodiazépines sont connues depuis les années 60, et près de 20 molécules sont actuellement utilisées en thérapie humaine comme anxiolytiques, myorelaxants et/ou hypnotiques. La majorité de ces médicaments sont des 1,4-benzodiazépines, à l'exception du Tofizopam qui présente un châssis de 1,2-benzodiazépine. Ce dernier est utilisé en Europe comme anxiolytique atypique, ainsi que pour le traitement de l'alcoolisme. Le cycle à 7 chaînons des benzodiazépines est particulièrement intéressant car cela confère à ces molécules des géométries tridimensionnelles tout à fait particulières.

La synthèse de benzo-2,3-oxazépin-4-one s'est révélée particulièrement difficile, et de très nombreuses voies de synthèse ont été testées. Néanmoins, nous avons réussi à développer une voie de synthèse efficace et reproductible (Schéma 3). La structure finale de ce premier exemple de benzo-2,3-oxazépin-4-one a été confirmée par cristallographie au rayon X. Nous travaillons actuellement à tester sa réactivité chimique et sa capacité à être fonctionnalisé.

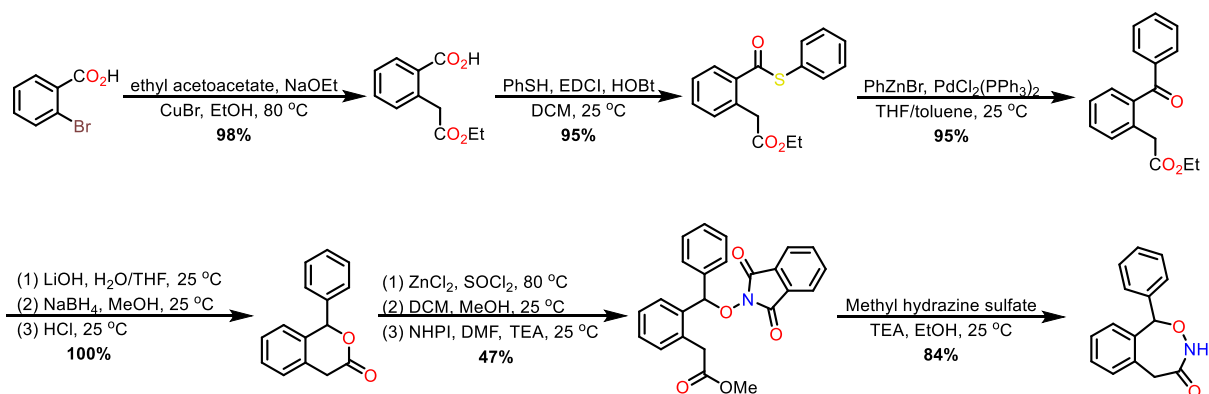
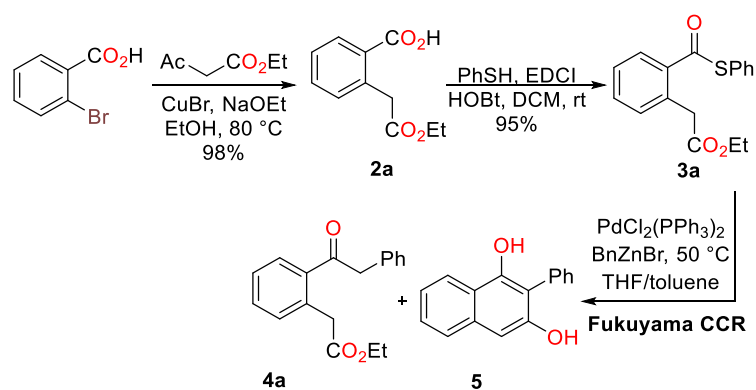


Schéma 3: Synthèse de la benzo-2,3-oxazépin-4-one

Durant la mise au point de cette synthèse, nous avons notamment travaillé sur la formation de la phénylacétophénone **4a** (Tableau 1) via une réaction de Fukuyama pallado-catalysée. La présence du groupement ester à proximité rend cette synthèse particulièrement difficile à réaliser à cause d'une réaction de cyclisation intramoléculaire. Après analyse des mécanismes en jeu, nous avons émis l'hypothèse qu'une accélération de la réaction de couplage devrait permettre d'éviter la cyclisation de Dieckman. L'utilisation de précatalyseurs commerciaux (PEPPSI-IPr ou XPhos-Pd-G4), mis au point pour la réaction de Negishi, n'a pas permis d'améliorer la réaction (Tableau 1, entrées 9 et 10). Nous avons par conséquent développé un nouveau précatalyseur que nous avons nommé POxAP pour « Post-Oxydative Addition Precatalyst » (Tableau 1, entrée 11).

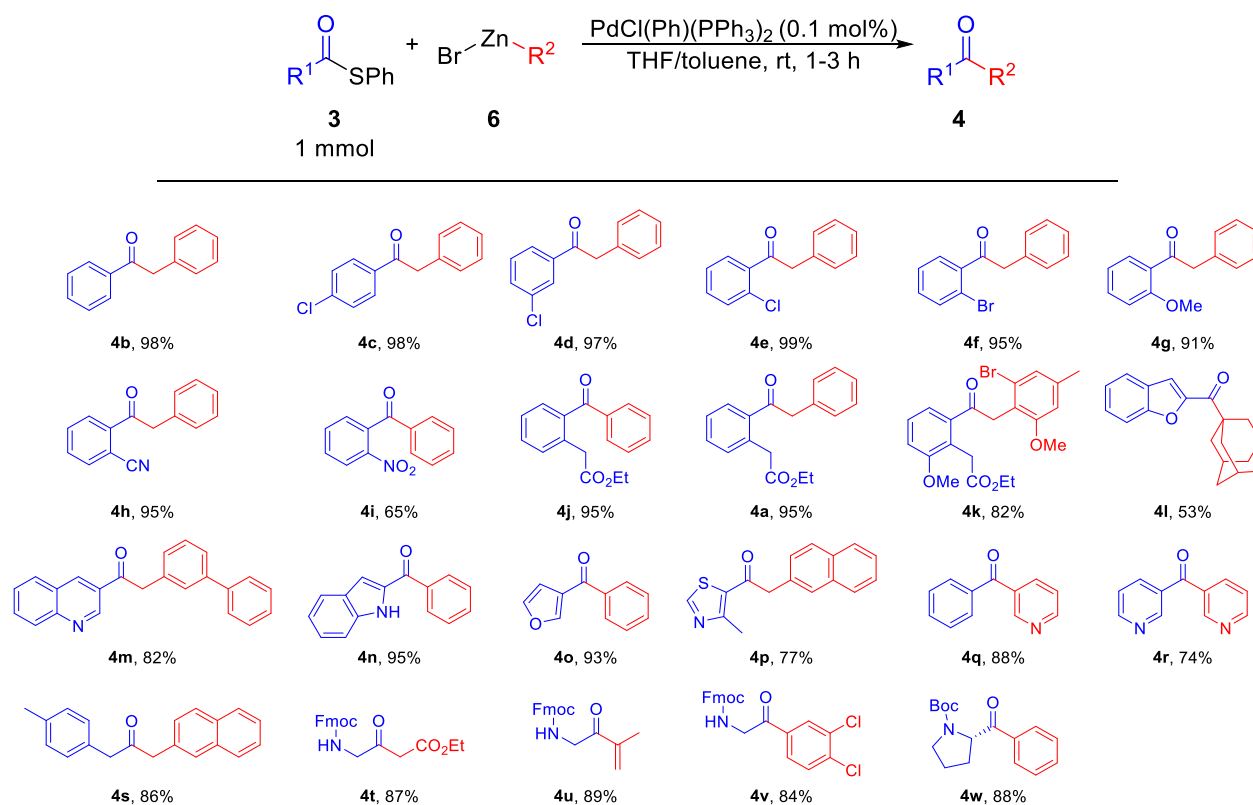
Tableau 1. Réaction de Fukuyama appliquée au thioester **3a**

entry ^a	cat	temp (°C)	time (min)	yield (%) ^b	
				4a	5
1	PdCl ₂ (PPh ₃) ₂	25	15	9	27
2	PdCl ₂ (PPh ₃) ₂	50	15	8	62
3 ^c	Pd(dba) ₂ /P(Fu) ₃	50	45	19	14
4 ^d	Pd ₂ (dba) ₃ /PCy ₃ /ZnCl ₂	50	45	31	53
5 ^e	Ni(acac) ₂	50	45	0	0
6	NiCl ₂ (PPh ₃) ₂	50	45	19	44
7	Cu(TMHD) ₂	50	45	27	41
8	Fe(acac) ₃	50	45	15	22
9	XPhos-Pd-G4	50	30	trace	0
10	PEPPSI-IPr	50	30	15	51
11 ^f	PdCl(Ph)(PPh ₃) ₂ [POxAP]	50	5	95	0

^aReaction conditions: Thioester **3a** (0.14 mmol), catalyst (1 mol %), BnZnBr (0.21 mmol, 0.82 M in THF), toluene (0.26 mL), rt. ^bIsolated yield. ^c1.4 mol % P(Fu)₃. ^d2 mol % PCy₃ and 1 equiv ZnCl₂ were used. ^e10 mol % Ni(acac)₂. ^f0.1 mol %

Grâce à ce précatalyseur de formule générique PdX(Ar)(PPh₃)₂, 0.001 mol% de catalyseur sont suffisants pour réaliser le couplage de Fukuyama avec d'excellent rendements, ouvrant l'accès à une très large variété de cétones (Tableau 2).

Tableau 2: Scope de la réaction de Fukuyama en utilisant le précatalyseur PdCl(Ph)(PPh₃)₂



^aReaction conditions: Thioester **3** (1 mmol), PdCl(Ph)(PPh₃)₂ (0.1 mol %), R²ZnBr **6** (1.5 mmol in THF), toluene (2.5 mL), rt, 1–3 h.

Ce nouveau précatalyseur POxAP nous a ainsi permis de synthétiser des analogues de la benzo-2,3-oxazepin-4-one, mais nous avons également valorisé ce nouveau réactif en réalisant la synthèse d'un précurseur de l'isoprekinamycine (IPK), un produit naturel connu pour ses propriétés antiparasitaires et anticancéreuses. Alors que la synthèse de ce précurseur de l'IPK avait été décrite dans la littérature en 16 étapes et 3% de rendement global, notre précatalyseur POxAP nous a permis de développer une stratégie alternative de synthèse conduisant au précurseur attendu en seulement 11 étapes et 29% de rendement global (Schéma 4). Ce travail a fait l'objet d'une publication dans *Organic Letters* (Tang, S. Q.; Bricard, J.; Schmitt, M.; Bihel, F. Fukuyama Cross-Coupling Approach to Isoprekinamycin: Discovery of the Highly Active and Bench-Stable Palladium Precatalyst POxAP. *Org. Lett.* **2019**, *21* (3), 844–848. <https://doi.org/10.1021/acs.orglett.9b00031>). Par ailleurs, nous avons montré également que POxAP est également efficace dans d'autres réactions telles que la réaction de Negishi, et ce travail est en cours de rédaction pour publication en 2019.

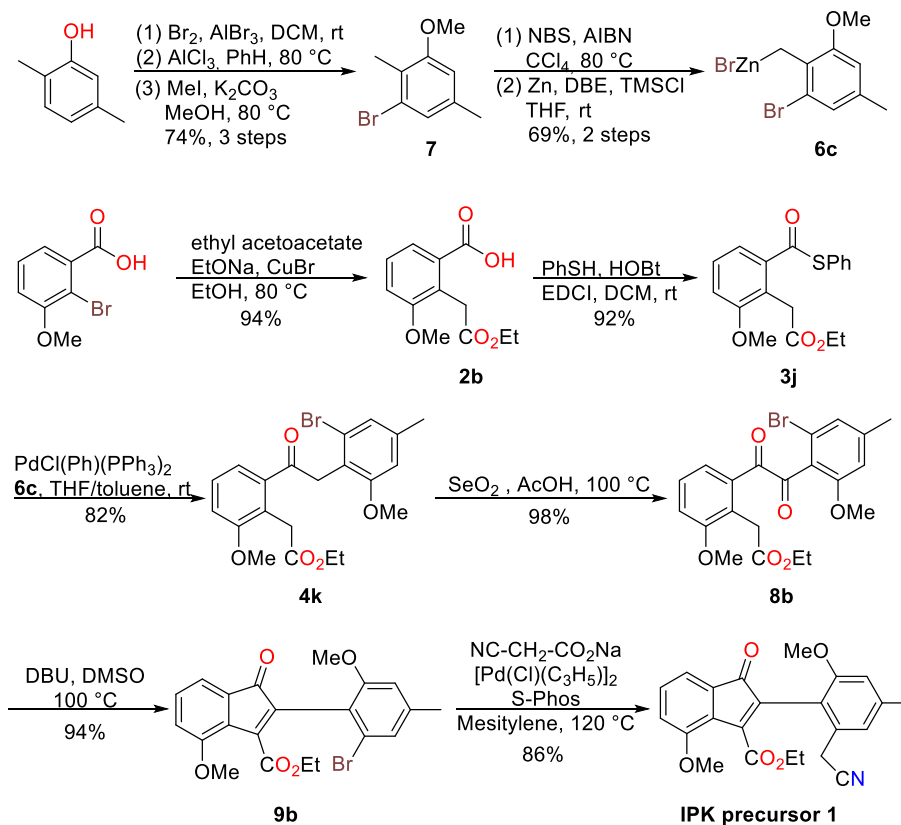


Schéma 4: Synthèse du précurseur de l'isoprékynamycine en 11 étapes et 29% de rendement global

3. Conclusion générale

Au cours de ce travail de thèse, j'ai pu remplir mes 2 objectifs principaux, à savoir la synthèse de nouveaux châssis moléculaires hétérocycliques et non aromatiques présentant une liaison N-O. Un important travail d'optimisation de voies de synthèse a été accompli, incluant la mise au point de nouvelles méthodologies (2 articles publiés en 1^{er} auteur). Grâce à la cristallographie, nous avons pu par ailleurs démontrer la géométrie non planaire de ces molécules, et les mesures de pKa ont montré également l'effet alpha de l'oxygène sur la basicité de l'azote. La suite de ce travail consistera à évaluer les possibilités de fonctionnalisation de ces châssis moléculaires, mais également évaluer leur pertinence en chimie médicinale. Ainsi, les propriétés d'ADME (stabilités métaboliques et plasmatiques, perméabilité, solubilité, etc.) seront mesurées, et des dérivés spécifiques seront synthétisés pour être testés sur des cibles biologiques spécifiques. A titre d'exemple, les 3-amino-1,2,4-oxadiazines seront testées pour leur capacité à moduler le système PFAR dans des tests anti-prions.

Table of Contents

I. Introduction	1
IA. Heterocycles in medicinal chemistry	3
IB. Nitrogen or oxygen heterocycles as privileged structures	8
IC. Molecular complexity in drug discovery	12
ID. Increase complexity: from N-N heterocycles to N-O heterocycles	15
IE. Common synthetic strategies to N-O heterocycles	23
II. Synthetic strategies and applications	27
III. Synthesis of 3-amino-1,2,4-oxadiazines and their physicochemical properties	33
IIIA. Synthesis of 6-(3,4-dichlorophenyl)-5,6-dihydro-4 <i>H</i> -1,2,4-oxadiazin-3-amine 10a	38
IIIB. Synthesis of (1 <i>R</i> ,8 <i>aS</i>)-1-phenyl-6,7,8,8 <i>a</i> -tetrahydro-1 <i>H</i> -pyrrolo [1,2- <i>d</i>][1,2,4]oxadiazin-4-amine 10b	48
IIIC. Synthesis of (5 <i>S</i> ,6 <i>R</i>)-5-isopropyl-6-phenyl-5,6-dihydro-4 <i>H</i> -1,2,4-oxadiazin-3-amine 10c	58
IIID. Physicochemical studies of 3-amino 1,2,4-oxadiazines	61
IIIE. Conclusion	64
IV. Total synthesis of alchornedine	67
IVA. Total synthesis of 40 from <i>N</i> -Boc glycine	70
IVB. Other methods to synthesize 43	79
IVC. Verification of the structure of alchornedine	84
IVD. Conclusion	87
V. Dioxygenation of styrenes with molecular oxygen in water, a green approach to introduce N-O moiety	89
VI. Synthesis of 2,3-benzoxazepin-4-one scaffold	93
VI A. Synthesis of 1-phenyl-2,3-benzoxazepin-4-one scaffold	98
VI B. Other methods to synthesize 1-phenyl-2,3-benzoxazepin-4-one	

scaffold	116
VI C. Synthesis of 1-benzyl-2,3-benzoxazepin-4-one scaffold	122
VI D. Conclusion	124
VII. Summary	127
VIII. Experiment section and NMR spectra	133
VIII A. General information	135
VIII B. Physicochemical studies of 1,2,4-oxadiazines	136
VIII C. Synthetic procedures and analytic data	138
IX. Appendix	205
Appendix I. Crystallographic data and structure refinement parameters of cpd 10a	207
Appendix II. Crystallographic data and structure refinement parameters of cpd 10b	212
Appendix III. Crystallographic data and structure refinement parameters of cpd 48	218
Appendix IV. Crystallographic data and structure refinement parameters of cpd 102	226
Appendix V. Crystallographic data and structure refinement parameters of cpd 81	232
Appendix VI. 2D NMRs of cpd 48	238
Appendix VII. NOESY and HMBC of cpd 45 and 43	240
Appendix VIII. Dioxygenation of styrenes with molecular oxygen in water	242
Appendix IX. Fukuyama cross-coupling approach to isoprekinamycin: discovery of the highly active and bench-stable palladium precatalyst POxAP	251
X. Reference	291

LIST OF ABBREVIATIONS

ADME	absorption, distribution, metabolism and excretion
Boc	<i>t</i> -butyloxycarbonyl
BOP	(benzotriazol-1-yloxy)tris(dimethylamino)phosphonium hexafluorophosphate
CCR	cross-coupling reaction
CDI	1,1'-carbonyldiimidazole
COSY	homonuclear chemical shift correlation spectroscopy
cpd	compound
CYP450	cytochrome P450
DBE	dibromoethane
DBU	1,8-diazabicyclo(5.4.0)undec-7-ene
DCM	dichloromethane
DEAD	diethyl azodicarboxylate
DIAD	diisopropyl azodicarboxylate
DIBAL-H	diisobutyl aluminium hydride
DMAP	4-dimethylaminopyridine
DMB	2,4-dimethoxybenzyl
DMEAD	di-2-methoxyethyl azodicarboxylate
DMF	<i>N,N</i> -dimethylformamide
EDCI	1-ethyl-3-(3-dimethylaminopropyl)carbodiimide
FDA	Food and Drug Administration
Fmoc	9-fluorenylmethoxycarbonyl
Fsp ³	fraction of saturated carbons
GABA _A receptor	type A γ -aminobutyric acid receptor
HBA	H-bond acceptor
HMBC	heteronuclear multiple bond correlation
HOBt	1-hydroxybenzotriazole

HSAB	hard and soft acids and bases
HSQC	heteronuclear single quantum correlation
log D	distribution coefficient
MsCl	methanesulfonyl chloride
NHPI	<i>N</i> -hydroxyphthalimide
NOESY	nuclear overhauser effect spectroscopy
NPFFR	neuropeptide FF receptors
N-N heterocycles	heterocycles including two adjacent nitrogen atoms
N-O heterocycles	heterocycles including adjacent nitrogen and oxygen atoms
PDE4	phosphodiesterase4
pK_a	ionization constant
PMP	<i>para</i> -methoxyphenyl
POxAP	post-oxidative-addition precatalyst
rt	room temperature
SPhos	2-dicyclohexylphosphino-2',6'-dimethoxybiphenyl
S-CDI	1,1'-thiocarbonyldiimidazole
TEA	triethylamine
TMSCl	trimethyl chlorosilane
(<i>S</i>)-2-Me-CBS	(<i>S</i>)-3,3-diphenyl-1-methylpyrrolidino[1,2- <i>c</i>]-1,3,2-oxazaborole

I. Introduction

I. Introduction

IA. Heterocycles in medicinal chemistry

For more than a century, heterocycles have constituted one of the largest areas of research in organic chemistry and been on the forefront of attention because of their numerous uses in pharmaceutical applications such as antimicrobial, anti-inflammatory, anticancer, antiviral, anticonvulsant and antidepressant (*Figure 1.1*).¹⁻⁶

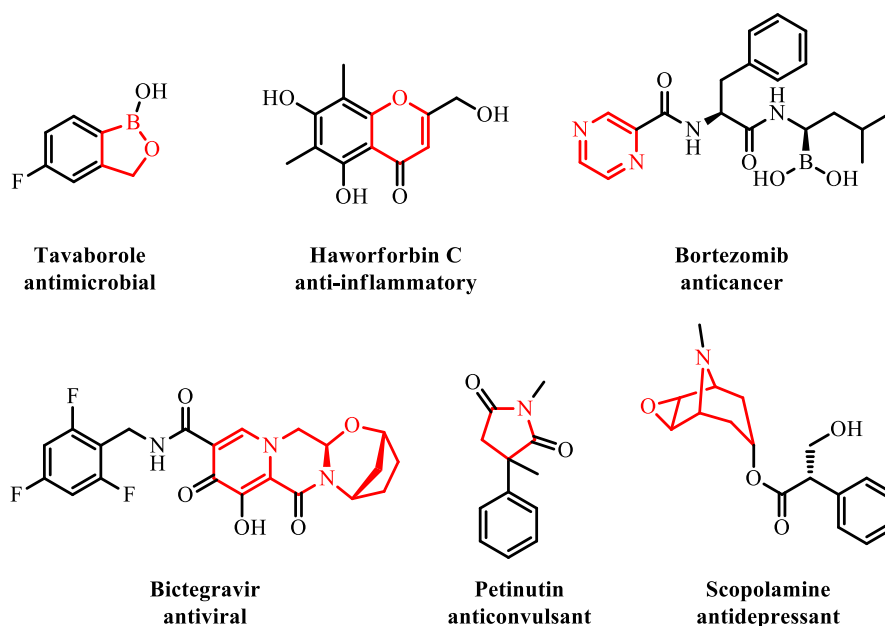


Figure 1.1. Heterocycles in pharmaceutical applications.

In particular, nitrogen- and oxygen-containing heterocycles are the two most common type of heterocycles that appear as structural components of U.S. Food and Drug Administration (FDA) approved pharmaceuticals. The analysis of the nitrogen or oxygen heterocyclic composition of U.S. FDA approved unique small-molecule pharmaceuticals shows that 59% of small-molecule drugs contain nitrogen heterocycle(s) and 27% contain oxygen heterocycle(s).^{7, 8}

Figure 1.2 displays the structures of the 20 most frequent nitrogen heterocycles

from 640 FDA approved unique nitrogen heterocycle-containing small molecule drugs (excluding pharmaceuticals with different international nonproprietary names) in order of decreasing frequency, which highlights the various ring system classes. Piperidine, pyridine and piperazine are the top three most common nitrogen heterocycles, appearing in 72, 62 and 59 unique small-molecule drugs, respectively. Significantly behind the top three is cephem, a β -lactam core found in 41 approved drugs followed by pyrrolidine accounting for 37 drugs. Two more five-membered nitrogen heterocycles, thiazole and imidazole, are sixth and seventh most prevalent nitrogen heterocycles followed by penam. Rounding off the top 10, with approximately equal representation, are indole, tetrazole, phenothiazine, and pyrimidine. It is interesting to note that 4 of the 10 most commonly used nitrogen heterocycles also contain a sulfur atom (cephem, thiazole, penam, and phenothiazine). Despite the similarity in frequency of the remaining top 20 nitrogen heterocycles, remarkable diversity in structures could be observed, ranging from simple five-membered rings (benzimidazole and imidazolidine) to complex natural motifs (morphinan, tropane and ergoline).

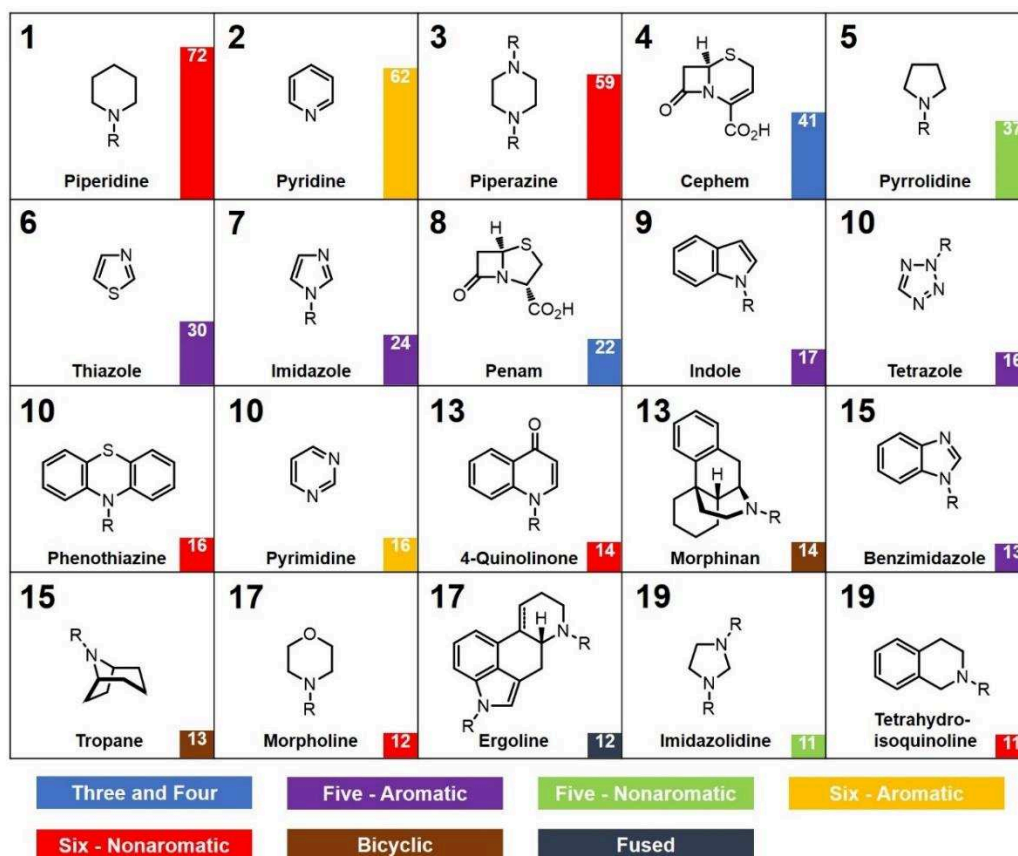


Figure 1.2. Top 20 most frequent nitrogen heterocycles in U.S. FDA approved drugs in order of decreasing frequency represented by a drawn to scale solid colored bar.

(adapted from Njardarson, J. T. et al⁷)

Figure 1.3. displays the 20 most frequent oxygen heterocycles from 311 FDA approved unique oxygen heterocycle-containing drugs in order of decreasing frequency. The two most frequently used oxygen heterocycles are originated from carbohydrate-based drugs, where pyranoses are number 1 with 62 appearances followed by furanoses in a distant second place with 34 appearance. Macrolactones, morpholines, and dioxolanes account for the remaining top five with 26, 26 and 24 appearance, respectively. When compared the frequency of the top two oxygen heterocycles or nitrogen heterocycles, a 45% decrease in frequency is observed between pyranose and furanose, while for nitrogen heterocycles, the decrease in frequency is 14% between piperidine and pyridine, suggesting the oxygen heterocycles are far more top heavy.

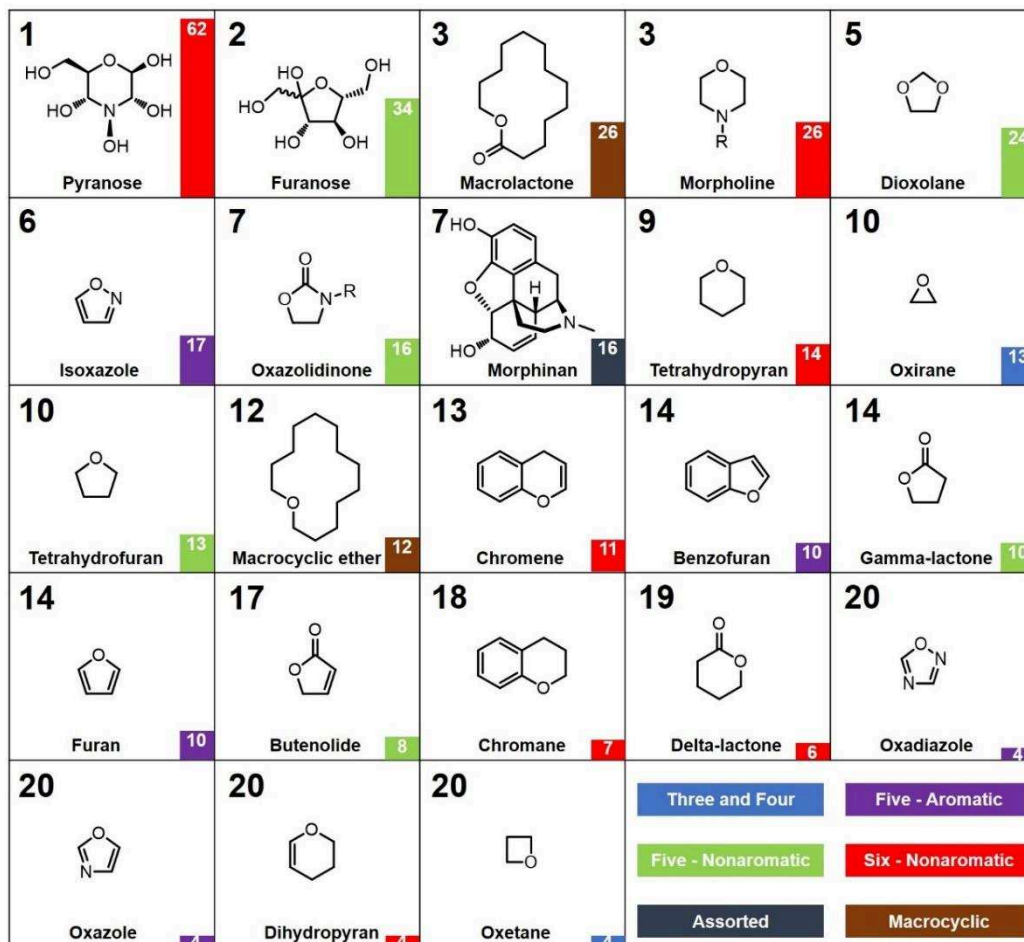


Figure 1.3. Top 20 most frequent oxygen heterocycles in U.S. FDA approved drugs, in order of decreasing frequency represented by a drawn to scale solid colored bar.

(adapted from Njardarson, J. T. et al⁸)

A closer look at these FDA approved pharmaceuticals containing nitrogen or oxygen heterocycles revealed that the majority are non-aromatic heterocycles (Figure 1.4). Although the rigidity of the non-aromatic heterocycles is decreased compared with the corresponding aromatic ones, the intercalation between molecules will be impaired and a better solubility will be obtained. Moreover, the non-aromatic scaffolds usually imply the presence of stereogenic elements, which increase the selectivity for targets and decrease the side effects. All these aspects lead to good druggability of the non-aromatic heterocycles.

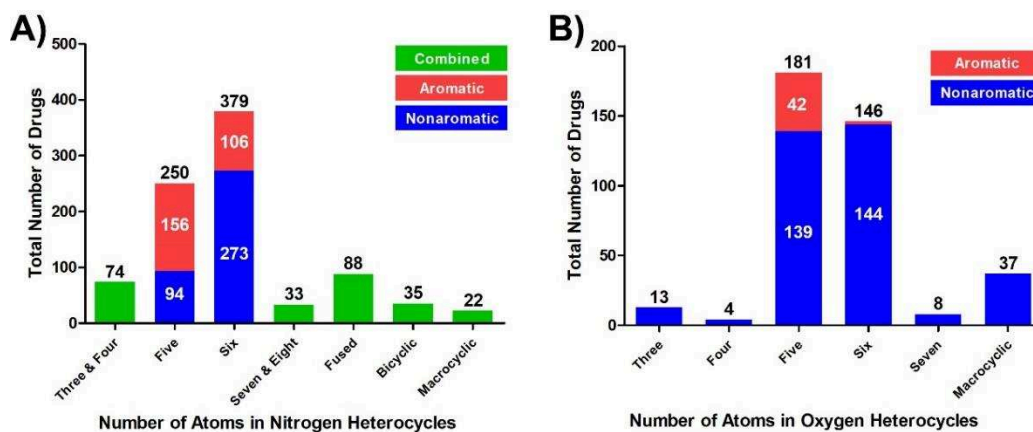
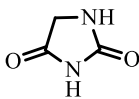
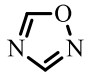
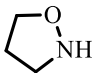
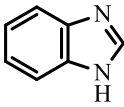
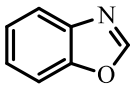


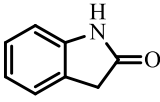
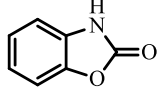
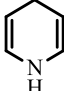
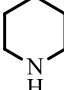
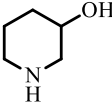
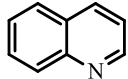
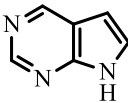
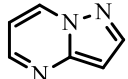
Figure 1.4. Structural classes and relative distribution of nitrogen (A) or oxygen (B) heterocycles in FDA approved drugs. (adapted from Njardarson, J. T. et al ^{7,8})

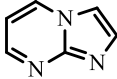
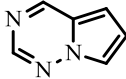
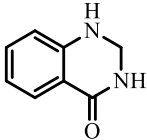
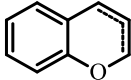
IB. Nitrogen or oxygen heterocycles as privileged structures

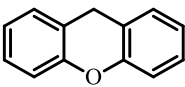
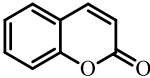
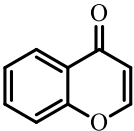
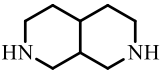
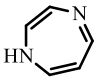
The concept of privileged structures is the idea that certain structural features produce biological effects more often than others. More formally, privileged structures have been defined in the context of a minimal substructure capable of binding several types of receptors.⁹ As frequently appeared in drugs, nitrogen and oxygen heterocycles are always regarded as privileged structures in medicinal chemistry. *Table 1.1* showed several examples of privileged structures containing nitrogen or oxygen heterocycles. Various biological activities of these heterocycles have been discovered, such as antibacterial, antiviral, anti-inflammatory, anticancer, antioxidant, antiplasmodial, antiglycation, anticonvulsant, antitubercular, antipsychotic, herbicidal, etc.

Table 1.1. Privileged structure containing nitrogen or oxygen heterocycles.

Heterocyclic Privileged Structures			Biological Activities
Five-membered heterocycles	hydantoin ¹⁰		anticancer, anti-inflammatory, antidiabetic, antimicrobial, adrenoceptor modulating, anticonvulsant, antiplatelet, anti-HIV
	1,2,4-Oxadiazole ¹¹		anti-inflammatory, analgesic
	isoxazolidine ¹²		Anticancer, antifungal, antimicrobial, anti-inflammatory, antiglycation
Fused five-membered heterocycles	benzimidazole ¹³		anti-HIV, anti-HCV, anti-HBV, anti-HCMV, anti-RSV and anti-rhino/enteroviruses
	benzoxazole ^{14, 15}		antimicrobial, antiglycation, anticonvulsant, antitubercular,

			antipsychotic, anticancer, herbicidal, antioxidant
	2-oxindole ^{16, 17}		antibacterial, anti-oxidant, anti-cancer, anti-HIV, anti-fungal, anti-tubercular, anti-inflammatory, neuroprotective
	2(3 <i>H</i>)-benzoxazolone ¹⁸		Analgesic, anti-inflammatory, antipsychotic, neuroprotective, anticonvulsant
Six-membered heterocycles	1,4- dihydropyridine ^{19, 20}		antihypertensive, antianginal, antitubercular, anticonvulsant, antitumor, analgesic, anti-inflammatory, stress protection, antiulcer, antioxidant
	piperidine ²¹		anticancer, antihypertensive, antimalarial, antibacterial, anticonvulsant, anti-inflammatory, monoamine oxidase inhibitory
	3-hydroxypiperidine ²²		Anticancer, antibiotic, anaesthetic, antifungal
Fused six-membered heterocycles	quinoline ^{23, 24}		antibacterial, antifungal, antiviral, neuroprotective, anticancer
	pyrrolo[2,3- <i>d</i>]pyrimidine ²⁵		antitumor, antiviral
	pyrazolo[1,5- <i>a</i>]pyrimidine ²⁶		antischistosomal, antitrypanosomal, sedative,

			anxiolytic, antimalarial, antifungal
	imidazo[1,2- <i>a</i>]pyrimidine ²⁷		anticancer, antiviral, antimicrobial, antibacterial, antifungal, anti-inflammatory, local anaesthetic
	pyrrolo[2,1- <i>f</i>][1,2,4]triazine ²⁸		Inhibitor of anaplastic lymphoma kinase (ALK), Janus kinase 2 (JAK2), VEGFR-2, EGFR, HER2, Met kinase, p38 α mitogenactivated protein (MAP) kinase and insulin-like growth factor receptor (IGF-1R) kinase
	2,3-Dihydroquinazolin-4(1 <i>H</i>)-one ²⁹		Antihypertensive, diuretic, neurotransmitter, thermogenic, stimulant, sedative, muscle-relaxant, hypnotic, antineoplastic, anti-inflammatory, antifungal
	chromene ³⁰		antitumor, antihepatotoxic, antioxidant, anti-inflammatory, diuretic, anticoagulant, antispasmodic, estrogenic, antiviral, antifungal, antimicrobial, anti-helminthic, hypothermal, vasodilatory, antitubercular, herbicidal, anticonvulsant, analgesic

	Xanthene ³¹		antibacterial, antiviral, anti-inflammatory, antitumor, antioxidant, antiplasmodial
	coumarin ³²⁻³⁴		antibacterial, antitubercular, antifungal, antiviral, antimutagenic, antioxidant, anti-inflammatory, antithrombotic, anticancer, anticoagulant, cyclooxygenase inhibitory, lipoxygenase inhibitory, cholinesterase inhibitory, monoamine oxidase inhibitory, CNS stimulant, vasodilator, and cytotoxic
	chromone ^{5, 35, 36}		Anticancer, anti-inflammatory, antidyslipidemic, estrogenic, immunosuppressant, antioxidant, antimicrobial
	bispidine ³⁷		Antiviral, antibacterial, antifungal, antidote, anticancer
Seven-membered heterocycles	1,4-diazepine ³⁸		anticonvulsant, sedative, and anxiolytic, anticancer, anti-inflammatory

IC. Molecular complexity in drug discovery

Since many drugs are derived from complex natural products (*Figure 1.5*),³⁹ the medicinal chemistry community has become increasingly aware of the requirement to creating drug-like compounds containing a high degree of structural diversity and architectural complexity,⁴⁰⁻⁴⁴ to increase the chance to find bioactive compounds. Molecular complexity has been associated with major aspects in the drug development process such as success in progressing into clinical development, target selectivity and compound safety.⁴⁵ However, like molecular similarity and chemical space, molecular complexity is an intuitive and subjective concept that is not easy to quantify in a unique and “best” manner.

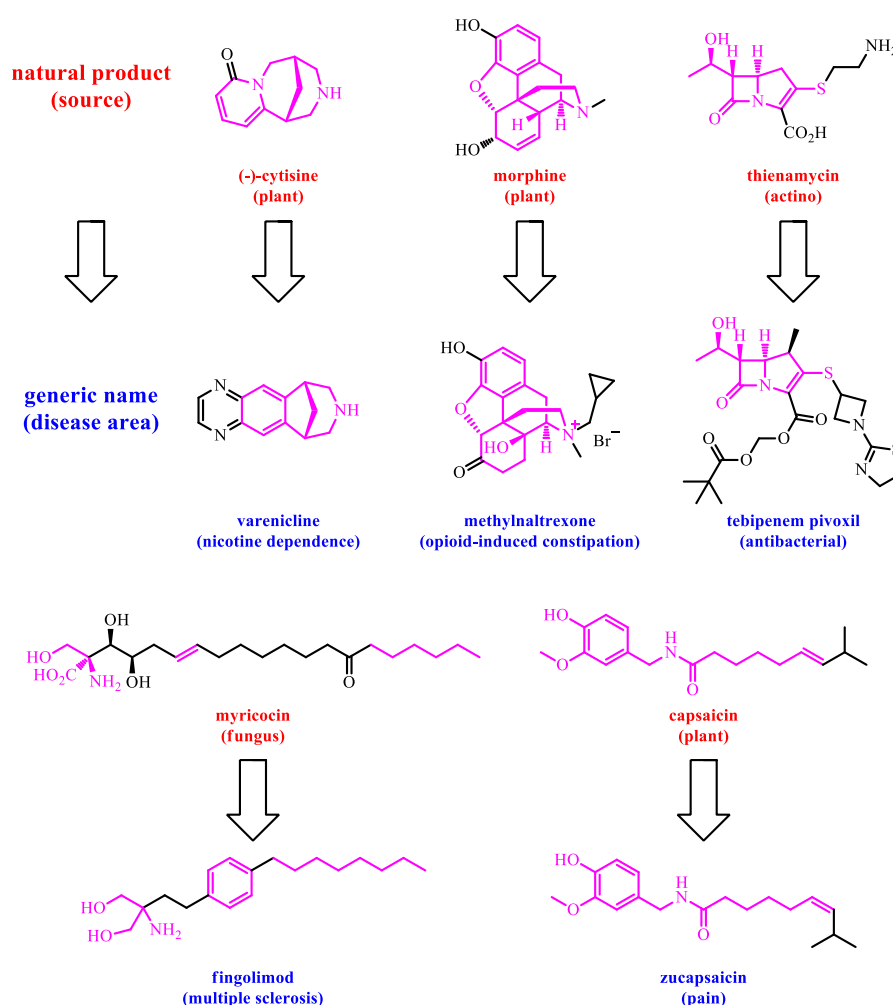


Figure 1.5. Nature product derived drugs.

Although routinely used in absorption, distribution, metabolism and excretion (ADME) prediction models and scrutinized as compounds progress from hit-to-lead, physicochemical indicators such as Lipinski's "rule of five" (H-bond donors or Log P < 5, molecular weight < 500, H-bond acceptors < 10),⁴⁶ topological polar surface area ($\leq 140 \text{ \AA}^2$) and rotatable bonds (≤ 10)⁴⁷ did not describe the complexity of the molecules, but help to determine the potential or the risk factors of a compound in drug development. As a result, several approaches describing molecular complexity have been reported. Based on the concepts of graph theory and information theory, Bertz proposed a mathematical approach for evaluating the complexity of chemical structures,⁴⁸ while Whitlock proposed an intuitive (metric) approach for molecular complexity,⁴⁹ which was then ameliorated by Barone with a more empirical approach.⁵⁰ After that, Allu proposed a new metric based on relative atomic electronegativities and bond parameters that evaluate both synthetic and molecular complexity starting from chemical structures.⁵¹ However, it reduced the correlation of complexity to molecular weight. More recently, Lovering proposed the descriptor of molecular complexity by using the fraction of saturated carbons (F_{sp^3} = number of sp^3 hybridized carbons/ total carbon count) and carbon chirality within a molecule.⁵² More importantly, he indicated that both complexity (as measured by F_{sp^3}) and the presence of chiral centers correlate with success as compounds transition from discovery, through clinical testing, to drugs. Without increasing molecular weight significantly, saturation and chirality allow the preparation of architecturally more complex molecules, resulting in the exploration of more diverse chemical space. As a result, it increases opportunity to design in out-of-plane substituents and to adjust molecular shape, increasing receptor/ligand complementarity. This might also allow the engineering of additional protein-ligand interactions not accessible to a flat aromatic ring, and thus improve potency and selectivity to a given target while mitigating off-target effects. Although aromatic features can provide an opportunity to develop π - π interactions or π -cation interactions,^{53, 54} an overall level of saturation may provide the molecule with an opportunity to better place these types of moieties.

Furthermore, increasing sp^3 character may improve several molecular attributes that contribute to clinical success. For instance, saturation increased solubility and decreased melting point, two experimental physical properties important to success in the drug discovery setting, as any compound with an intravenous mode of delivery should necessarily be very water soluble and a melting point above 250 °C will negatively impact oral bioavailability.⁵⁵ Increasing complexity (measured by F_{sp^3} and chiral carbon count) also reduces promiscuity and cytochromeP450 (CYP450) inhibition, which were linked to toxicity.⁵⁶

ID. Increase complexity: from N-N heterocycles to N-O heterocycles

It is widely accepted that heterocycles including two adjacent nitrogen atoms (N-N heterocycles) are excellent drug candidates. More particularly, the five-membered ring pyrazole, as well as both six-membered rings pyridazine and 1,2,4-triazine, were extensively used in drug design (Figure 1.6).⁵⁷⁻⁵⁹ Indeed, thanks to the nitrogen atoms, these three aromatic scaffolds exhibit 2 to 3 H-bond acceptors, capable to interact with target proteins. Moreover, these nitrogen atoms allow to decrease the lipophilicity of these heterocycles in comparison with benzene. However, due to their aromatic character, these 3 scaffolds have still a planar geometry, partly contributing to the fact that they are widely used in developing pharmacological tools, but poorly represented in FDA-approved drugs.

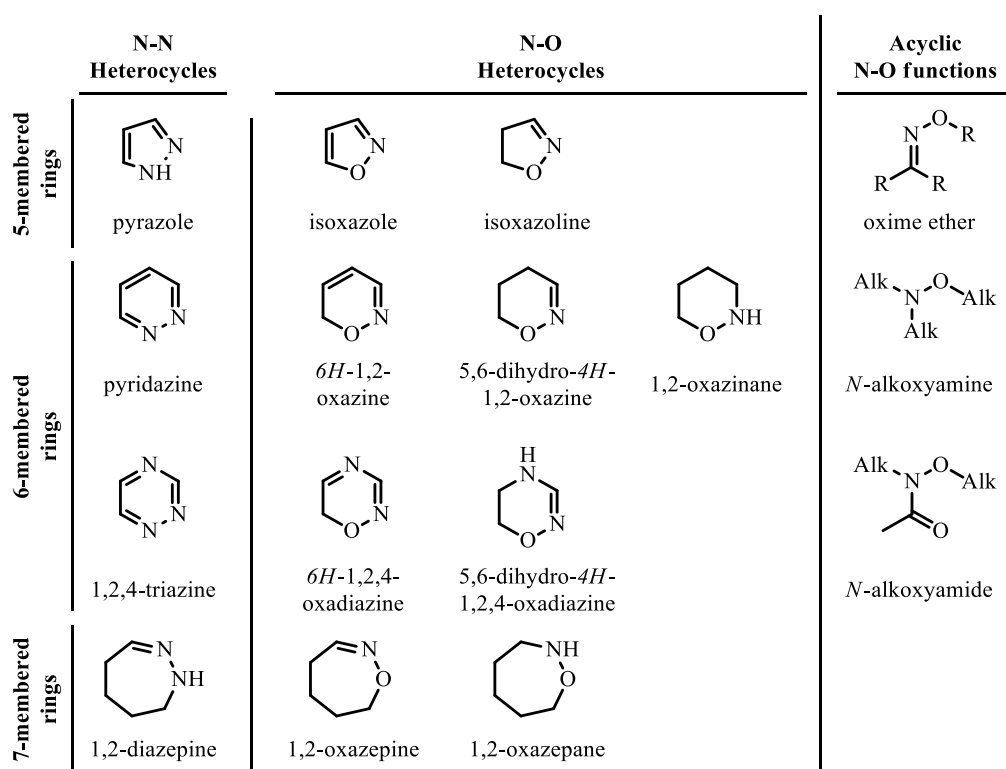


Figure 1.6. N-N heterocycles, N-O heterocycles and acyclic N-O functions.

1,2,4-triazine ring is widely described as scaffold of many biological active compounds, natural or synthetic, with a great variety of pharmacological effects,

especially active as anti-inflammatory, antiproliferative, neuroprotective, antibacterial and antitumor agents (*Figure 1.7*).⁶⁰⁻⁶⁴

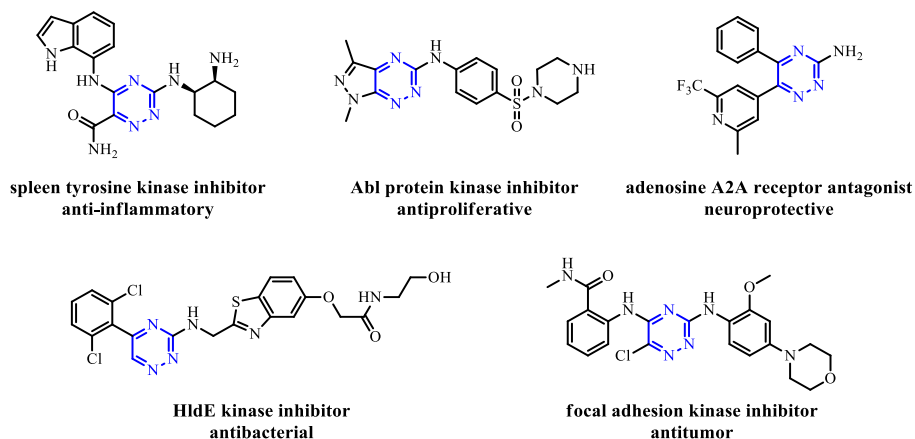


Figure 1.7. Bioactive 1,2,4-triazines.

Compound (cpd) **1** is an N-N heterocycle containing 1,2,4-Triazine nucleus previously developed in our group as a neuropeptide FF receptors (NPFFR) antagonist (*Figure 1.8*). When we increased the complexity of cpd**1** by saturated one of the C=N double bond in the 1,2,4-triazine scaffold, cpd **2** (acid dissociation constant (pK_a) \approx 9.3) was obtained with a higher activity. Then, the cyclic iminoguanidine scaffold **2** was replaced by the conjugated cyclic guanidine **3** (pK_a \approx 10.6) according to isosterism concept. Cpd **3** appeared to be a potent selective NPFF₁R antagonist, which could significantly reduce the long lasting fentanyl-induced hyperalgesia in rodents.⁶⁵ However, removing the conjugation between the guanidine and phenyl moiety in **3** by saturating the C=C double bond in-between increased pK_a (\approx 13) and impaired the biological activity, indicating the importance of a proper basicity to activity.

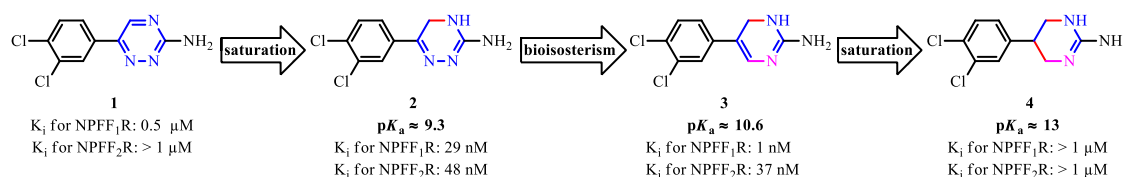


Figure 1.8. Previous research on six-membered N-N heterocycle 1,2,4-triazine.

Besides 1,2,4-triazine, the seven-membered N-N heterocycle, 2,3-benzodiazepin-4-one also has attracted huge interest because of their diverse pharmacological activities, including neuroprotective, anticonvulsant, and antitumor effect (*Figure 1.9*).⁶⁶⁻⁶⁸

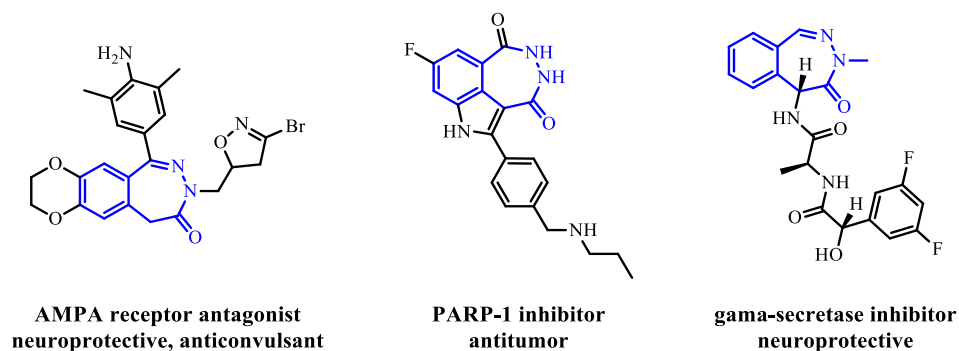


Figure 1.9. Bioactive 2,3-benzodiazepin-4-ones.

By pharmacophoric comparison between papaverine **5** (ring expansion) and tofisopam **6** (bioisosterism), cpd **7** was developed by our group as a novel class of phosphodiesterase4 (PDE4) inhibitor, which appears as a potential target for the development of new anti-asthmatic and anti-inflammatory drugs (*Figure 1.10*).⁶⁹ As a result of the insertion of a saturated carbon into **5** and saturation one of the C=N double bond in **6**, the 2,3-benzodiazepin-4-one nucleus in **7** shown a non-planar boat-shaped conformation,⁷⁰ which might be crucial to the target cognization.

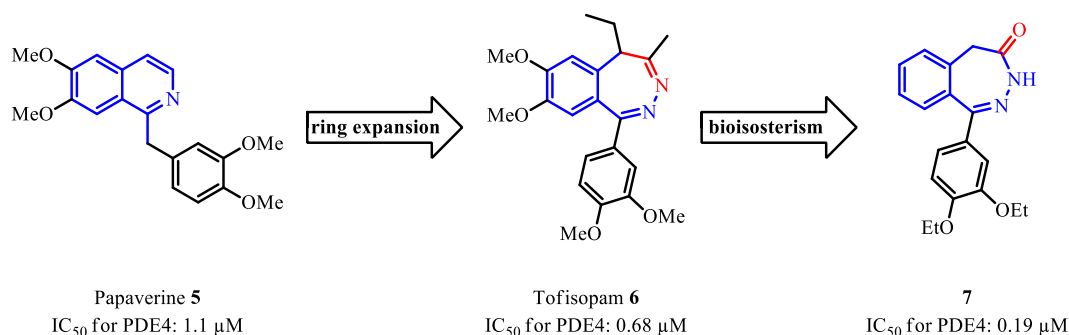


Figure 1.10. Previous research on seven-membered N-N heterocycle 2,3-benzodiazepin-4-one.

As shown in *Figure 1.9* and *1.10*, increasing the complexity through the concept of “escape the flatland” (saturating carbon bonds and introducing chiral sp^3 carbon atoms) enhanced the biological activity and target selectivity. Thus, in this project, we will continue to increase the complexity of two scaffolds, 4,5-dihydro-1,2,4-triazine **2** and 2,3-benzodiazepin-4-one **7**, by developing non-planar heterocycles including adjacent nitrogen and oxygen atoms (N-O heterocycles), as bioisosteres of the corresponding N-N heterocycles. By transposing one of the two adjacent nitrogen atoms in cpd **2** and **7** by an oxygen atom, we will obtain two new scaffolds 1,2,4-oxadiazine **8** and 2,3-benzoxazepin-4-one **9** exhibiting an intracyclic N-O bond (*Figure 1.11*). As the oxygen atom is a H-bond acceptor (HBA), these scaffolds can be considered as biomimetic structures of the corresponding N-N heterocycles. However, thanks to the bivalent character of oxygen atom, these N-O heterocycles cannot be aromatic, and so show an interesting non-planar geometry. Moreover, a supplementary complexity can be obtained by introducing chirality on saturated carbon atoms.

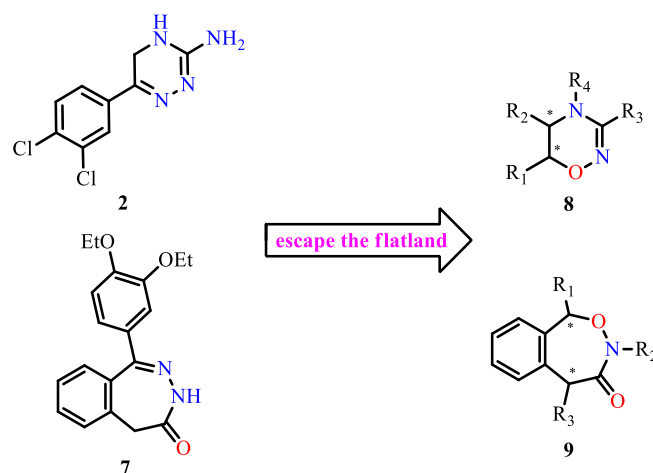


Figure 1.11. Developing N-O heterocycles from N-N heterocycles.

Drug-likeness rules consider N-O single bonds as “structural alerts” which should not be present in a perspective drug candidate (*Figure 1.6*), in particular *N*-alkoxyamines such as TEMPO. In most cases this concern is correct, since the

general weakness of the *O*-alkyl bond in the *N*-alkoxyamine moieties, these compounds can undergo a C-ON bond homolysis to release a persistent nitroxyl radical NO· particularly useful in controlled radical polymerization but triggering serious side effects in drugs.^{71, 72} Thus, *N*-alkoxyamine cannot be used as a scaffold of interest for biological applications. However, the same type of metabolic behavior of *N*-alkoxyamine should not be expected when the nitrogen atom is “conjugated”, either with an aromatic ring or with a chemical function including a double bond such as amide, amidine, etc...

In contrast to acyclic *N*-alkoxyamine, oxime ethers (*Figure 1.6*) are not sensitive to homolysis and are widely used in medicinal chemistry. Indeed, thanks to its resistance to protonation, oxime ethers possess greater intrinsic hydrolytic stability than hydrazones (>N=N=<) or imines (-N=<). This stability to hydrolysis allowed several acyclic oxime ethers to be pushed in clinical trials. Today, more than 15 are marketed in various indications including multiple sclerosis, bacterial infections or depression (*Figure 1.12*). This stability to hydrolysis is also true for the non-aromatic cyclic oxime ethers.

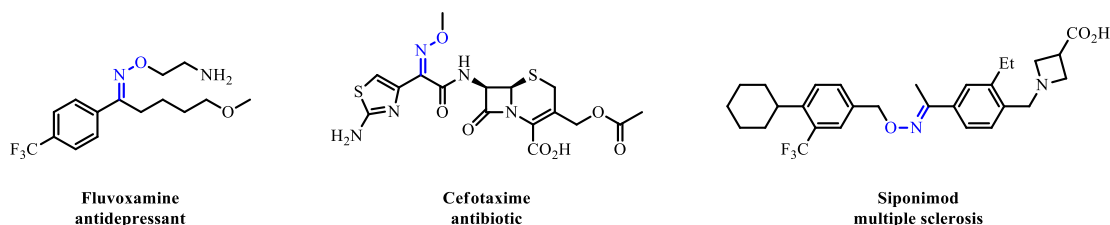


Figure 1.12. Marketed drugs presenting acyclic oxime ether moiety.

Whereas the five-membered cyclic oxime ethers (*Figure 1.6*, isoxazole, isoxazoline) were used in organic and medicinal chemistry as early as the 60s, with several marketed drugs (*Figure 1.13*), the synthetic and/or biologic potential of the six and seven-membered cyclic oxime ethers, also called 1,2-oxazines and 1,2-oxazepines (*Figure 1.6*), remained poorly explored because of the absence of convenient methods for the synthesis of these scaffolds. This is actually quite understandable if one

considers the preconceived idea that saturated N-O heterocycles are more difficult to prepare and the knowledge on their physicochemical properties are limited.

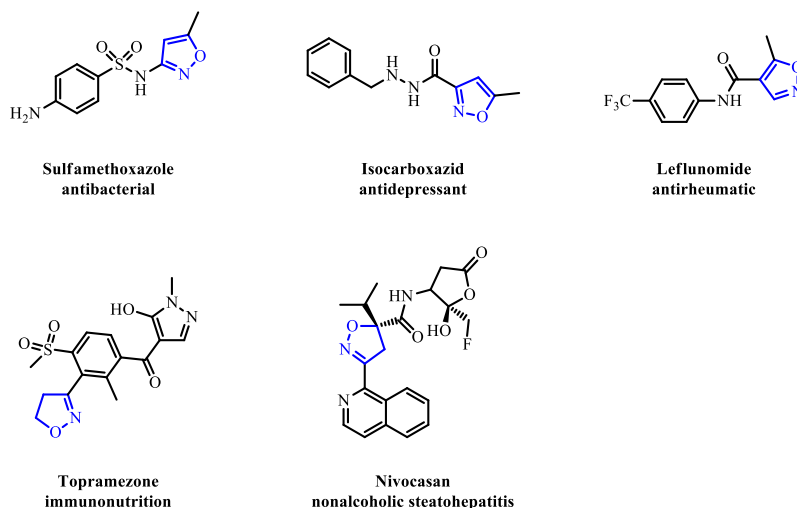
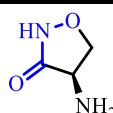
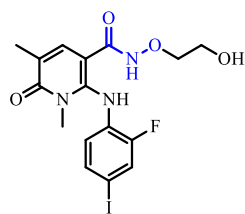


Figure 1.13. Examples of marketed drugs presenting isoxazole or isooxazoline moiety.

As oxime ethers, alkoxyamides are not sensitive to homolysis and were widely used in organic chemistry, especially with the famous Weinreb amide. However, alkoxyamides have recently raised a growing interest in medicinal chemistry, 9 drugs are currently marketed or under clinical trials, including two cyclic alkoxyamide (Table 1.2).

Table 1.2. Alkoxyamides drugs marketed or under clinical trials.

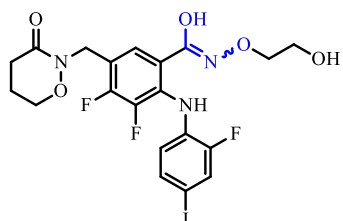
Alkoxyamide	Disease	State
 Cycloserine	infection	Marketed (2019-01-18)



breast cancer

Phase I

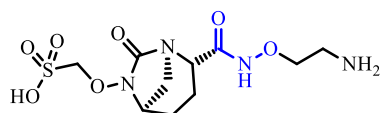
AZD-8330



neoplasms

Phase I

RO-4987655



infection

Phase I

Nacubactam

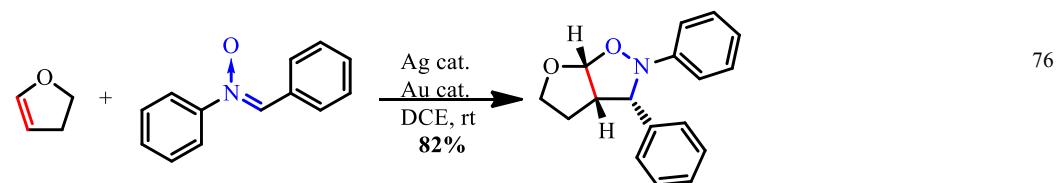
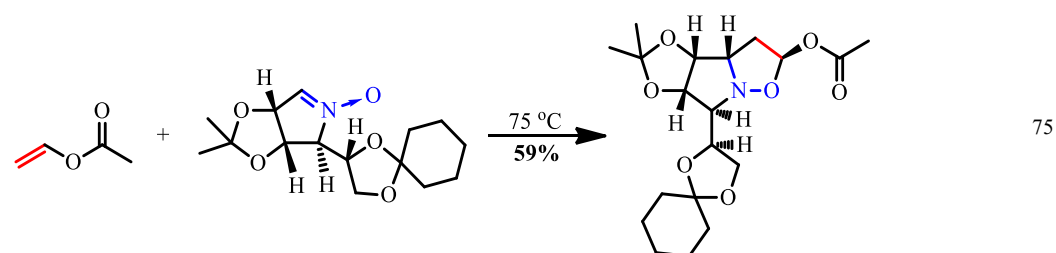
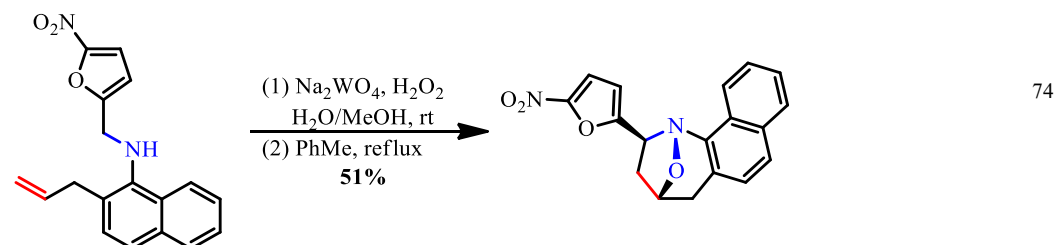
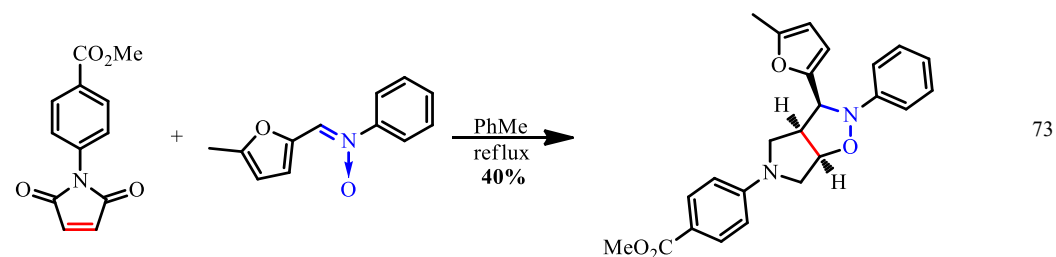
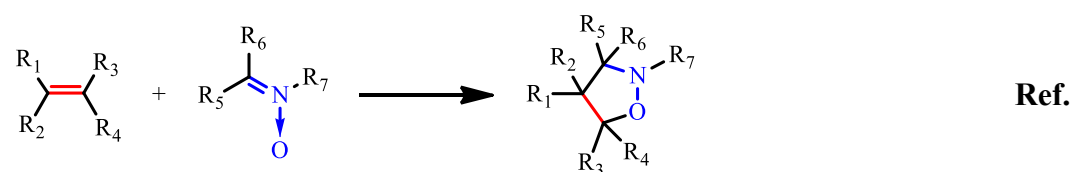
Based on the forementioned stability of oxime ethers and alkoxyamides, we proposed the 1,2,4-oxadiazine and 2,3-benzoxazepin-4-one scaffolds described in *Figure 1.11* should be stable in biological media and constitute promising building blocks for drug design.

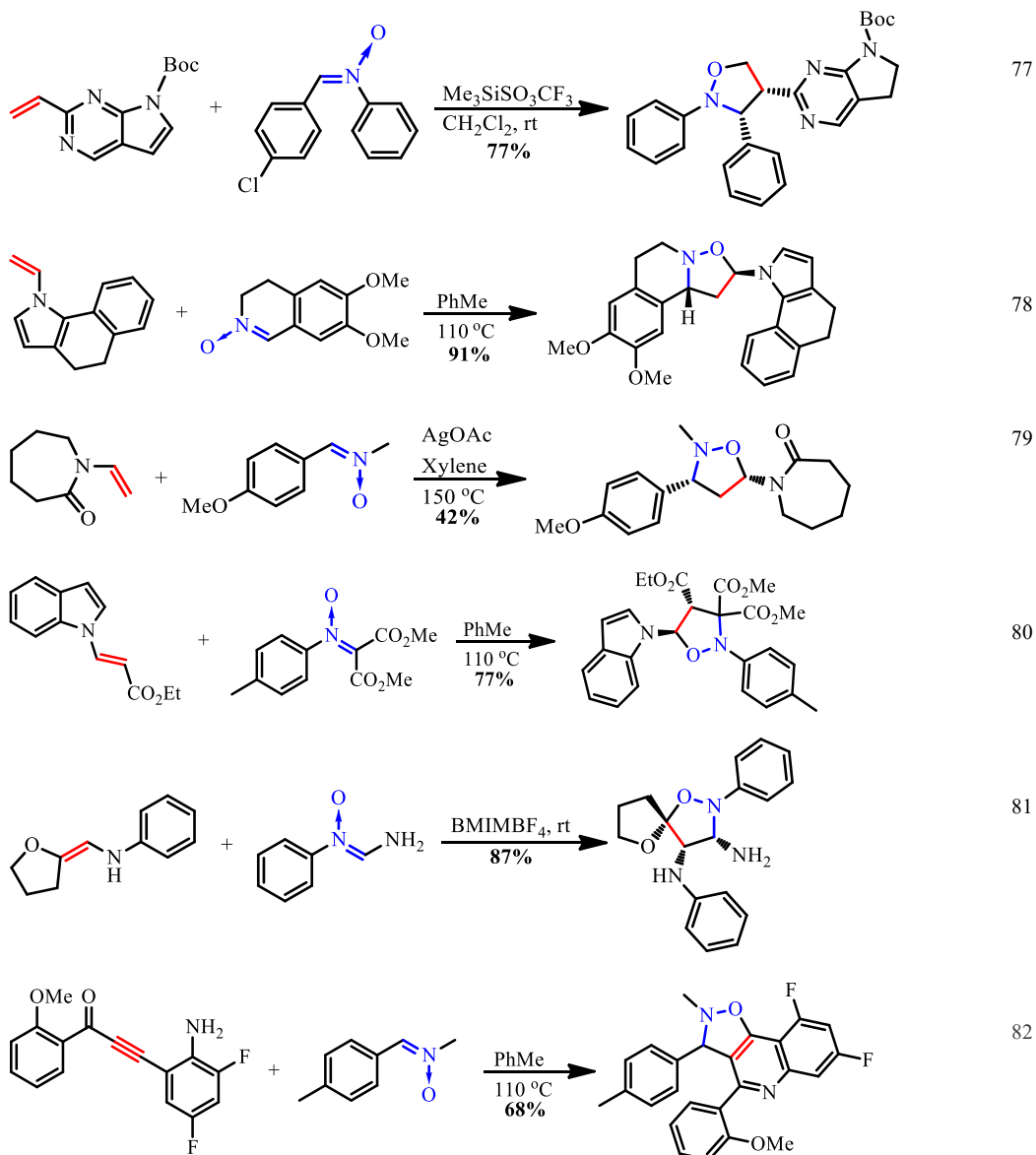
IE. Common synthetic strategies to N-O heterocycles

Despite the importance of N-O heterocycles, limited synthetic strategies were reported on these scaffolds, which could be mainly divided into two types: (1) cycloaddition, and (2) acylation. Here the general equations and presentative examples are listed.

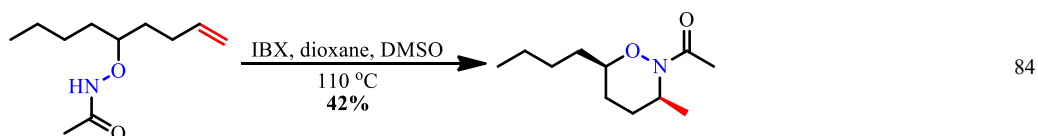
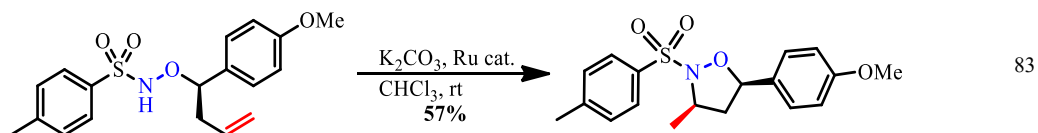
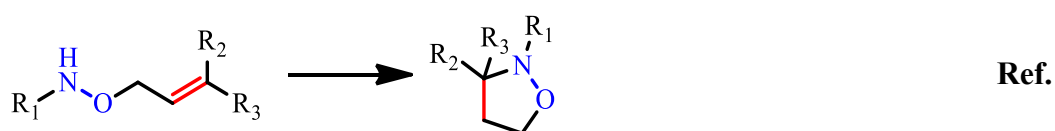
1. Cycloaddition:

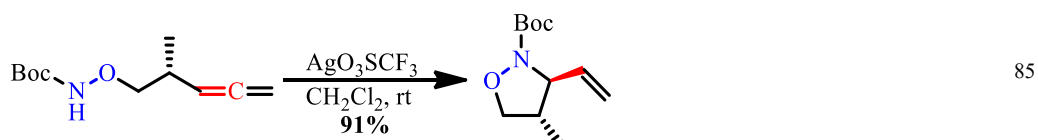
(1) with nitrones



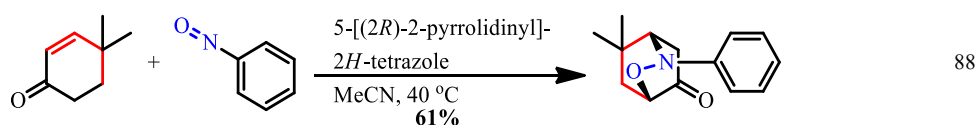
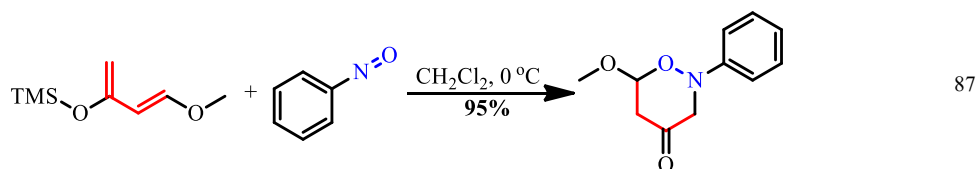
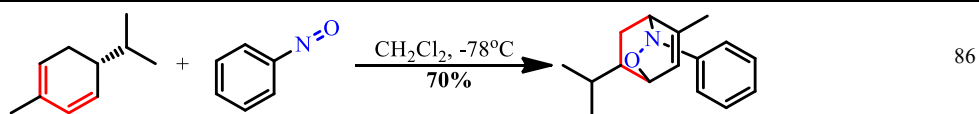
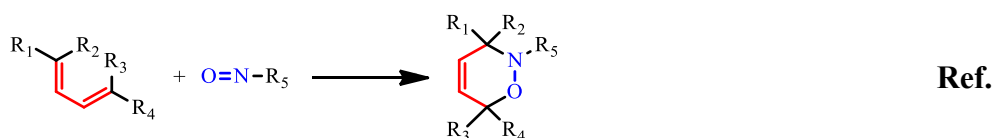


(2) with hydroxylamine analogs

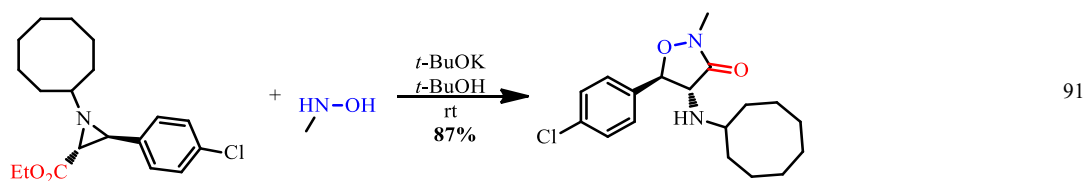
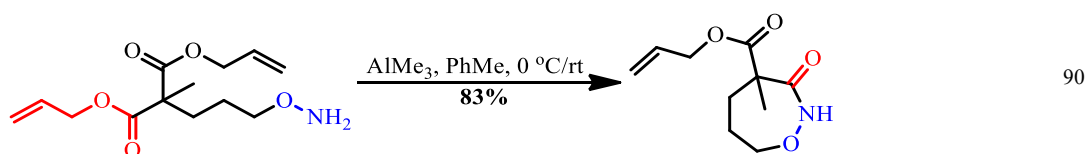
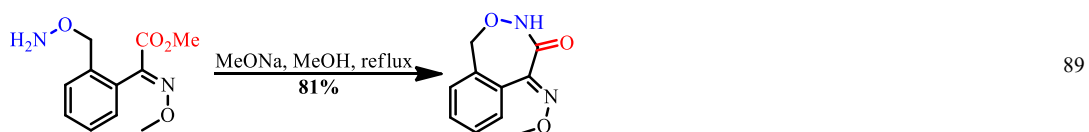
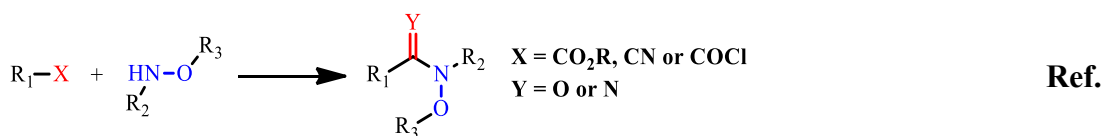


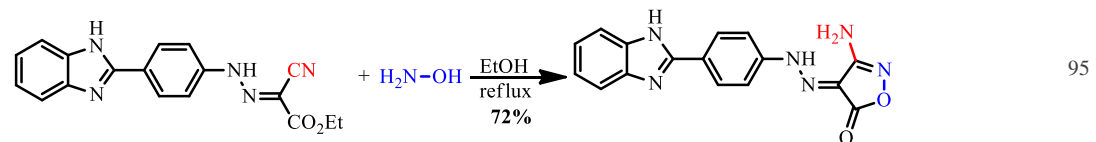
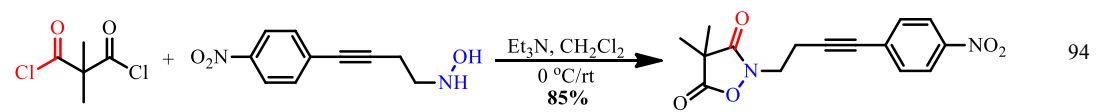
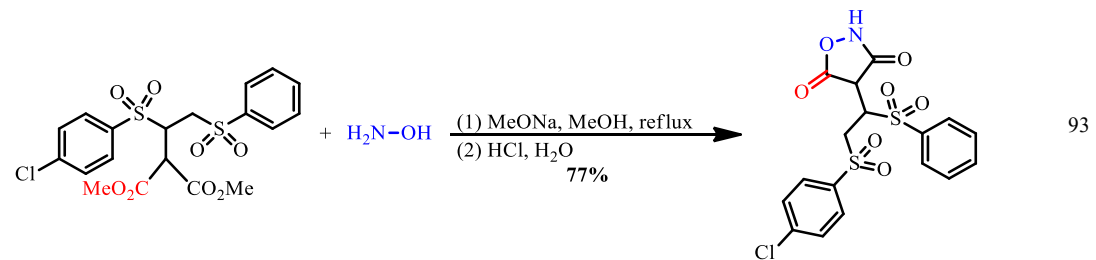
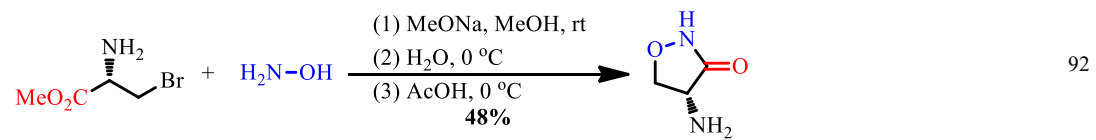


(3) with nitrosos



2. Acylation:





II. Synthetic strategies and applications

II. Synthetic strategies and applications

New drugs with better efficacy and low toxicity are continually required to combat the unmet medical needs across diverse therapeutic areas and pharmaceutical industries are facing immense pressure to supply these drugs to the market. For the delivery of new drugs, molecular complexity is becoming a crucial concept in drug discovery due to its close association with target selectivity and success in progressing into clinical development⁹⁶. One way to reach this complexity introduced in Chapter IC is to avoid aromatics, in favor of saturated carbon bonds (Fsp³) and chiral sp³ carbon atoms, a concept that Franck Lovering called “Escape from Flatland”. The rationale of this approach is that these non-planar molecules will be more natural product-like, and more amenable to explore additional areas of chemical space. Moreover, significant gains are expected in terms of ADME properties (solubility, biological selectivity, lipophilicity, etc).^{56, 97, 98}

Based on the “Escape from Flatland” theory, 1,2,4-oxadiazine **8** and 2,3-benzoxazepin-4-one **9** exhibiting an intracyclic N-O bond were designed to learn the geometries and physicochemical properties (pK_a and distribution coefficient (log D)) from their corresponding N-N heterocycles **2** and **7**, two biologically active compounds previously developed in our group (*Figure 1.11*)

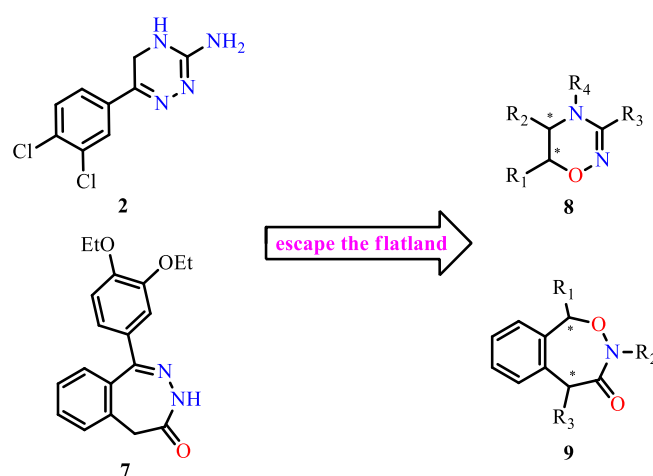
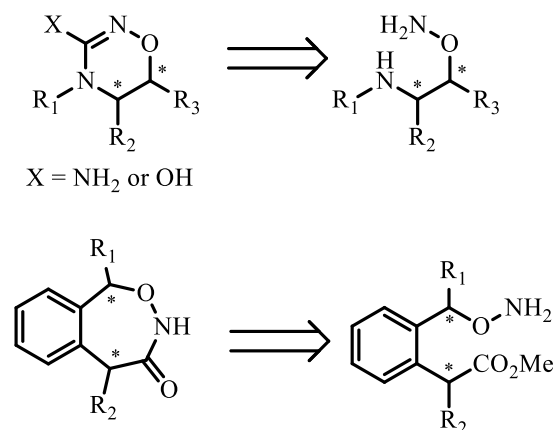


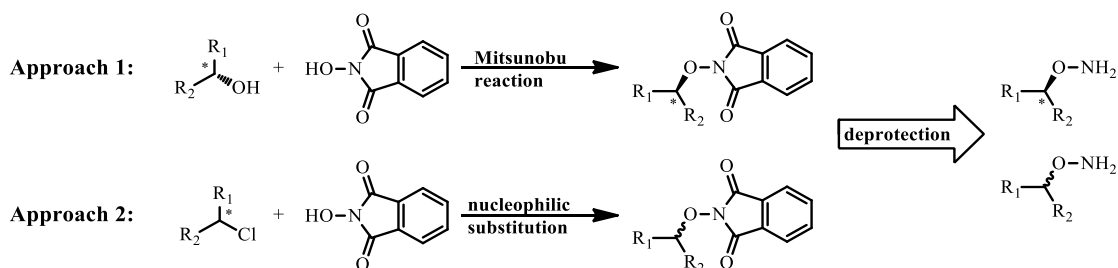
Figure 1.11. Developing N-O heterocycles from N-N heterocycles.

Although the cycloaddition reaction of nitron, nitroso or hydroxylamine analogs with olefins or alkynes shown in Chapter IE opened an efficient synthetic pathway to N-O heterocycles, these reactions cannot be applied to the synthesis of 1,2,4-oxadiazine and 2,3-benzoxazepin-4-one scaffolds due to the presence of the second nitrogen atom and the carbonyl group, respectively. “Acylation” of alkoxyamine seems to be a better approach for the following reasons: (1) alkoxyamines are more stable than nitroso or nitron, (2) the chirality of the carbon adjacent to the oxygen atom can be easily controlled when introduction the C-ON moiety by the classical Mitsunobu reaction of a secondary alcohol with *N*-hydroxyphthalimide (NHPI) (*Scheme 2.1*).



Scheme 2.1. Generate N-O heterocycles by “Acylation” of alkoxyamine.

In this project, the first choice we proposed to construct the C-ON bond is using Mitsunobu reaction of chiral alcohol with NHPI, as this approach generally inverted the chirality of alcohol (*Scheme 2.2*). However, the limitation of this approach is that the Mitsunobu reaction does not work with bulky alcohols in some cases. As a result, nucleophilic substitution of NHPI with alkyl halides is proposed as an alternative approach. Despite the chirality of the reaction center might be difficult to control (S_N1 vs S_N2 depending of the hydroxy substituents), the nucleophilic substitution is less vulnerable by the steric hinderance compared with the Mitsunobu reaction.



Scheme 2.2. Two approaches to construct C-ON bond.

Applying the synthetic method towards **8**, the structure of the natural product alchornedine, previously proposed based on the NMRs and mass spectra, will be verified by total synthesis (*Figure 2.1*).

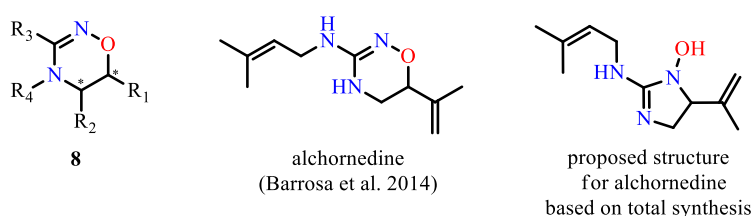
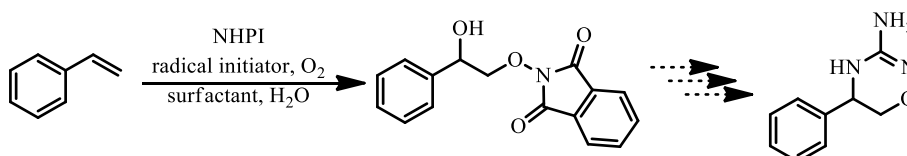


Figure 2.1. Published structure for alchornedine and our proposition.

As the environment impact of the chemical industry has become a major issue and around 80% of the chemical waste in a reaction originated from the usage of organic solvent. A radical reaction of styrenes and NHPI under oxygen in water will also be developed to construct the C-ON bond, which could be easily transformed into 1,2,4-oxadiazine scaffolds (*Scheme 2.3*).



Scheme 2.3. Construction the C-ON bond in water.

Exploring the synthetic method of 2,3-benzoxazepin-4-one scaffold **9** led to the discovery of a new precatalyst named post-oxidative-addition precatalyst (POxAP),

which will be applied in Fukuyama CCR to investigate the catalytic activity and compatibility with different functional groups (*Figure 2.2*).

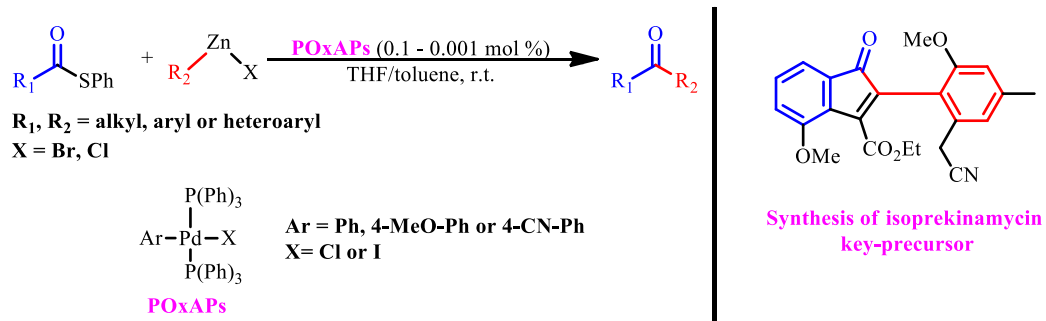


Figure 2.2. POxAP catalyzed Fukuyama cross-coupling reaction.

III. Synthesis of 3-amino-1,2,4-oxadiazines and their physicochemical properties

III. Synthesis of 3-amino-1,2,4-oxadiazines and their physicochemical properties

1,2,4-triazine nucleus is a prominent structural core system present in numerous pharmacologically active compounds. Till date, various 1,2,4-triazine analogs, possessing a wide range of potent pharmacological activities, have been reported.⁵⁹ Among them, four drugs are already marketed, including one 3-amino-1,2,4-triazine Lamotrigine (Figure 3.1).

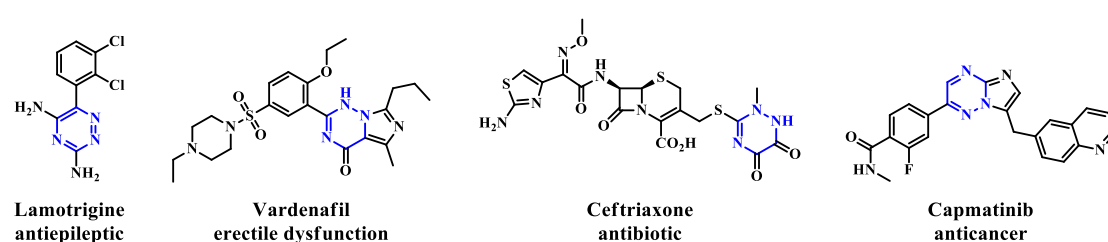


Figure 3.1. Marketed drugs presenting 1,2,4-triazine nucleus.

In our recent study, a NPFFRs antagonist **2** was obtained when we reduced one of the C=N double bond of 3-amino-1,2,4-triazine **1**. The biological evaluations showed that **2** exhibits two-digit nanomolar affinity for both NPFFRs leading to a significant reduction of the long lasting fentanyl-induced hyperalgesia in rodents.⁶⁵ These results prompt us to further increase the complexity of **2** by transposing one of the two adjacent nitrogen atoms by an oxygen atom, leading to a non-planar N-O heterocycle 3-amino-1,2,4-oxadiazine **10a**, as an unsaturated bioisostere of **1** and **2** (Figure 3.2).

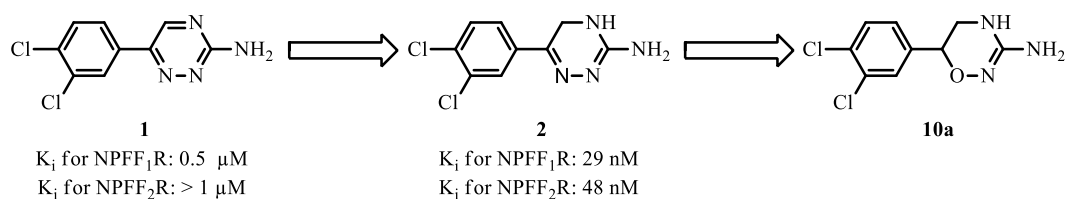
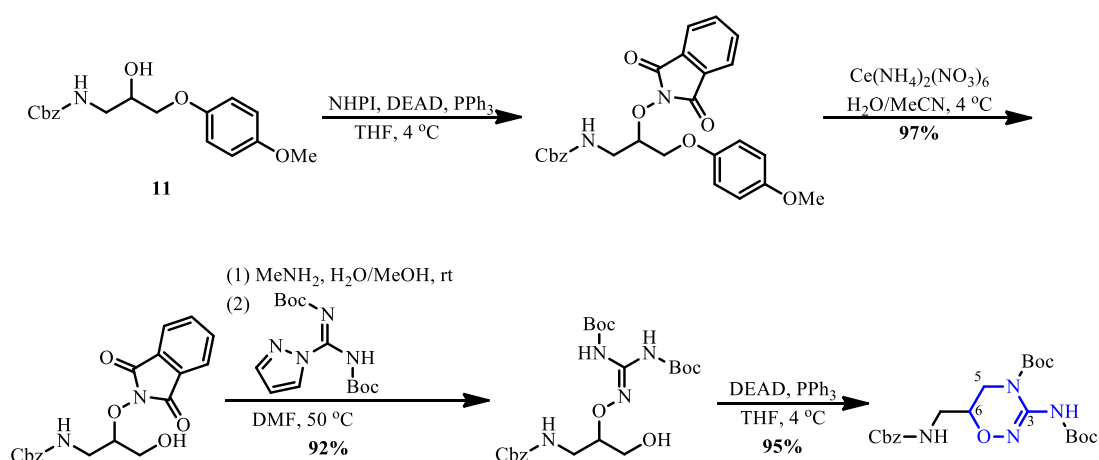


Figure 3.2. Development of 3-amino-1,2,4-oxadiazine **10a**.

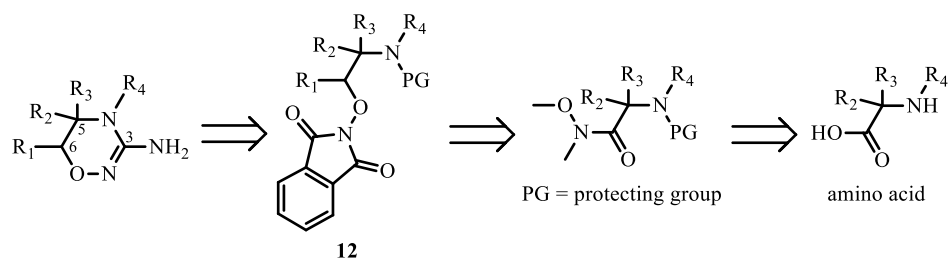
To synthesize **10a**, 3-amino-1,2,4-oxadiazine scaffold was searched as substructure in SciFinder and only one patent was founded,⁹⁹ which used **11** as a precursor (*Scheme 3.1*). The N-O bond was introduced into **11** by a Mitsunobu reaction with NHPI. Then, *para*-methoxyphenyl (PMP) ether was cleaved by ceric ammonium nitrate, followed by the deprotection of alkoxyamine with methylamine. The Boc-protected alkoxyguanidine moiety was formed using *N,N'*-bis-Boc-1-guanylpiprazole. Finally, the 3-amino-1,2,4-oxadiazine scaffold was cyclized after an intra-molecular Mitsunobu reaction.



Scheme 3.1. The exclusive reported method to synthesize 3-amino-1,2,4-oxadiazine scaffold.

Although the patented synthetic pathway in *Scheme 3.1* provided a possibility to synthesize the achiral 3-amino-1,2,4-oxadiazine **10a**, the method is not adapted to introduce stereogenic centers at positions 5 and 6, which would constitute an interesting perspective in terms of molecular complexity.

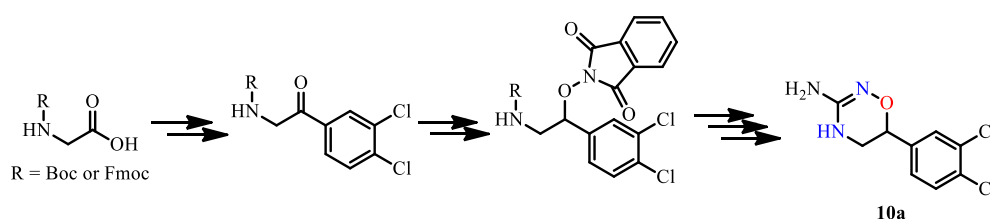
Herein, an approach is proposed, starting from amino acid (*Scheme 3.2*). The key intermediate **12** could be synthesized through the preparation of Weinreb amide, (stereo-selective) reduction and Mitsunobu reaction. After deprotection and cyclized with bromocyanide, 1,2,4-oxadiazine scaffold with one or two chiral centers at position 5 or 6 will be obtained. Compared with the approach in *Scheme 3.1*, *N*-protected amino acids are readily available and most of them already bear a chiral center at the α position.



Scheme 3.2. Proposed synthetic approach of 3-amino-1,2,4-oxadiazine from amino acid.

III.A. Synthesis of 6-(3,4-dichlorophenyl)-5,6-dihydro-4H-1,2,4-oxadiazin-3-amine 10a

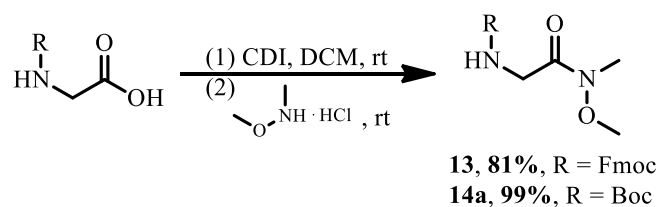
To verify the feasibility of the synthetic approach of 3-amino-1,2,4-oxadiazine scaffold proposed in *Scheme 3.2*, cpd **10a** was synthesized from *N*-Boc or *N*-Fmoc glycine (*Scheme 3.3*). The advantage of *N*-Fmoc glycine is that the deprotection of Fmoc and phthalimide could be realized in one pot.¹⁰⁰⁻¹⁰² While for *N*-Boc glycine, both deprotections will have to be done in a sequential manner. However, Boc group can be easily removed under acidic condition without requiring any purification step.^{103, 104}



Scheme 3.3. Synthesis of 10a from N-Boc or N-Fmoc glycine.

III.A1. Synthesis of Weinreb amide from *N*-Boc or *N*-Fmoc glycine

N-Boc or *N*-Fmoc glycines was used to synthesize the corresponding Weinreb amides as precursors of ketones (*Scheme 3.4*).



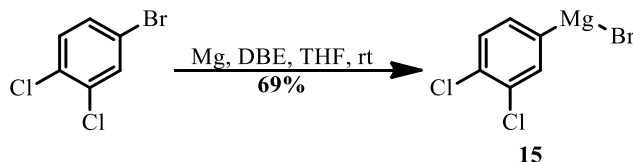
Scheme 3.4. Synthesis of Weinreb amides 13 and 14a.

Although 1-ethyl-3-(3-dimethylaminopropyl)carbodiimide (EDCI) and 1-hydroxy-benzotriazole (HOBt) are two most commonly used coupling reagents for

the synthesis of Weinreb amide from carboxylic acid, here 1,1'-carbonyldiimidazole (CDI) was used.¹⁰⁵⁻¹⁰⁸ Acylimidazoles of corresponding *N*-Boc or *N*-Fmoc glycine formed as the intermediates by the addition of CDI. The advantage of this method is that the work up is much easier, as resulting side product imidazole can be easily removed by liquid-liquid extraction. Weinreb amide **13** and **14a** were obtained in 81% (Fmoc) and 99% (Boc) yields, respectively.

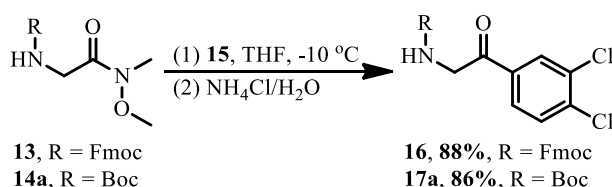
III A2. Synthesis of ketone from Weinreb amide

Grignard reagent **15** was prepared from 1-bromo-3,4-dichlorobenzene (*Scheme 3.5*). A catalytical amount of dibromoethane (DBE) was added to remove the oxidized magnesium at the surface of the metal (giving MgBr₂ and ethylene gas), leading to the formation of Grignard reagent **17** in 69% yield (determined by titration with a solution of menthol and 1,10-phenanthroline in THF).¹⁰⁹



Scheme 3.5. Synthesis of Grignard reagent 15.

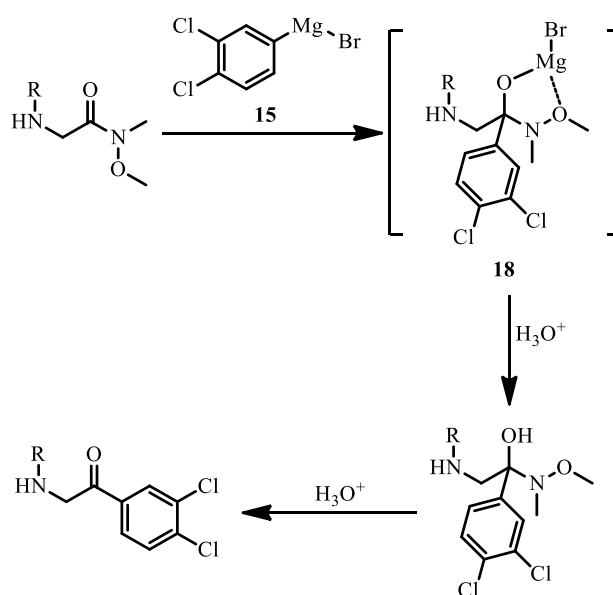
The reaction of Weinreb amides **13** or **14a** with excess amount of Grignard reagent **15** gave ketones **16** and **17a** in 88% (Fmoc) and 86% (Boc) yields, respectively (*Scheme 3.6*).



Scheme 3.6. Synthesis of ketones 16 and 17a.

The successful acylation by excess Grignard reagent **15** is due to the putative and

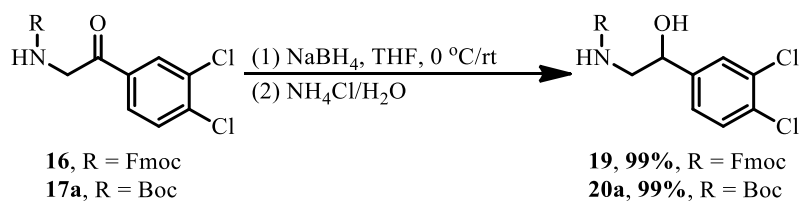
stable tetrahedral intermediate **18** formed upon addition of the first equivalent of **17** (*Scheme 3.8*). This stability precludes the collapse of **18** to a ketone under the reaction conditions and thus prevents any additional reaction of **15** on the resulting ketone to form a tertiary alcohol. The aqueous workup not only facilitates the collapse of tetrahedral intermediate **18** to furnish the respective ketone, but also ensures simultaneous quenching of **15** in excess, thereby explaining why no over-addition product was formed despite the use of excess Grignard reagent.¹¹⁰⁻¹¹³



Scheme 3.7. Mechanism of the reaction between Weinreb amide and Grignard reagent.

IIIA3. Reduction of ketone into alcohol

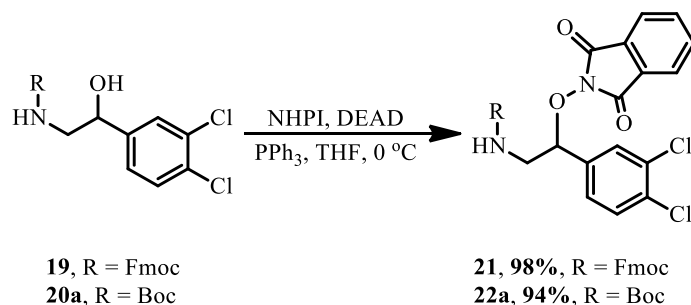
In consideration of the difficulty to identify enantiomers and current primary objective was to verify the feasibility of the synthetic approach of **10a** proposed in *Scheme 3.3*, the chiral reduction for ketone **16** or **17a** was not taken into account here. Instead, the two ketones were directly reduced by NaBH₄, giving alcohol **19** and **20a** in quantitative yields (*Scheme 3.8*).



Scheme 3.8. Reduction of ketone 18 and 19a.

IIIA4. Introduction of N-O moiety by Mitsunobu reaction

One of the key steps to synthesize 1,2,4-oxadiazine was the building of the C-ON bond. Mitsunobu reaction between alcohol and NHPI seemed to be an ideal method using mild reaction conditions. More importantly, the reaction is supposed to be stereospecific, which will be favorable in controlling the stereogenic centers when a chiral alcohol will be used.¹¹⁴⁻¹¹⁸ The Mitsunobu reaction of **19** or **20a** with NHPI was easily managed, producing the key intermediate **21** and **22a** in 98% (Fmoc) and 94% (Boc) yields, respectively (*Scheme 3.9*).

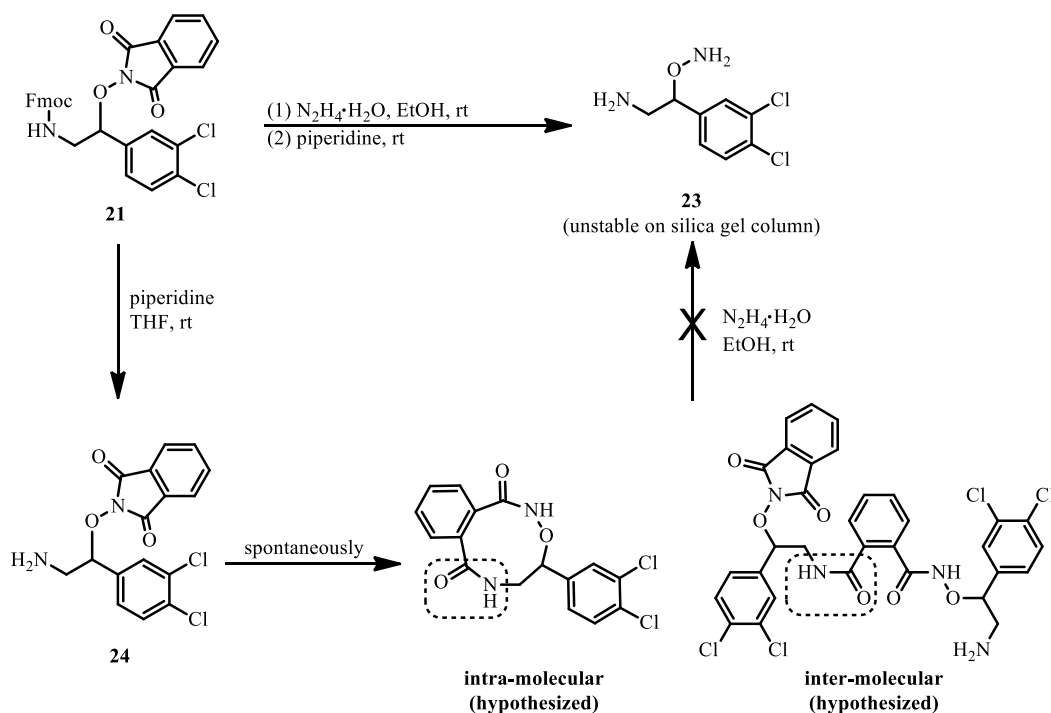


Scheme 3.9. Mitsunobu reaction with alcohols 19 and 20a.

IIIA5. Deprotection of the key intermediates 21 and 22a

Hydrazine hydrate, followed by piperidine was used to deprotect the phthalimide and Fmoc moieties of **21** in a one-pot reaction (*Scheme 3.10*). Although HPLC analysis of the crude reaction shown a high conversion, **23** could not be isolated due to its instability during purification steps whether in normal phase or in reverse phase chromatography.

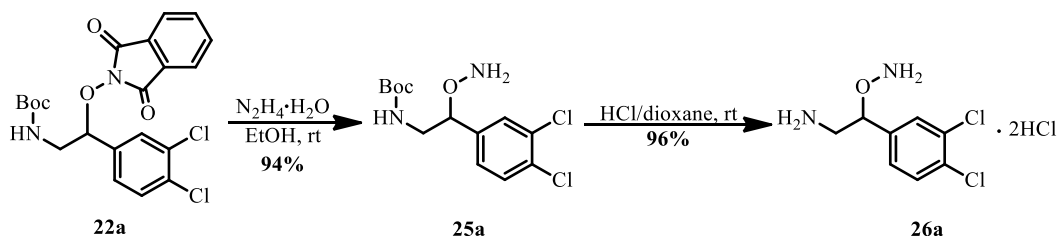
As 2,3-dihydrophthalazine-1,4-dione, formed from the deprotection of phthalimide with hydrazine, could be easily removed by precipitation from EtOH, we tried to prepare **24** by using piperidine, before deprotecting the phthalimide moiety with hydrazine hydrate and removing 2,3-dihydrophthalazine-1,4-dione by precipitation in EtOH (*Scheme 3.10*). This process would avoid any final purification of **23** on silica gel. However, based on the characteristic UV absorption of phthalimide moiety at 220 nm, traces of **24** were detected by HPLC. This is likely due to the nucleophilic amine of **24** which can intra- or inter-molecularly attack the carbonyl of the phthalimide moiety, leading to the formation of stable amides (*Scheme 3.10*).



Scheme 3.10. Deprotection of Fmoc and phthalimide moiety.

In consideration of the instability of **23** on silica gel and spontaneous nucleophilic reaction between amine and phthalimide in **24**, Boc protected **22a** seemed to be a more suitable precursor for the preparation of the deprotected amino alkoxyamine **26a**. The phthalimide moiety in **22a** was first deprotected by hydrazine hydrate and the resulting **25a** was obtained in 94% yield. Then, Boc was removed by HCl in dioxane

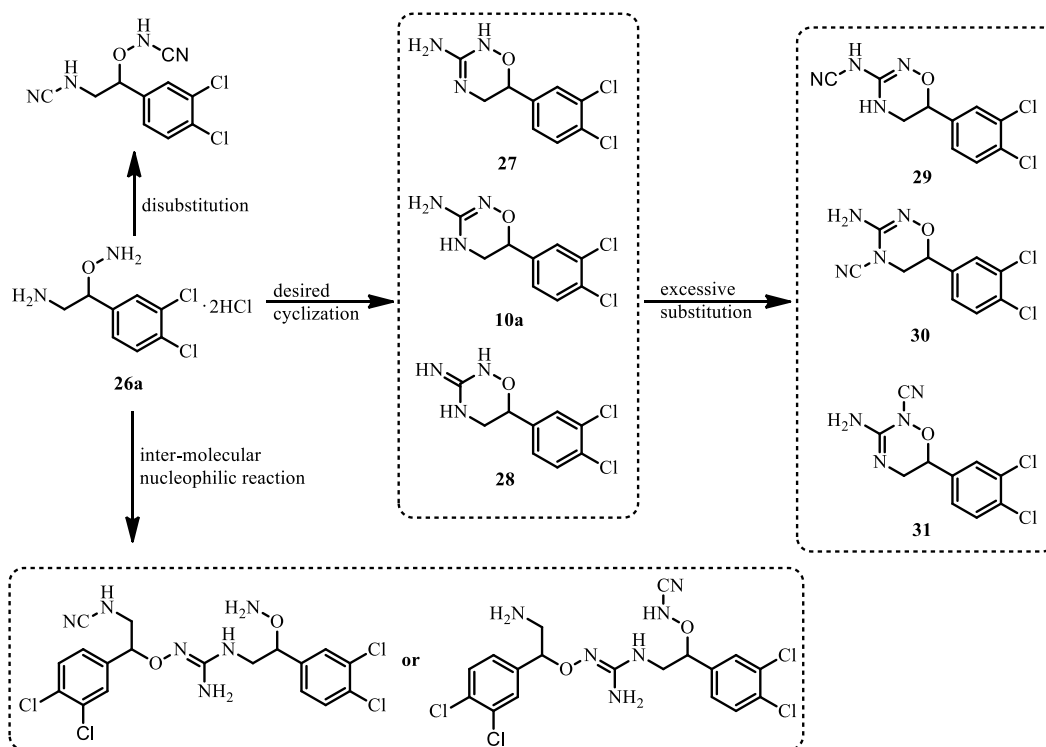
without additional purification, affording hygroscopic hydrochloride **26a** in 96% yield (Scheme 3.11).



Scheme 3.11. Deprotection of phthalimide moiety and Boc.

III A6. Cyclization of amino alkoxyamine **26a**

Amino alkoxyamine **26a** was cyclized using BrCN. The reaction was run under diluted concentration (0.04 M of **26a** in MeCN) at 0 °C to avoid: (1) disubstitution of CN group on **26a**, (2) inter-molecular nucleophilic reaction of amino group and (3) excessive substitution of CN group on **10a** (Scheme 3.12).



Scheme 3.12. Desired and possible side reactions during cyclization of **26a**.

Two products were isolated from the cyclization reaction of **26a** with BrCN. Several possible structures were proposed based on ^1H and ^{13}C NMRs in $\text{DMSO-}d^6$ (Figure 3.3 and 3.4). The chemical shifts and integrations in ^1H NMR spectra shown that both compounds had an AB spin system for $-\text{CH}_2\text{-N}$ moiety in a cyclized structure, excluding the products of disubstitution and inter-molecular reaction shown in Scheme 3.12. The main difference of the two ^1H NMR spectra was that one compound contained a $-\text{NH}-$ peak at 6.17 ppm and a $-\text{NH}_2$ peak at 4.47 ppm, suggesting that the structure of this compound was **10a**, since **28** should show three $-\text{NH}$ peaks, while **27** should show a $-\text{NH-O}-$ peak at a lower field due to its acidity. ^{13}C NMR spectrum was also in agreement with **10a**.

The second isolated product shown only one active proton peak, $-\text{NH}_2$ at 5.79 ppm, suggesting the formation of excessive substitution products **30** or **31** (**29** should show two $-\text{NH}$ peaks). ^{13}C NMR spectrum confirmed this hypothesis with an obvious $-\text{CN}$ peak at 110.14 ppm.

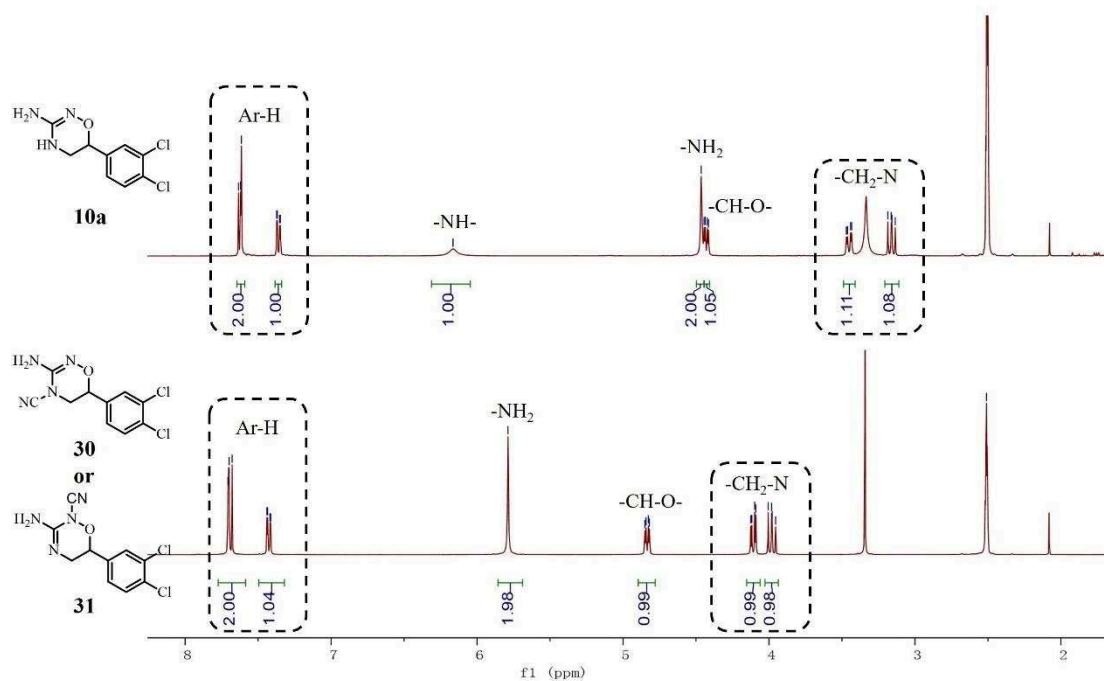


Figure 3.3. ^1H NMR ($\text{DMSO-}d^6$) and proposed structures of the two products isolated from cyclization reaction of alkoxyamine **26a**.

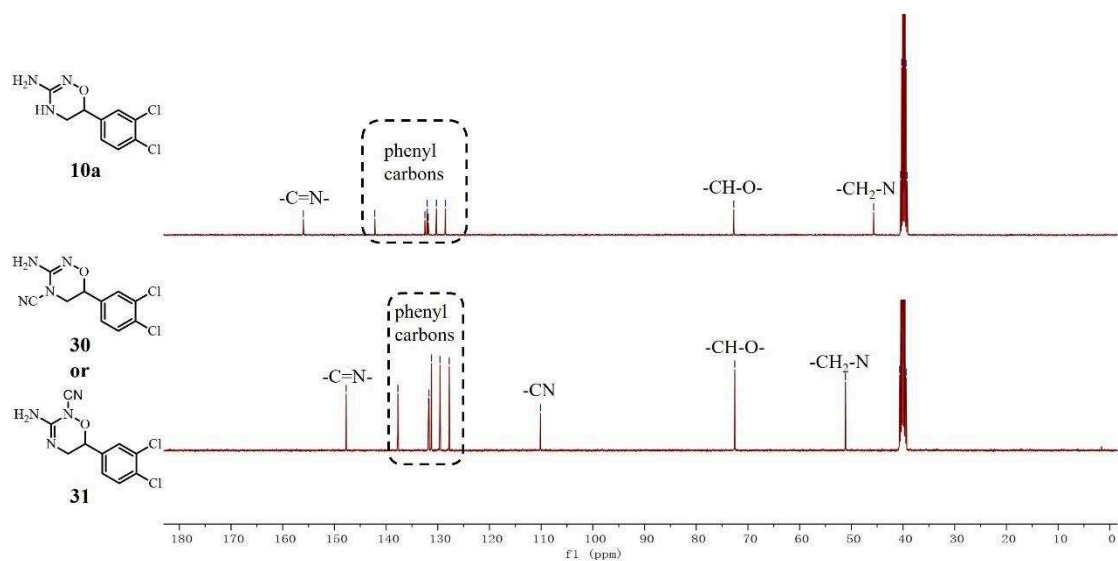


Figure 3.4. ^{13}C NMR (DMSO- d_6) and proposed structures of the two products isolated from cyclization reaction of alkoxyamine **26a**.

To clearly associate NMR spectra to **30** or **31**, a 2D HMBC NMR experiment was performed (Figure 3.5). Obvious correlation was observed between protons in $-\text{CH}_2-\text{N}$ moiety (3.98 and 4.11 ppm) and the carbon in $-\text{CN}$ group (110.14 ppm), indicating the structure of the side product was **30** as this kind of correlation would not be observed in **31**.

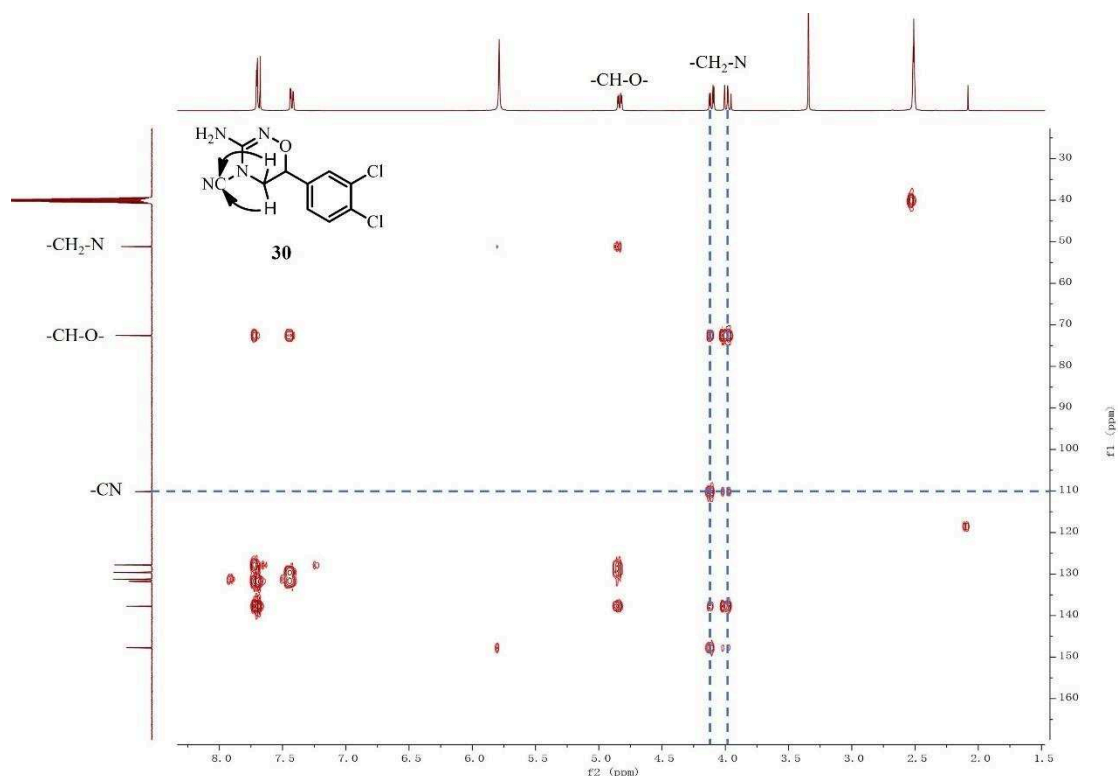
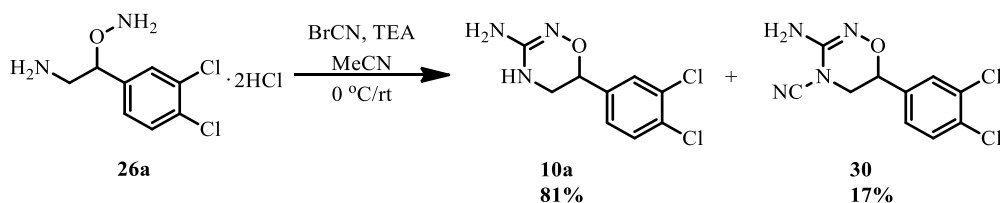


Figure 3.5. HMBC (DMSO-d_6) of **30**.

In summary, **26a** could be cyclized in MeCN using BrCN at 0 °C, affording **10a** and **30** in 81% and 17% yields, respectively (Scheme 3.13). The appearance of **30** also indicated that the secondary nitrogen atom (-HN-CH₂-) of **10a** was more nucleophilic than the primary and tertiary ones (-NH₂ and >C=N-O-) towards BrCN.



Scheme 3.13. Cyclization of amino alkoxyamine **26a**.

To further confirm the correctness of the synthesis and geometry of **10a**, it was recrystallized by slow evaporation from MeCN solution. Single-crystal X-ray diffraction analysis shown that the crystal structure of **10a** belongs to 3-amino-1,2,4-oxadiazine (Figure 3.6). The C=N double bond located between N2

and C3, rather than C3 and N4. This is comprehensible since the p - π conjugative effect between oxygen atom and C=N double bond in **10a** is more stable than the σ - π hyperconjugative effect between C-H bond on C5 and C=N double bond in **27**. Due to the bivalent character of the oxygen atom, the 1,2,4-oxadiazine scaffold shown a non-planar geometry in which C6 is located far out of the plane constituted by N=C-NH moiety. Moreover, the N-O bond and NH-CH₂ bond is unparallel due to the different bond angles between N-O-C and N-C-C. It also could be observed that the oxadiazine ring is approximately vertical to the phenyl ring since this orthogonal conformation decreased the steric hinderance. The details of the crystallographic data and structure refinement parameters were summarized in Appendix I.

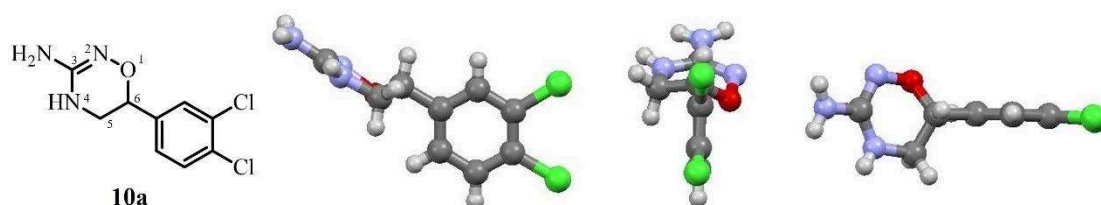


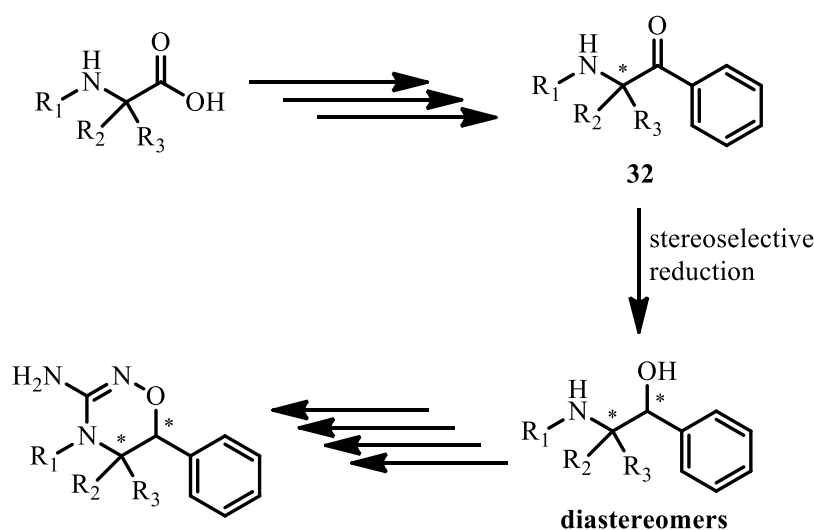
Figure 3.6. X-ray crystallography of 10a displayed with front view, right view and top view.

In conclusion, **10a** was synthesized from *N*-Boc glycine in 7 steps in 58% overall yield. The structures of the products were identified by NMR spectra and the geometry of **10a** was confirmed by X-ray crystallography. The unsaturation of the 1,2,4-oxadiazine ring and the bivalent character of oxygen atom result in a non-planar geometry of **10a**.

IIIB. Synthesis of (1*R*,8*aS*)-1-phenyl-6,7,8,8*a*-tetrahydro-1*H*-pyrrolo

[1,2-*d*][1,2,4]oxadiazin-4-amine 10b

Now that the method to synthesize racemic 3-amino-1,2,4-oxadiazine scaffold from *N*-Boc glycine has been established (Section IIIA), we focused our interest on producing chiral 3-amino-1,2,4-oxadiazine scaffolds. L-proline was selected as starting material for the synthesis of chiral 3-amino-1,2,4-oxadiazine scaffolds exhibiting two stereogenic centers. Compared with glycine, L-proline already bears a stereogenic center at the α position of carboxyl group. After reduction of the targeted ketone **32**, up to two diastereomers would be obtained (Scheme 3.14). It will facilitate isolation and characterization of the stereoisomers, since diastereomers have different chromatographic and NMR properties under commonly used achiral silica gel and deuterated solvent.¹¹⁹⁻¹²¹

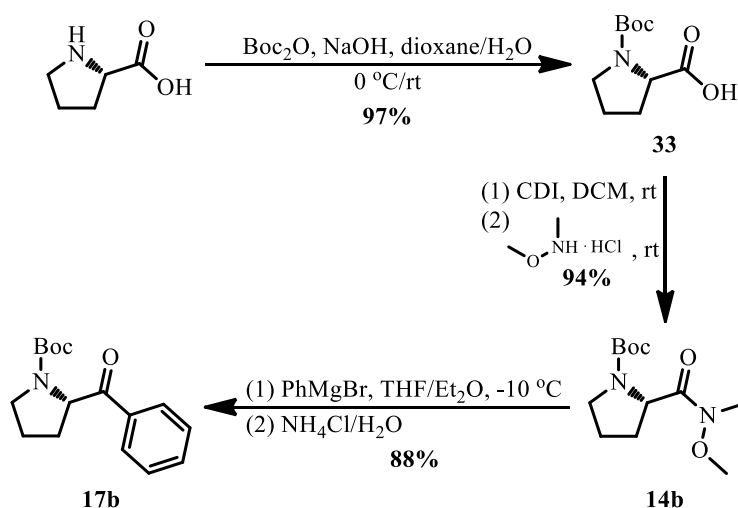


Scheme 3.14. Synthesis of chiral 3-amino-1,2,4-oxadiazine scaffold.

IIIB1. Synthesis of ketone 17b from L-proline

Ketone **17b** was synthesized from L-proline by similar methods described in Section IIIA (Scheme 3.15). First, the amino group in L-proline was protected by Boc_2O under basic condition in dioxane/ H_2O ,¹²² affording *N*-Boc L-proline **33** in 97%

yield. After activation by CDI and substitution with *N,O*-dimethylhydroxylamine,¹²³ **33** was transformed into Weinreb amide **14b** in 94% yield. The addition-elimination reaction between Weinreb amide **14b** and phenyl magnesium bromide furnished ketone **17b** in 88% yield.¹²⁴



Scheme 3.15. Synthesis of ketone **17b** from *L*-proline.

IIIB2. Stereoselective reduction of ketone **17b**

A non-stereoselective reduction of ketone **17b** would lead to a mixture 1:1 of two diastereoisomers. However, our goal was to find stereoselective conditions allowing to favor one diastereoisomer over the other. Several conditions were then tried to reduce ketone **17b** (Table 3.1) and the structures of some complex reductants were presented in Figure 3.7. The two reduced diastereomeric alcohols could be distinguished by comparing their ¹H NMR spectra with the ones reported in literature, and obtained with a different strategy.¹²⁵

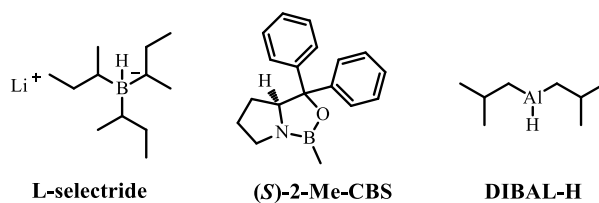
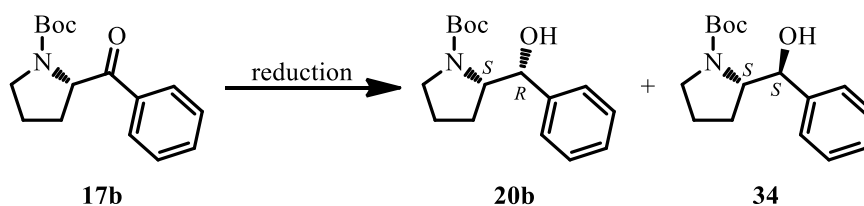


Figure 3.7. Structures of several complex reductants.

Chiral reductant L-selectride led to a poor enantioselective reduction, producing **20b** (*S/R*) and **34** (*S/S*) in 57% and 43% yields, respectively, while almost no reaction happened with (*S*)-3,3-diphenyl-1-methylpyrrolidino[1,2-*c*]-1,3,2-oxazaborole ((*S*)-2-Me-CBS). Surprisingly, reduction of **17b** by NaBH₄ appeared more enantioselective with the formation of both diastereomers **20b** (*S/R*) and **34** (*S/S*) in 24% and 72% yields, respectively. The weaker reductant NaBH₃(CN) failed to reduce ketone **17b**. Aluminum-type reductants were tested, and while LiAlH₄ appeared poorly enantioselective, producing **20b** and **34** in 45% and 55% yields, respectively, the bulky reductant diisobutyl aluminium hydride (DIBAL-H) enantioselectively reduced ketone **17b** into the diastereoisomer **20b** in quantitative yield and **34** was not detected.

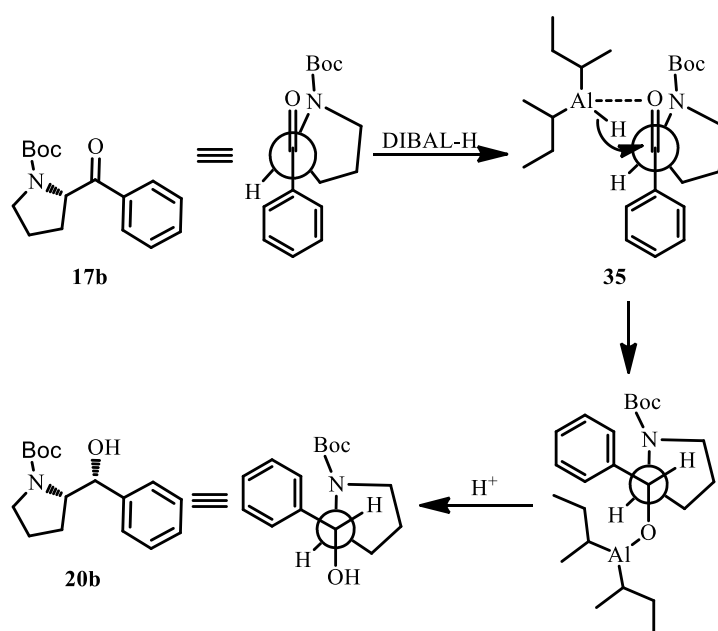
Table 3.1. Reduction of ketone **17b**.



Entry	Conditions	20b (<i>S/R</i>) (%)	34 (<i>S/S</i>) (%)
1	L-selectride, THF, 0 °C	57	43
2	(<i>S</i>)-2-Me-CBS, BH ₃ , THF, 0 °C /rt	trace	0
3	NaBH ₄ , MeOH, -20 °C	24	72
4	NaBH ₃ (CN), THF, rt	0	0
5	LiAlH ₄ , THF, rt	45	55
6	DIBAL-H, THF, 0 °C	100	0

The Newman projection formula of **17b** explains the selectivity of DIBAL-H reduction originated from two effects in intermediate **35** (Scheme 3.16): (1) the complexation between aluminum atom of DIBAL-H and the oxygen atom of ketone **17b**, (2) the steric hinderance between isobutyls of DIBAL-H and Boc of **17b**. These

two effects orientated the attack of DIBAL-H on ketone **17b**, favoring the formation of intermediate **35** and producing alcohol **20b** after hydrolysis under acidic condition. The two effects also explained why other reductants in *Table 3.1* were less selective: (1) attenuation of the complexation between the boron atom of borane-type reductants and the oxygen atom of ketone **17b** (2) disappearance of the steric hinderance between LiAlH_4 and **17b**. At this stage, we did not find conditions to stereoselectively reduce ketone **17b** into the diastereoisomer **34**.

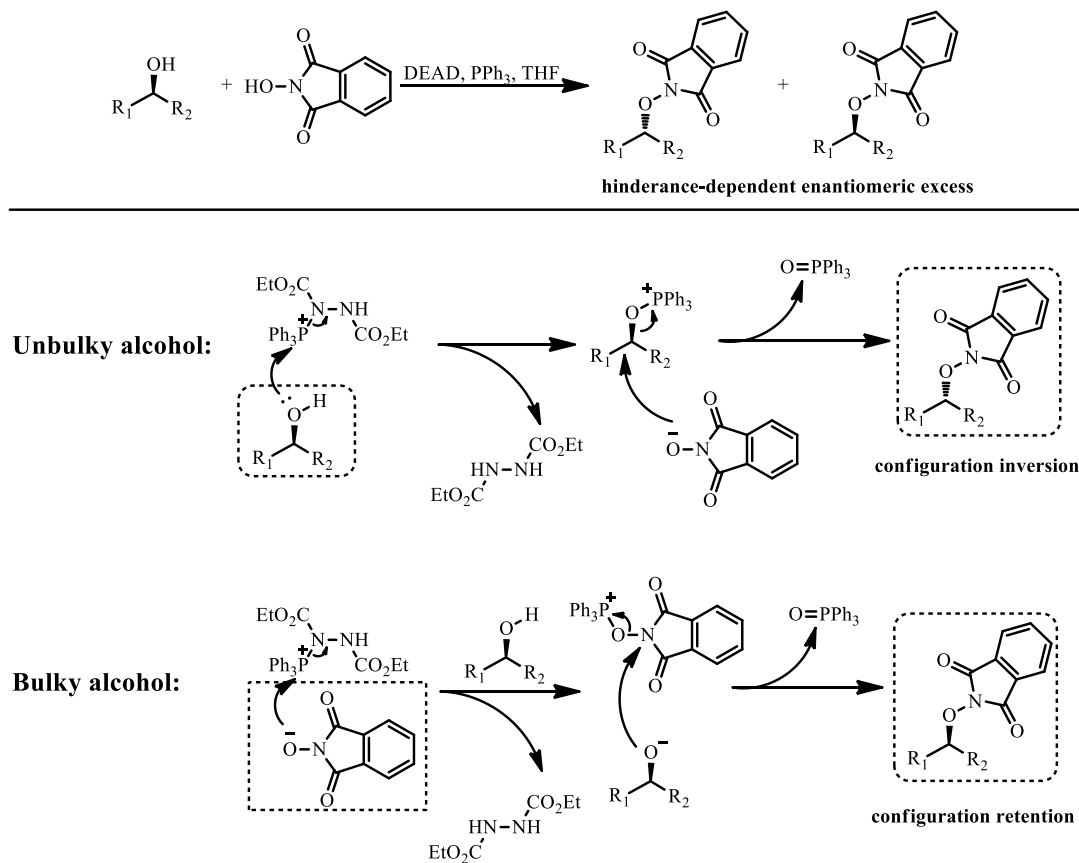


Scheme 3.16. Mechanism of selective reduction of ketone 17b by DIBAL-H.

III B3. Introduction of N-O moiety by Mitsunobu reaction

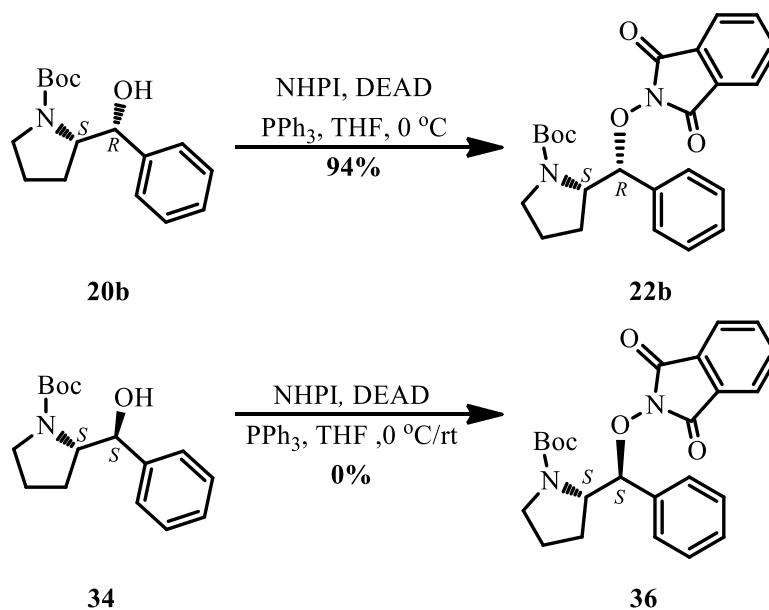
Starting with **20b** (*S/R*), Mitsunobu reaction with NHPI led to **22b** in 94% yield. Due to the inversion of configuration related to Mitsunobu mechanism, **22b** was expected to show a *S/S* configuration. However, when we performed X-ray crystallography of the final oxadiazine resulting from **22b**, we were surprised to observe that the Mitsunobu reaction did not led to an inversion of configuration, but to a retention (See *Figure 3.9*). It is not a frequent case, but this kind of retention of configuration has already been reported when the Mitsunobu reaction is performed on

sterically hindered substrate.¹²⁶ Using alcohol and NHPI as substrates, *Scheme 3.17* shown two commonly accepted mechanisms of Mitsunobu reaction with configuration inversion or retention.



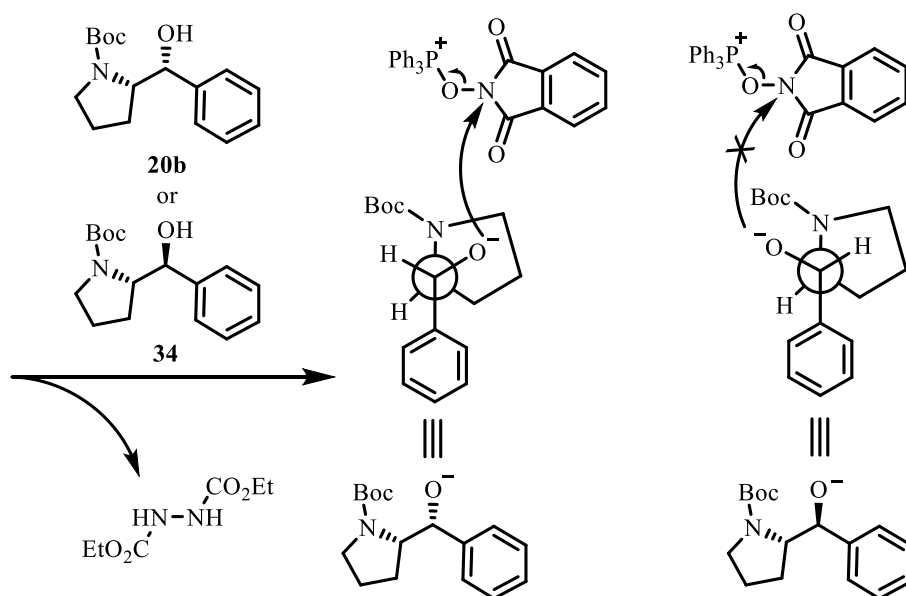
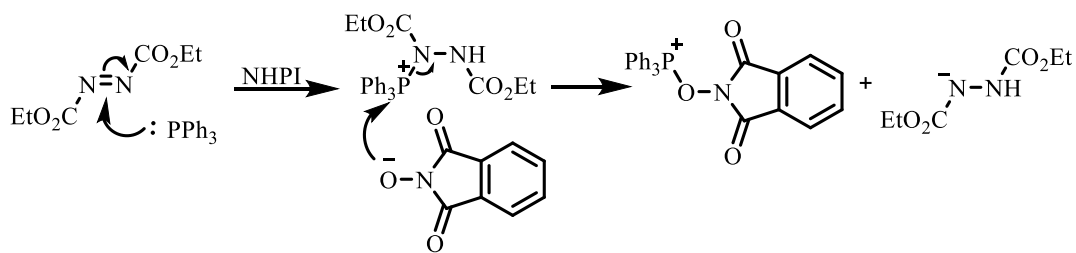
Scheme 3.17. Mechanism of Mitsunobu reaction with configuration inversion or retention.

We were also surprised to observe that the same condition of Mitsunobu reaction failed to transform diastereoisomer **34** into **36** and the starting material was recovered quantitatively (*Scheme 3.18*).



Scheme 3.18. Configuration retained Mitsunobu reaction between 20b or 34 and NHPI.

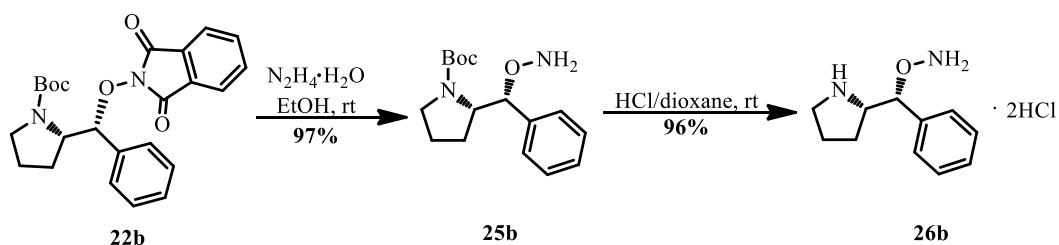
The difference reactivity of diastereomers **20b** (*S/R*) and **34** (*S/S*) in Mitsunobu reaction might originate from the hinderance between Boc and PPh_3^+ moiety, which interfere attack of alcohol (*Scheme 3.19*). To surmount this hinderance, the Mitsunobu reaction between **34** and NHPI was tried at rt. Disappointedly, raising the reaction temperature resulted into a complex reaction mixture and no desired product was observed (based on the characteristic absorption of phthalimide moiety at 220 nm).



Scheme 3.19. Hinderance of Boc in **34** prohibited Mitsunobu reaction.

IIIB4. Deprotection of the key intermediate **22b**

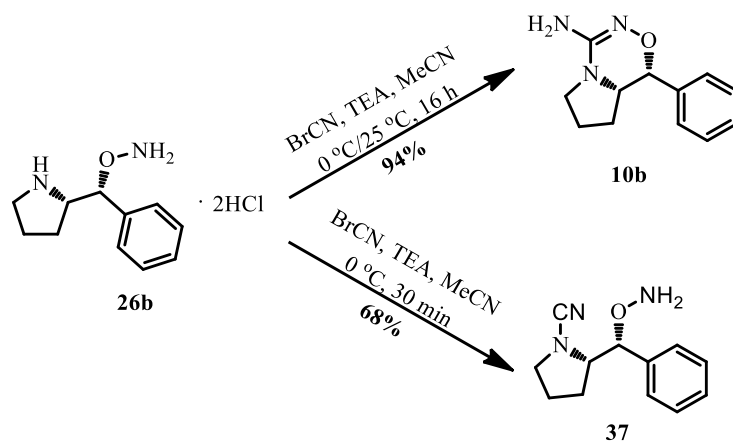
The phthalimide moiety in **22b** was deprotected by hydrazine hydrate, producing **25b** in 97% yield. Then, Boc was removed by HCl in dioxane without additional purification, affording highly hygroscopic **26b** in 96% yield (Scheme 3.20).



Scheme 3.20. Deprotection of the key intermediate **22b**.

III B5. Cyclization of amino alkoxyamine 26b

In a similar way to synthesize **10a**, **26b** was cyclized in MeCN with BrCN, affording chiral 3-amino-1,2,4-oxadiazine **10b** in 94% yield (*Scheme 3.21*).



Scheme 3.21. Synthesis of chiral 3-amino 1,2,4-oxadiazine scaffolds 10b.

It is noteworthy that intermediate **37** could be isolated if ceasing reaction after 30 minutes (*Scheme 3.21*). In ^1H NMR spectrum of intermediate **37** (*Figure 3.8*), one $-\text{NH}_2$ peak rather than two $-\text{NH}$ peaks were observed, indicating the cyano group is linked to pyrrolidine moiety, which means the secondary amine of **26b** is more nucleophilic than the alkoxyamine towards BrCN. Despite the similarity in ^1H NMR, intermediate **37** and desired product **10b** could be easily distinguished by ^{13}C NMR, since **37** shown a $-\text{CN}$ peak at 117.48 ppm, while **10b** shown a $-\text{C}=\text{N}-$ at 155.84 ppm (*Figure 3.8*).

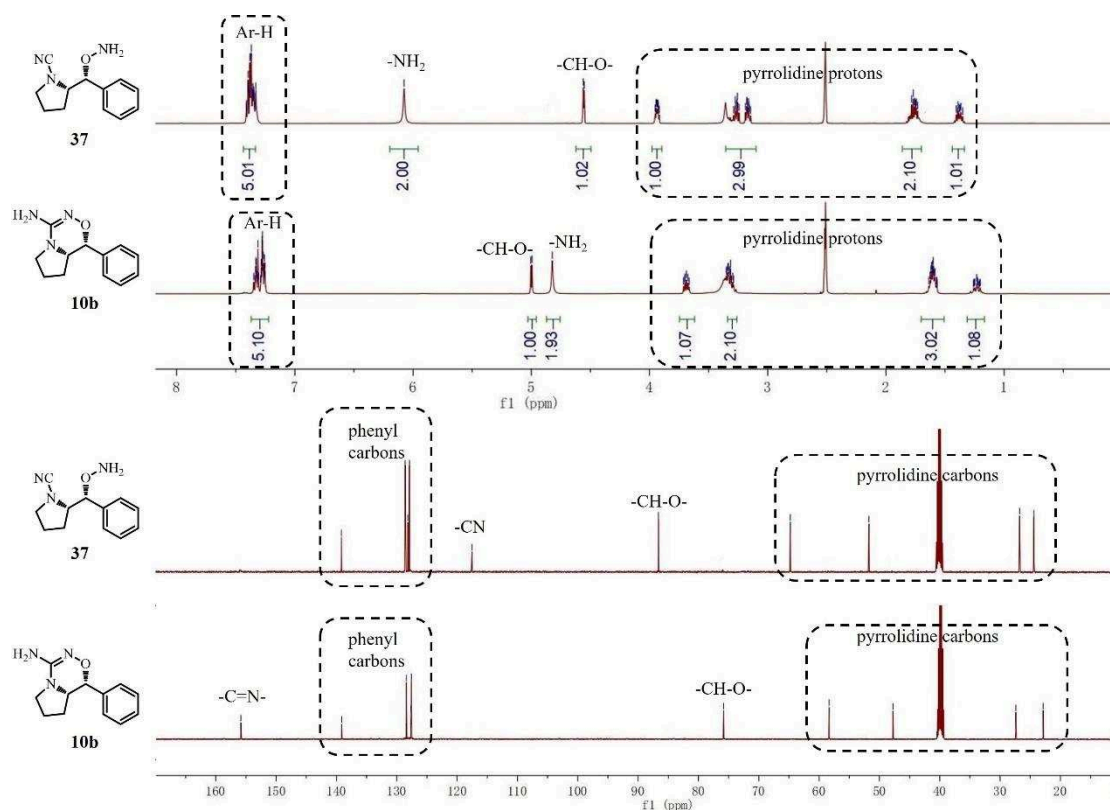


Figure 3.8. ^1H and ^{13}C NMR of **37** and **10b** in $\text{DMSO}-d^6$.

To further confirm the structure and geometry of expected oxadiazine, **10b** was recrystallized by slow evaporation from MeCN solution. Single-crystal X-ray diffraction analysis shown that the crystal structure of **10b** belongs to (5*S*, 6*R*)-3-amino-1,2,4-oxadiazine (Figure 3.9), highlighting the configuration retention of **22b** during the Mitsunobu reaction (Scheme 3.18). Compared with **10a** (Figure 3.6), the presence of the pyrrolidine ring in **10b** decreases the mutual perpendicularity between oxadiazine and phenyl rings. The details of the crystallographic data and structure refinement parameters were summarized in Appendix II.

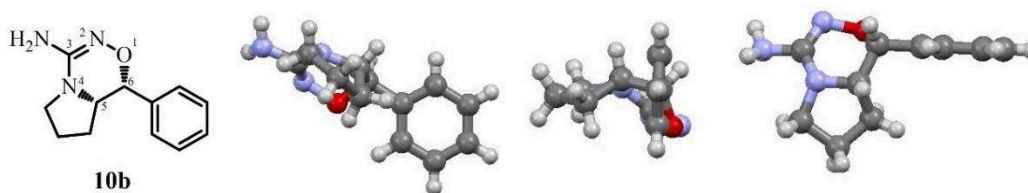


Figure 3.9. X-ray crystallography of **10b** displayed with front view, right view and top view.

In conclusion, starting from L-proline, chiral 3-amino-1,2,4-oxadiazine **10b** could be stereoselectively synthesized through DIBAL-H reduction and Mitsunobu reaction. The bulkiness of Boc plays a crucial role in the stereoselective reduction of ketone and consequent Mitsunobu reaction. Both stereogenic centers in **10b** increases the spatial geometric complexity of the 1,2,4-oxadiazine scaffold.

IIIC. Synthesis of (5*S*,6*R*)-5-isopropyl-6-phenyl-5,6-dihydro-4*H*-1,2,4-oxadiazin-3-amine **10c**

The results in Section IIIB shown that the stereoselectivity of DIBAL-H reduction and the reactivity of Mitsunobu reaction were originated from the bulkiness of Boc. However, the effect of the rigidity of pyrrolidine ring in these two reactions were not discussed. Here, *N*-Boc L-valine was used as the starting material to learn whether the stereoselectivity of DIBAL-H reduction and the reactivity of Mitsunobu reaction remained if the rigidity was impaired (*Figure 3.10*).

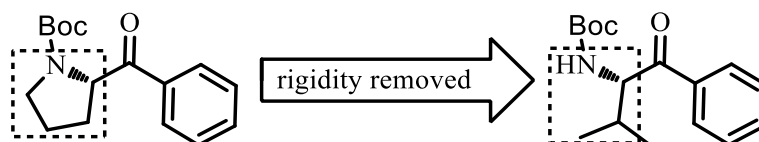
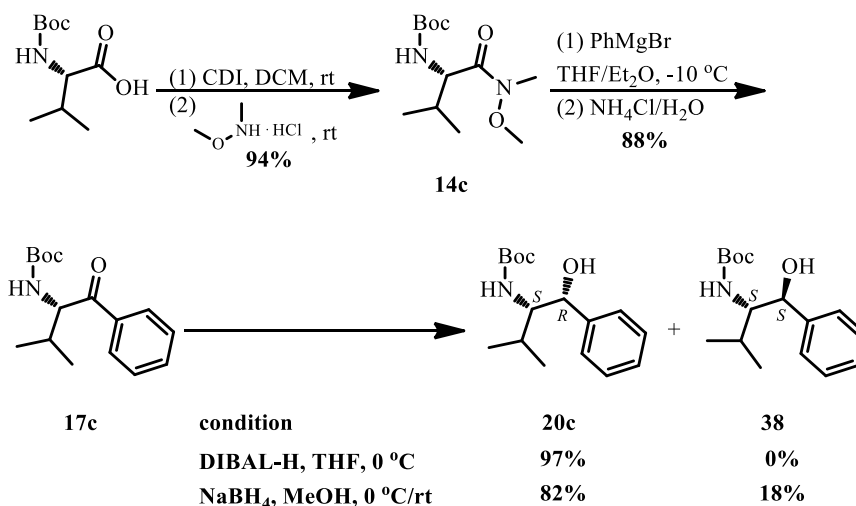


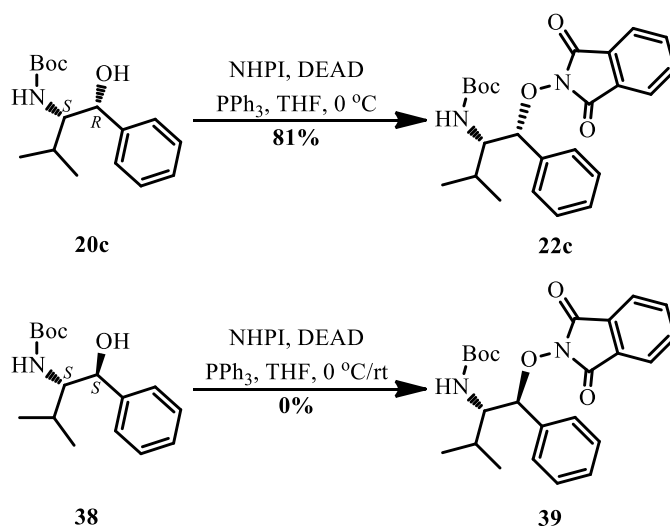
Figure 3.10. Removal of the rigidity in ketone.

In the same way, *N*-Boc L-valine was activated by CDI and substituted with *N,O*-dimethylhydroxylamine, producing Weinreb amide **14c** in 94% yield. It was then reacted with PhMgBr, affording ketone **17c** in 88% yield. Similar to the reduction of **17b**, DIBAL-H could stereoselectively reduce ketone **17c** into the only diastereomer **20c** in 97% yield, while NaBH₄ reduction produced both diastereomers **20c** and **38** in 82% and 18% yields, respectively (*Scheme 3.22*). The structures of both diastereomers could be identified by comparing their ¹H NMR spectra with the ones reported in literature.^{127, 128} The similarity of these results as those described in Section IIIB2 indicates that the stereoselective reduction of DIBAL-H is originated from the bulkiness of Boc, rather than the rigid frame between the nitrogen and α carbon atoms of ketone.



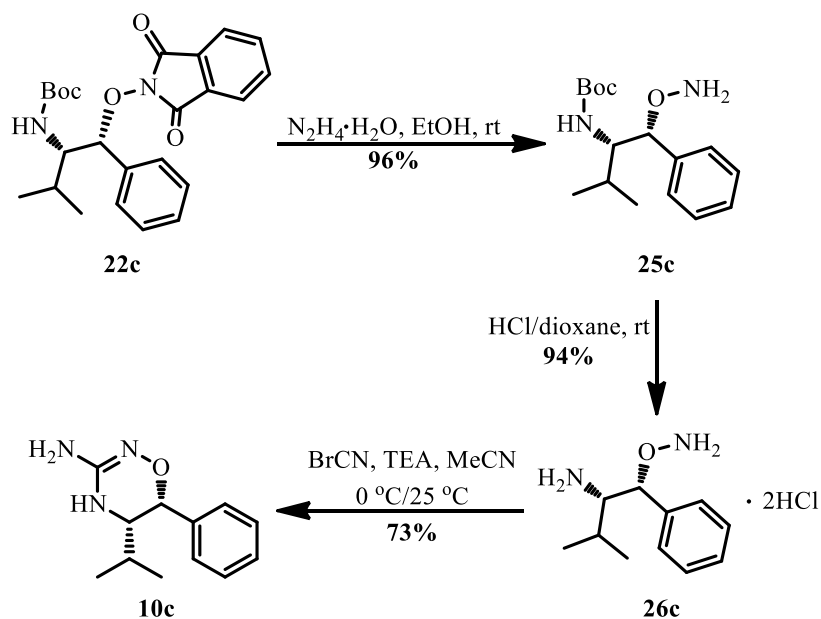
Scheme 3.22. Reduction of ketone **17c** synthesized from *N*-Boc *L*-valine.

The N-O moiety was introduced into diastereomer **20c** (*S/R*) by Mitsunobu reaction with NHPI at 0 °C and key intermediate **22c** (*S/R*) was obtained in 81% yield. However, as observed before, the same Mitsunobu conditions failed to transform diastereomer **38** (*S/S*) into key intermediate **39** (*S/S*) and the starting material was recovered quantitatively (Scheme 3.23). Again, the similarity of these results as those described in Section IIIB3 indicates that the different reactivity of the two diastereomers **20c** (*S/R*) and **38** (*S/S*) in Mitsunobu reaction is independent of the rigid frame between the nitrogen and α carbon atoms of alcohol.



Scheme 3.23. Mitsunobu reaction of diastereomer **20c** or **38** with NHPI.

The phthalimide moiety in **22c** was deprotect by hydrazine hydrate, producing **25c** in 96% yield. Then, Boc was removed by HCl in dioxane without additional purification, affording highly hygroscopic amino alkoxyamine **26c** in 94% yield. Finally, **26c** was cyclized in diluted MeCN solution by BrCN, affording chiral 3-amino-1,2,4-oxadiazine **10c** in 73% yield (*Scheme 3.24*).



Scheme 3.24. Synthesis of 10c from key intermediate 22c.

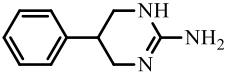
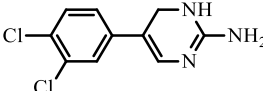
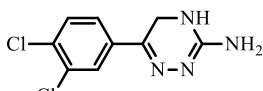
In conclusion, chiral 3-amino-1,2,4-oxadiazine **10c** could be stereoselectively synthesized as **10b**, indicating the absence of rigid frame between the nitrogen and α carbon atoms of amino acids did not influence the stereoselective reduction of DIBAL-H and the reactivity of Mitsunobu reaction. These results also revealed the versatility of DIBAL-H reduction and Mitsunobu reaction in synthesizing chiral 1,2,4-oxadiazine scaffold from Boc amino acids.

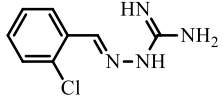
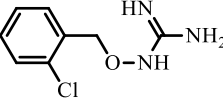
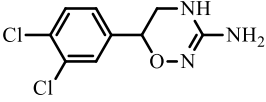
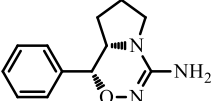
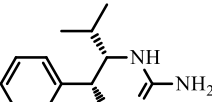
IIID. Physicochemical studies of 3-amino 1,2,4-oxadiazines

Modern drug-discovery chemistry is based on a multidimensional optimization approach, in which the optimization of physicochemical properties, aspects of ADME and safety of a lead compound are considered at an equal level together with potency and selectivity.¹²⁹ A large fraction of the drugs currently on the market or in development contain one or more basic nitrogen atoms. Whether or not basic nitrogen atoms are protonated in the biological environment may be critical not only for the variability of the biopharmaceutical characteristics of drugs but also parameters such as log D and solubility.^{130, 131} Therefore, it is important to know pK_a and modulate its basicity in a rational, structure-based fashion.

In previous sections, three 3-amino-1,2,4-oxadiazines were synthesized as biomimetic compounds of cyclic amino guanidine. To investigate the influence of oxygen atom on the physicochemical properties of neighboring guanidine moiety, pK_a and log D of 3-amino-1,2,4-oxadiazines (**10a**, **10b** and **10c**) will be measured by pH-metric and HPLC methods, respectively.¹³² pK_a and log D of acyclic alkoxy guanidine (**42**) and cyclic/acyclic (imino)guanidine (**2**, **3**, **40** and **41**) were also measured as reference points (*Table 3.2*).

Table 3.2. pK_a and log $D_{7.4}$.

Compound	$pK_{a \text{ MeOH}60\%}$ ^[a]	$pK_{a \text{ aq}}$ ^[b]	log $D_{7.4}$ ^[c]
 40	> 11	> 11	-0.64 ± 0.06
 3	10.6 ± 0.1	11.4	1.90 ± 0.04
 2	9.29 ± 0.05	10.0	1.70 ± 0.03

 41	8.50 ± 0.05	9.2	1.50 ± 0.09
 42	7.29 ± 0.05	8.0	1.07 ± 0.03
 10a		under progress	
 10b		under progress	
 10c		under progress	

[a] $pK_{a \text{ MeOH60\%}}$ was determined based on pH- V_{NaOH} titration curve (ionic strength 0.1 M, temperature 25 °C) and calculated by HYPERQUAD program.

[b] $pK_{a \text{ aq}} = (pK_{a \text{ MeOH60\%}} + 0.43)/0.97$.

[c] Average of two individual samples (aqueous phase from tested compounds in the mixture PBS (pH 7.4) and octanol at 20 °C) measured by HPLC at 280 nm.

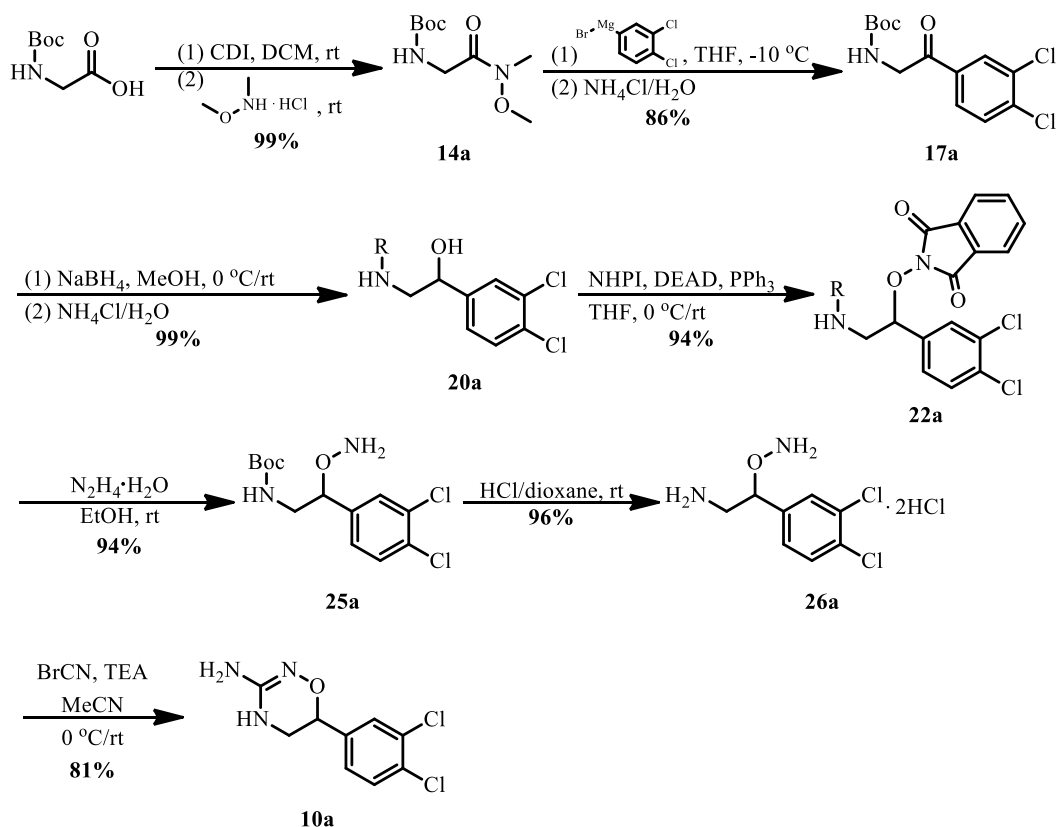
Due to the strong basicity of guanidine group, $pK_{a \text{ MeOH60\%}}$ of **40** is too high to be measured under the titration condition and $pK_{a \text{ aq}}$ of **40** is estimated >11 as $pK_{a \text{ MeOH60\%}}$. $\log D_{7.4}$ of **40** is negative -0.64 ± 0.06 , which means it is hydrophilic and unfavorable for membrane permeability by passive diffusion. Introducing one double bond and two chlorine atoms in **40** resulted in cpd **3**, which is prepared in form of TFA salt. The presence of $-\text{C}=\text{C}-$ and chlorine atoms decreases $pK_{a \text{ aq}}$ to 11.4 and increases $\log D_{7.4}$ to 1.90 ± 0.04 , indicating cpd **3** is approximately 100 times more soluble in octanol than in PBS. This kind of hydrophobicity is not only due to the decrease of pK_a but also partially due to the presence of CF_3COO^- which formed an ion pair with the protonated compound. Replacing one carbon atom in cpd **3** by a

nitrogen atom led to cyclic iminoguanidine **2** (TFA form) with $pK_{a\text{aq}} = 10$ and $\log D_{7.4} = 1.70 \pm 0.03$, which means it's approximately 50 times more soluble in octanol than in PBS. As cpd **3**, the hydrophobicity of protonated cpd **2** is partially due to ion pair formed with CF_3COO^- . Replacing 3,4-dichlorophenyl by 2-chlorophenyl and breaking the iminoguanidine ring in cpd **2** by removing a carbon atom gave cpd **41** with $pK_{a\text{aq}} = 9.2$ and $\log D_{7.4} = 1.50 \pm 0.09$, a weak but sufficient hydrophobicity for crossing biological membrane. Acyclic alkoxyguanidine **42** was obtained by transposing the α nitrogen atom in acyclic iminoguanidine **41** by an oxygen atom, decreasing $pK_{a\text{aq}}$ to 8 and $\log D_{7.4}$ to 1.07 ± 0.03 . The order of magnitude of $\log D_{7.4}$ is 1, which means it's approximately 10 times more soluble in octanol than in PBS, sufficient for crossing biological membrane.

Comparing with the original cyclic guanidine **40**, acyclic alkoxyguanidine **42** is three orders of magnitude less basic ($\Delta pK_{a\text{aq}} < -3$) and more favorable for membrane permeability ($\Delta \log D_{7.4} = 1.71 \pm 0.03$) (Table 3.2). The electron-withdrawing nature of oxygen atom seems to be responsible for the reduction in basicity of the adjacent nitrogen atom in guanidine moiety. Due to 3-amino-1,2,4-oxadiazines, a kind of cyclic alkoxyguanidine is more structural complex relative to acyclic **42**, better target selectivity is expected besides good physicochemical properties. As a result, several 3-amino-1,2,4-oxadiazines (**10a**, **10b** and **10c**) have been synthesized and the measurements of their pK_a and $\log D_{7.4}$ are current under progress.

III.E. Conclusion

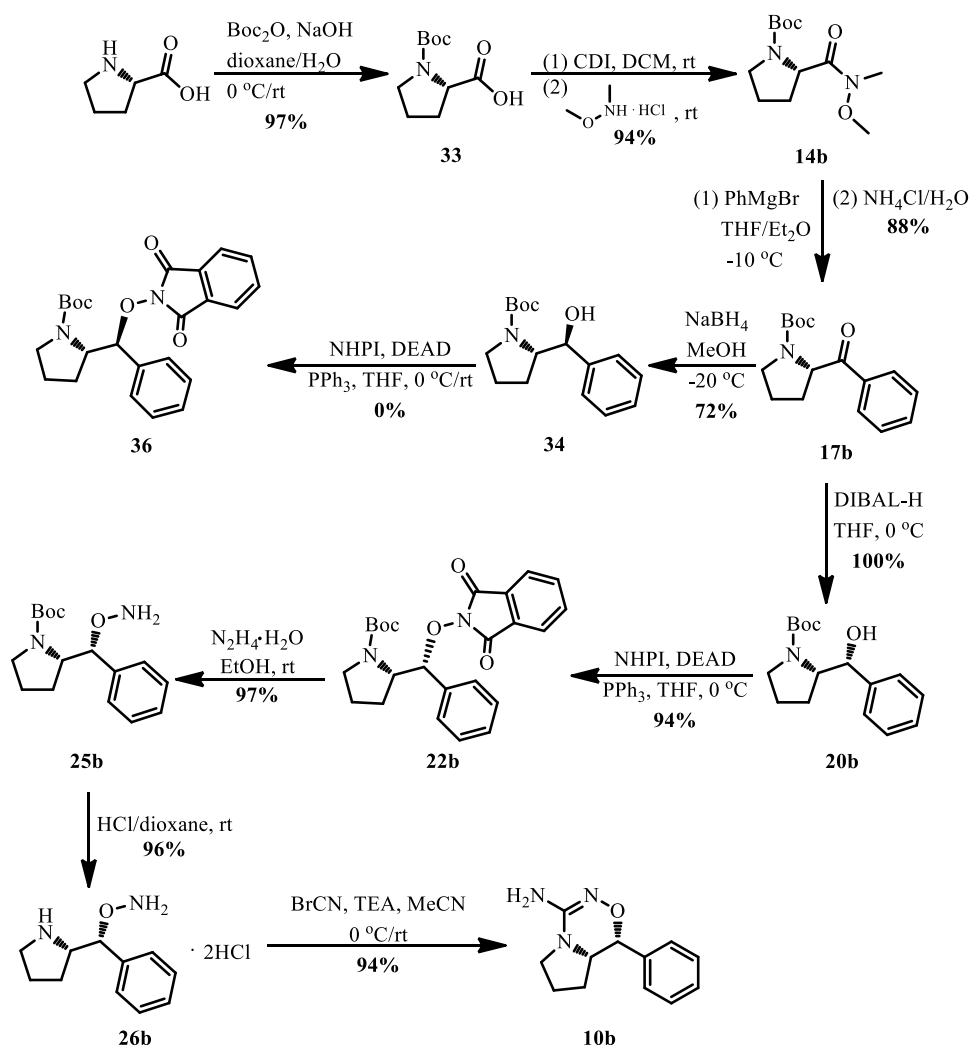
In this chapter, racemic 6-(3,4-dichlorophenyl)-5,6-dihydro-4*H*-1,2,4-oxadiazin-3-amine **10a** was synthesized in 7 steps in 58% overall yield from *N*-Boc glycine to verify the feasibility of the synthetic approach (Scheme 3.25). The X-ray crystallography of **10a** shown a non-planar geometry of the 3-amino-1,2,4-oxadiazine scaffold which was perpendicular with the phenyl ring.



Scheme 3.25. Synthesis of **10a** from *N*-Boc glycine.

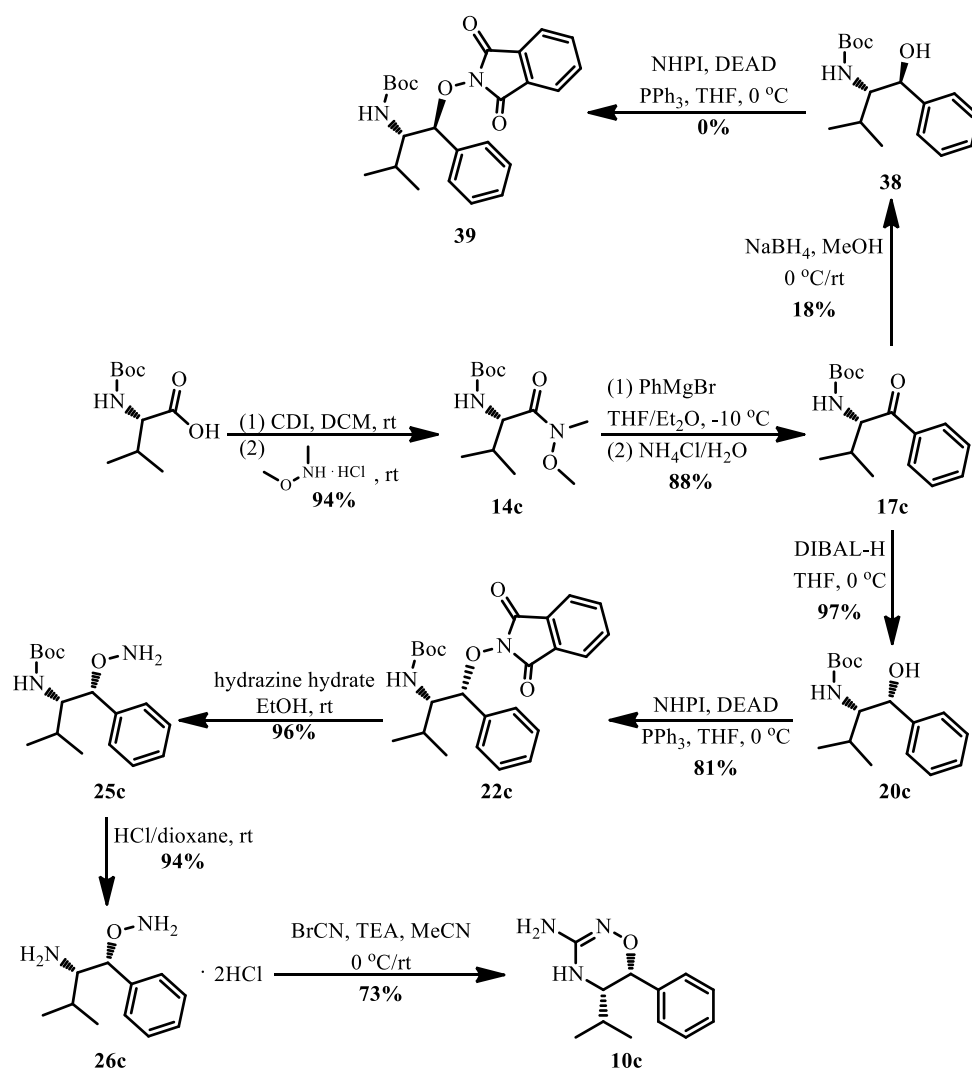
By chiral reduction of alcohol with DIBAL-H, (1*R*,8*aS*)-1-phenyl-6,7,8,8*a*-tetrahydro-1*H*-pyrrolo[1,2-*d*][1,2,4]oxadiazin-4-amine **10b** could be synthesized from L-proline based on the established methods (Scheme 3.26). Due to the steric hinderance of alcohol, Mitsunobu reaction works only with diastereomer **20b** and the configuration is retained. X-ray crystallography of **10b** shown the presence of pyrrolidine ring decreased the mutual perpendicularity between the oxadiazine and

phenyl rings.



Scheme 3.26. Synthesis of **10b** from *L*-proline.

To know whether the stereoselectivity of DIBAL-H reduction and the reactivity of Mitsunobu reaction would change if the rigidity of the pyrrolidine ring in **19b** was removed, *N*-Boc *L*-valine was used as the starting material. (5*S*,6*R*)-5-isopropyl-6-phenyl-5,6-dihydro-4*H*-1,2,4-oxadiazin-3-amine **10c** still could be stereoselectively synthesized by applying DIBAL-H reduction and Mitsunobu reaction as key steps, indicating the versatility of the established methods in synthesis chiral 3-amino-1,2,4-oxadiazine scaffold from Boc amino acid (Scheme 3.27).



Scheme 3.27. Synthesis of **10c** from *N*-Boc *L*-valine.

To fully conclude about the effects of Boc vs amino acid side chain hindrance on the stereoselectivity of the DIBAL-H reduction or the Mitsunobu reaction, an 1,2,4-oxadiazin-3-amine will be synthesized starting from Boc-alanine, bearing a simple methyl group at the alpha position.

In preliminary results of physicochemical studies, significant decrease in *pK_a* and improvement in log *D* were observed in acyclic alkoxy guanidine compared with cyclic/acyclic guanidine. To have a better comprehension of the influence of oxygen atom on the physicochemical properties of neighboring guanidine moiety, the measurements of *pK_a* and log *D*_{7.4} of 3-amino-1,2,4-oxadiazines are currently under progress.

IV. Total synthesis of alchornedine

IV. Total synthesis of alchornedine

In 2014, Barrosa et al isolated a new natural guanidine alkaloid with 3-amino-1,2,4-oxadiazine scaffold, named alchornedine, from the leaves of *Alchornea glandulosa*, which is effective against both clinical forms of *Trypanosoma cruzi* and could be used as a scaffold for future drug designed against American trypanosomiasis (Figure 4.1).¹³³ As the total synthesis of alchornedine has never been described, the structure was proposed by the authors based on the NMR spectra in MeOD- d^4 , rather than DMSO- d^6 or X-ray crystallography. In fact, it's not a reliable way to confirm the exact structure of alchornedine because a hydrogen–deuterium exchange of NH proton signals is occurring in MeOD- d^4 . In this chapter, the aim of our work was to propose the total synthesis of **43** and its NMR spectra would be compared with the literature to confirm the correctness of Barrosa's proposed structure for alchornedine¹³³

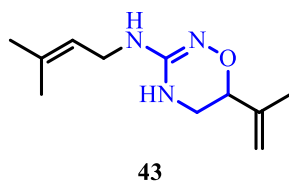
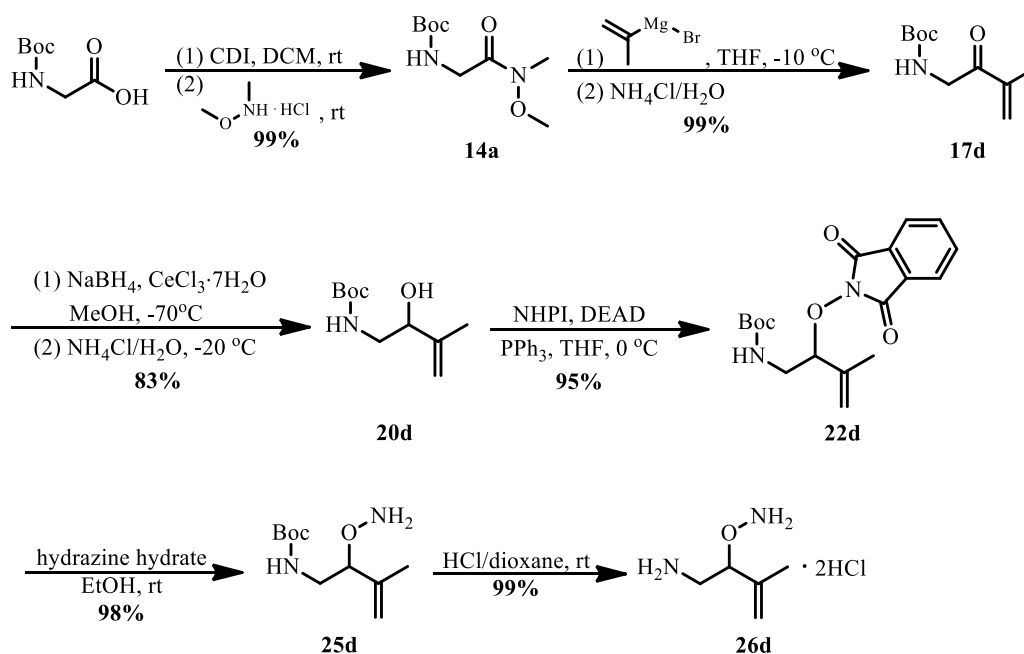


Figure 4.1. Barrosa's proposed structure of alchornedine.

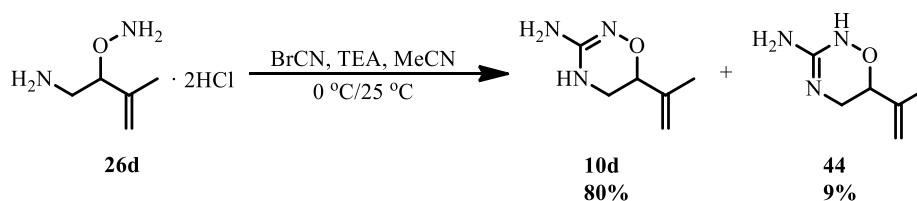
IVA. Total synthesis of **40** from *N*-Boc glycine

Based on the established method to synthesize 3-amino-1,2,4-oxadiazine scaffold in Chapter III, **43** was synthesized using *N*-Boc glycine as the starting material. Weinreb amide **14a** was prepared quantitatively from *N*-Boc glycine using CDI as activating group and then reacted with isopropenyl magnesium bromide, furnishing α , β -unsaturated ketone **17d** in 99% yield. It is noteworthy that **17d** was sensitive to temperature as the product degraded when it was concentrated in EtOAc/Heptane solution at 40° C. Due to the alternant polarization of α , β -unsaturated ketone **17d**, 1,4-reduction happened when NaBH₄ was used without carbonyl activation agents, giving access to the α , β -saturated ketone, *tert*-butyl (3-methyl-2-oxobutyl)carbamate. To realize 1,2-reduction, CeCl₃ was used as carbonyl activation agent before the addition of NaBH₄, furnishing α , β -unsaturated alcohol **20d** in 83% yield. The N-O moiety was introduced by Mitsunobu reaction of **20d** with NHPI, providing **22d** in 95% yield. The phthalimide moiety in **22d** was then deprotected by hydrazine hydrate, followed by the deprotection of Boc by HCl in dioxane, affording amino alkoxyamine **26d** in 99% yield (*Scheme 4.1*).



Scheme 4.1. Synthesis of amino alkoxyamine 26d from N-Boc glycine.

Amino alkoxyamine **26d** was cyclized into 3-amino-1,2,4-oxadiazine using BrCN. Two isomers **10d** and **44** were separated in 80 and 9% yield, respectively (*Scheme 4.2*).



Scheme 4.2. Cyclization of amino alkoxyamine 26d.

The structure of **10d** and **44** were identified by NMR spectra (*Figure 4.2*). Although the two compounds are similar in ^{13}C NMR, the electron-withdrawing effect of oxygen atom makes the ^1H chemical shift of -NH- in **44** located at 8.83 ppm compared to the one in **10d** at 6.07 ppm. Tautomeric transformation between **10d** and **44** won't happen since the chemical shifts remained unchanged when the ^1H NMR was measured at 50 $^{\circ}\text{C}$.

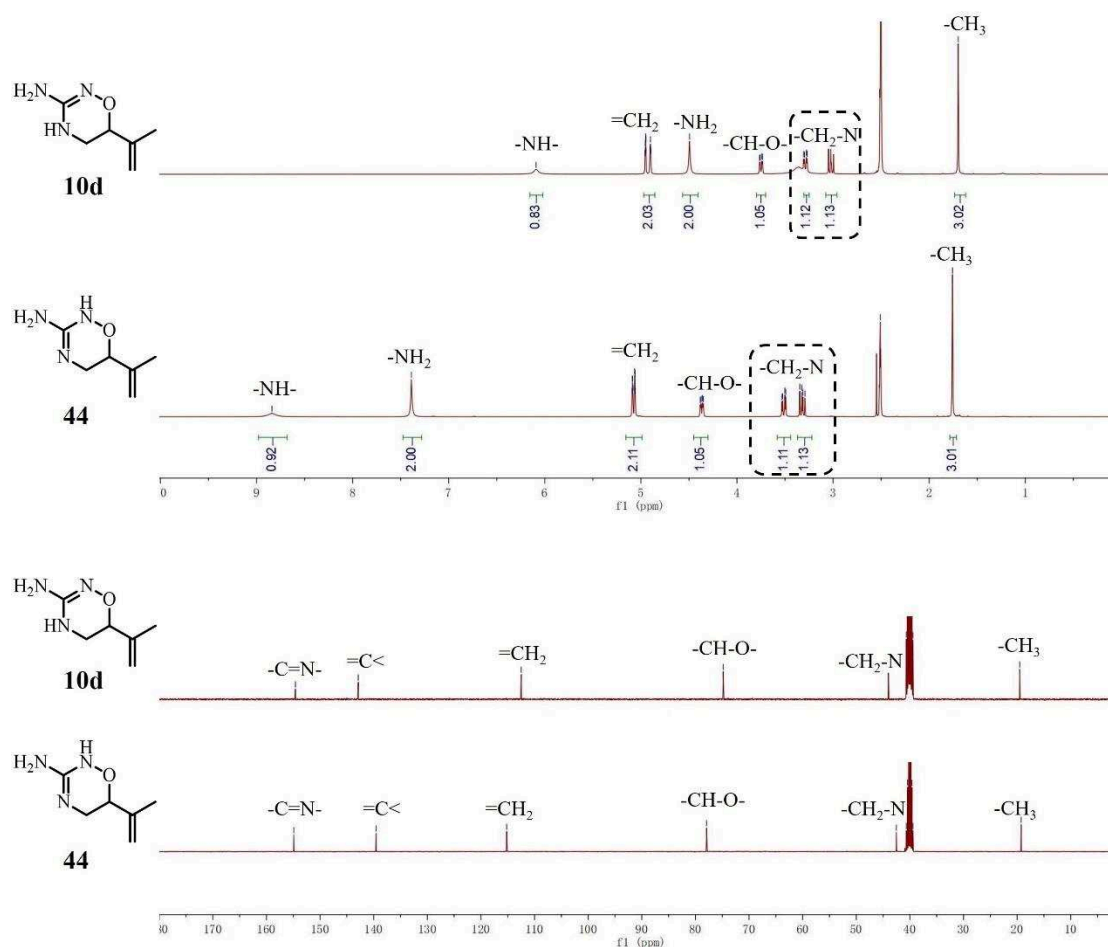


Figure 4.2. ¹H and ¹³C NMR spectra of **10d** and **44** in DMSO-*d*⁶.

To clearly identify **10d** and **44**, NOESY of both compounds were also measured (Figure 4.3 and 4.4). In NOESY of **10d**, -NH- moiety is correlated with both -CH₂-N and -NH₂ moieties. However, correlation between -NH- and -CH₂-N moiety could not be observed in **44** and only -NH₂ moiety is correlated with -NH- moiety.

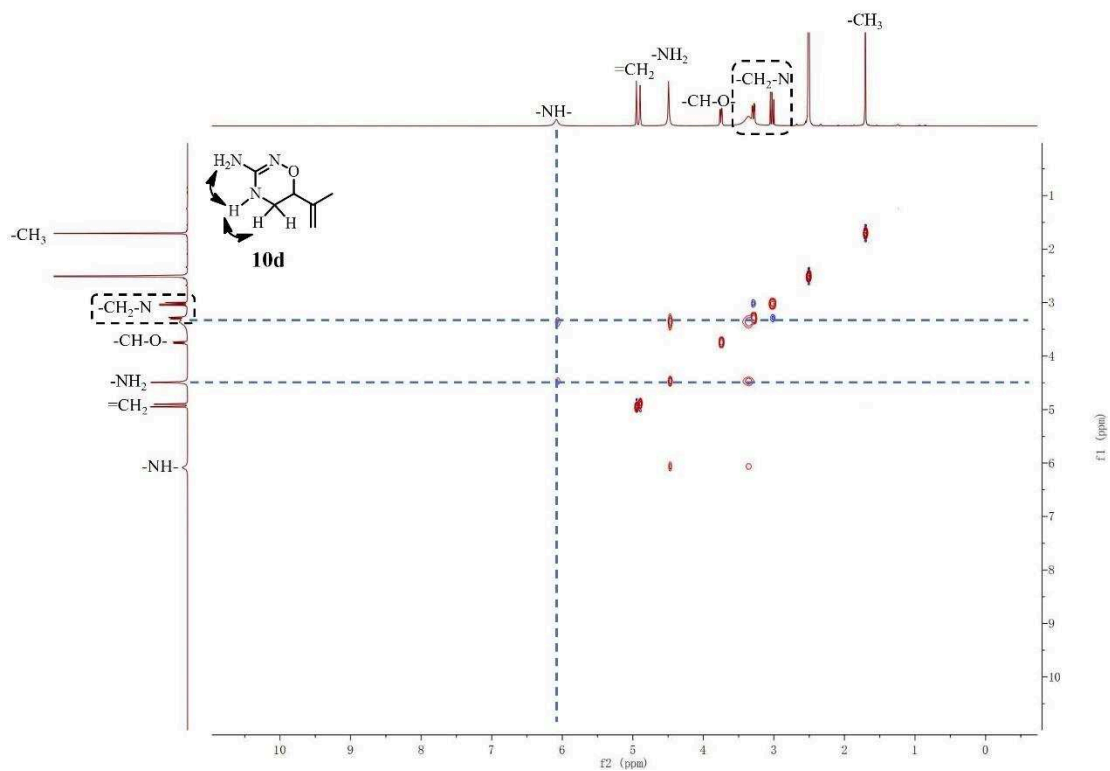


Figure 4.3. NOESY of **10d** in $\text{DMSO-}d^6$.

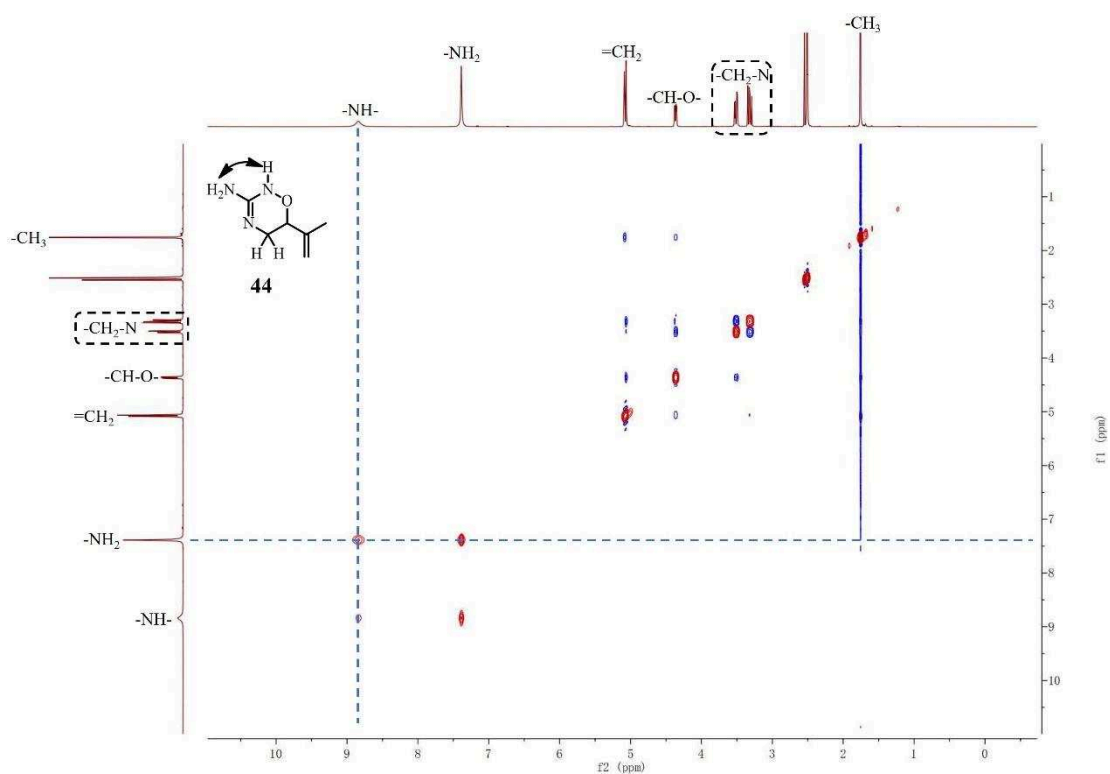
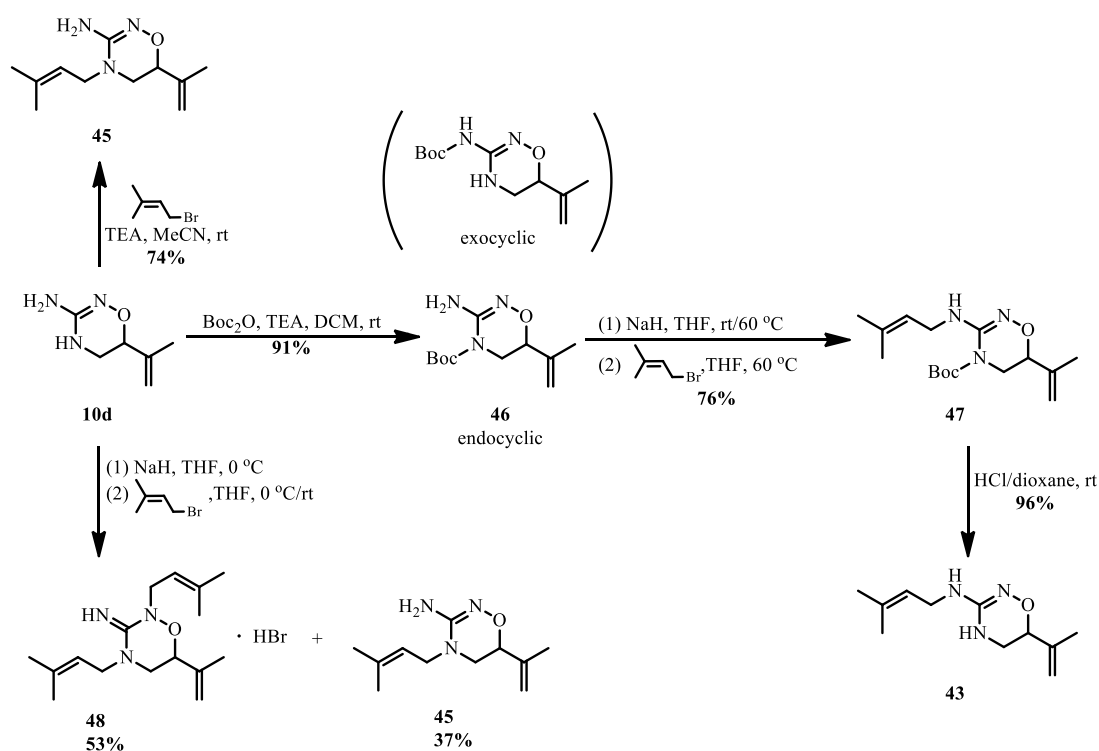


Figure 4.4. NOESY of **44** in $\text{DMSO-}d^6$.

Direct alkylation of **10d** by 3,3-dimethyl allylic bromide with TEA produced **45** in 74% yield. Consistent with the concept of hard and soft acids and bases (HSAB), alkylation of **10d** in presence of excess of NaH and 3,3-dimethyl allylic bromide, led to a mixture of the dialkylated cpd **48** and the monoalkylated cpd **45** in 53% and 37% yields, respectively (*Scheme 4.3*). X-ray crystallography of **48** exhibited a C=N bond out of the oxadiazine ring (*Figure 4.5*). The details of 2D NMRs, crystallographic data and structure refinement parameters of **48** were summarized in Appendix III and VI. As the synthesis of **43** from **10d** by direct alkylation was challenging, cpd **10d** was first protected by (Boc)₂O. Although exocyclic *N*-Boc protection was expected according to HSBA theory, endocyclic *N*-Boc protected **46** was obtained in 91% yield, which was indicated by the presence of a -NH₂ peak at 5.25 ppm in ¹H NMR with CDCl₃. The amino group in **46** was then deprotonated by NaH and alkylated by 3,3-dimethyl allylic bromide in THF, producing **47** in 76% yield. Other bases such as K₂CO₃ or TEA in DMF failed to alkylate **46** into **47**. After Boc deprotection, cpd **43** was obtained in 96% yield (*Scheme 4.3*).



Scheme 4.3. Alkylation of 10d.

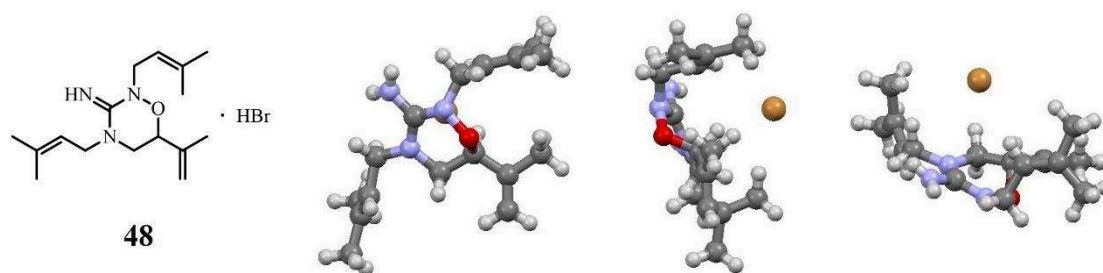


Figure 4.5. X-ray crystallography of **48** displayed with front view, right view and top view.

Because NOESY and HMBC of **45** and **43** did not provide sufficient information (Appendix VII), as well as the difficulty in crystallization to obtain good crystals, **45** and **43** were distinguished from their isomers (Figure 4.6) by referring to ^1H NMR spectra of **10d**, **44** and **48** in $\text{DMSO-}d^6$ (Figure 4.2 and Figure 4.7). By comparing the chemical shifts of $-\text{CH}_2-$ in allylic moieties of **48** and **45** (Figure 4.7), we could distinguish **45** from isomer **49** (Figure 4.6), as the chemical shift of allylic $-\text{CH}_2-$ will locate at a lower field if it links to the nitrogen atom adjacent to oxygen atom. ^1H NMR of **44** indicates that the chemical shift of $-\text{NH-O-}$ moiety is located at around 9 ppm (Figure 4.2) and no such acidic proton signal is observed in ^1H NMR of **43** (Figure 4.7), thus, the three isomers of **43** bearing $-\text{NH-O-}$ moiety could be excluded (Figure 4.6.). Cpd **43** and **50** could be distinguished based on the chemical shift of $-\text{CH-O-}$ moiety. Referring to ^1H NMR of **48** (Figure 4.7), we could estimate that the chemical shift of $-\text{CH-O-}$ moiety in **50** should locate around 4.56 ppm due to their similarity in scaffold. However, the chemical shift of $-\text{CH-O-}$ moiety in **43** locates at 3.72 ppm (Figure 4.7), which is far from 4.56 ppm, while quite close to **10d** at 3.74 ppm (Figure 4.2), excluding the formation of isomer **50**. At this point, **45** and **43** have been distinguished from all their isomers (Figure 4.6) based on their characteristic peaks in ^1H NMR.

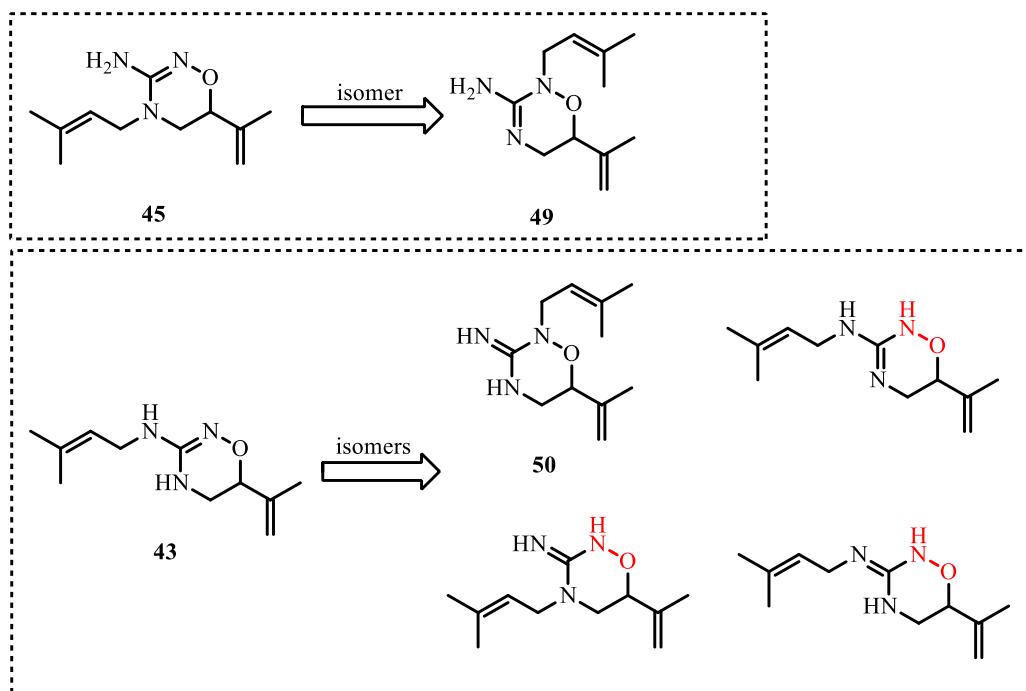


Figure 4.6. Isomers of 45 and 43.

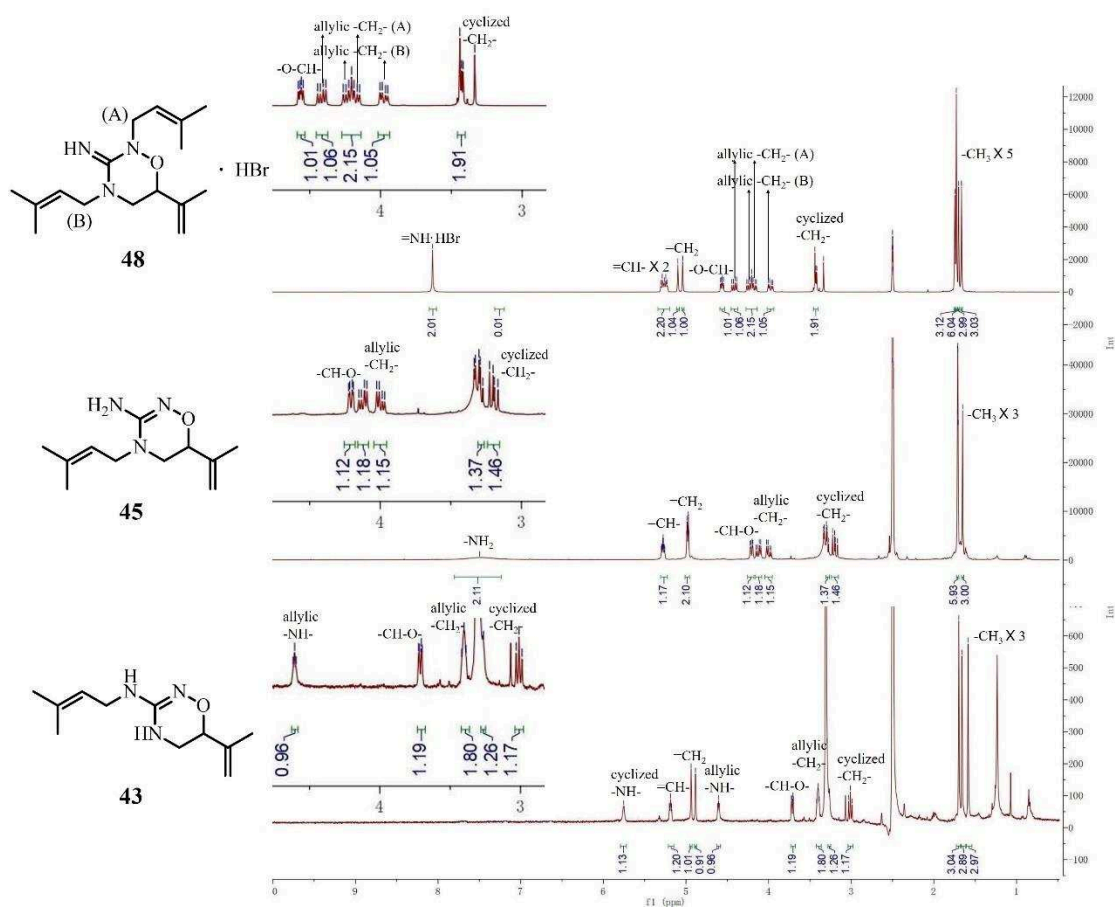


Figure 4.7. ^1H NMR spectra of 48, 45 and 43 in $\text{DMSO}-d_6$.

To know the correctness of the synthetic approach towards the proposed structure of alchornedine, ^1H NMR spectra of **45** and **43** were also measured in $\text{MeOD-}d^4$ (Figure 4.8). However, neither of them was consistent with the ^1H NMR reported in literature (Figure 4.9).¹³³

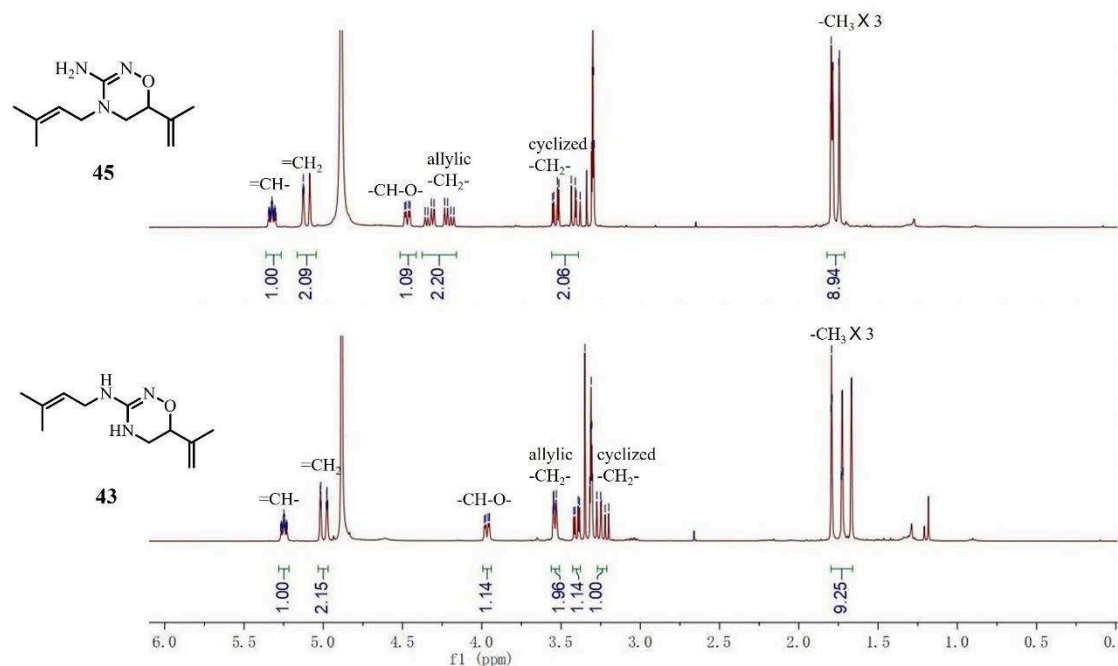


Figure 4.8. ^1H NMR spectra of **45** and **43** in $\text{MeOD-}d^4$.

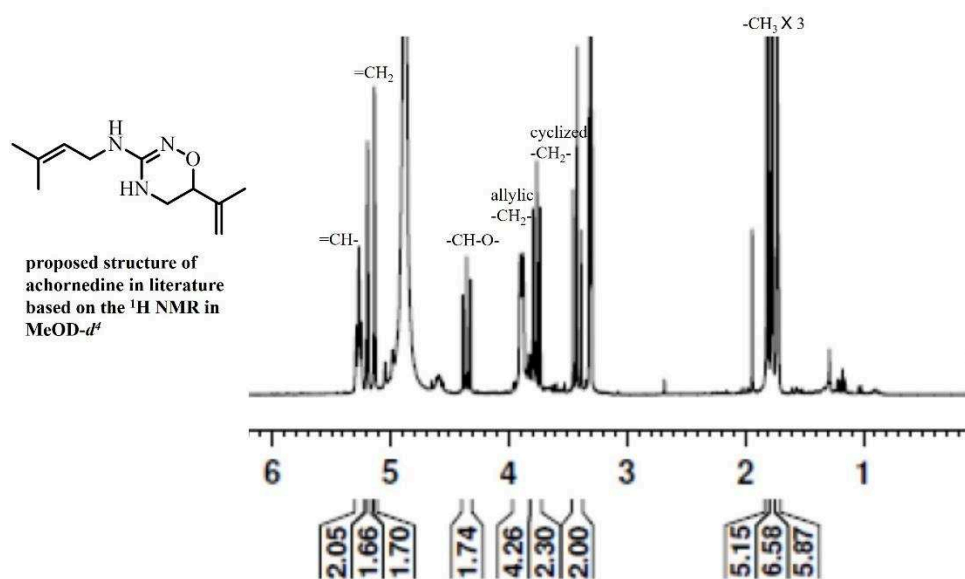
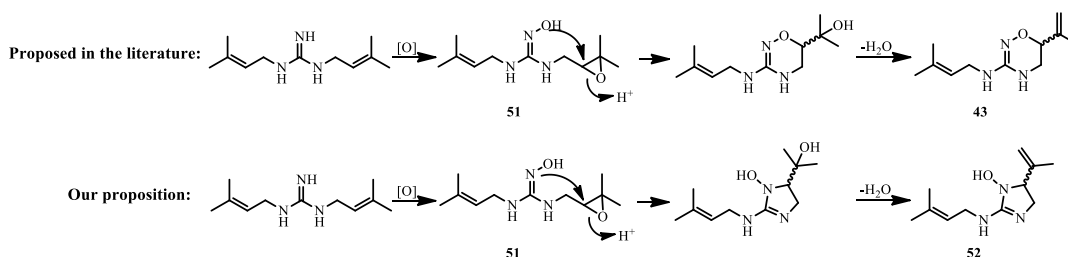


Figure 4.9. ^1H NMR spectra of alchornedine in $\text{MeOD-}d^4$ reported in literature.

This fact suggested that the structure of alchornedine proposed in literature was not correct. Since the mass spectrum of alchornedine in literature shown a M+1-16 peak, a dissociated hydroxy group might exist in the structure of alchornedine. The biogenetic formation of alchornedine proposed in literature showed the oxirane moiety in **51** was attacked by the oxygen atom and finally formed a six-membered ring **43**, the proposed structure of alchornedine. However, this structure seemed not consistent with the aforementioned M+1-16 peak in mass spectra. Thus, we proposed the oxirane moiety in **51** might be attacked the nitrogen atom and finally formed a five-membered ring **52**, the corrected structure of alchornedine (*Scheme 4.4*). The rationality of this speculation is that **52** bears a hydroxy group, which is consistent with the M+1-16 peak in mass spectrum of alchornedine provided in the literature, indicating the structure of alchornedine should be **52**, not **43**.

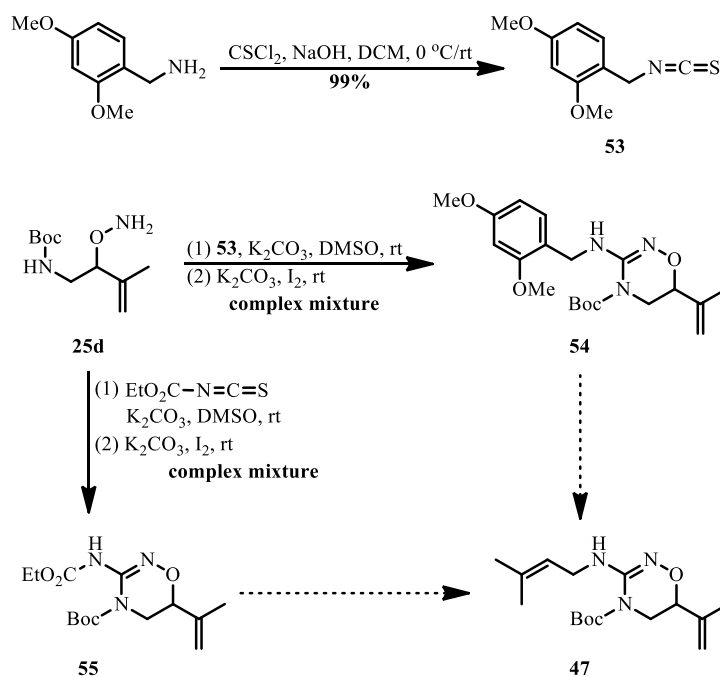


Scheme 4.4. Proposed structure of alchornedine by biogenetic formation.

IVB. Other methods to synthesize 43

IVB1. Starting from Boc amino alkoxyamine 25d

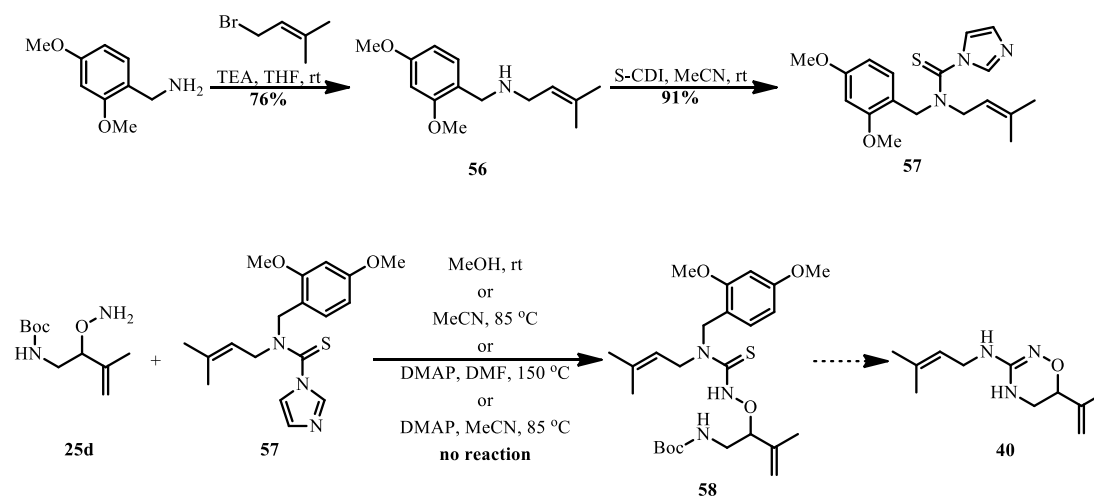
Due to the fact that endocyclic nitrogen in 3-amino-1,2,4-oxadiazine **10d** is more nucleophilic than the exocyclic one towards 3,3-dimethyl allylic bromide, the use of appropriate *N*-2,4-dimethoxybenzyl (DMB) protected isothiocyanate derivative **53** could be a way to directly cyclize **25d** into Boc protected 1,2,4-oxadiazines **54** or **55**. An iodine-mediated cyclodesulfurization was tried as it was reported in literature to synthesize cyclic guanidine from *N*-Boc amine and isothiocyanate.¹³⁴ Despite HPLC of the reaction mixture shown a total consumption of the starting material **25d**, the purification of the two reactions were difficult due to the complexity of the crude (Scheme 4.5).



Scheme 4.5. Synthesis of **47** from **25d** with isothiocyanate derivatives.

Direct introduction of 3,3-dimethyl allylic amine moiety into **25d** was also tried using carbothioamide **57**, which was prepared from the reaction of *N*-DMB allylic amine **56** with 1,1'-thiocarbonyldiimidazole (S-CDI). Solvents such as MeOH, MeCN

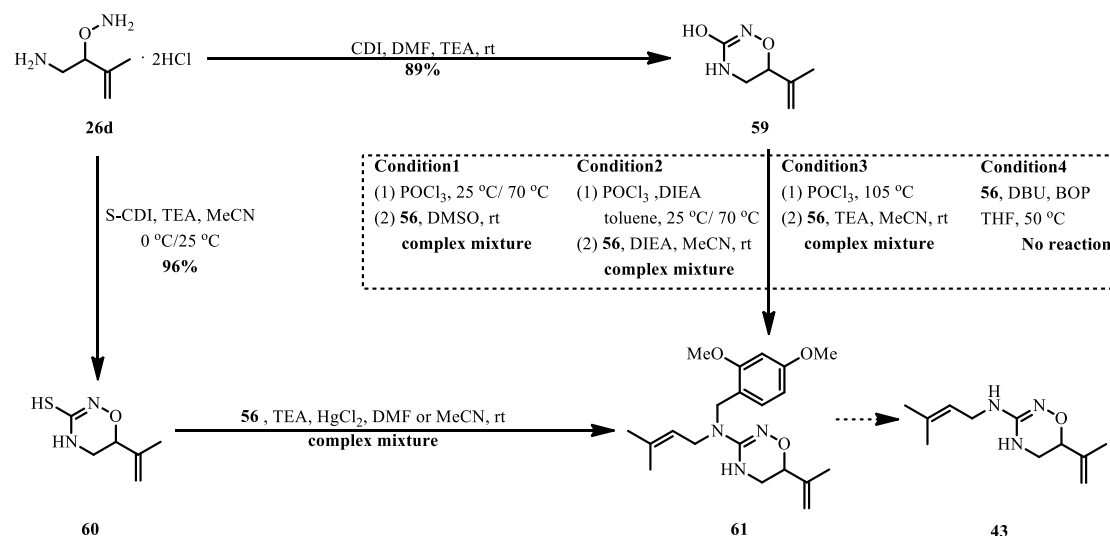
and DMF with/without catalytic amount of 4-dimethylaminopyridine (DMAP) were tried. However, no reaction happened even heated at 150 °C (*Scheme 4.6*).



Scheme 4.6. Synthesis of 58 from 25d with carbothioamide 57.

IVB2. Starting from 26d

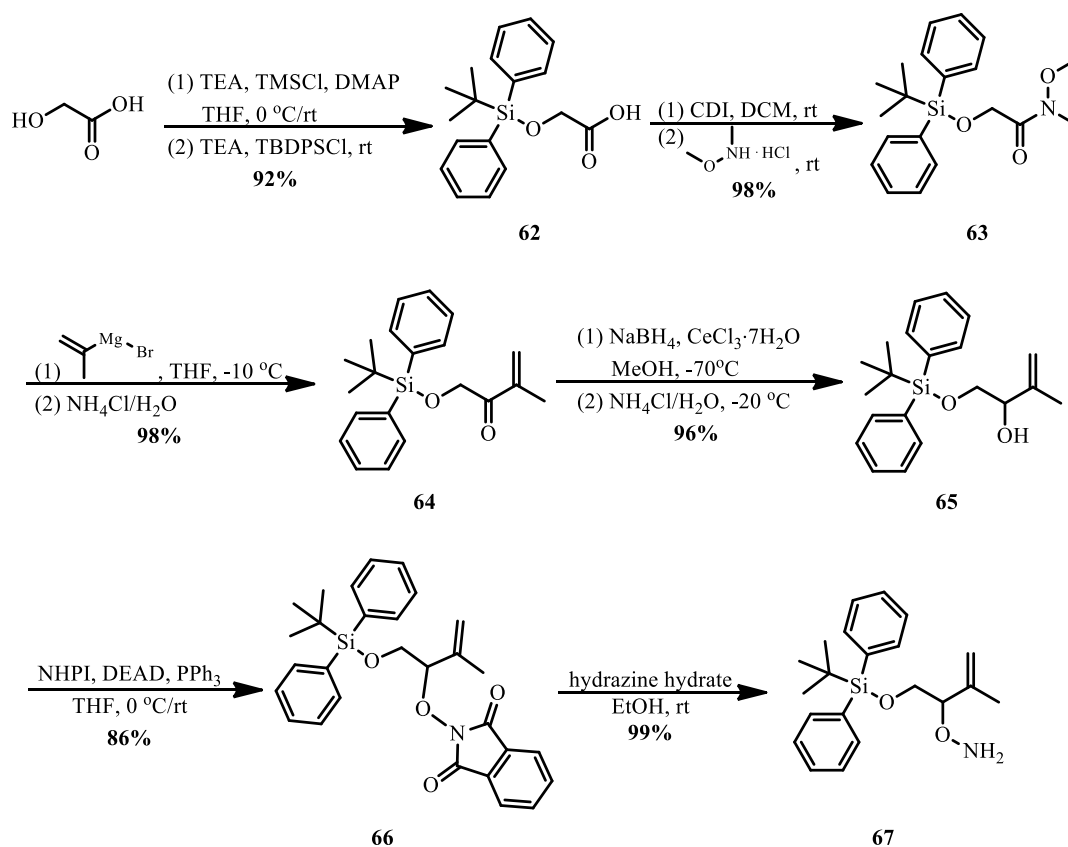
Another strategy to avoid the formation of **45** was to focus on umpollung reactions involving the introduction of allylic moiety on oxadiazine-3-ol **59** or its corresponding thiol **60** by nucleophilic substitution with the help of the *N*-DMB amine **56** (*Scheme 4.7*). Although **26d** could be transformed into **59** and **60** easily in 89% and 96% yields, respectively, the synthesis of **61** was difficult. Three conditions were tried to transform **59** into the corresponding iminochloride with POCl_3 , while subsequent substitution with amine **56** gave a complex reaction mixture. Directly transformation of **59** into **61** with 1,8-diazabicyclo(5.4.0)undec-7-ene (DBU) and (benzotriazol-1-yloxy)tris(dimethylamino)phosphonium hexafluorophosphate (BOP) in THF was unsuccessful and starting material was recovered quantitatively. Introduction of the allylic moiety into **60** with amine **56**, HgCl_2 and TEA in DMF or MeCN also failed and gave a complex reaction mixture. Moreover, 3-mercapto-1,2,4-oxadiazine **60** is instable since degradation happened after it was stored at room temperature for several days.



Scheme 4.7. Synthesis of **61** from **26d** via 3-hydroxy-1,2,4-oxadiazine **59** or 3-mercapto-1,2,4-oxadiazine **60**.

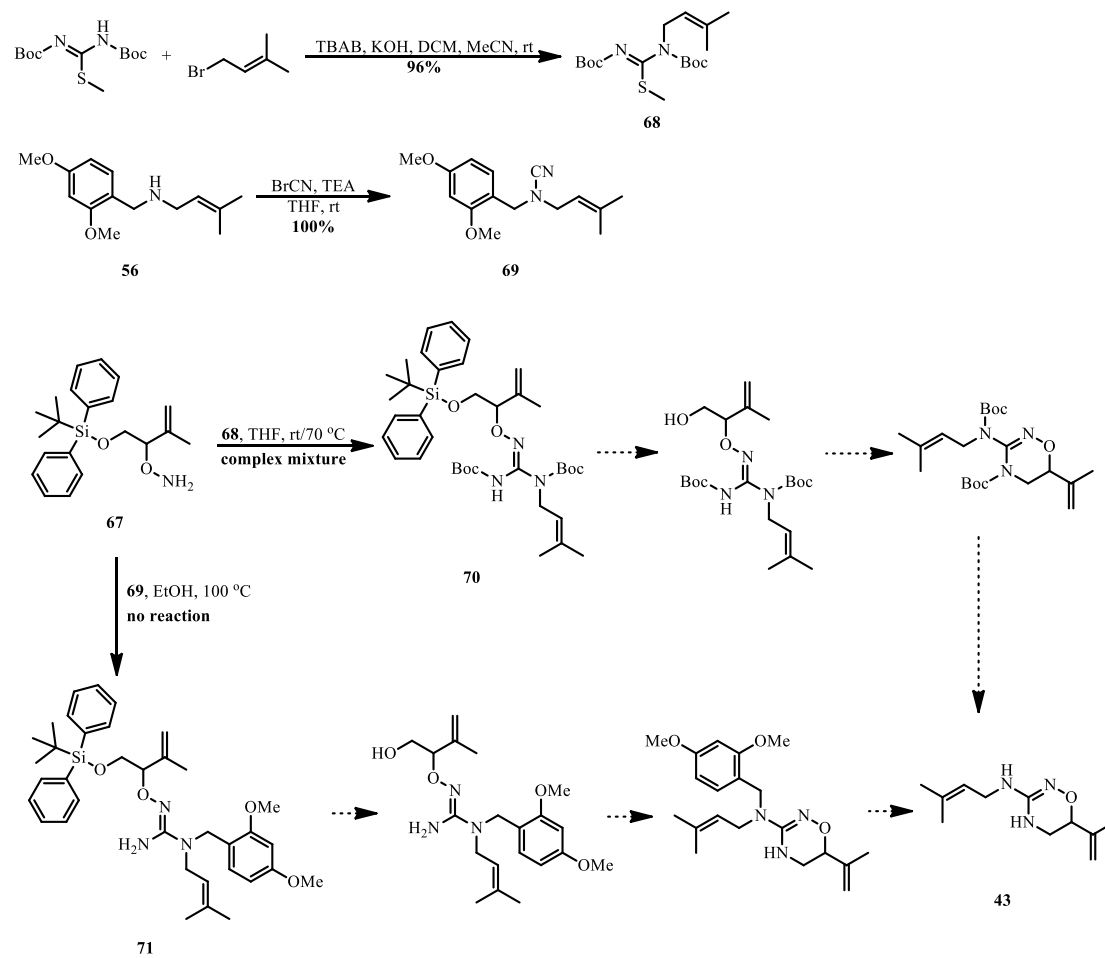
IVB3. Starting from 2-hydroxyacetic acid

In *Scheme 3.1* (see Chapter III), an exclusive reported method to synthesize 3-amino-1,2,4-oxadiazine scaffold was described in which it introduced the guanidine moiety on alkoxyamine by *N, N'*-bis-Boc-1-guanylpyrazole.⁹⁹ Here, a similar method was tried using 2-hydroxyacetic acid as starting material. Hydroxyl group in 2-hydroxyacetic acid was first protected by *tert*-butyldiphenylsilyl group, obtaining **62** in 92% yield. The resulting product was then transformed into Weinreb amide **63** in 98% yield. The reaction of **63** with isopropenyl magnesium bromide furnished α , β -unsaturated ketone **64** in 98% yield, which was then reduced into alcohol **65** by NaBH₄ in the presence of CeCl₃ as a carbonyl activating agent. The N-O moiety was introduced into **65** by Mitsunobu reaction with NHPI, followed by the deprotection of phthalimide moiety with hydrazine hydrate, affording alkoxyamine **67** in 99% yield (*Scheme 4.7*).



Scheme 4.7. Synthesis of alkoxyamine **67** from 2-hydroxyacetic acid.

To avoid the substitution of undesired nitrogen atom in final oxadiazine ring, we have previously introduced the allylic moiety on the starting reagents: *N,N'*-bis-Boc-*S*-Methyl-thiourea or *N*-DMB-3-methylbut-2-en-1-amine (Scheme 4.8). The key step of this approach was introducing the guanidine moiety by the reaction of hydroxylamine **67** with the previously synthesized *S*-methyl-thiourea **68** or cyanamide **69**, then transformed the resulting cpds **70** and **71** into **43** after a sequence of deprotection-Mitsunobu-deprotection reactions. Despite the synthesis of alkoxyamine **67** went smoothly from 2-hydroxyacetic acid, the reaction of **67** with *S*-methyl thiourea **68** gave a complex reaction mixture. In contrary, no reaction happened between **67** and cyanogen amide **69** even heated at 100 °C (Scheme 4.8).

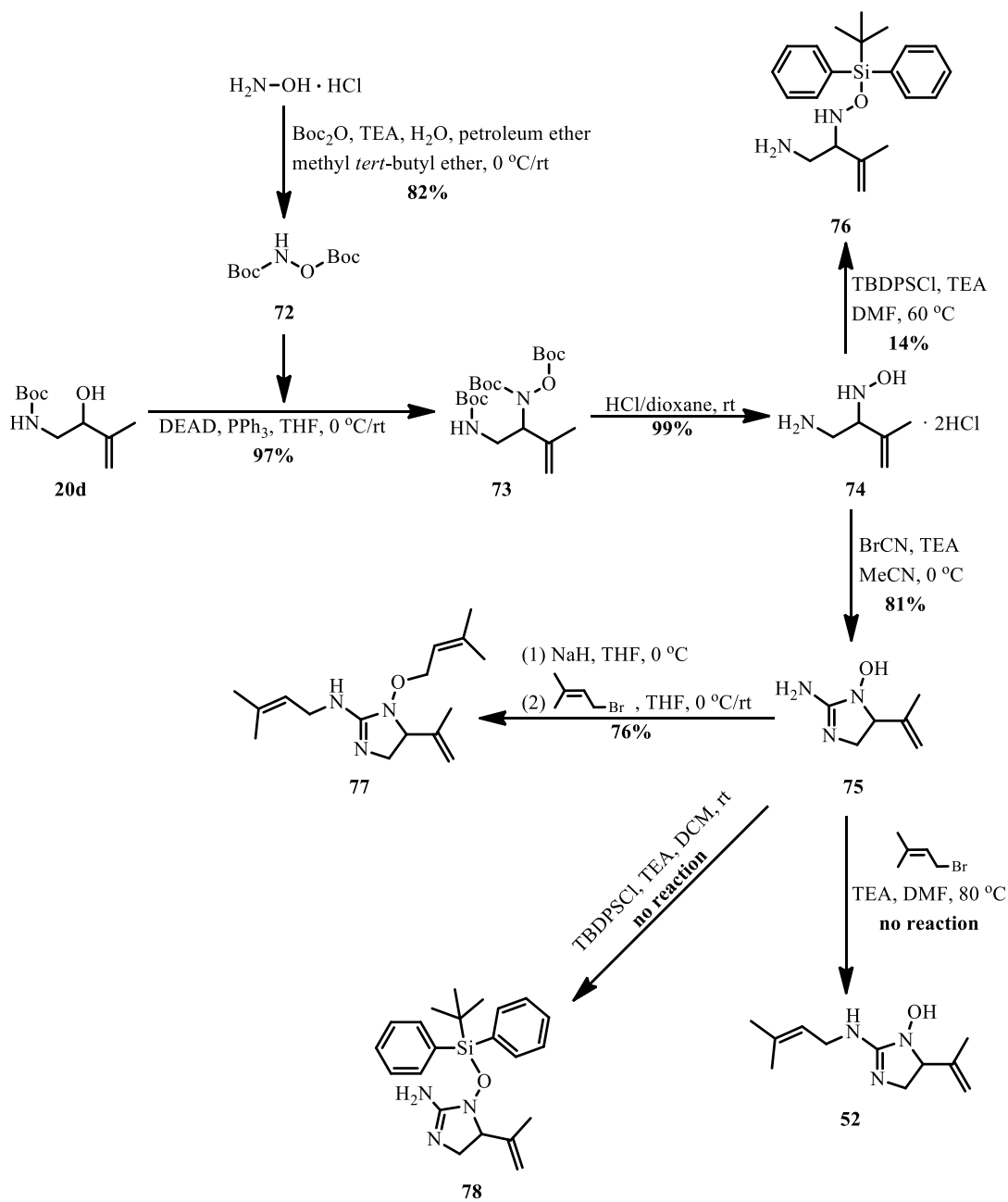


Scheme 4.8. Synthesis of 70 and 71 from alkoxyamine 67.

IVC. Verification of the structure of alchornedine

In Section IVA, we apprehended the total synthesis of cpd **43** as it was previously proposed to be alchornedine, a new natural product isolated from the leaves of *Alchornea glandulosa*. However, the NMRs of **43** did not conform to those provided in literature, indicating the true structure of alchornedine was not **43**. Based on the proposed biogenetic formation of alchornedine and M+1-16 peak in mass spectrum, 2-amino-imidazol-1-ol **52** was proposed to be the right structure of alchornedine, rather than **43** (*Scheme 4.4*). In this section, **52** would be synthesized to confirm our proposition for the structure of alchornedine.

The synthesis **52** was started from a previously synthesized alcohol **20d** (*Scheme 4.9*). Mitsunobu reaction of **20d** with *N,O*-diBoc hydroxylamine furnished the key intermediate **73** in 97% yield. The deprotection of **73** by HCl in dioxane provided *N*-alkyl hydroxylamine **74** in 99% yield, which was then cyclized into **75** by BrCN in 81% yield. 3,3-dimethyl allylic bromide and TEA in DMF failed to directly alkylated **75** into **52** even heated at 80 °C. When a stronger base NaH was used, **75** was *N,O*-dialkylated affording **77** in 76% yield. As shown in *Figure 4.10*, ¹H NMR of **77** in MeOD-*d*⁴ is quite similar to the one of alchornedine reported in literature (*Figure 4.9*), supporting our proposed structure of alchornedine. To block the nucleophilicity of the oxygen atom, TBDPSCl was used to protect the hydroxyl group in **74** or **75**. However, **76** was obtained in a low yield and TBDPSCl failed to protect the hydroxyl group in **75**.



Scheme 4.9. Synthesis of **52** via direct alkylation of **75** or TBDPS pre-protection.

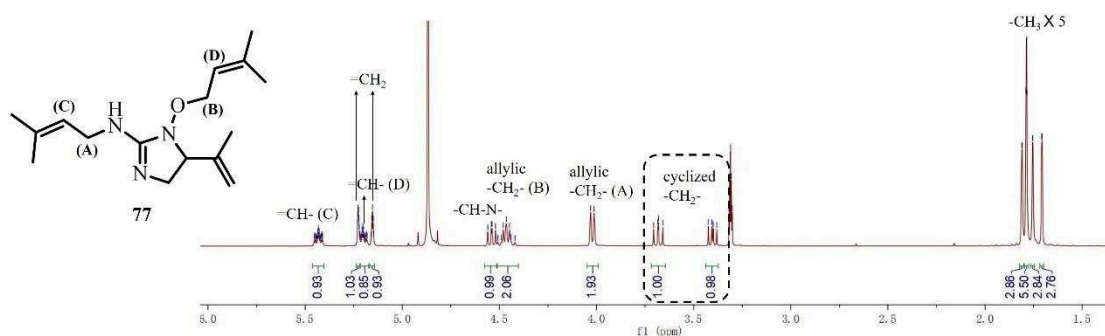
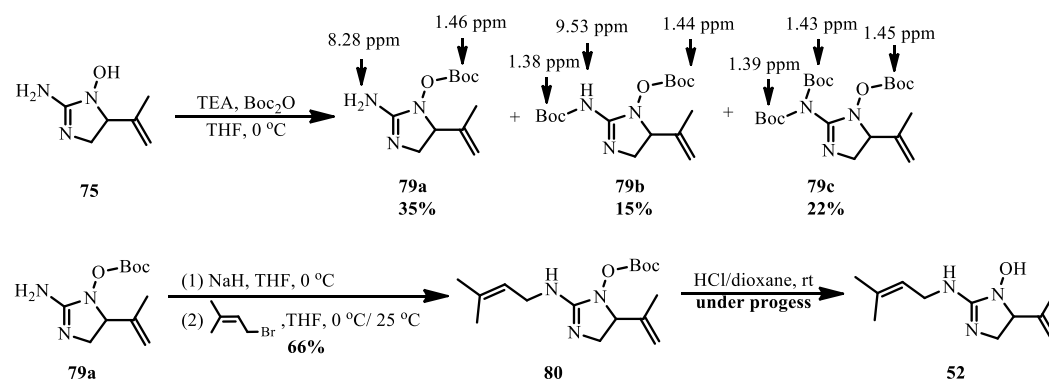


Figure 4.11. ^1H NMR of **77** in $\text{MeOD}-d^4$.

Since it is difficult to protect the hydroxyl group in **74** or **75** by TBDPSCl, Boc₂O was tried to protect **75** (2.1 eq. Boc₂O was used, decrease the equivalent of Boc₂O led to the remaining of **75**). As expected, three products, **79a**, **79b** and **79c** were separated by reverse phase chromatography in 35%, 15% and 22% yields, respectively. Their structures were identified by characteristic signals in ¹H NMR in DMSO-*d*⁶ (Scheme 4.10). 3,3-dimethyl allylic moiety was then introduced into **79a** after deprotonating the amino group with NaH, providing **80** in 66% yield. The structure of **80** was confirmed by ¹H NMR in DMSO-*d*⁶ where a -NH- peak (7.5 ppm), three =C-CH₃ peaks (1.74 ppm, 1.69 ppm, 1.64 ppm) and a Boc peak (1.47 ppm) were observed. The Boc deprotection of **80** with HCl in dioxane is currently under progress (Scheme 4.10). After **52** was obtained, ¹H NMR will be compared with the one in Figure 4.9 so that confirm our proposition for the corrected structure of alchornedine.



Scheme 4.10. Synthesis of **52** from **75** via Boc protection.

IVD. Conclusion

In this chapter, we try to synthesized **43** as it was proposed to be natural product alchornedine.¹³³ However, the inconsistency in ¹H NMRs indicated that **43** was not right structure of alchornedine (*Figure 4.8 and 4.9*). Based on mass spectrum and biogenetic formation (*Scheme 4.4*), we proposed the structure of alchornedine should be **52**. To confirm the proposition, the synthesis of **52** is currently under progress and its NMR will be compare with the one in literature (*Figure 4.9*).

**V. Dioxygenation of styrenes with
molecular oxygen in water, a green
approach to introduce N-O moiety**

V. Dioxygenation of styrenes with molecular oxygen in water, a green approach to introduce N-O moiety

Recently, green chemistry awareness attempts to address the environmental impact of both chemical products and the processes by which these are produced. Around 80 % of the chemical waste from a reaction mixture corresponds to the organic solvent.¹³⁵ Hence, the development of alternatives to organic solvents has emerged as a research topic of great interest. Water is commonly considered as a benign solvent in view of its environmentally safe and abundantly available in nature. Unfortunately, most organic reactants have poor solubility in water, leading to low yield and reaction rate. The development of organic synthesis in aqueous medium using surfactants appears as a promising ecofriendly strategy¹³⁶. Indeed, thanks to their amphiphilic nature, surfactants in water undergo spontaneous self-assembly into micelles, which then act as nanoreactors, as their hydrophobic cores play the role of reaction vessels in which the organic transformation involving water-insoluble reagents can occur (*Figure 5.1*).¹³⁷

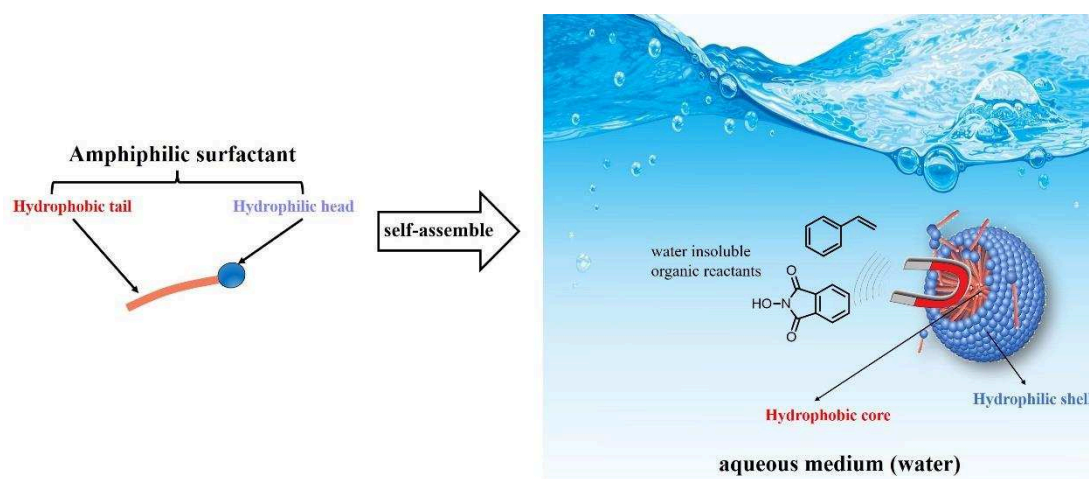
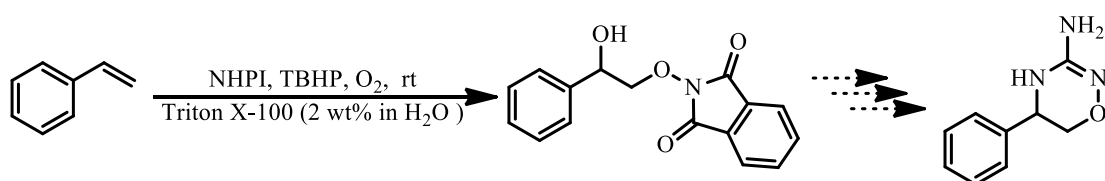


Figure 5.1 Surfactant assisted organic reaction in water.

In Chapter III and IV, various 1,2,4-oxadiazines have been synthesized and the key step was the introduction of N-O moiety by Mitsunobu reaction in THF. In view of

the importance of this key step and its environment concerns, a radical reaction was established to introduce the N-O moiety by dioxygenation of styrenes with molecular oxygen in water. The products obtained could be easily transformed into compounds with 1,2,4-oxadiazine scaffolds (*Scheme 5.1*). This part of work has been published in *Tetrahedron Letters* (Tang et al, DOI: [10.1016/j.tetlet.2018.03.009](https://doi.org/10.1016/j.tetlet.2018.03.009)) and the article has been inserted in Appendix VIII.¹³⁸



Scheme 5.1. Dioxygenation of styrenes with molecular oxygen in water.

VI. Synthesis of 2,3-benzoxazepin-4-one scaffold

VI. Synthesis of 2,3-benzoxazepin-4-one scaffold

Compounds containing diazepine moieties are of significant interest in medicinal and pharmaceutical research because of their important biological activities. Among them, seven-membered ring 1,4-benzodiazepine heterocycles have captured the imagination of medicinal and organic chemists for the past 60 years.¹³⁹ Besides being the core unit of traditional anxiolytics such as diazepam, oxazepam, lorazepam, clonazepam, and ketazolam (*Figure 6.1*), there are numerous 1,4-benzodiazepines under research (*Figure 6.2*), which exhibits biological activities such as anti-ulcer,¹⁴⁰ anti-viral,¹⁴¹ anti-toxin,¹⁴² anti-inflammatory,¹⁴³ anti-cancer,¹⁴⁴ and anti-bacterial.¹⁴⁵

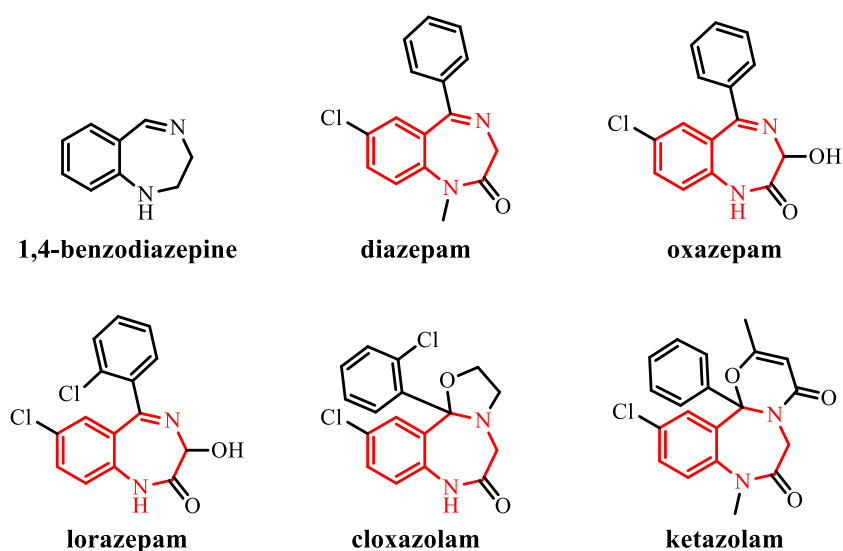


Figure 6.1. Examples of drugs exhibiting a 1,4-benzodiazepine scaffold

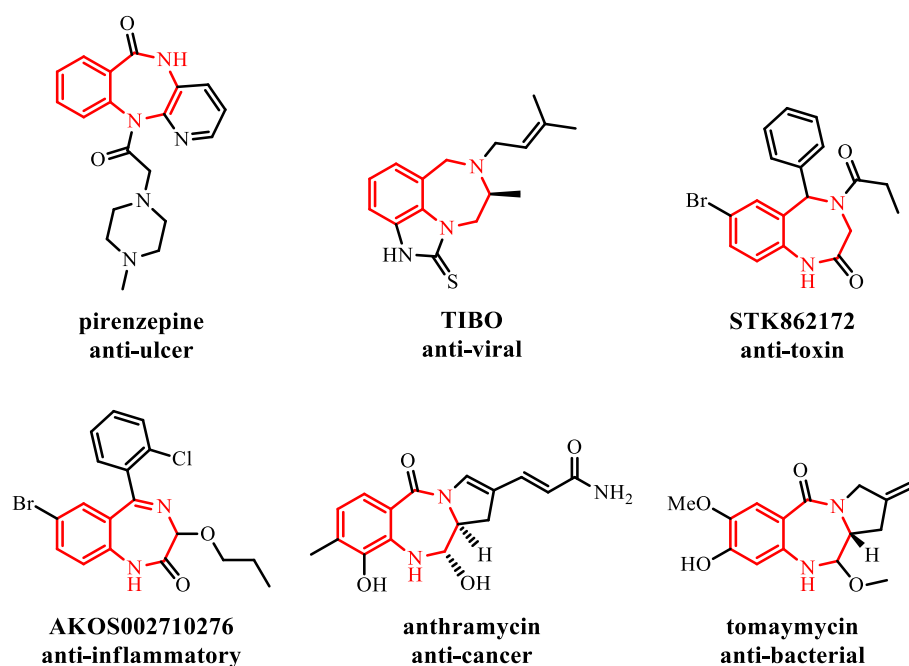


Figure 7.2. 1,4-benzodiazepines with different biological activities.

Changing the position of the nitrogen atoms in classical structure of 1,4-benzodiazepines leads to 2,3-benzodiazepines, which exhibit extremely rich pharmacological activities.¹⁴⁶ The first remarkable 2,3-benzodiazepine is tofisopam, a phosphodiesterases inhibitor which has been claimed to exert anxiolytic effects without sedation (Figure 6.3).^{147, 148} Further modifications of the substituents on the pharmacophore of tofisopam led to the discovery of GYKI 52466 (Figure 6.3). Similar to tofisopam, GYKI 52466 is a 2,3-benzodiazepine pharmacologically different from conventional 1,4-benzodiazepines, such as diazepam, in that they do not bind to type A γ -aminobutyric acid receptor (GABA_A receptor), and lack sedative-hypnotic activity. In addition, GYKI 52466 also acts as a noncompetitive AMPA receptor antagonist with anticonvulsant and neuroprotective properties, which induced growing interest focused on 2,3-benzodiazepines.¹⁴⁹ One major modification of the 2,3-benzodiazepine scaffold in GYKI 52466 is replacing the methyl by an oxygen or sulfur atom, leading to 1-aryl-2,3-benzodiazepine-4-one or 1-aryl-2,3-benzodiazepine-4-thione scaffold with higher anti-convulsant potency (Figure 6.3).¹⁴⁹⁻¹⁵⁹

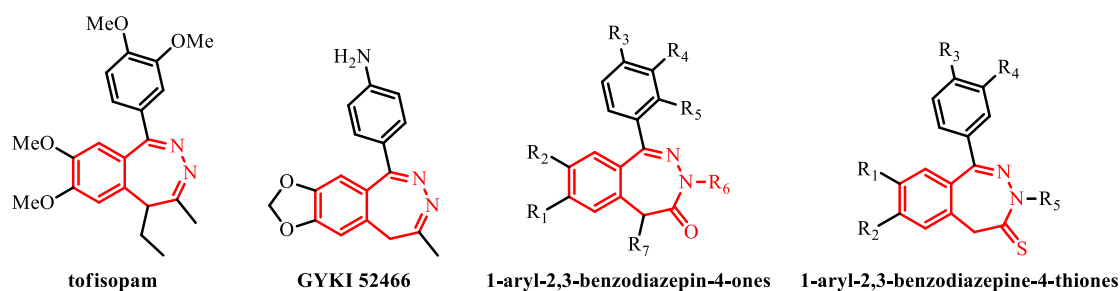


Figure 6.3. Tofisopam, GYKI 52466 and 1-aryl-2,3-benzodiazepine-4-(thi)ones.

Several 2,3-benzodiazepin-4-one derivatives were also developed as PDE-4 inhibitors in our group by pharmacophoric comparison between papaverine and tofisopam (Figure 1.10, Chapter I). Since most current researches of benzodiazepine focused on modifying the position of the two nitrogen atoms, the complexity of the scaffold is not significantly increased. In this chapter, one of the two adjacent nitrogen atoms in 2,3-benzodiazepine-4-one scaffold will be transposed by an oxygen atom to form 2,3-benzoxazepin-4-one scaffold (Figure 6.4). Due to the bivalent character of the oxygen atom, an additional stereogenic center will be obtained, making the geometry of 2,3-benzoxazepin-4-one more complex than the corresponding N-N heterocycle.

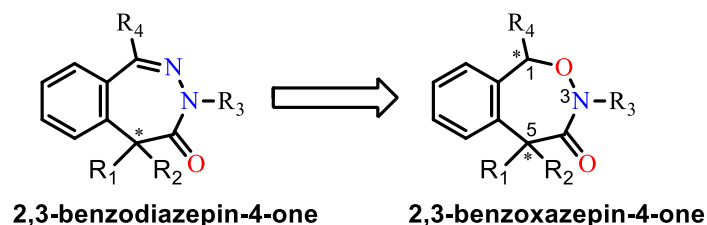
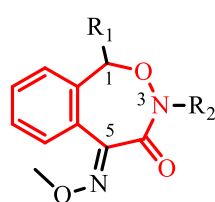


Figure 6.4. Development of 2,3-benzoxazepin-4-one from 2,3-benzodiazepine-4-one.

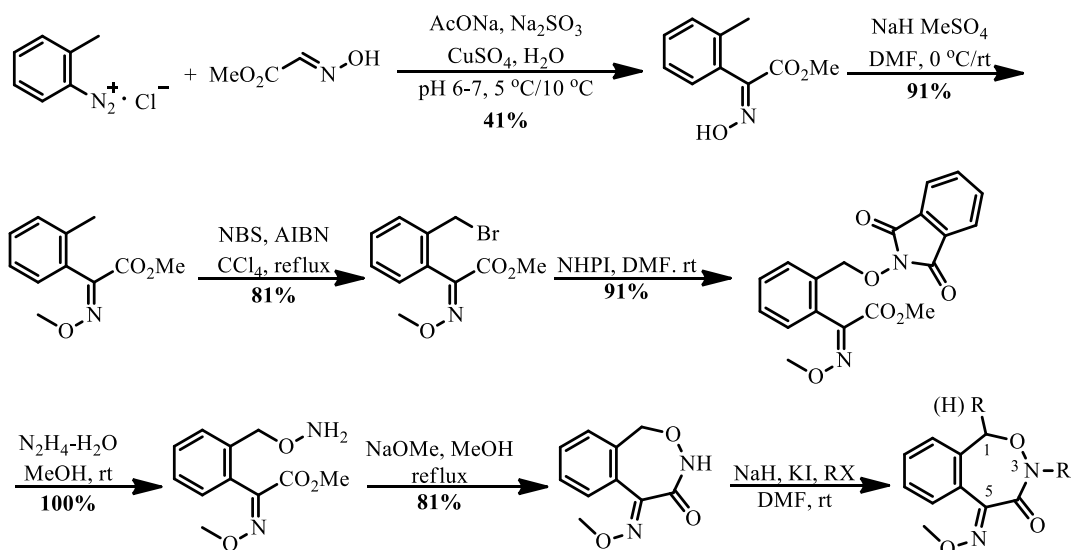
VIA. Synthesis of 1-phenyl-2,3-benzoxazepin-4-one scaffold

Contrary to benzodiazepine, little research has been done with benzoxazepine (49694 vs 842 references in Scifinder, using “benzodiazepine” or “benzoxazepine” as research topic). Only one reference was found when using 2,3-benzoxazepin-4-one as substructure in Scifinder (*Figure 6.5*).⁸⁹ Although this reported scaffold can be easily obtained in 6 steps, the methoxyimino function at position 5 is indispensable since “Meerwein arylation” between diazonium chloride and methyl 2-hydroxyiminoacetate was used as the initial step (*Scheme 6.1*).^{89, 160} Furthermore, most of these benzoxazepin-4-ones are achiral due to the unalterable methoxyimino function at position 5 and the limited substitution at position 1.



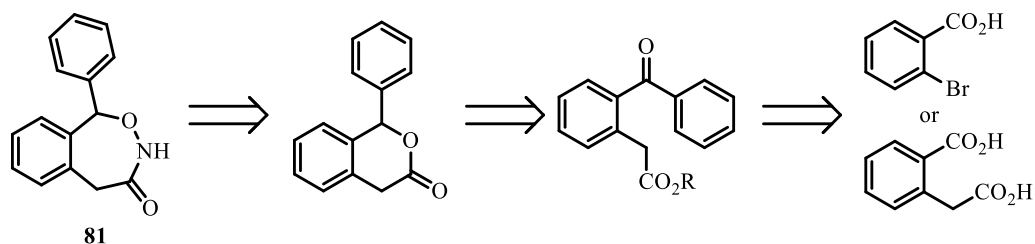
R ₁	R ₂	R ₁	R ₂
H	H	H	4-Me-benzyl
H	Me	H	4-CN-benzyl
H	Et	H	4-NO ₂ -benzyl
H	<i>n</i> -Pr	H	2-Cl-benzyl
H	allyl	H	(6-Cl-3-pyridinyl)methyl
H	propargyl	H	(2-chloro-5-thiazolyl)methyl
H	<i>n</i> -butyl	allyl	allyl
H	<i>n</i> -pentyl	2-Cl-benzyl	2-Cl-benzyl
H	<i>n</i> -hexanyl		
H	<i>n</i> -heptanyl		

Figure 6.5. Reported fungicidal 2,3-benzoxazepin-4-one.



Scheme 6.1. Reported method to synthesize 2,3-benzoxazepin-4-one scaffold.

As shown above, no synthetic approach has been reported so far to synthesize 1,5 positions modifiable 2,3-benzoxazepine-4-ones. Indeed, relative to five- or six-membered N-O heterocycles, the seven-membered one is more difficult to synthesize. Here, a general approach to synthesize 1-phenyl-2,3-benzoxazepin-4-one scaffold was proposed (*Scheme 6.2*), which mainly relies on the formation of a benzolactone as key-intermediate.

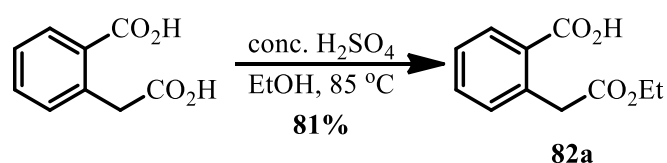


Scheme 6.2. Retrosynthesis of 1-phenyl-2,3-benzoxazepin-4-one scaffold.

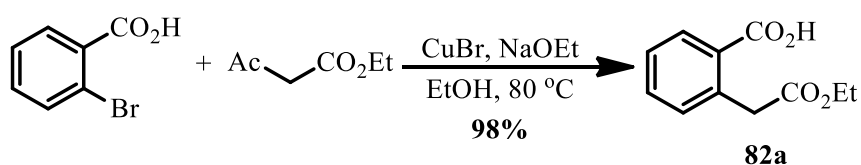
VIA1. Synthesis of 2-(2-ethoxy-2-oxoethyl)benzoic acid **82a**

One concise way to synthesize **82a** was the esterification of homophthalic acid with EtOH under the catalysis of concentrated H₂SO₄, furnishing **82a** in 81% yield (*Scheme 6.3*). Another method to synthesize **82a** involved the Hurtley reaction, a

copper-mediated acetylation of 2-halobenzoic acid with 1,3-dicarbonyl compounds.¹⁶¹ 2-bromobenzoic acid was coupled with ethyl acetoacetate in the presence of NaOEt and catalytic amount of CuBr in EtOH, which was then deacetylated *in situ* via retro-Claisen condensation to afford **2a** in 98% yield (*Scheme 6.4*). Although this method is relatively more complex than the one in *Scheme 6.3*, it has a better availability in starting materials with functionalized aryles.

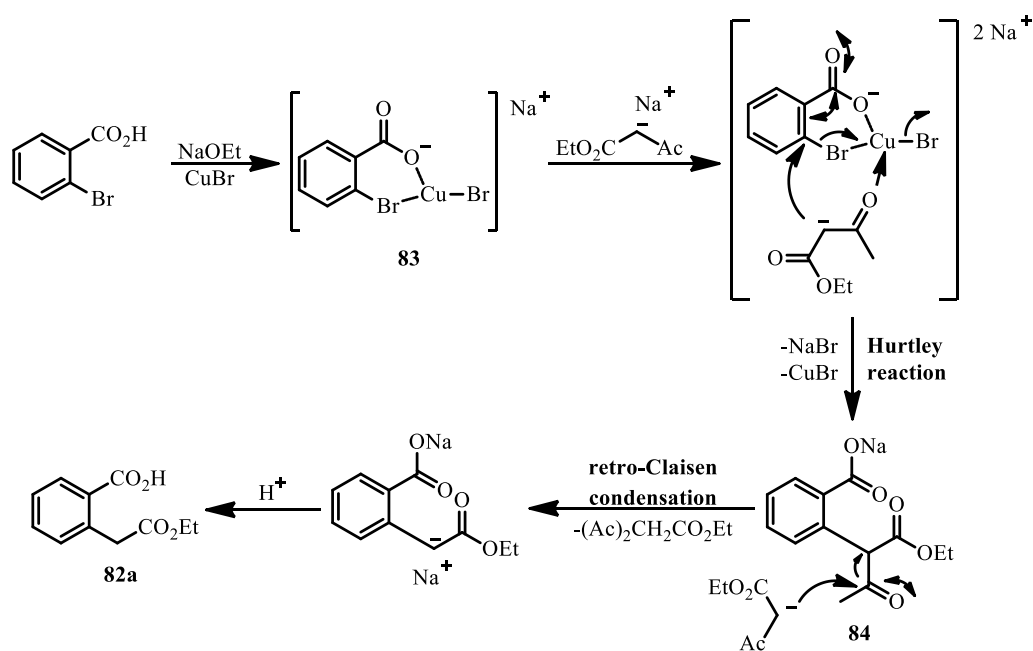


Scheme 6.3. Synthesis of 82a by esterification of homophthalic acid.



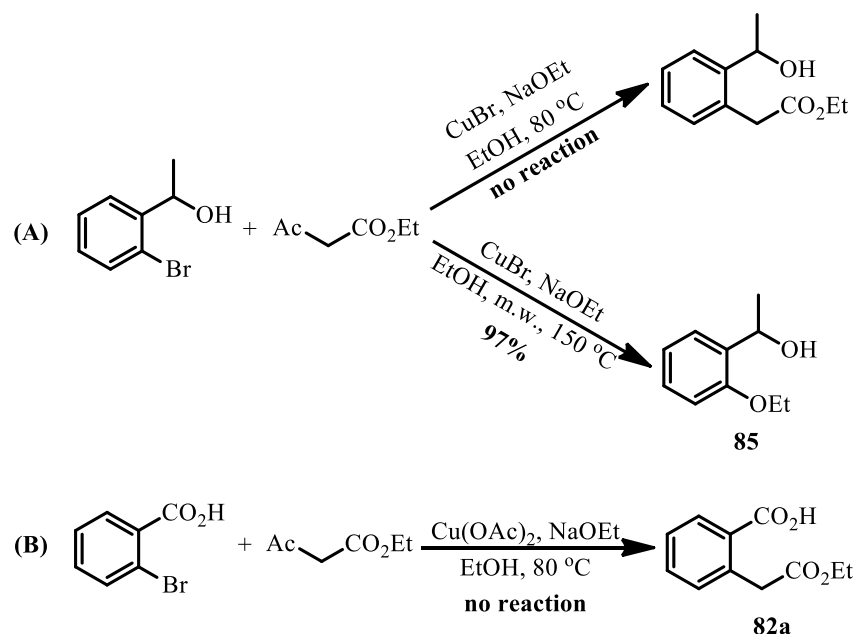
Scheme 6.4. Synthesis of 82a by tandem Hurtley–retro-Claisen reaction (2-bromobenzoic acid:ethyl acetoacetate:NaOEt = 1:2:3).

Scheme 6.5 shows a proposed mechanism of the tandem Hurtley–retro-Claisen reaction. The copper (I) carboxylate **83** is the essential intermediate for Hurtley reaction in that the polarization of the C-Br bond is augmented by intra-molecular coordination of the bromine atom to the copper (I) atom, facilitating the attack of ethyl acetoacetate carbanion and promoting the formation of the coupling product **84**.¹⁶²⁻¹⁶⁴ As EtONa (3 eq.) is fully used to deprotonate 2-bromobenzoic acid (1 eq.) as well ethyl acetoacetate (2 eq), the carbonyl of **84** is attacked by remaining ethyl acetoacetate carbanion and undergoes a retro-Claisen condensation by removing an ethyl diacetoacetate. Acidification of the reaction mixture finally gave the desired product **82a**.



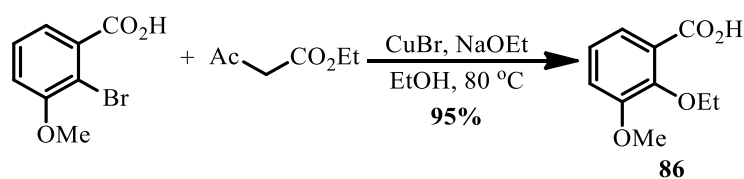
Scheme 6.5. Mechanism of Hurtley-retro-Claisen reactions.

It is noteworthy that the carboxylic group is indispensable since no reaction happened when replacing 2-bromobenzoic acid by 1-(2-bromophenyl)ethanol. Moreover, under microwave irradiation at 150 °C, ethoxylation rather than Hurtley reaction happened (*Scheme 6.6A*). In the literature, Cu(II) catalysts were efficiently used in Hurtley reaction.^{165, 166} Surprisingly, replacement of Cu(I)Br by Cu(II)(OAc)₂ prevented Hurtley reaction (*Scheme 6.6B*).



Scheme 6.6. (A) Hurltley reaction in the absence of carboxylic group. (B) Hurltley reaction in the absence of CuBr.

The ratio of the reactants (2-halobenzoic acid:ethyl acetoacetate:NaOEt = 1:2:3) was also important to Hurltley–retro-Claisen reaction. An excess of NaOEt (2-halobenzoic acid:ethyl acetoacetate:NaOEt = 1:2:4) led to the formation of ethoxylated product **86** in 95% yield (Scheme 6.7).



Scheme 6.7. Ethoxylation, rather than Hurltley reaction in an excess NaOEt (2-bromo-3-methoxybenzoic acid:ethyl acetoacetate:NaOEt = 1:2:4).

To explore the scope of the tandem Hurltley–retro-Claisen reaction, different 2-halobenzoic acids were used as starting material (Figure 6.6). The reactions worked well with 2-bromo or 2-iodobenzoic acids bearing electro-donating/withdrawing substituents (**82b-82h**, **82k**). For 2-chlorobenzoic acids, the synthesis of **82j** needed a

longer reaction time but led to a good 89% yield, while no reaction happened with 2,3-dichlorobenzoic acid (**82i**).

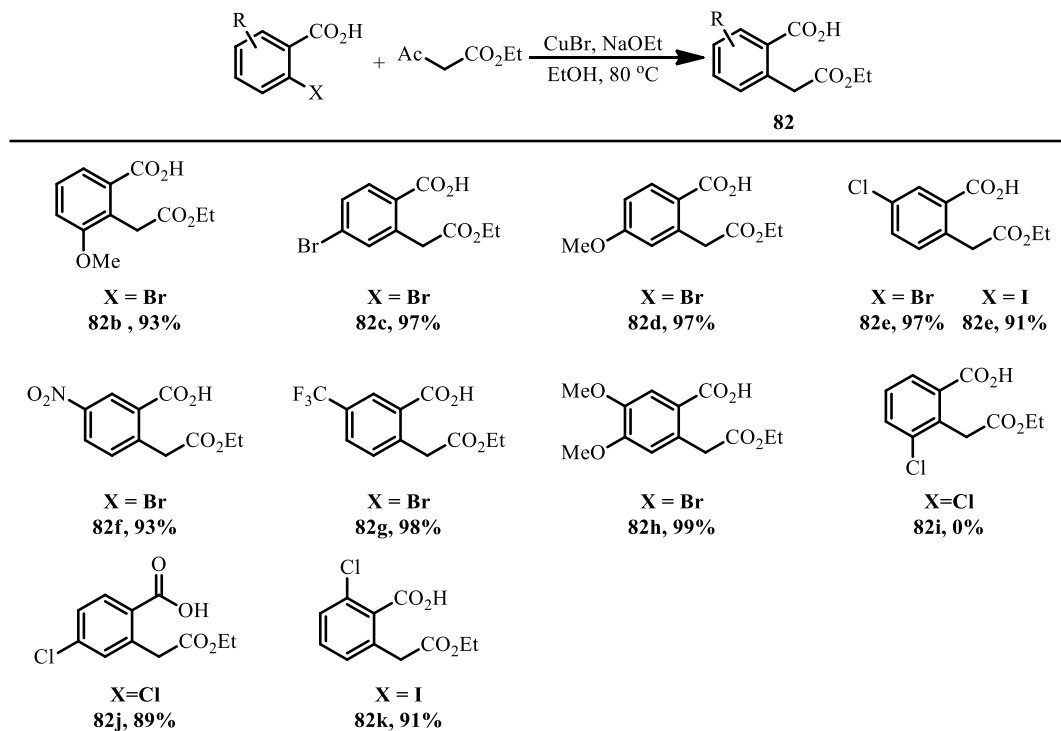
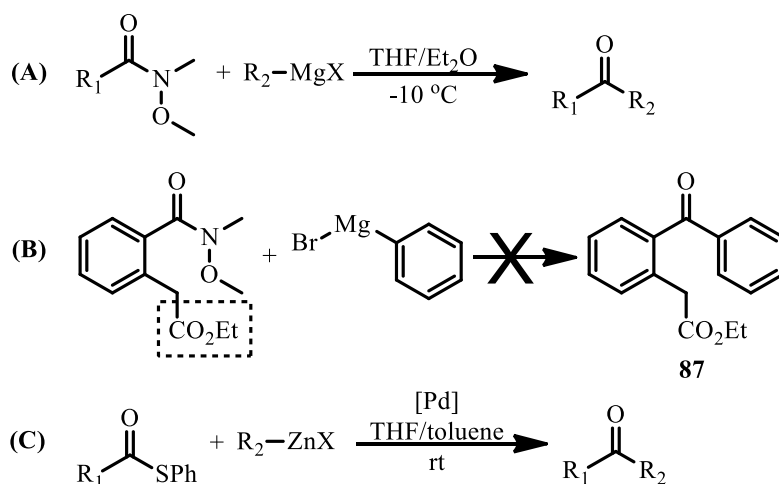


Figure 6.6. CuBr catalyzed tandem Hurtley–retro-Claisen reaction.

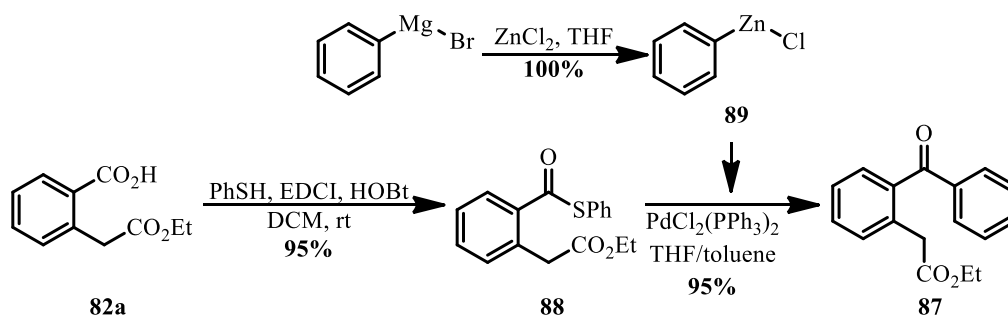
VIA2. Synthesis of ethyl 2-(2-benzoylphenyl)acetate **87**

During the synthesis of 1,2,4-oxadiazine scaffolds, the ketone intermediates were synthesized through the reaction of Weinreb amide with Grignard reagent (*Scheme 6.8A*). However, this method was not suitable for the synthesis of ketone **87** because of the presence of ester function, which could be attacked by the organo-magnesium reagents (*Scheme 6.8B*). Since the organo-zinc reagents were less active relative to the corresponding organo-magnesium, the Fukuyama CCR between thioester and organo-zinc reagent was applied to form the diaryketone **87** (*Scheme 6.8C*).



Scheme 6.8. (A) Ketone synthesis through Weinreb amide and Grignard reagent. (B) Ester function incompatible with Grignard reagent. (C) Fukuyama cross-coupling reaction.

By using HOBt and EDCI as coupling reagents, **82a** was thioesterified into **88** in 95% yield (*Scheme 6.9*). Organo-zinc reagent **89** was afforded in quantitative yield by adding PhMgBr into excess anhydrous ZnCl₂/THF solution. PdCl₂(PPh₃)₂ successfully catalyzed the Fukuyama reaction between thioester **88** and organo-zinc reagent **89**, giving diarylketone **87** in 95% yield (*Scheme 7.9*).



Scheme 6.9. Synthesis of diarylketone 87 via Fukuyama cross-coupling reaction of thioester 88 and organo-zinc reagent 89.

VIA3. Reduction of ethyl 2-(2-benzoylphenyl)acetate **87**

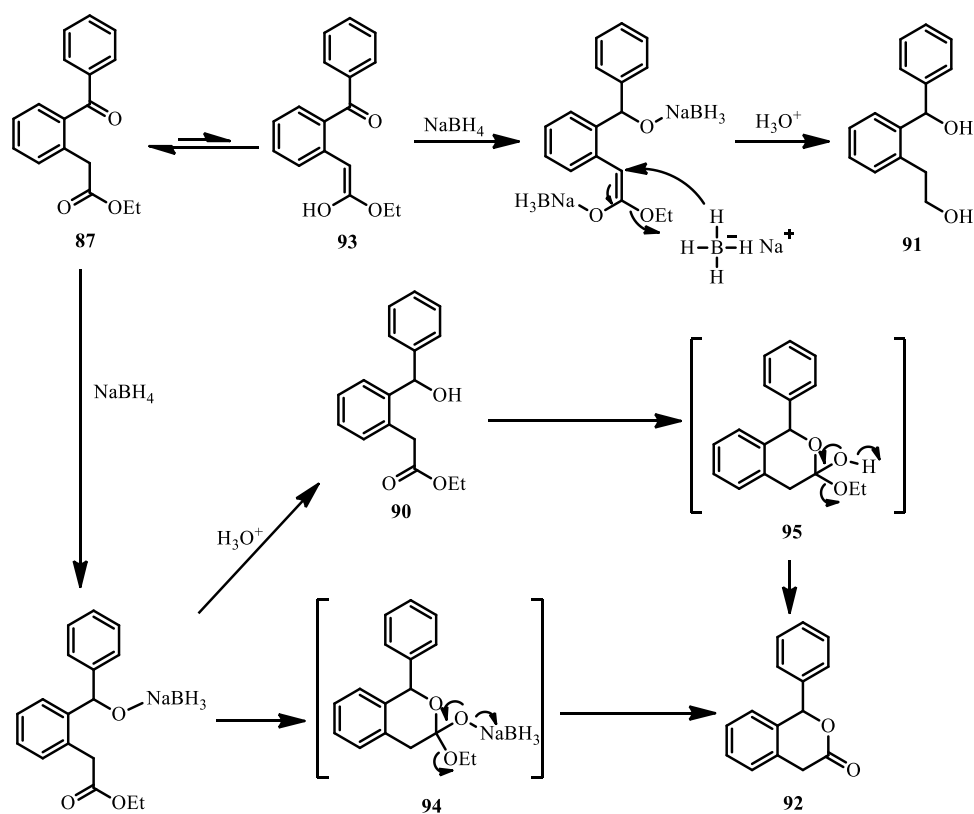
As a prerequisite condition to introduce the N-O bond, several methods were tried

to reduce diarylketone **87** into alcohol **90** (Table 6.1). However, both Zn/NaOH at 100 °C or NaBH₄ at rt reduced the ester group, leading to the formation of diol **91** in 100% and 94% yields, respectively. Reduction of ester group by NaBH₄ was inevitable even when the temperature was decreased to -70 °C, leading to a mixture of the desired product **90**, diol **91** and lactone **92**. Purification of the reaction mixture by normal phase chromatography resulted in total transformation of **90** into **92**, lactone **92** and diol **91** were obtained in 51% and 47% yields, respectively. A weaker reductant, Na(CN)BH₃ failed to reduce ketone **87**.

Table 6.1. Reduction of diarylketone **87**.

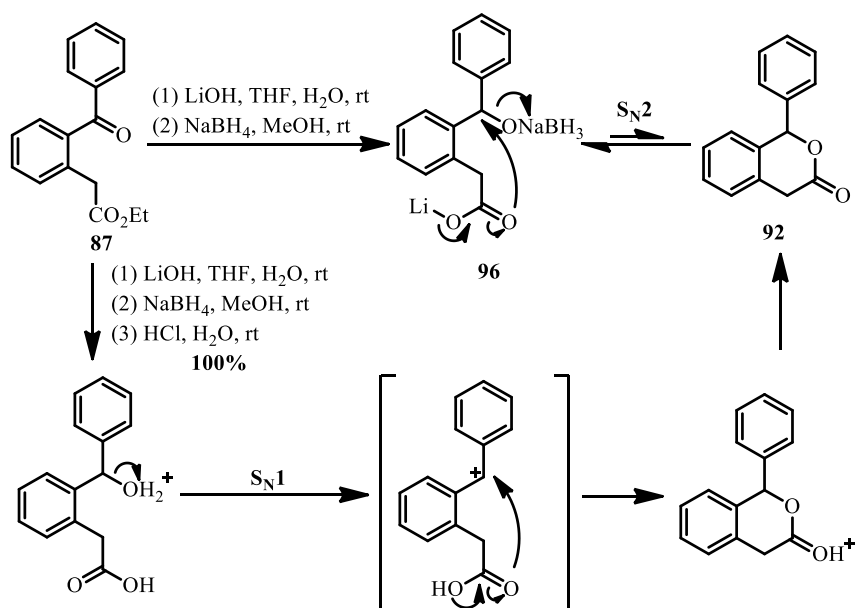
Conditions	90 (%)	91 (%)	92 (%)
Zn, NaOH, H ₂ O, 100 °C	-	100	-
NaBH ₄ , EtOH, rt	-	94	-
NaBH ₄ , EtOH, -70 °C	instable	47	51
Na(CN)BH ₃ , EtOH, rt	no reaction		

Generally, ester groups could not be reduced by NaBH₄ at -70 °C. However, due to the benzophenone moiety at the α -carbon of ester function in **87**, the enol tautomer **93** will be stabilized by the presence of a long conjugation system. As electron-withdrawing groups, the hydroxy and ethoxy groups in **93** enhance the polarity of the enol double bond, facilitating the attack of NaBH₄ and leading to the formation of diol **91**. In a different mechanism, lactone **92** is formed through two kinds of favored six-membered transition states **94** and **95** after the desired reduction of **87**. (Scheme 6.11)



Scheme 6.11. Proposed mechanism for NaBH_4 reduction of diarylketone **87**.

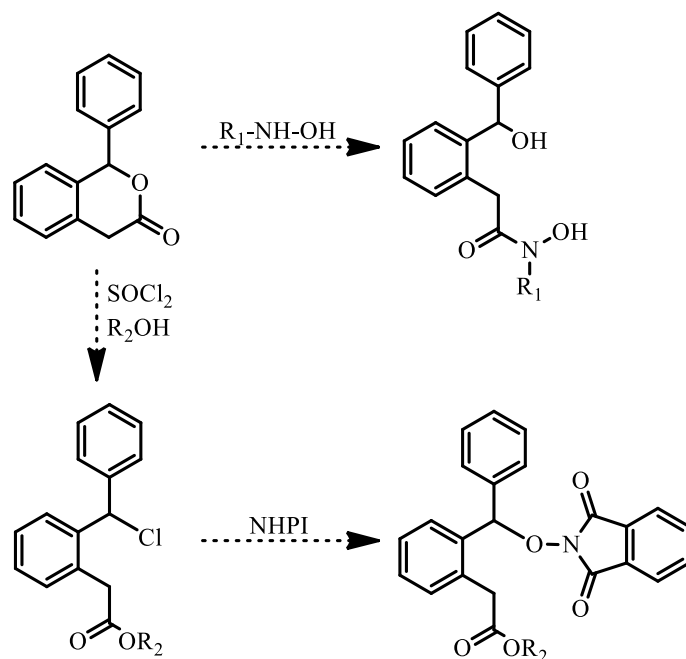
To avoid the formation of diol **91**, the ester group in diarylketone **87** was first hydrolyzed into carboxylic group as it is more tolerant towards NaBH_4 reduction. Diarylketone **87** was hydrolyzed by LiOH , followed by NaBH_4 reduction, leading to a mixture of intermediate **96** and lactone **92**. However, further acidification of the reaction mixture produced lactone **92** in quantitative yield through an expected $\text{S}_{\text{N}}1$ mechanism favoring the lactone formation (Scheme 7.12).



Scheme 6.12. Synthesis and mechanism of lactone 92 from diarylketone 87 in a tandem hydrolysis, reduction and acidification.

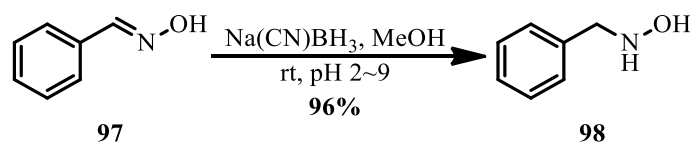
VIA4. Introduction of the N-O moiety

During the synthesis of 1,2,4-oxadiazine scaffold, the N-O moiety was introduced by Mitsunobu reaction between alcohol and NHPI. However, as shown in *Scheme 6.12*, reduction of diarylketone **87** led to lactone **92**, which means N-O moiety cannot be readily introduced by Mitsunobu reaction with NHPI anymore. As a result, two methods were proposed here to open the lactone ring, either by nucleophilic attack of the ester group with hydroxylamine, or by chlorination of the diphenylmethyl position followed by the introduction of NHPI (*Scheme 6.13*).



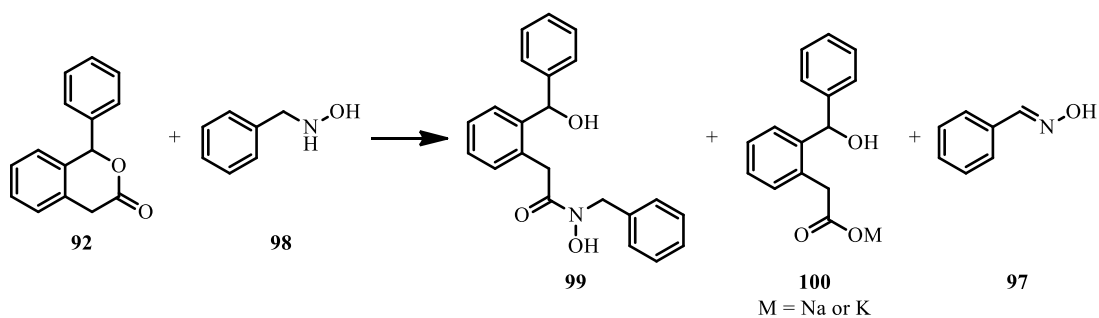
Scheme 6.13. Introduction of the N-O moiety in lactone.

N-benzylhydroxylamine **98**, which was prepared from $\text{Na}(\text{CN})\text{BH}_3$ reduction of oxime **97** (Scheme 6.14), was first tried to insert the N-O moiety into **92**. As shown in Table 6.2, coupling reagents DCC and DMAP in DCM led to a complex mixture, while no reaction happened between lactone **92** and *N*-benzylhydroxylamine **98** in MeOH with/without TEA. Strong bases such as KOH in MeOH or NaOEt in EtOH quantitatively oxidized **98** into oxime **97**, along with the formation of carboxylate **100**, which was easily cyclized into lactone **92** after acidification (mechanism discussed in Scheme 6.12.).



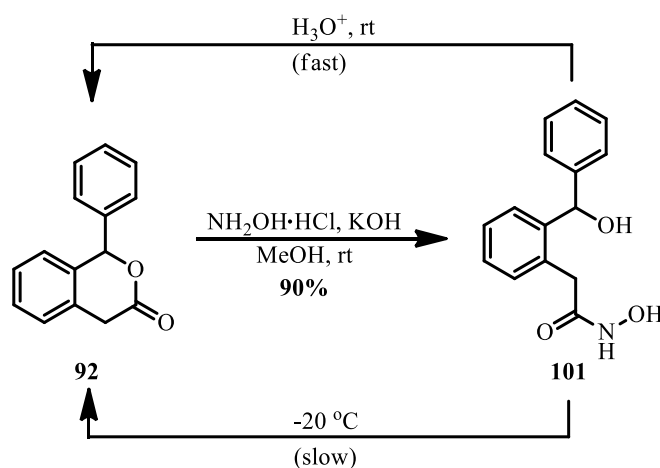
Scheme 6.14. Reduction of (*E*)-benzaldehyde oxime **97**.

Table 6.2. Insertion N-O moiety with *N*-benzylhydroxylamine **98**.



Conditions	99 (%)	100 (%)	97 (%)
DCC, DMAP, DCM, rt		complex mixture	
MeOH, rt		no reaction	
TEA, MeOH, rt		no reaction	
KOH, MeOH, rt	0%	100%	100%
NaOEt, EtOH, rt	0%	60%	100%

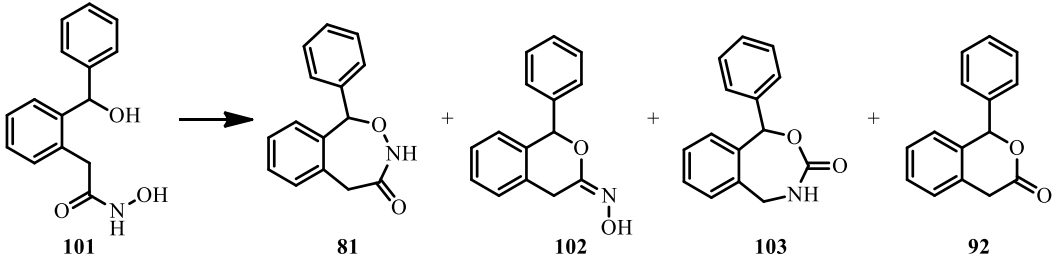
Because of the instability of **98** under basic conditions, hydroxylamine in MeOH was used to insert N-O moiety into lactone **92**, affording an instable hydroxamic acid **101** in 90% yield (*Scheme 6.15*). Similar to carboxylate **100**, hydroxamic acid **101** could be easily cyclized into lactone **92** under acidic condition. Even stored at $-20\text{ }^{\circ}\text{C}$, spontaneous cyclization of **101** was observed although in relatively slow rate.



Scheme 6.15. Synthesis of hydroxamic acid 101 and its instability.

In agreement with its poor stability, **101** was used immediately for next step. So far, no efficient method was found to cyclize hydroxamic acid **101** into benzoxazepinone **81** (Table 6.3). The first attempt we tried was to transform the benzylic hydroxyl group of **101** into a good leaving group such as mesylate or bromide, which would facilitate the cyclization. Unexpectedly, MsCl or PBr₃ under basic conditions led to lactone **92** as major product. Intra-molecular Mitsunobu reaction of **101** produced oxime **102**, carbamate **103** and lactone **92** in 18%, 41% and 34% yields, respectively. Similarly, application of CDI at room temperature led to the cyclization of hydroxamic acid **101** into oxime **102**, carbamate **103** and lactone **92** in 56%, 27% and 11% yields, respectively. Finally, microwave irradiation of **101** with CDI at 120 °C led to lactone **92** in quantitative yield.

Table 6.3. Cyclization of hydroxamic acid **101**.



The reaction scheme shows the cyclization of hydroxamic acid **101** into four products: benzoxazepinone **81**, alkoxy oxime **102**, cyclic carbamate **103**, and lactone **92**. The starting material **101** is a 2-phenyl-2-(2-hydroxy-1-phenylethyl)acetohydroxamic acid derivative. The products are shown as a mixture of **81**, **102**, **103**, and **92**.

Conditions	81 (%)	102 (%)	103 (%)	92 (%)
TEA, MsCl, DMAP, toluene, rt	0	trace	trace	64
TEA, MsCl, DMAP, THF, rt	0	trace	trace	83
pyridine, PBr ₃ , Et ₂ O, 0 °C	0	trace	trace	91
DIAD, PPh ₃ , THF, 0 °C /rt	0	18	41	34
CDI, THF, rt	0	56	27	11
CDI, THF, m.w., 120 °C	0	0	0	100

Here we proposed a potential mechanism for the CDI-mediated formation of alkoxy oxime **102** and cyclic carbamate **103** (Scheme 6.16). Tautomerism of hydroxamic acid **101** into imino-diol and subsequent reaction with CDI led to the

formation of a dioxazolone ring, which was then opened by hydroxyl group nearby to form the cyclic oxime **102**.¹⁶⁷ Although NMR spectra (See *Figure 6.8*) as well as exact mass of **102** were in agreement with the initially expected 6/7 fused bicycle benzoxazepinone **81**, X-ray crystallography of single crystals recrystallized by slow evaporation from MeCN solution allowed us to formally identify the 6/6 fused bicycle **102** (*Figure 6.7*). The details of the crystallographic data and structure refinement parameters are summarized in Appendix IV.

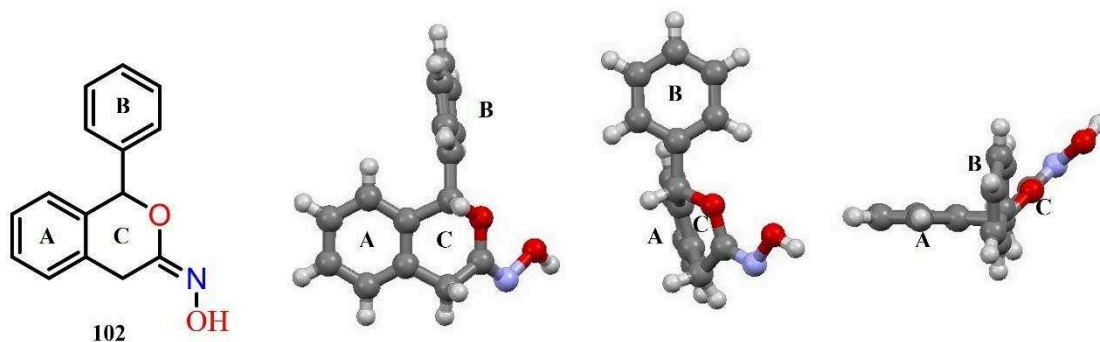
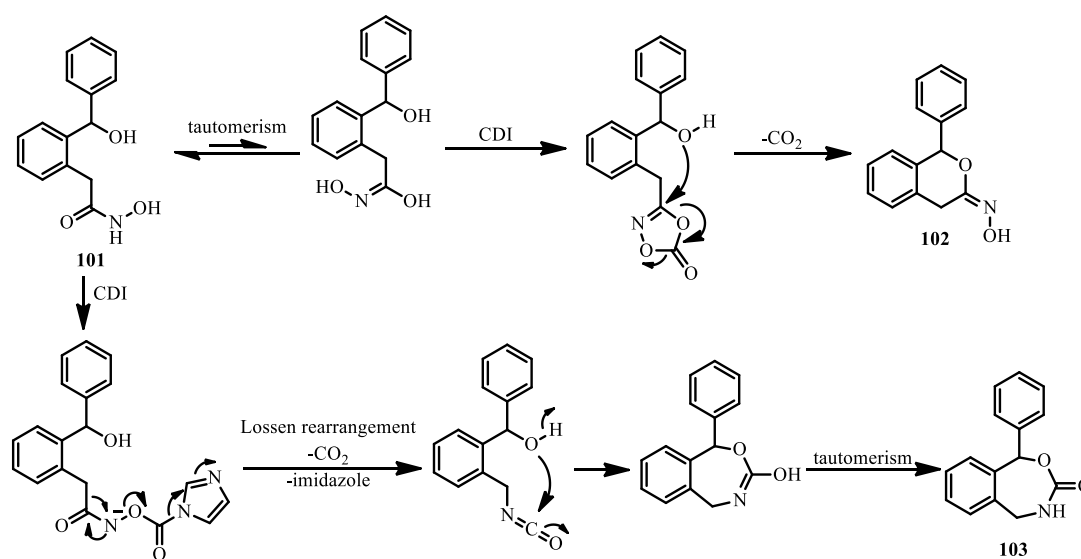


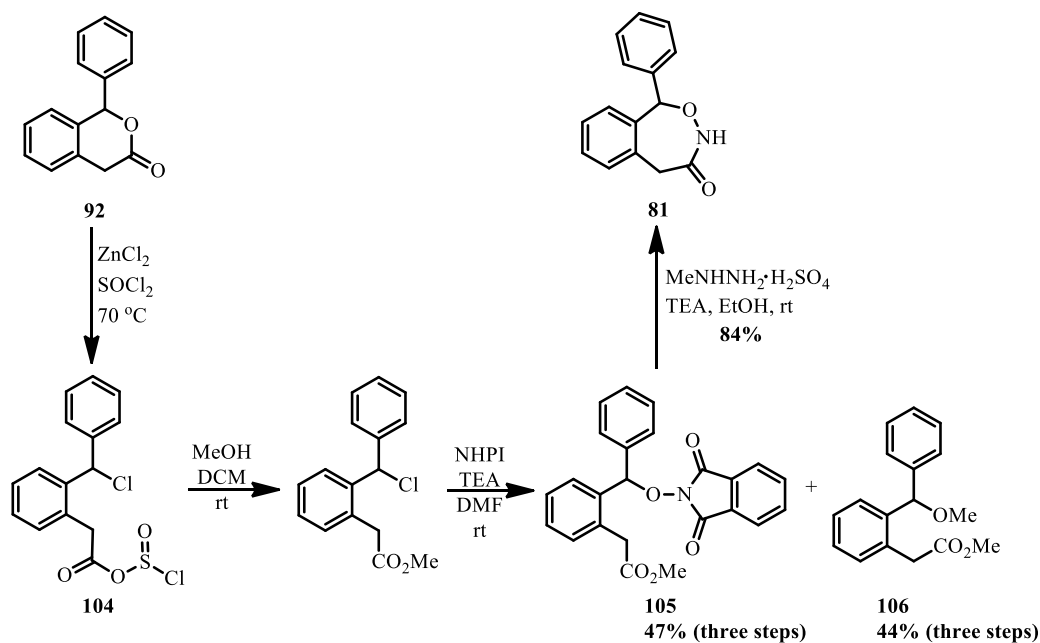
Figure 6.7. X-ray crystallography of oxime 102 displayed with front view, right view and top view.

Concomitantly with the formation of **102**, direct nucleophilic attack of **101** towards CDI generated an amidoacetate, which underwent Lossen rearrangement and produced an isocyanate (*Scheme 6.16*). Intra-molecular nucleophilic addition of the benzylic hydroxyl group on isocyanate and subsequent tautomerism resulted into the formation of **103**. Its structure was confirmed by comparison with literature.¹⁶⁸ Similar mechanism may be proposed under Mitsunobu conditions (DIAD/PPh₃).



Scheme 6.16. Mechanism for the formation of oxime 102 and carbamate 103.

As shown above, inserting N-O moiety on carbonyl group of **92** under basic conditions and subsequent cyclization by intra-molecular Mitsunobu reaction or CDI finally led to the formation of oxime **102** and carbamate **103**, rather than the desired benzoxazepinone **81**. Thus, a tandem approach was tried to first introduce N-O moiety at benzylic position (*Scheme 6.17*). SOCl₂ with catalytic amount of ZnCl₂ successfully transformed **92** into benzyl acyl dichloride **104**, which was subsequently esterified by MeOH. The addition of NHPI under basic condition afforded the expected alkoxyamine **105** as well as the alkoxy ester **106** in 47% and 44% yields, respectively. Deprotection of **105** with methyl hydrazine directly led to the cyclized 2,3-benzoxazepin-4-one **81** in 84% yield (*Scheme 6.17*).



Scheme 6.17. Introduction of N-O moiety at benzylic position.

As isomers, the structure of oxime **102**, carbamate **103** and benzoxazinone **81** could be identified by NMRs (*Figure 6.8 and 6.9*). The main difference of oxime **102** from the other two is that it shown a =N-OH peak at 9.35 ppm in ^1H NMR, a $-\text{CH}_2-$ peak at 30.1 ppm and a $-\text{C}=\text{N}-$ peak at 150.77 ppm in ^{13}C NMR. In ^1H NMR of carbamate **103**, it shown a $-\text{NH}-$ peak at 7.74 ppm and one of the two protons in $-\text{CH}_2-$ shown a *dd* peak at 4.06 ppm due to the presence of the adjacent $-\text{NH}-$ group. Because of the electro-withdrawing effect of bilateral oxygen atom and carbonyl group, the $-\text{NH}-$ peak of benzoxazinone **1** locates at 11.01 ppm in ^1H NMR. Far different from the carbamate $>\text{C}=\text{O}$ peak of **103** at 154.59 ppm., the hydroxamate $>\text{C}=\text{O}$ peak of benzoxazinone **81** locates at 176.48 ppm in ^{13}C NMR.

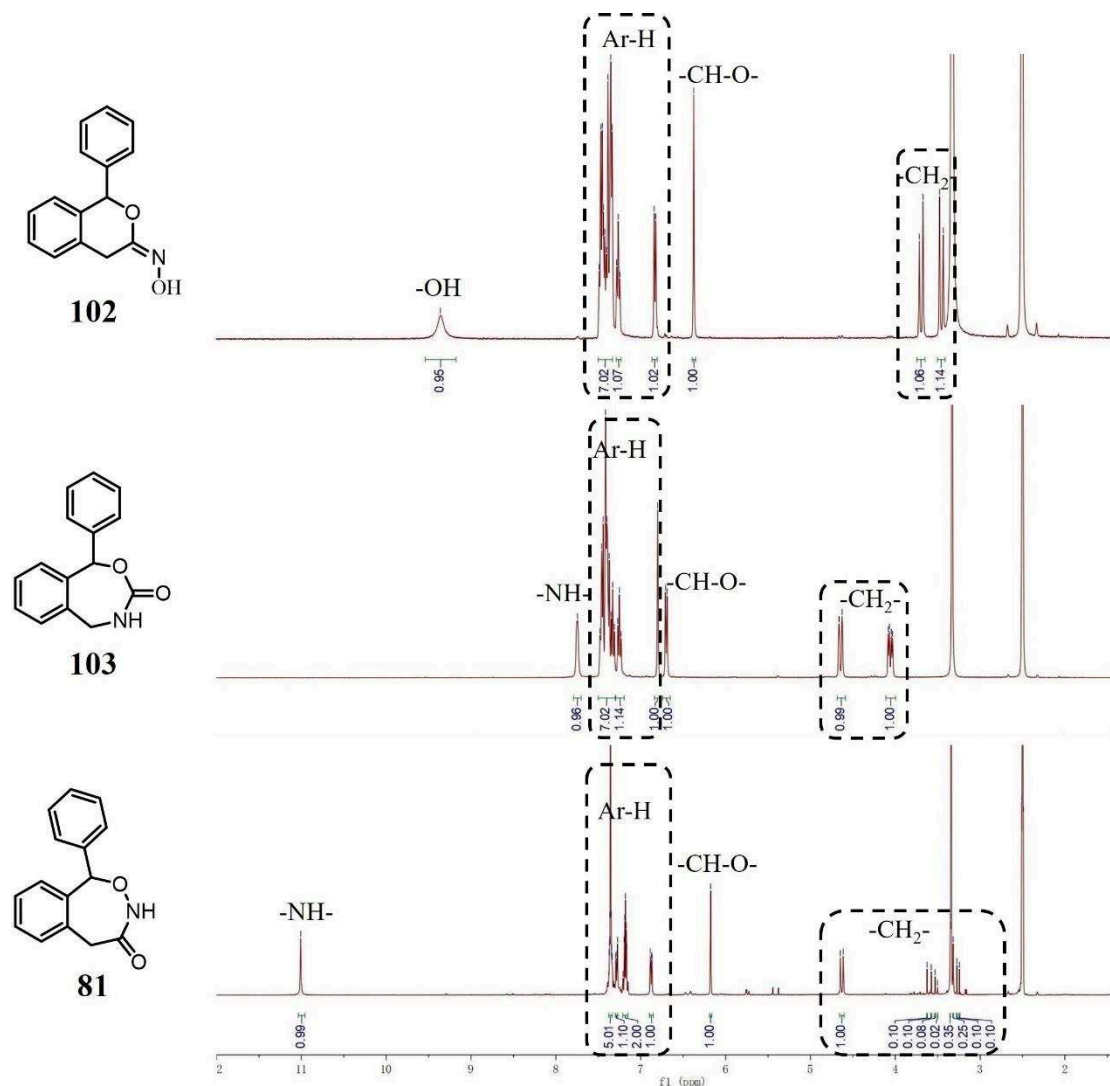


Figure 6.8. ^1H NMRs of oxime **102**, carbamate **103** and benzoxazepinone **81**.

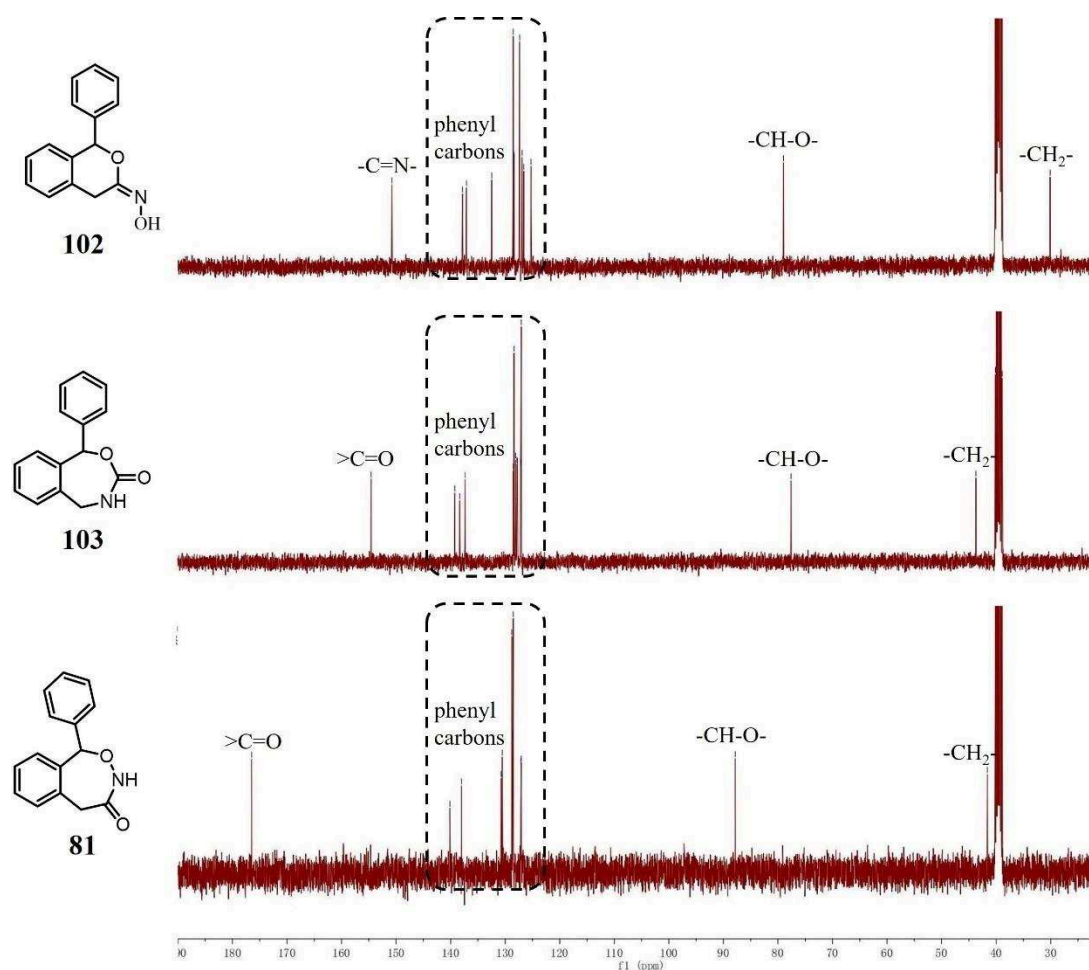


Figure 6.9. ^{13}C NMRs of oxime **102**, carbamate **103** and benzoxazepinone **81**.

To provide more evidence for the structures of **81**, it was recrystallized by slow evaporation from MeCN solution. Single-crystal X-ray diffraction analysis showed that the crystal structure **81** belongs to 2,3-benzoxazepin-4-one scaffold (Figure 6.10). The details of the crystallographic data and structure refinement parameters are summarized in Appendix V.

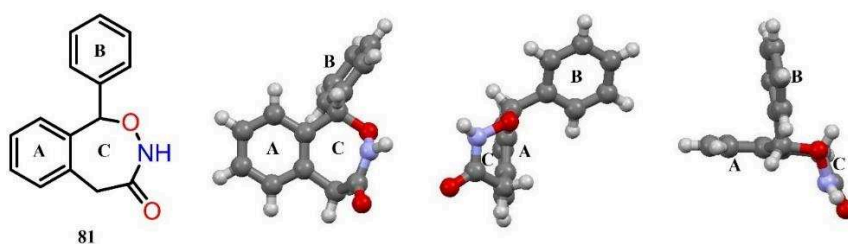
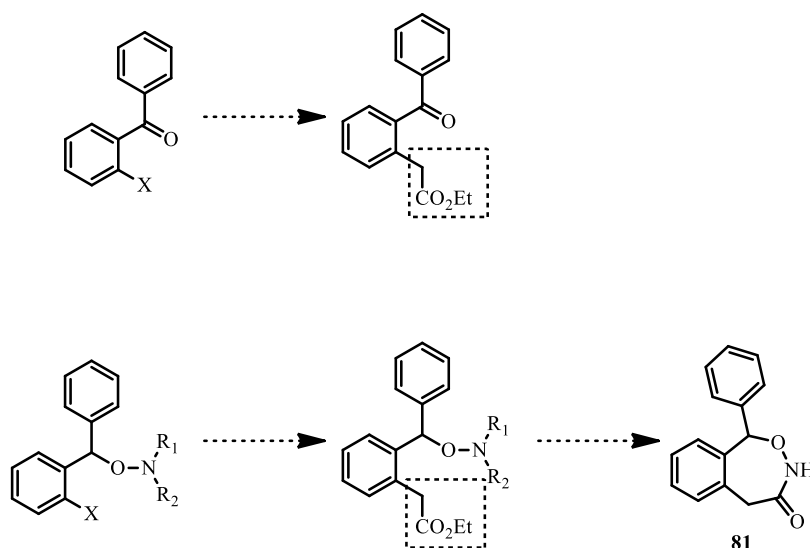


Figure 6.10. X-ray crystallography of 1-phenyl-2,3-benzoxazepin-4-one **81** displayed with front view, right view and top view.

VIB. Other methods to synthesize 1-phenyl-2,3-benzoxazepin-4-one scaffold

During the development of aforementioned method to synthesize 1-phenyl-2,3-benzoxazepin-4-one **81**, other synthetic approaches were attempted in which 2-bromobenzaldehyde or 2-iodobenzoic acid was used as starting material. The general idea of these approaches was to couple the ester moiety on diaryl ketone or alkoxyamine (Scheme 6.18).

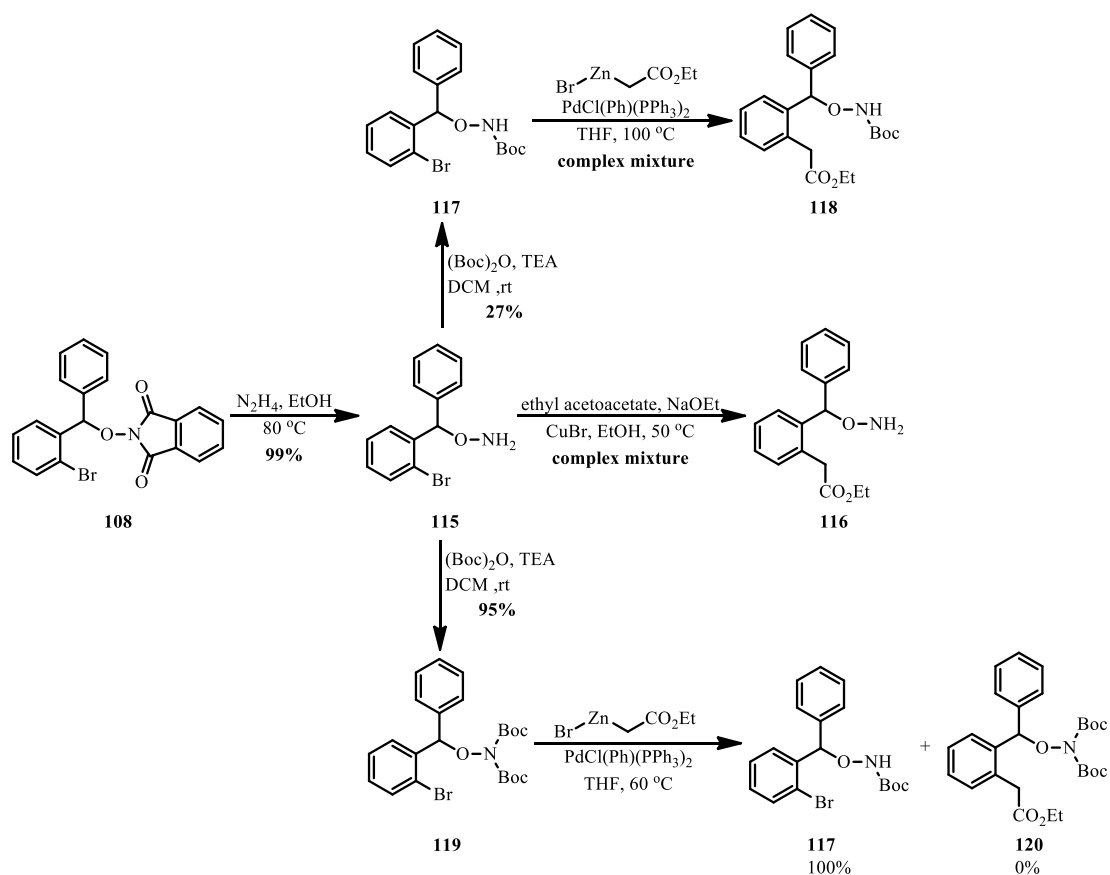


Scheme 6.18. Coupling the ester moiety on diaryl ketone or alkoxyamine.

VIB1. Starting from 2-bromobenzaldehyde

To construct the diaryl scaffold, 2-bromobenzaldehyde was used as starting material (Scheme 6.19). By addition reaction between 2-bromobenzaldehyde and PhMgBr at $-30\text{ }^{\circ}\text{C}$, diaryl alcohol **107** was obtained in 87% yield. Since direct substitution of alcohol **107** by NHPI did not work under the catalysis of tris(pentafluorophenyl)borane, alcohol **107** was brominated into **109** by PBr₃ in 99% yield. Three reactants were tried to substitute bromide by a N-O moiety. While *N*-protected hydroxylamine **98** or **111** led to complex reaction mixtures, NHPI with

TEA in DMF at rt successfully transformed bromide **109** into *N*-alkoxyl phthalimide **108** in 98% yield. The attempt to directly introduce the ester moiety into **108** by tandem Hurtley–retro-Claisen reaction led to a complex reaction mixture. PdCl(Ph)(PPh₃)₂ (a precatalyst developed in our lab, see Appendix IX) catalyzed Negishi CCR between **108** and organo-zinc reagent also failed to furnish **114**. Another method to obtain **114** was by first performing a Pd-catalyzed cyanation of **108** into **113**, followed by hydrolysis of the cyano group into ester.^{169, 170} Despite methyl cyanation of **108** by sodium cyanoacetate under the catalysis of allylpalladium chloride dimer and 2-dicyclohexylphosphino-2',6'-dimethoxybiphenyl (S Phos) gave **33** in a modest 34% yield, the hydrolysis of the cyano group with trimethyl chlorosilane (TMSCl) in EtOH resulted in a complex reaction mixture. Because of the inability to introduce the ester moiety into bromide **108**, it was deprotected into **115** by hydrazine in EtOH in 99% yield (*Scheme 6.20*). Unfortunately, tandem Hurtley–retro-Claisen reaction on **115** led also to complex reaction mixture. To limit side-reactions, the amino group in **115** was first protected with Boc group(s) (mono-Boc **117** & di-Boc **119**) before applying a Negishi CCR. PdCl(Ph)(PPh₃)₂ catalyzed Negishi CCR between **117** and organo-zinc reagent at 100 °C resulted in a complex reaction mixture, while the same reaction between **119** and organo-zinc reagent at 60 °C led to the loss of one Boc group and the formation of **117** in quantitative yield. Steric hindrance due to Boc protection is likely preventing the Negishi CCR.

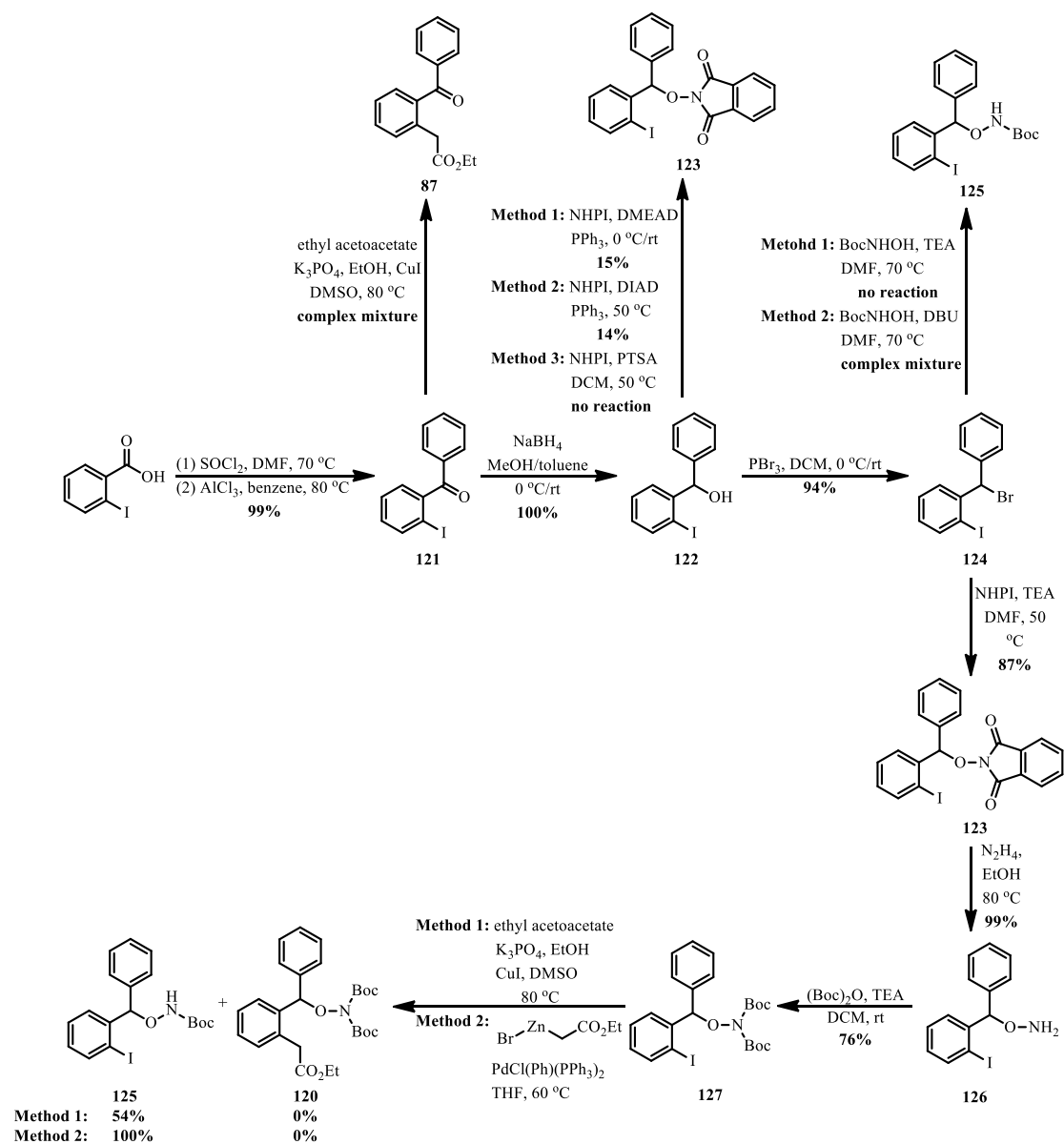


Scheme 6.20. Introduction of ester moiety on O-diphenylmethylhydroxyamine.

VIB2. Starting from 2-iodobenzoic acid

As iodine atom is a better leaving group than bromo, the synthetic approach using 2-iodobenzoic acid as starting material was also tried (Scheme 6.21). Friedel-Craft acylation of benzene worked well with 2-iodobenzoyl chloride under the catalysis of AlCl_3 , furnishing ketone **121** in 99% yield. As discussed in Section VI A1, carboxylic group at the α position of halogen is essential for Hurtley reaction, so an ethanol-assisted CuI-catalyzed coupling reaction was attempted, leading to complex reaction mixture.¹⁷¹ Reduction of ketone **121** with NaBH_4 produced alcohol **122** in quantitative yield. Three methods were tried to substitute alcohol **122** by a N-O moiety. Di-2-methoxyethyl azodicarboxylate (DMEAD) or diisopropyl azodicarboxylate (DIAD) mediated Mitsunobu reaction between **122** and NPHI gave the desired product **123** in 15% and 14% yields, respectively. No reaction happened

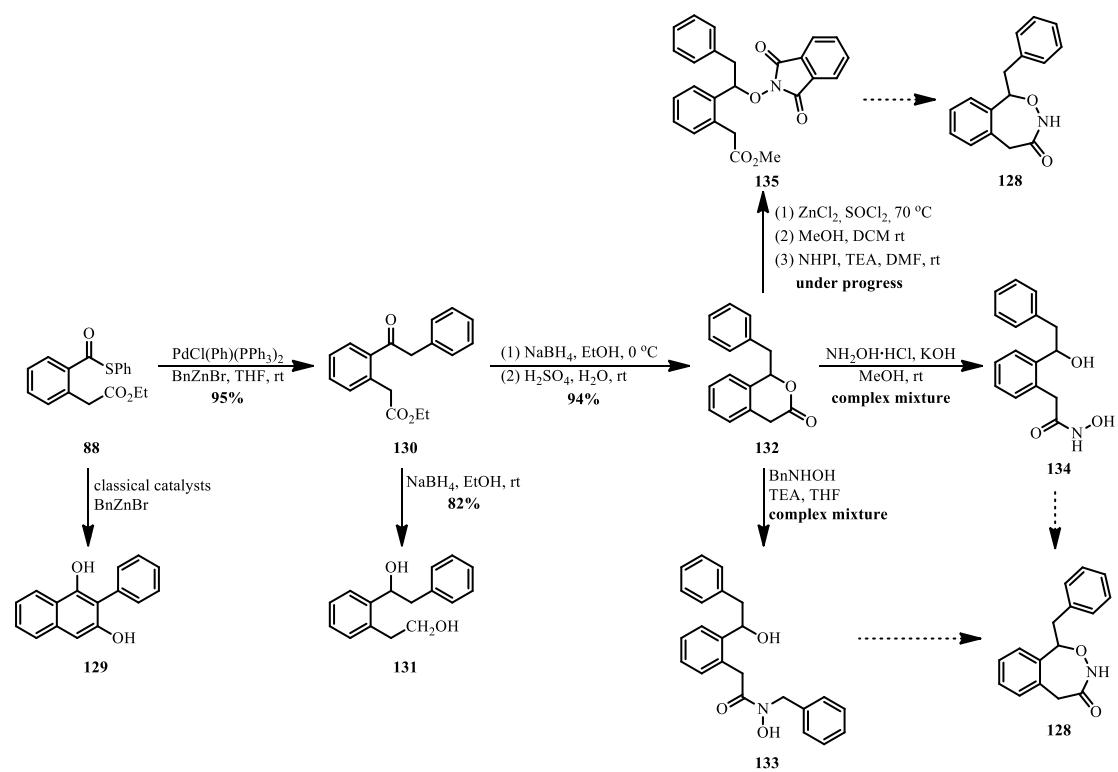
when PTSA was used to assist the substitution reaction between **122** and NHPI.¹⁷² As it was difficult to directly transform **122** into **123**, alcohol **122** was first brominated with PBr₃ in DCM, affording **124** in 94% yield. However, substitution of the resulting bromide **124** by BocNHOH in presence of TEA or DBU failed. In contrary, by using NHPI with TEA in DMF, compound **123** was obtained in 87% yield. Since the phthalimide moiety was incompatible with Negishi or Hurtley reaction conditions, **123** was deprotected by hydrazine and re-protected by diboc, affording **127** in 76% yield. To introduce the ester moiety in **127**, an ethanol-assisted CuI-catalyzed coupling reaction with ethyl acetoacetate was applied, but led to mono boc protected alkoxyamine **125** (54% yield) and unreacted starting material **127** (37%), while no desired product **120** was obtained. Similarly, the PdCl(Ph)(PPh₃)₂ catalyzed Negishi CCR between **126** and organo-zinc reagent BrZnCH₂CO₂Et led to undesired compound **125** in quantitative yield.



Scheme 6.21. Synthetic approach starting from 2-iodobenzoic acid.

VIC. Synthesis of 1-benzyl-2,3-benzoxazepin-4-one scaffold

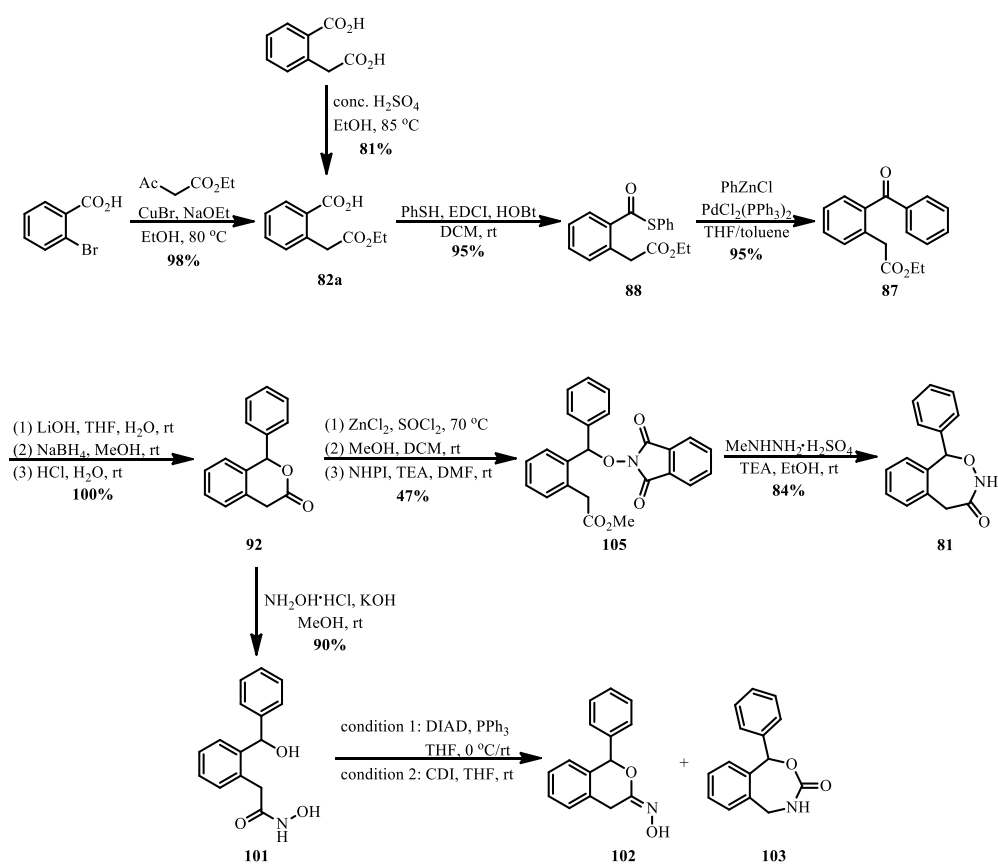
In section VI A, we managed to synthesize the first 1-phenyl-2,3-benzoxazepin-4-one **81**. The next challenge in terms of molecular diversity was to insert a benzyl group at position 1 instead of the benzene ring. Based on the established synthetic approach of 1-phenyl-2,3-benzoxazepin-4-one **81**, we attempted here to synthesize 1-benzyl-2,3-benzoxazepin-4-one **128** (*Scheme 6.22*). Several classical catalysts for Fukuyama CCR were tried to synthesize ketone **130**. However, the competition between Dieckman condensation and Fukuyama CCR led to naphthalenediol **129**, rather than ketone **130** as the major product. To accelerate the Fukuyama CCR, PdCl(Ph)(PPh₃)₂, a post-oxidative-addition precatalyst (POxAP) was developed (For more details on POxAPs, see Appendix IX). Thanks to this novel precatalyst POxAP, Fukuyama CCR between thioester **88** and BnZnBr afforded the desired ketone **130** in 95% yield. In agreement with previous results described in *Table 6.1*, reduction of ketone **130** with NaBH₄ at rt led to diol **131** in 82% yield. In contrary, reduction at 0°C followed by acidification afforded the expected lactone **132** in 94% yield. As expected, reaction between lactone **132** and BnNHOH or NH₂OH under basic condition led to complex reaction mixtures. We will next investigate the synthetic strategy including a chlorination step with SOCl₂/ZnCl₂, followed by a substitution with NHPI and its deprotection with methylhydrazine to obtain the expected 1-benzyl-2,3-benzoxazepin-4-one **128**.



Scheme 6.22. Synthesize 1-benzyl-2,3-benzoxazepin-4-one **128** through lactone **132**.

VID. Conclusion

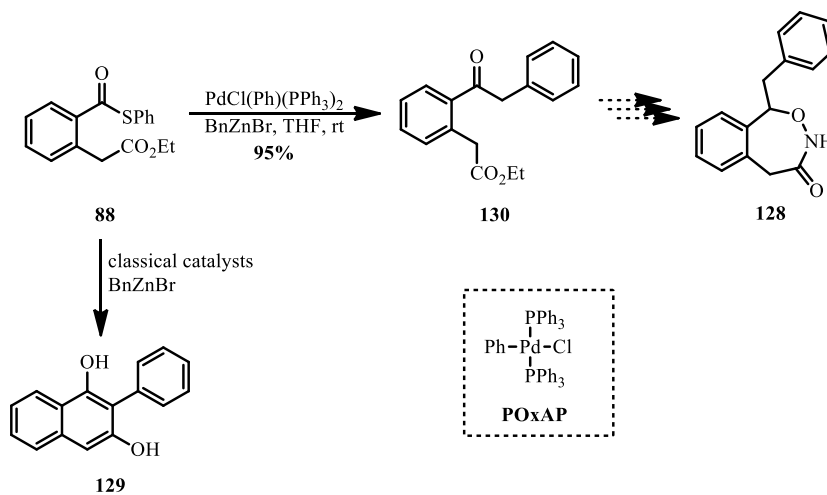
In this chapter, the new scaffold 1-phenyl-2,3-benzoxazepin-4-one **81** was synthesized in 10 steps in 35% overall yield. The key step was introducing the N-O moiety into lactone **92**. Opening the lactone ring under acidic condition followed by NHPI substitution and cyclization gave the desired product **81**. An overall view of the synthesis is shown in *Scheme 6.23*. The structure of benzoxazepinone **1** was identified by NMRs and X-ray crystallography (*Figure 6.10*).



Scheme 6.23. Synthesis of 1-phenyl-2,3-benzoxazepin-4-one 81.

Several attempts were also tried to synthesize 1-benzyl-2,3-benzoxazepin-4-one **128**, an analog of **81**. Although none of these synthetic approaches worked well till now, a novel catalyst, named POxAP, was developed during the synthesis of ketone **130** (*Scheme 6.24*). The application of POxAP in Fukuyama CCR provided a novel synthetic approach towards isoprekinamycin, a natural product with anti-cancer

activities. This part of my PhD work was recently published in *Organic Letters* (Tang et al, DOI: [10.1021/acs.orglett.9b00031](https://doi.org/10.1021/acs.orglett.9b00031)) and this article has been inserted in Appendix IX.¹⁷³



Scheme 6.24. Attempts to synthesize 1-benzyl-2,3-benzoxazepin-4-one 128 leading to the discovery of POxAP.

VII. Summary

VII. Summary

The guanidine moiety is widely used in the development of pharmacological tools such as NPPF receptors antagonists, inhibitors of FXa, NOS, as well as urokinase. However, due to the significant basicity of guanidine ($pK_a \approx 13$), as well as its capacity to form numerous hydrogen bonds, it's difficult to develop the molecules with good pharmacological profiles, especially in terms of oral absorption, distribution in center nervous system or duration of action. The iminoguanidine system is an interesting way to decrease the basicity of guanidine as shown by the development of the antihypertensive guanabenz (Wytensin®). Yet this molecule is entirely flat and shows a certain sensibility to hydrolysis. In a previous project, Dr Bihel's group has developed a cyclic guanabenz which shown an inhibitory effect on prions while less sensitive to hydrolysis.

In this project, we proposed to develop 3-amino-1,2,4-oxadiazines as the biomimetic structure of guanidines et iminoguanidines. Although the synthesis of six-membered ring 1,2-oxadiazines were widely developed thanks to [4+2] nitroso-Diels Alder cyclization, the synthesis of 3-amino-1,2,4-oxadiazines system is nearly unknown in literature.

Starting from *N*-Boc glycine, a multi-step synthetic approach has been established without the control of chiral center at position 6, providing a rapid access to cyclic 3-amino-1,2,4-oxadiazine with high yields (*Scheme 3.25*). When using L-proline or *N*-Boc L-valine, cyclic 4-amino or 4-hydroxypyrrolo-[1,2-d]-1,2,4-oxadiazine could be enantioselectively synthesized by stereoselective reduction of the ketone intermediate (*Scheme 3.26* and *3.27*). The structure and geometry of these new heterocycles were identified by X-ray crystallography (*Figure 3.6* and *3.9*). Preliminary results of pK_a indicated a significant decrease in basicity of these alkoxyguanidines ($pK_a \approx 8$) compared with iminoguanidines ($pK_a \approx 10$) and guanidines ($pK_a \approx 13$) (*Table 3.2*).

Up to now, the only one natural product presenting a 3-amino-1,2,4-oxadiazine scaffold is alchornedine, a molecule with anti-parasite effects isolated from the leaves

of *Alchornea glandulosa*. Since alchornedine has never been synthesized and its structure was deduced by NMR analysis (*Figure 4.9*), we synthesized this alkaloid for the first time. However, the results shown that the structure named alchornedine described in the literature is not correct. We proposed alchornedine presented a five-membered 2-amino-*N*-hydroxy-imidazole ring rather than six-membered 3-amino-1,2,4-oxadiazine ring (*Scheme 4.4*). The synthesis of this scaffold is currently under progress.

During the course of synthesizing 1,2,4-oxadiazine, several methods were tried to introduce the N-O moiety, one of which was inserting NHPI at the α position of styrene derivatives, followed by oxidation at β position (*Appendix VIII*). In presence of Triton X-100, the reaction could be run in water, meeting the principles of green chemistry. This method has been published in *Tetrahedron Letters* (Tang, S.-Q.; Wang, A.-P.; Schmitt, M.; Bihel, F. Dioxygenation of Styrenes with Molecular Oxygen in Water. *Tetrahedron Lett.* 2018. <https://doi.org/10.1016/j.tetlet.2018.03.009>).

Benzodiazepines have been known since 1960s and near 20 molecules are used in clinic as anxiolytics, muscle relaxants or hypnotics. Most of these benzodiazepines belong to 1,4- benzodiazepines except Tofizopam which presents a 1,2-benzodiazepine scaffold and is used for the treatments of atypical anxiety and alcoholism. The seven-membered ring in benzodiazepine is particularly interesting since it endowed the molecule a specific three-dimensional geometry. During the development and characterization of new N-O heterocycles, 2,3-benzoxazepin-4-one was also synthesized as a bioisostere of 2,3-benzodiazepin-4-one. Although the synthesis of 2,3-benzoxazepin-4-one is extremely difficult, an effective synthetic approach was established after numerous methods were tried (*Scheme 6.23*). The structure of this first 2,3-benzoxazepin-4-one was confirmed by X-ray crystallography (*Figure 6.10*) and the research on the physicochemical properties is under progress.

During the synthesis of 2,3-benzoxazepin-4-one, several attempts were also tried to synthesize 1-benzyl-2,3-benzoxazepin-4-one. Although none of these synthetic approaches worked well till now, a novel catalyst, named POxAP, was developed. The

application of POxAP in Fukuyama CCR provided a novel synthetic approach towards isoprekinamycin, a natural product with anti-cancer activities (Appendix IX). This method has been published in *Tetrahedron Letters* (Tang, S. Q.; Bricard, J.; Schmitt, M.; Bihel, F. Fukuyama Cross-Coupling Approach to Isoprekinamycin: Discovery of the Highly Active and Bench-Stable Palladium Precatalyst POxAP. *Org. Lett.* 2019, 21 (3), 844–848. <https://doi.org/10.1021/acs.orglett.9b00031>).

VIII. Experiment section and NMR spectra

VIII. Experiment section and NMR spectra

VIIIA. General information

All commercial reagents were used without additional purification. Analytical TLC was performed using silica gel plates Merck 60 F₂₅₄ and plates were visualized by exposure to ultraviolet light (254 nm). Compounds were purified on silica gel Merck 60 (particle size 0.040-0.063 nm).

¹H and ¹³C NMR spectra were recorded on Bruker Avance Spectrometer operating at 400 or 500 MHz and 100 or 125 MHz, respectively. All chemical shift values δ and coupling constants *J* are quoted in ppm and in Hz, respectively, multiplicity (s= singlet, d= doublet, t= triplet, q= quartet, quin = quintet, sex= sextet m= multiplet, br= broad).

Analytical RP-HPLC-MS was performed using a LC 1200 Agilent with quadrupole-time-of-flight (QTOF) (Agilent Accurate Mass QToF 6520) with a Zorbax Agilent C18-column (C18, 50 mm x 2.1 mm; 1.8 μ m) using the following parameters: 1) The solvent system: A (0.05% of formic acid in acetonitrile) and B (0.05% of formic acid in H₂O); 2) A linear gradient: t= 0 min, 98% B; t = 8 min, 0% B; t = 12.5 min, 0% B; t = 12.6 min, 98% B; t = 13 min, 98% B; 3) Flow rate of 0.5 mL/min; 4) Column temperature: 35 °C; 5) DAD scan from 190 nm to 700 nm; 6) Ionization mode : ESI⁺ or ESI⁻.

HPLC were performed using a Dionex UltiMate 3000 using the following parameters: Flow rate of 0.5 mL/min, column temperature: 30 °C, solvent system: A (MeOH) and B (0.05% of TFA in H₂O), t = 0 min to 1 min: 50 to 60% of B, then t = 1 min to t = 10 min: 60 to 100% of B and t = 10 min to t = 15 min: 100% of B.

The single-crystal structure analysis was performed using X-ray diffraction with a Thermo Fisher ESCALAB 250 diffractometer.

VIIIB. Physicochemical studies of 1,2,4-oxadiazines

VIIIB1. Measurement of pK_a ¹³²

m mg compound was dissolved in v mL H₂O containing 60% MeOH, 0.005M HCl and NaCl in sufficient quantity to adjust the ionic strength to 0.1 M. 1 mL forementioned solution was transferred by a micropipette into a 2 mL glass tube and titrated by the solution of NaOH (0.1 M) in MeOH/H₂O (60%/40%). pK_a in 60% MeOH ($pK_{a \text{ MeOH}60\%}$) was determined based on pH- V_{NaOH} titration curve and calculated by HYPERQUAD program. Aqueous pK_a ($pK_{a \text{ aq}}$) is estimated by the following equation: $pK_{a \text{ MeOH}60\%} = 0.97 \times pK_{a \text{ aq}} - 0.43$.

VIIIB2. Measurement of log D ¹⁷⁴

1. Preparation of stock, reference and tested solutions:

(1) PBS buffer: 150 mM NaCl and 100 mM Na₂HPO₄ in H₂O

(2) Stock solution (10 mM): tested compound was dissolved in DMSO and conserved at 4 °C.

(3) Reference solution (100 μM): 10 μL stock solution diluted with 990 μL MeCN/H₂O.

(4) Tested solution (100 μM): (1) 10 μL stock solution + 20 μL octanol + 970 μL PBS; (2) 10 μL stock solution + 200 μL octanol + 790 μL PBS; (3) 10 μL stock solution + 660 μL octanol + 330 μL PBS. The three mixtures were mixed on a rotary agitator at 20 °C for 1 h and centrifuged at 10,000g for 5 min. The aqueous phase was collected for analysis.

2. The reference solution and aqueous phases of tested solutions were analyzed by HPLC equipped with a C18 column (kinetex 2.6μ C18 100A 50x4.6 mm) an automatic injector and a diode array detector. The inject volume was 10 μL and column temperature was 30 °C. Detected wave length was 280 nm. The solvent system: A (0.05% of TFA in H₂O) and B (MeCN), flow rate 2 mL/min, t = 0 min to

0.1 min: 5% B, then t = 2.6 min to t = 3.1 min: 95% B and t = 3.3 min to t = 6 min: 5% of B. The measurements were first carried out in octanol/PBS with three different proportions. Then, the repeated measurement was carried out with best adapted octanol/PBS proportion. Log D was calculated by area under curve of the reference solution and tested solution.

3. Due to logD of DMSO in octanol/H₂O is -1.35 and 10 μL DMSO was added in each tube, we assume 9.6 μL DMSO is in H₂O and 0.4 μL is in octanol.

LogD of the tested compounds can be calculated with the following equation:

$$\log D = \log ((V_{\text{ref}} \times A_{\text{ref}} - V_{\text{aq}} \times A_{\text{aq}}) / (V_{\text{oct}} \times A_{\text{aq}}))$$

V_{ref}: volume of reference solution = 1 mL

A_{ref}: area under curve of the reference solution

V_{aq}: Volume of the aqueous phase (979.6 μL; 799.6 μL; 339.6 μL)

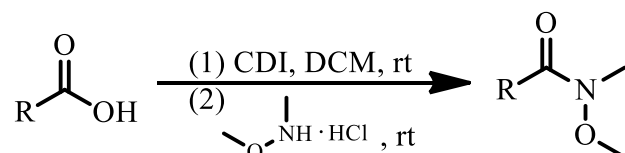
A_{aq}: area under curve of the tested solution

V_{oct}: volume of the organic phase (20.4 μL; 200.4 μL; 660.4 μL)

VIIIC. Synthetic procedures and analytic data

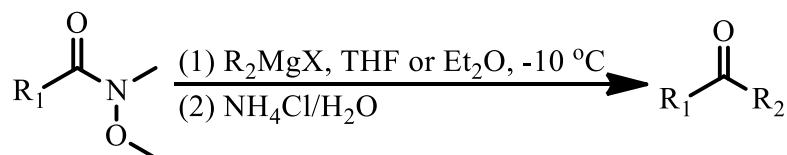
VIIIC1 Typical procedures

1. Typical procedures 1 (TP1)



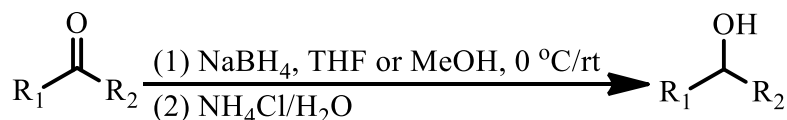
To a solution of *N*-Boc amino acid (1 eq.) in DCM was slowly added CDI (1.2 ~ 1.3 eq.) and stirred at rt for 30 minutes until CO₂ evolution ceased. *N,O*-dimethylhydroxylamine hydrochloride (1.2 ~ 1.3 eq.) was then added to the reaction mixture and stirred at rt for 16 h. The mixture was quenched with water and extracted with DCM thrice. The combined organic phases were washed brine, dried over anhydrous Na₂SO₄ and filtered. The filtrate was concentrated in vacuo to afford the product.

2. Typical procedures 2 (TP2)



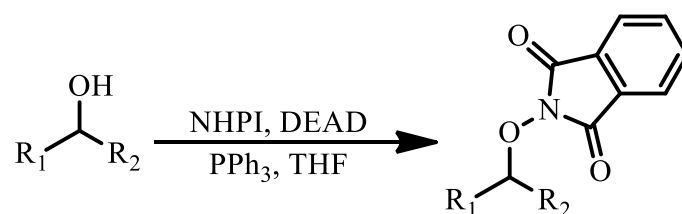
Grignard reagent (1.4 ~ 4 eq.) in THF was added dropwise to a solution of Weinreb amide (1 eq.) in THF or Et₂O at -10 °C under Ar. After stirred at -10 °C overnight, the reaction mixture was poured slowly into saturated NH₄Cl aqueous solution at 0 °C under stirring. After 10min, the resulting mixture was extracted with EtOAc thrice. The combined organic phases were washed with brine, dried over Na₂SO₄ and filtered. The filtrate was concentrated in vacuo and purified by silica gel chromatography to afford the product.

3. Typical procedures 3 (TP3)



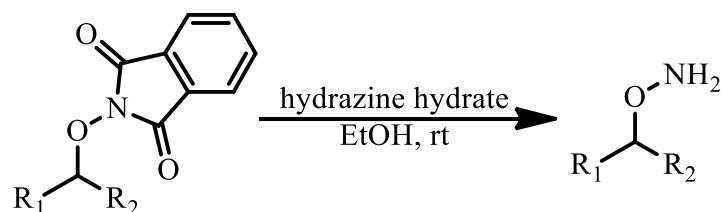
To a solution of ketone (1 eq.) in THF or MeOH was slowly added NaBH₄ (2 ~ 4 eq.) at 0°C. The mixture was then stirred at rt for 1 ~ 3 h. After completion, the reaction mixture was poured slowly into saturated NH₄Cl aqueous solution at 0 °C under stirring. After 10min, the resulting mixture was extracted with EtOAc thrice (if MeOH was used as solvent, removed under reduced pressure before extraction). The combined organic phases were washed with brine, dried over Na₂SO₄ and filtered. The filtrate was concentrated in vacuo to afford the product.

4. Typical procedures 4 (TP4)



After degassed and back filled with Ar thrice, a solution of alcohol (1 eq.), NHPI (1.3 ~ 1.5 eq.) and PPh₃ (1.3 ~ 1.8 eq.) in THF was cooled to the given temperature. Then, DEAD (1.3 ~ 1.8 eq.) was added dropwise to the solution and stirred at the given temperature overnight. The reaction mixture quenched by the addition of water and extracted with EtOAc thrice. The combined organic phases were washed with brine, dried over Na₂SO₄ and filtered. The filtrate was concentrated and purified by silica gel chromatography to afford the product.

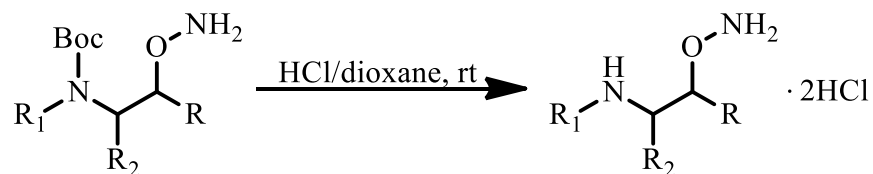
5. Typical procedures 5 (TP5)



Hydrazine hydrate (15 eq.) was added dropwise to a solution of *N*-alkoxyphthalimide (1 eq.) in EtOH and stirred at rt for the given time. The reaction mixture was concentrated in vacuo, and purified by reverse chromatography (MeOH/H₂O) to

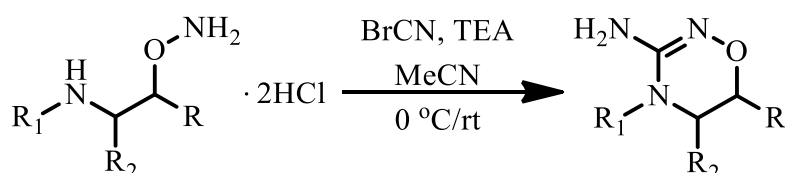
afford the product.

6. Typical procedures 6 (TP6)



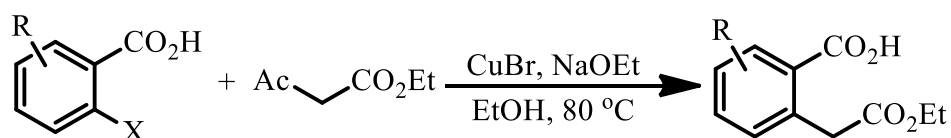
A solution of Boc amino alkoxyamine (1 eq.) in HCl/dioxane (4M) was stirred at rt for 16 h. The reaction was concentrated in vacuo and dried under reduced pressure overnight to afford the product.

7. Typical procedures 7 (TP7)



TEA (4 eq.) was slowly added to a solution of amino alkoxyamine dihydrochloride (1 eq.) in MeCN at 0 °C and stirred for 5 min. Then a solution of BrCN (1.1 ~ 1.2 eq.) in MeCN was slowly added at 0°C. After stirring at 0 °C for 30 min, the mixture was stirred at rt overnight. The crude was concentrated in vacuo and purified by reverse phase chromatography (ACN/H₂O) to afford the product.

8. Typical procedures 8 (TP8)

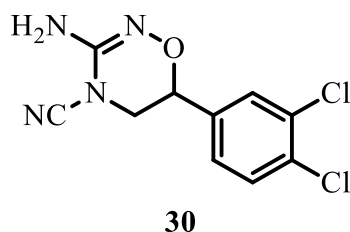
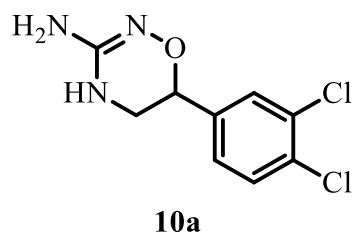


To an oven dried microwave tube prefilled with Ar was added NaOEt (3 or 4 eq.), anhydrous ethanol and sonicated until the suspension became clear. Ethyl acetoacetate (2 eq.) was then added and stirred at rt for 2 min. After the addition of CuBr (0.1 eq.) and 2-bromobenzoic acid (1 eq.), the reaction mixture was stirred under Ar at 80°C for the given time. The reaction was concentrated in vacuo and water was added. The

aqueous mixture was washed with EtOAc, acidified by HCl_{aq} (2M) until pH~3 and extracted by EtOAc thrice, the organic phases were washed with brine, dried over anhydrous Na₂SO₄ and filtered. The filtrate was concentrated in vacuo to afford the product.

VIIIC2 Preparation and and analytic data

Preparation of 6-(3,4-dichlorophenyl)-5,6-dihydro-4*H*-1,2,4-oxadiazin-3-amine (10a) and 3-amino-6-(3,4-dichlorophenyl)-5,6-dihydro-4*H*-1,2,4-oxadiazine-4-carbonitrile (30)



According to typical procedure **TP7**, the reaction was performed with **26a** (1 eq., 20 mg, 0.068 mmol) in MeCN (1.43 mL), TEA (4 eq., 0.0378 mL, 0.272 mmol) and a solution of BrCN (1.2 eq., 8.65 mg, 0.0816 mmol) in MeCN (0.286 mL), affording **10a** (13.6 mg, 81%) and **30** as white solids (3.2 mg, 17%).

¹H NMR (400 MHz, DMSO-*d*⁶) of **10a**: δ 7.66 – 7.57 (m, 2H), 7.35 (dd, *J* = 8.3, 2.0 Hz, 1H), 6.16 (s, 1H), 4.46 (s, 2H), 4.42 (dd, *J* = 9.0, 3.1 Hz, 1H), 3.45 (dd, *J* = 11.4, 3.2 Hz, 1H), 3.15 (dd, *J* = 11.4, 9.0 Hz, 1H).

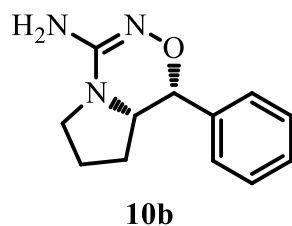
¹³C NMR (101 MHz, DMSO-*d*⁶) of **10a**: δ 154.08, 140.44, 130.89, 130.44, 130.25, 128.70, 126.98, 71.97, 45.30.

¹H NMR (400 MHz, DMSO-*d*⁶) of **30**: δ 7.71 – 7.65 (m, 2H), 7.42 (dd, *J* = 8.4, 2.0 Hz, 1H), 5.78 (s, 2H), 4.82 (dd, *J* = 9.4, 3.1 Hz, 1H), 4.10 (dd, *J* = 11.0, 3.2 Hz, 1H), 3.97 (dd, *J* = 11.0, 9.5 Hz, 1H).

¹³C NMR (101 MHz, DMSO-*d*⁶) of **30**: δ 147.23, 137.23, 131.30, 131.21, 130.74, 129.08, 127.30, 109.65, 72.06, 50.65.

Preparation of (1*R*,8*aS*)-1-phenyl-6,7,8,8*a*-tetrahydro-1*H*-pyrrolo[1,2-*d*][1,2,4]

oxadiazin-4-amine (**10b**)

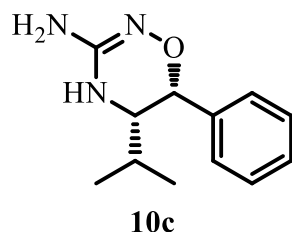


According to typical procedure **TP7**, The reaction was performed with **26b** (1 eq., 20 mg, 0.0754 mmol) in MeCN (1.5 mL), TEA (4 eq., 0.0419 mL, 0.302 mmol) and a solution of BrCN (1.2 eq., 9.59 mg, 0.0905 mmol) in MeCN (0.3 mL), affording **10b** as a white solid (15.4 mg, 94 %).

^1H NMR (400 MHz, DMSO- d^6): δ 7.36 – 7.21 (m, 5H), 4.99 (d, J = 4.4 Hz, 1H), 4.81 (s, 2H), 3.67 (dt, J = 9.6, 5.0 Hz, 1H), 3.33 – 3.25 (m, 2H), 1.69 – 1.49 (m, 3H), 1.30 – 1.15 (m, 1H).

^{13}C NMR (101 MHz, DMSO- d^6): δ 155.83, 139.18, 128.43, 127.67, 127.62, 75.92, 58.47, 47.87, 27.53, 23.00.

Preparation of (5*R*,6*S*)-5-isopropyl-6-phenyl-5,6-dihydro-4*H*-1,2,4-oxadiazin-3-amine (**10c**)



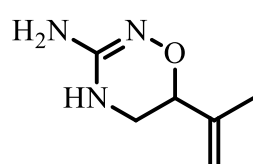
According to typical procedure **TP7**, the reaction was performed with a solution of **26c** (1 eq., 40 mg, 0.15 mmol) in MeCN (3.48 mL), TEA (4 eq., 0.0832 mL, 0.599 mmol) and a solution of BrCN (1.1 eq., 17.4 mg, 0.165 mmol) in MeCN (0.174 mL), affording **10c** as a white solid (24 mg, 73 %).

^1H NMR (400 MHz, DMSO- d^6): δ 7.38 – 7.30 (m, 5H), 5.86 (s, 1H), 4.44 (s, 2H), 4.09 (d, J = 8.2 Hz, 1H), 3.34 – 3.31 (m, 1H), 1.42 (pd, J = 6.9, 2.7 Hz, 1H), 0.86 (d, J = 7.1 Hz, 3H), 0.79 (d, J = 6.8 Hz, 3H).

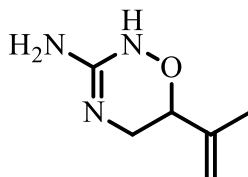
^{13}C NMR (101 MHz, DMSO- d^6): δ 154.95, 138.83, 128.21, 127.99, 127.75, 77.02,

59.63, 28.15, 19.29, 15.10.

Preparation of 6-(prop-1-en-2-yl)-5,6-dihydro-4*H*-1,2,4-oxadiazin-3-amine (10d) and 6-(prop-1-en-2-yl)-5,6-dihydro-2*H*-1,2,4-oxadiazin-3-amine (44)



10d



44

According to typical procedure **TP7**, The reaction was performed with a solution of **26d** (1 eq., 152 mg, 0.804 mmol) in MeCN (18.5 mL), TEA (4 eq., 0.447 mL, 3.22 mmol) and a solution of BrCN (1.1 eq., 93.7 mg, 0.884 mmol) in MeCN (1 mL), affording **10d** (91 mg, 80 %) and **44** as white solids (10 mg, 9 %).

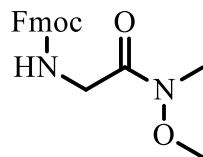
^1H NMR (400 MHz, DMSO- d^6) of **10d**: δ 6.07 (s, 1H), 4.94 (dt, $J = 2.2, 1.1$ Hz, 1H), 4.89 (t, $J = 1.9$ Hz, 1H), 4.48 (s, 2H), 3.74 (dd, $J = 9.4, 3.0$ Hz, 1H), 3.28 (dd, $J = 11.2, 3.1$ Hz, 1H), 3.02 (dd, $J = 11.2, 9.5$ Hz, 1H), 1.70 (s, 3H).

^{13}C NMR (101 MHz, DMSO- d^6) of **10d**: δ 154.08, 142.36, 111.95, 74.27, 19.01.

^1H NMR (400 MHz, DMSO- d^6) of **44**: δ 8.83 (s, 1H), 7.38 (s, 2H), 5.09 – 5.07 (m, 1H), 5.05 (q, $J = 1.2$ Hz, 1H), 4.36 (dd, $J = 9.0, 3.3$ Hz, 1H), 3.50 (dd, $J = 12.6, 3.5$ Hz, 1H), 3.31 (dd, $J = 12.6, 9.1$ Hz, 1H), 1.75 (s, 3H).

^{13}C NMR (101 MHz, DMSO- d^6) of **44**: δ 154.90, 139.56, 115.17, 77.90, 42.51, 19.24.

Preparation of (9*H*-fluoren-9-yl)methyl (2-(methoxy(methyl)amino)-2-oxoethyl) carbamate (13)



13

CDI (1.2 eq., 2.62 g, 16.1 mmol) was slowly added to a solution of *N*-Fmoc glycine (1 eq., 4 g, 13.5 mmol) in DCM (30 mL) and the resulting mixture was stirred at rt for 30 minutes until CO₂ evolution ceased. *N,O*-dimethylhydroxylamine hydrochloride (1.2

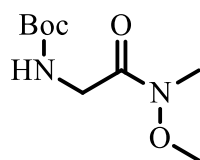
eq., 1.57 g, 16.1 mmol) was then added and stirred at rt for 16 h. The reaction mixture was concentrated in vacuo, diluted with water and extracted with EtOAc thrice. The combined organic phase was washed with brine, dried over Na₂SO₄, and concentrated in vacuo. The crude was purified by silica gel chromatography (heptane:EtOAc = 2:1 to 1:1) to afford **13** as a colorless oil (3.7 g, 81%).

Rf: 0.5 (EtOAc:heptane = 3:1).

¹H NMR (400 MHz, CDCl₃): δ 7.76 (d, *J* = 7.5 Hz, 2H), 7.62 (d, *J* = 7.4 Hz, 2H), 7.40 (t, *J* = 7.3 Hz, 2H), 7.32 (td, *J* = 7.4, 1.1 Hz, 2H), 5.64 (s, 1H), 4.39 (d, *J* = 7.2 Hz, 2H), 4.25 (t, *J* = 7.2 Hz, 1H), 4.17 (d, *J* = 4.4 Hz, 2H), 3.72 (s, 3H), 3.22 (s, 3H).

These data are consistent with the previously reported characterization.¹⁷⁵

Preparation of *tert*-butyl (2-(methoxy(methyl)amino)-2-oxoethyl)carbamate (**14a**)



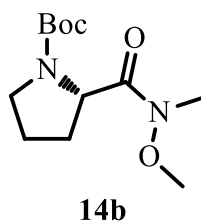
14a

The reaction was performed with *N*-Boc glycine (1 eq., 4 g, 22.8 mmol), CDI (1.2 eq., 4.44 g, 27.4 mmol) and *N,O*-dimethylhydroxylamine hydrochloride (1.2 eq., 2.67 g, 27.4 mmol) in DCM (45 mL) according to typical procedure **TP1**, , affording **14a** as a white solid (4.9 g, 99%).

¹H NMR (400 MHz, CDCl₃): δ 5.26 (s, 1H), 4.07 (d, *J* = 3.8 Hz, 2H), 3.70 (s, 3H), 3.19 (s, 3H), 1.45 (s, 9H).

These data are consistent with the previously reported characterization.¹⁷⁶

Preparation of (*S*)-*tert*-butyl 2-(methoxy(methyl)carbamoyl)pyrrolidine-1-carboxylate (**14b**)

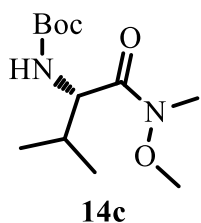


The reaction was performed with **33** (1 eq., 3 g, 13.9 mmol), CDI (1.2 eq., 2.71 g, 16.7 mmol) and *N,O*-dimethylhydroxylamine hydrochloride (1.2 eq., 1.63 g, 16.7 mmol) in DCM (28 mL) according to typical procedure **TP1**, affording **14b** as a colorless oil (3.4 g, 94%).

¹H NMR (400 MHz, CDCl₃, mixture of rotamers): δ 4.63 (m, 1H), 3.76 (s, 1.4H), 3.69 (s, 1.6H), 3.60 – 3.34 (m, 2H), 3.17 (s, 3H), 2.25 – 2.07 (m, 1H), 1.99 – 1.79 (m, 3H), 1.43 (s, 4.7H), 1.39 (s, 4.3H).

These data are consistent with the previously reported characterization.¹²⁴

Preparation of (*S*)-*tert*-butyl (1-(methoxy(methyl)amino)-3-methyl-1-oxobutan-2-yl)carbamate (**14c**)

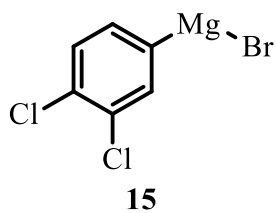


The reaction was performed with *N*-Boc L-valine (1 eq., 3 g, 13.8 mmol), CDI (1.2 eq., 2.69 g, 16.6 mmol) and *N,O*-dimethylhydroxylamine hydrochloride (1.2 eq., 1.62 g, 16.6 mmol) in DCM (27.9 mL) according to **TP1**, affording **14c** as a colorless oil (3.37 g, 94 %).

¹H NMR (400 MHz, CDCl₃): δ 5.12 (d, *J* = 9.9 Hz, 1H), 4.55 (t, *J* = 8.0 Hz, 1H), 3.74 (s, 3H), 3.19 (s, 3H), 1.96 (dq, *J* = 13.4, 6.7 Hz, 1H), 1.41 (s, 9H), 0.93 (d, *J* = 6.8 Hz, 3H), 0.88 (d, *J* = 6.8 Hz, 3H).

These data are consistent with the previously reported characterization.¹⁷⁷

Preparation of (3,4-dichlorophenyl)magnesium bromide (**15**)

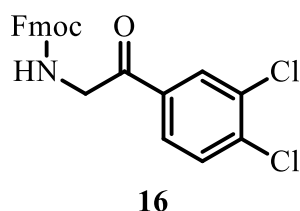


To a flame-dried 25 mL round bottom flask was charged activated Mg (1.5 eq., 0.365 g, 15 mmol) and anhydrous THF (10 mL). The suspension was then degassed and back filled with Ar thrice, followed by the addition of 1,2-dibromoethane (3 %, 0.025 mL, 0.3 mmol). After 5 min, a solution of 1-bromo-3,4-dichlorobenzene (1 eq., 2.26 g, 10 mmol) in anhydrous THF (10 mL) was slowly added to the suspension of Mg and stirred at rt for 3h to afford a brown solution of **15** in 20 mL THF (0.34 M, 6.85 mmol, 69%).

The obtained Grignard reagent was titrated by the following method¹⁰⁹: A 20 mL microwave tube fitted with a magnetic stirring bar was charged with menthol (42.8 mg, 0.274 mmol) and 1,10-phenanthroline (6 mg, 0.03 mmol) before being capped with a rubber septum and flushed with dry Ar. Dry THF (3 mL) was introduced, and the resulting solution was stirred at rt for 2min. The Grignard solution was then added dropwise by the syringe until a distinct burgundy color persisted for longer than one minute. [RMgX] in M = mmol of menthol/volume of RMgX in mL

In this reaction, 0.8 mL Grignard reagent was consumed for titration.

Preparation of (9*H*-fluoren-9-yl)methyl (2-(3,4-dichlorophenyl)-2-oxoethyl) carbamate (**16**)



The reaction was performed with **13** (1 eq., 0.5 g, 1.47 mmol) in THF (8 mL) and a THF solution of **15** (2 eq., 0.34 M, 8.64 mL, 2.94 mmol) according to typical procedure **TP2**. The crude was purified by silica gel chromatography (heptane:EtOAc

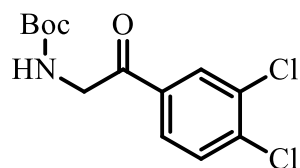
= 5:1 to 4:1) to afford **16** as a white solid (0.55 g, 88%).

Rf: 0.3 (heptane:EtOAc = 3:1).

¹H NMR (400 MHz, CDCl₃): δ 8.06 (d, *J* = 2.0 Hz, 1H), 7.81 - 7.75 (m, 3H), 7.65 - 7.59 (m, 3H), 7.41 (t, *J* = 7.3 Hz, 2H), 7.33 (t, *J* = 7.3 Hz, 2H), 5.75 (s, 1H), 4.69 (d, *J* = 4.6 Hz, 2H), 4.44 (d, *J* = 7.1 Hz, 2H), 4.26 (t, *J* = 7.0 Hz, 1H).

These data are consistent with the previously reported characterization.¹⁷³

Preparation of *tert*-butyl (2-(3,4-dichlorophenyl)-2-oxoethyl)carbamate (**17a**)



17a

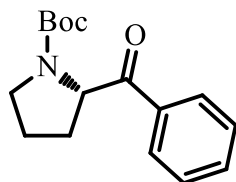
The reaction was performed with **14a** (1 eq., 0.4 g, 1.83 mmol) in THF (9 mL) and a THF solution of **15** (2 eq., 0.5 M, 7.33 mL, 3.67 mmol) according to typical procedure **TP2**. The crude was purified by silica gel chromatography (heptane:EtOAc = 5:1) to afford **17a** as a white solid (0.48 g, 86%).

Rf: 0.35 (heptane:EtOAc = 3:1).

¹H NMR (400 MHz, CDCl₃): δ 8.04 (d, *J* = 1.9 Hz, 1H), 7.78 - 7.74 (m, 1H), 7.58 (d, *J* = 8.4 Hz, 1H), 5.46 (s, 1H), 4.60 (d, *J* = 4.6 Hz, 2H), 1.47 (s, 9H).

These data are consistent with the previously reported characterization.¹⁷⁸

Preparation of (*S*)-*tert*-butyl 2-benzoylpyrrolidine-1-carboxylate (**17b**)



17b

The reaction was performed with **14b** (1 eq., 1.5 g, 5.81 mmol) in Et₂O (50 mL) and a THF solution of PhMgBr (1.4 eq., 1 M, 8.13 mL, 8.13 mmol) according to typical procedure **TP2**. The crude was purified by silica gel chromatography (heptane:EtOAc

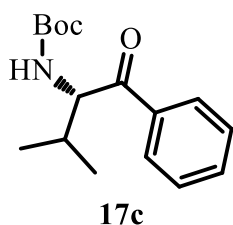
= 20:1 to 5:1) to afford **17b** as a white solid (1.4 g, 88%).

¹H NMR (400 MHz, CDCl₃, mixture of rotamers): δ 8.02 – 7.89 (m, 2H), 7.62 – 7.50 (m, 1H), 7.45 (m, 2H), 5.32 (dd, *J* = 9.3, 2.9 Hz, 0.35H), 5.18 (dd, *J* = 8.7, 3.7 Hz, 0.55H), 3.57 (m, 2H), 2.31 (m, 1H), 2.01 – 1.84 (m, 3H), 1.45 (s, 3.5H), 1.25 (s, 5.5H).

Rf: 0.5 (heptane:EtOAc = 2:1).

These data are consistent with the previously reported characterization.¹²⁴

Preparation of (*S*)-*tert*-butyl (3-methyl-1-oxo-1-phenylbutan-2-yl)carbamate (**17c**)



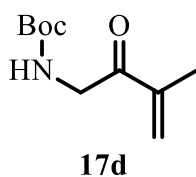
The reaction was performed with **14c** (1 eq., 2.6 g, 9.99 mmol) in Et₂O (27.9 mL) and a THF solution of PhMgBr (3 eq., 1 M, 30 mL, 30 mmol) according to typical procedure **TP2**. The crude was purified by silica gel chromatography (heptane:EtOAc = 10:1) to afford **17c** as a colorless oil (2.45 g, 88 %).

¹H NMR (400 MHz, CDCl₃): δ 8.00 – 7.92 (m, 2H), 7.63 – 7.55 (m, 1H), 7.48 (m, 2H), 5.43 (d, *J* = 9.1 Hz, 1H), 5.23 (dd, *J* = 9.1, 4.1 Hz, 1H), 2.14 (m, 1H), 1.45 (s, 9H), 1.03 (d, *J* = 6.8 Hz, 3H), 0.75 (d, *J* = 6.8 Hz, 3H).

Rf: 0.4 (heptane:EtOAc = 5:1).

These data are consistent with the previously reported characterization.¹⁷⁹

Preparation of *tert*-butyl (3-methyl-2-oxobut-3-en-1-yl)carbamate (**17d**)



The reaction was performed with **14a** (1 eq., 2 g, 9.16 mmol) in THF (30 mL) and a

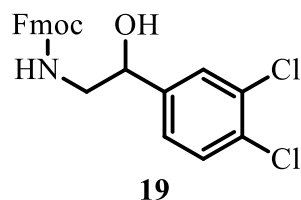
THF solution of isopropenylmagnesium bromide (4 eq., 0.5 M, 73.3 mL, 36.7 mmol) according to typical procedure **TP2** without further purification to afford **17d** as a yellow oil (1.8 g, 99 %).

^1H NMR (400 MHz, CDCl_3): δ 5.99 (s, 1H), 5.83 (q, $J = 1.4$ Hz, 1H), 5.36 (s, 1H), 4.35 (d, $J = 4.5$ Hz, 2H), 1.90 (t, $J = 1.2$ Hz, 3H), 1.44 (s, 9H).

^{13}C NMR (101 MHz, CDCl_3): δ 196.11, 155.88, 142.47, 125.54, 79.89, 46.74, 28.49, 17.54.

Rf: 0.8 (heptane:EtOAc = 1:1).

Preparation of (9H-fluoren-9-yl)methyl (2-(3,4-dichlorophenyl)-2-hydroxyethyl) carbamate (**19**)



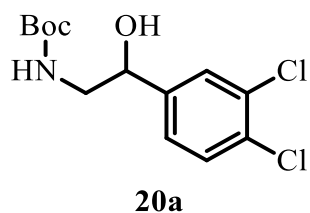
The reaction was performed with **16** (1 eq., 500 mg, 1.17 mmol) in THF (10 mL) with NaBH_4 (4 eq., 177 mg, 4.69 mmol) according to typical procedure **TP3** in 1 h, affording **19** as a white solid (496 mg, 99%).

^1H NMR (400 MHz, CDCl_3): δ 7.80 – 7.74 (m, 2H), 7.60 – 7.55 (m, 2H), 7.49 – 7.29 (m, 6H), 7.16 (d, $J = 7.6$ Hz, 1H), 5.15 (s, 1H), 4.84 – 4.74 (m, 1H), 4.51 – 4.40 (m, 2H), 4.21 (t, $J = 6.5$ Hz, 1H), 3.57 – 3.18 (m, 2H), 3.11 (s, 1H).

^{13}C NMR (101 MHz, CDCl_3): δ 155.56, 144.46, 143.88, 141.53, 133.16, 131.97, 130.66, 128.07, 127.92, 127.25, 125.36, 125.07, 120.18, 72.82, 67.08, 48.64, 47.40.

Rf: 0.4 (heptane:EtOAc = 1:1).

Preparation of *tert*-butyl (2-(3,4-dichlorophenyl)-2-hydroxyethyl)carbamate (**20a**)



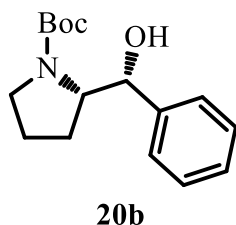
The reaction was performed with **17a** (1 eq., 500 mg, 1.64 mmol) in THF (15 mL) with NaBH₄ (4 eq., 177 mg, 4.69 mmol) according to typical procedure **TP3** in 1 h, affording **20a** as a white solid (498 mg, 99%).

¹H NMR (400 MHz, CDCl₃): δ 7.46 (d, *J* = 1.9 Hz, 1H), 7.40 (d, *J* = 8.3 Hz, 1H), 7.17 (dd, *J* = 8.4, 1.8 Hz, 1H), 4.98 (t, *J* = 5.6 Hz, 1H), 4.86 – 4.75 (m, 1H), 3.78 (s, 1H), 3.49 – 3.13 (m, 2H), 1.43 (s, 9H).

¹³C NMR (101 MHz, CDCl₃): δ 157.44, 142.30, 132.76, 131.71, 130.54, 128.12, 125.37, 80.50, 73.17, 48.50, 28.45.

Rf: 0.5 (heptane:EtOAc = 1:1).

Preparation of (*S*)-*tert*-butyl 2-((*R*)-hydroxy(phenyl)methyl)pyrrolidine-1-carboxylate (**20b**)



A solution of DIBAL-H (2 eq., 1 M, 0.145 mL, 0.145 mmol) in THF was added slowly to a solution of **17b** in THF (0.5 mL) under Ar at 0°C. The mixture was stirred at 0°C for 1 h and quenched with water and extracted with EtOAc thrice. The combined organic phases were washed with brine, dried over anhydrous Na₂SO₄, and filtered. The filtrate was concentrated in vacuo, then dissolved in 2 mL EtOAc/Heptane (1:1) and filtered through a silica gel pad with EtOAc/Heptane (1:1), the filtrate was concentrated in vacuo to afford **20b** as a colorless oil (20.1 mg, 100 %).

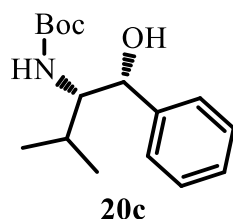
¹H NMR (400 MHz, CDCl₃): δ 7.41 – 7.24 (m, 5H), 5.47 (s, 0.68H), 5.17 (s, 0.28H),

4.89 (s, 0.64H), 4.33 (s, 0.57H), 4.03 (s, 0.34H), 3.57 (s, 0.44H), 3.32 (s, 1H), 2.84 (s, 0.66H), 2.30 (m, 0.34H), 1.94 (m, 1H), 1.79 (m, 1H), 1.54 (s, 9H), 1.25 – 1.09 (m, 1H).

Rf: 0.55 (heptane:EtOAc = 2:1).

These data are consistent with the previously reported characterization.¹²⁵

Preparation of *tert*-butyl ((1*R*,2*S*)-1-hydroxy-3-methyl-1-phenylbutan-2-yl) carbamate (**20c**)

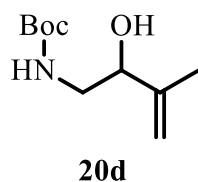


A solution of DIBAL-H (3 eq., 1 M, 0.541 mL, 0.541 mmol) in THF was slowly added to a solution of **17c** (1 eq., 50 mg, 0.18 mmol) in THF (1 mL) under Ar at 0°C. After stirred at 0°C for 3 h, the mixture was quenched with water and extracted with EtOAc thrice. The combined organic phases were washed with brine, dried over Na₂SO₄, and concentrated in vacuo. The crude was purified by reverse phase chromatography (MeOH/H₂O) to afford **20c** as a white solid (49 mg, 97 %).

¹H NMR (400 MHz, CDCl₃): δ 7.36 – 7.27 (m, 5H), 4.87 (t, *J* = 4.6 Hz, 1H), 4.35 (d, *J* = 9.8 Hz, 1H), 3.84 – 3.74 (m, 1H), 1.76 – 1.66 (m, 1H), 1.39 (s, 9H), 1.29 (s, 1H), 1.04 (d, *J* = 6.7 Hz, 3H), 0.89 (d, *J* = 6.7 Hz, 3H).

These data are consistent with the previously reported characterization.¹²⁷

Preparation of *tert*-butyl (2-hydroxy-3-methylbut-3-en-1-yl)carbamate (**20d**)



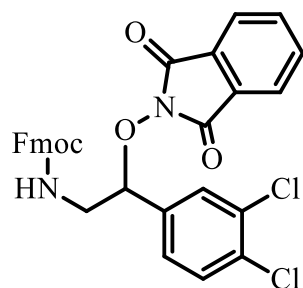
Trichlorocerium heptahydrate (1.6 eq., 2.74 g, 7.35 mmol) was added to a solution of **17d** (1 eq., 0.92 g, 4.59 mmol) in MeOH (20.8 mL) and stirred at rt until the

suspension became clear. Then, the mixture was cooled to -70°C and NaBH_4 (1.3 eq., 225 mg, 5.97 mmol) was added portionwise. The reaction was stirred at -70°C for 20 min and quenched by the addition of H_2O at -20°C . After MeOH was removed under reduced pressure, the aqueous suspension was extracted with EtOAc thrice. The combined organic phases were washed with brine, dried over anhydrous Na_2SO_4 and concentrated in vacuo. The crude was purified by silica gel chromatography (heptane:EtOAc = 2:1) to afford **20d** as a colorless oil (0.82 g, 89 %).

^1H NMR (400 MHz, CDCl_3): δ 5.04 (s, 1H), 4.92 (s, 1H), 4.14 (dt, $J = 7.3, 3.4$ Hz, 1H), 3.43 – 3.34 (m, 1H), 3.17 – 3.07 (m, 1H), 2.64 (s, 1H), 1.74 (s, 3H), 1.44 (s, 9H).
 ^{13}C NMR (101 MHz, CDCl_3): δ 156.95, 145.17, 111.82, 79.81, 75.05, 45.21, 28.51, 18.74.

Rf: 0.5 (heptane:EtOAc = 1:1).

Preparation of (9*H*-fluoren-9-yl)methyl (2-(3,4-dichlorophenyl)-2-((1,3-dioxoisindolin-2-yl)oxy)ethyl)carbamate (**21**)



21

According to typical procedure **TP4**, the reaction was performed by the addition of DEAD (1.3 eq., 71.4 μL , 0.455 mmol) into a solution of **19** (1 eq., 150 mg, 0.35 mmol), NHPI (1.3 eq., 74.3 mg, 0.455 mmol) and PPh_3 (1.3 eq., 119 mg, 0.455 mmol) in THF (4 mL) under Ar at 0°C and stirred at 0°C overnight. The crude was purified by silica gel chromatography (heptane:EtOAc = 5:1) to afford **21** as a white solid (196 mg, 98%).

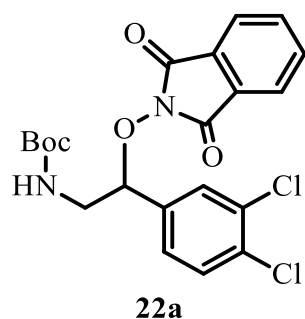
^1H NMR (400 MHz, CDCl_3): δ 7.82 (dd, $J = 5.5, 3.1$ Hz, 2H), 7.76 (dt, $J = 5.1, 3.4$ Hz, 4H), 7.65 (d, $J = 6.5$ Hz, 3H), 7.47 – 7.38 (m, 4H), 7.33 (t, $J = 7.4$ Hz, 2H), 5.97 (t, J

= 6.2 Hz, 1H), 5.27 (dd, $J = 7.5, 3.7$ Hz, 1H), 4.38 (dd, $J = 7.5, 2.3$ Hz, 2H), 4.26 (t, $J = 7.3$ Hz, 1H), 3.80 – 3.64 (m, 2H).

^{13}C NMR (101 MHz, CDCl_3): δ 163.89, 156.62, 144.08, 141.44, 136.14, 134.96, 133.52, 132.90, 130.72, 129.62, 128.81, 127.83, 127.22, 126.77, 125.40, 123.96, 120.10, 87.81, 67.39, 47.33, 45.03.

Rf: 0.5 (heptane:EtOAc = 1:1).

Preparation of *tert*-butyl (2-(3,4-dichlorophenyl)-2-((1,3-dioxoisindolin-2-yl)oxy)ethyl)carbamate (**22a**)



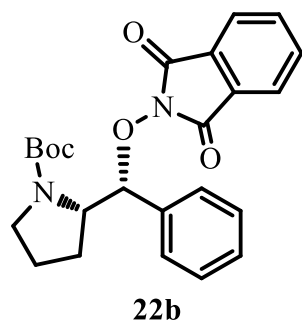
According to typical procedure **TP4**, the reaction was performed by the addition of DEAD (1.3 eq., 26.6 μL , 0.17 mmol) into a solution of **20a** (1 eq., 40 mg, 0.131 mmol), NHPI (1.3 eq., 27.7 mg, 0.17 mmol) and PPh_3 (1.3 eq., 44.5 mg, 0.17 mmol) in THF (1.49 mL) under Ar at 0°C and stirred at 0°C overnight. The crude was purified by silica gel chromatography (heptane:EtOAc = 5:1 to 4:1) to afford **22a** as a white solid (55.4 mg, 94%).

^1H NMR (400 MHz, CDCl_3): δ 7.83 – 7.78 (m, 2H), 7.77 – 7.72 (m, 2H), 7.63 (s, 1H), 7.45 (d, $J = 8.3$ Hz, 1H), 7.38 (dd, $J = 8.3, 2.1$ Hz, 1H), 5.50 (t, $J = 6.2$ Hz, 1H), 5.29 (t, $J = 5.3$ Hz, 1H), 3.61 (t, $J = 6.2$ Hz, 2H), 1.43 (s, 9H).

^{13}C NMR (101 MHz, CDCl_3): δ 163.88, 151.77, 134.89, 133.37, 132.80, 130.63, 129.72, 128.87, 126.93, 124.42, 123.92, 87.23, 84.52, 44.34, 28.48.

Rf: 0.6 (heptane:EtOAc = 1:1).

Preparation of (*S*)-*tert*-butyl 2-((*R*)-((1,3-dioxoisindolin-2-yl)oxy)(phenyl)methyl)pyrrolidine-1-carboxylate (**22b**)



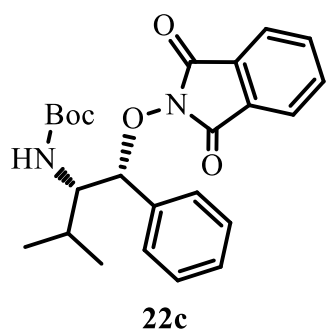
According to typical procedure **TP4**, the reaction was performed by the addition of DEAD (1.8 eq., 0.305 mL, 1.95 mmol) into a solution of **20b** (1 eq., 300 mg, 1.08 mmol), NHPI (1.5 eq., 264 mg, 1.62 mmol) and PPh₃ (1.8 eq., 510 mg, 1.95 mmol) in THF (12 mL) under Ar at 0°C and stirred at 0°C overnight. The crude was purified by silica gel chromatography (heptane:EtOAc = 4:1) to afford **22b** as a white solid (429 mg, 94%).

¹H NMR (400 MHz, CDCl₃): δ 7.72 – 7.38 (m, 6H), 7.30 – 7.19 (m, 3H), 5.88 (s, 0.45H), 5.68 (s, 0.55H), 4.03 (m, 1H), 3.59 – 3.32 (m, 2H), 2.50 – 2.19 (m, 1H), 2.05 (m, 1H), 1.75 (m, 2H), 1.40 (s, 4H), 1.36 (s, 5H).

¹³C NMR (101 MHz, CDCl₃): δ 163.61, 158.46, 134.37, 129.16, 128.57, 128.22, 127.75, 127.52, 123.45, 88.86, 77.36, 61.80, 29.86, 28.63, 22.84, 14.26.

Rf: 0.49 (heptane:EtOAc = 2:1).

Preparation of *tert*-butyl ((1*R*,2*S*)-1-((1,3-dioxoisindolin-2-yl)oxy)-3-methyl-1-phenylbutan-2-yl)carbamate (**22c**)



According to typical procedure **TP4**, the reaction was performed by the addition of DEAD (1.8 eq., 0.526 mL, 3.35 mmol) into a solution of **20c** (1 eq., 0.52 g, 1.86 mmol), NHPI (1.5 eq., 0.455 g, 2.79 mmol) and PPh₃ (1.8 eq., 0.879 g, 3.35 mmol) in

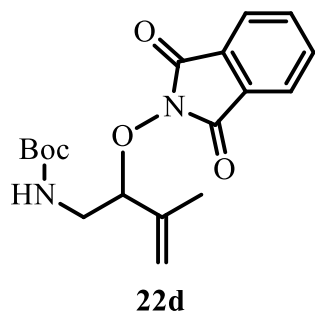
THF (13.5 mL) under Ar at 0°C and stirred at 0°C overnight. The crude was purified by silica gel chromatography (heptane:EtOAc = 4:1 to 3:1) to afford **22c** as a white solid (0.64 g, 81%).

¹H NMR (400 MHz, CDCl₃): δ 7.71 – 7.65 (m, 4H), 7.51 – 7.47 (m, 2H), 7.31 – 7.27 (m, 3H), 5.52 (d, *J* = 4.7 Hz, 1H), 5.12 (d, *J* = 10.2 Hz, 1H), 3.84 – 3.77 (m, 1H), 1.96 – 1.87 (m, 1H), 1.39 (s, 9H), 1.16 (d, *J* = 6.7 Hz, 3H), 0.95 (d, *J* = 6.8 Hz, 3H).

¹³C NMR (101 MHz, CDCl₃): δ 163.74, 156.09, 136.51, 134.46, 128.99, 128.94, 128.31, 128.14, 123.48, 88.21, 79.20, 60.00, 30.56, 28.54, 20.30, 18.47.

Rf: 0.35 (heptane:EtOAc = 3:1).

Preparation of *tert*-butyl (2-((1,3-dioxoisindolin-2-yl)oxy)-3-methylbut-3-en-1-yl)carbamate (**22d**)



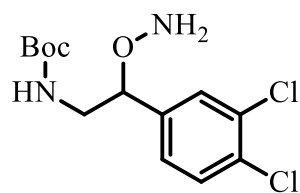
According to typical procedure **TP4**, the reaction was performed by the addition of DEAD (1.3 eq., 0.274 mL, 1.74 mmol) into a solution of **20d** (1 eq., 270 mg, 1.34 mmol), NHPI (1.3 eq., 284 mg, 1.74 mmol) and PPh₃ (1.3 eq., 457 mg, 1.74 mmol) in THF (8 mL) under Ar at 0°C and stirred at 0°C overnight. The crude was purified by silica gel chromatography (heptane:EtOAc = 5:1 to 3:1) to afford **22d** as a colorless oil (440 mg, 95 %).

¹H NMR (400 MHz, CDCl₃): δ 7.86 – 7.66 (m, 4H), 5.42 (s, 1H), 5.09 – 4.97 (m, 2H), 4.70 – 4.55 (m, 1H), 3.55 – 3.38 (m, 2H), 1.92 (s, 3H), 1.46 (s, 9H).

¹³C NMR (101 MHz, CDCl₃): δ 163.93, 156.16, 140.32, 134.65, 128.94, 123.69, 117.71, 90.65, 79.59, 42.00, 28.52, 17.91.

Rf: 0.6 (heptane:EtOAc = 1:1).

Preparation of *tert*-butyl (2-(aminooxy)-2-(3,4-dichlorophenyl)ethyl)carbamate (25a)



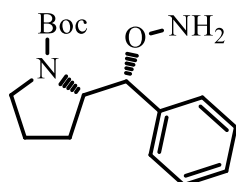
25a

According to typical procedure **TP5**, the reaction was performed with **22a** (1 eq., 400 mg, 0.886 mmol) and hydrazine hydrate (15 eq., 1.29 mL, 13.3 mmol) in EtOH (12 mL) in 30 min, affording **25a** as a white solid (267 mg, 94%).

^1H NMR (400 MHz, CDCl_3): δ 7.46 – 7.41 (m, 2H), 7.16 (dd, $J = 8.2, 1.8$ Hz, 1H), 5.44 (s, 2H), 4.86 (s, 1H), 4.60 (dd, $J = 7.9, 3.8$ Hz, 1H), 3.56 – 3.44 (m, 1H), 3.19 (ddd, $J = 14.4, 7.9, 4.8$ Hz, 1H), 1.43 (s, 9H).

^{13}C NMR (101 MHz, CDCl_3): δ 155.94, 139.87, 132.95, 132.19, 130.74, 128.78, 126.18, 84.70, 79.79, 44.93, 28.50.

Preparation of (*S*)-*tert*-butyl 2-((*R*)-(aminooxy)(phenyl)methyl)pyrrolidine-1-carboxylate (25b)



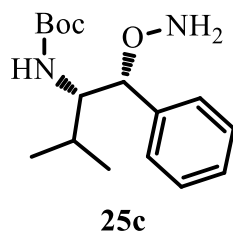
25b

According to typical procedure **TP5**, the reaction was performed with **22b** (1 eq., 100 mg, 0.237 mmol) and hydrazine hydrate (15 eq., 0.344 mL, 3.55 mmol) in EtOH (3 mL) in 16 h, affording **25b** as a colorless oil (67 mg, 97%).

^1H NMR (400 MHz, CDCl_3): δ 7.42 – 7.27 (m, 5H), 5.43 (s, 2H), 5.01 (m, 1H), 4.00 (m, 1H), 3.61 – 3.26 (m, 2H), 2.13 – 1.70 (m, 3H), 1.63 (m, 1H), 1.52 – 1.46 (m, 9H).

^{13}C NMR (101 MHz, CDCl_3): δ 154.62, 128.61, 127.63, 126.44, 125.97, 88.10, 79.68, 62.04, 47.04, 28.71, 25.79, 23.73.

Preparation of *tert*-butyl ((1*R*,2*S*)-1-(aminooxy)-3-methyl-1-phenylbutan-2-yl) carbamate (25c**)**

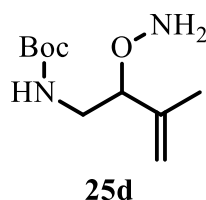


According to typical procedure **TP5**, the reaction was performed in 1 h using **22c** (1 eq., 45 mg, 0.106 mmol) and hydrazine hydrate (15 eq., 0.154 mL, 1.59 mmol) in EtOH (1.5 mL) in 1 h, affording **25c** as a white solid (30 mg, 96%).

¹H NMR (400 MHz, CDCl₃): δ 7.31 – 7.25 (m, 5H), 5.26 (s, 2H), 4.68 (d, *J* = 10.4 Hz, 1H), 4.60 (d, *J* = 4.9 Hz, 1H), 3.59 – 3.49 (m, 1H), 1.75 – 1.65 (m, 1H), 1.31 (s, 9H), 0.96 (d, *J* = 6.7 Hz, 3H), 0.86 (d, *J* = 6.8 Hz, 3H).

¹³C NMR (101 MHz, CDCl₃): δ 156.05, 139.67, 128.57, 127.88, 127.04, 86.77, 78.95, 60.04, 30.12, 28.48, 20.32, 18.33.

Preparation of *tert*-butyl (2-(aminooxy)-3-methylbut-3-en-1-yl)carbamate (25d**)**



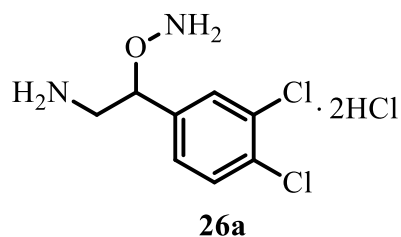
According to typical procedure **TP5**, the reaction was performed with **22d** (1 eq., 1.65 g, 4.76 mmol) and hydrazine hydrate (15 eq., 6.93 mL, 71.5 mmol) in EtOH (23.6 mL) in 1 h. The reaction mixture was concentrated in vacuo directly and purified by silica gel chromatography (heptane:EtOAc = 2:1 to 1:1) to afford **25d** as a white solid (1.01 g, 98 %).

¹H NMR (400 MHz, CDCl₃): δ 5.31 (s, 2H), 5.04 – 4.99 (m, 2H), 4.85 (s, 1H), 3.96 (dd, *J* = 7.7, 3.9 Hz, 1H), 3.46 – 3.34 (m, 1H), 3.14 – 3.01 (m, 1H), 1.71 (s, 3H), 1.43 (s, 9H).

¹³C NMR (101 MHz, CDCl₃): δ 156.06, 142.26, 113.93, 87.18, 79.42, 42.25, 28.52, 18.56.

Rf: 0.4 (heptane:EtOAc = 1:1).

Preparation of 2-(aminooxy)-2-(3,4-dichlorophenyl)ethanamine dihydrochloride (26a)

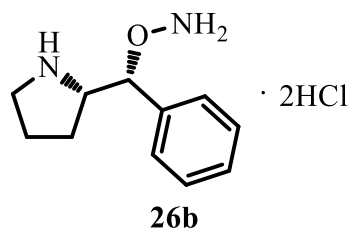


The reaction was performed with **25a** (1 eq., 91 mg, 0.283 mmol) in HCl/dioxane (4 M, 2.73 mL) according to typical procedure **TP6**, affording **26a** as a white solid (80 mg, 96%).

^1H NMR (400 MHz, DMSO- d^6): δ 10.48 (s, 3H), 8.42 (s, 3H), 7.76 – 7.72 (m, 2H), 7.46 (dd, J = 8.3, 2.0 Hz, 1H), 5.43 (dd, J = 8.6, 4.0 Hz, 1H), 3.34 – 3.17 (m, 2H).

^{13}C NMR (101 MHz, DMSO- d^6): δ 135.98, 132.06, 131.41, 130.95, 129.84, 128.11, 80.76, 41.66.

Preparation of *O*-((*R*)-phenyl((*S*)-pyrrolidin-2-yl)methyl)hydroxylamine dihydrochloride (26b)

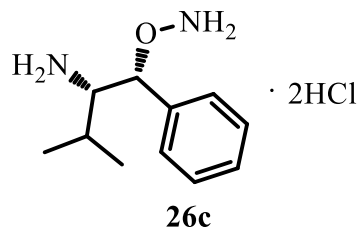


The reaction was performed with **25b** (1 eq., 60 mg, 0.205 mmol) in HCl/dioxane (4 M, 2 mL) according to typical procedure **TP6**, affording **26b** as a white solid (52.2 mg, 96 %).

^1H NMR (400 MHz, DMSO- d^6): δ 10.16 (s, 5H), 7.62 – 7.31 (m, 5H), 5.59 (d, J = 5.0 Hz, 1H), 3.85 (m, 1H), 3.24 – 3.06 (m, 2H), 1.88 (m, 4H).

^{13}C NMR (101 MHz, DMSO- d^6): δ 135.05, 129.14, 128.76, 127.03, 83.15, 61.72, 45.37, 24.56, 23.48.

Preparation of (1*R*,2*S*)-1-(aminooxy)-3-methyl-1-phenylbutan-2-amine dihydrochloride (26c)

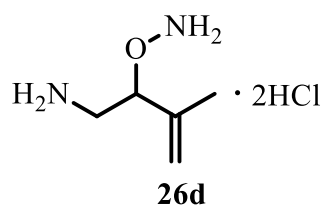


The reaction was performed with **25c** (1 eq., 285 mg, 0.968 mmol) in HCl/dioxane (4 M, 5 mL) according to typical procedure **TP6**, affording **26c** as a white solid (244 mg, 94 %).

^1H NMR (400 MHz, DMSO- d^6): δ 9.02 (s, 6H), 7.50 – 7.46 (m, 5H), 5.25 (d, J = 9.9 Hz, 1H), 3.44 (dd, J = 9.9, 2.5 Hz, 1H), 1.48 – 1.36 (m, 1H), 0.93 (d, J = 7.1 Hz, 3H), 0.81 (d, J = 7.0 Hz, 3H).

^{13}C NMR (101 MHz, DMSO- d^6): δ 130.29, 129.38, 128.93, 85.18, 58.57, 27.55, 19.58, 15.61.

Preparation of 2-(aminooxy)-3-methylbut-3-en-1-amine dihydrochloride (26d)

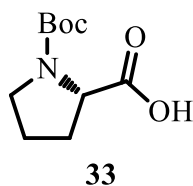


The reaction was performed with **25d** (1 eq., 300 mg, 1.39 mmol) in HCl/dioxane (4 M, 15 mL) according to typical procedure **TP6**, affording **26d** as a white solid (259 mg, 99 %).

^1H NMR (400 MHz, DMSO- d^6): δ 10.90 (s, 3H), 8.35 (s, 3H), 5.24 (s, 1H), 5.22 – 5.19 (m, 1H), 4.79 (dd, J = 8.2, 4.0 Hz, 1H), 3.09 – 2.98 (m, 2H), 1.72 (s, 3H).

^{13}C NMR (101 MHz, DMSO- d^6): δ 138.73, 118.52, 83.96, 66.82, 17.88.

Preparation of (*S*)-1-(*tert*-butoxycarbonyl)pyrrolidine-2-carboxylic acid (**33**)



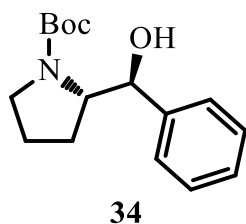
Boc₂O (1.2 eq., 11.4 g, 11.2 mL, 52.1 mmol) was added portionwise to a solution of proline (1 eq., 5 g, 3.7 mL, 43.4 mmol) in NaOH_{aq} (2 eq., 1 M, 87 mL, 87 mmol) and dioxane (21.7 mL) at 0 °C over 10 min. The resulting mixture was stirred at 0 °C for 30 min, then allowed to warm to rt and stirred overnight. The organic solvent was removed under reduced pressure. The remaining aqueous solution was acidified to pH ~2 with saturated aq. citric acid. The aqueous solution was extracted with DCM thrice. The combined organic layers were washed with brine, dried over Na₂SO₄, and concentrated in vacuo to afford **33** as a white solid (9.1 g, 97 %).

¹H NMR (400 MHz, CDCl₃, mixture of rotamers): δ 11.12 (s, 1H), 4.28 (m, 1H), 3.61 – 3.28 (m, 2H), 2.32 – 2.16 (m, 1H), 2.15 – 1.99 (m, 1H), 1.91 (m, 2H), 1.46 (s, 4.5H), 1.41 (s, 4.5H).

Rf: 0.58 (EtOAc with 0.1% AcOH).

These data are consistent with the previously reported characterization.¹⁸⁰

Preparation of (*S*)-*tert*-butyl 2-((*S*)-hydroxy(phenyl)methyl)pyrrolidine-1-carboxylate (**34**)



The reaction was performed with **17b** (1 eq., 400 mg, 1.45 mmol) in MeOH (6 mL) with NaBH₄ (4 eq., 219 mg, 5.81 mmol) according to typical procedure **TP3** in 1 h. The crude was purified by reverse phase chromatography (MeOH/H₂O) to afford **34** as a colorless oil (290 mg, 72%).

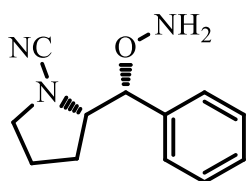
¹H NMR (400 MHz, CDCl₃): δ 7.37 – 7.27 (m, 5H), 5.94 – 5.74 (m, 1H), 4.52 (d, *J*=

8.9 Hz, 1H), 4.09 (td, $J = 8.3, 3.8$ Hz, 1H), 3.53 – 3.32 (m, 2H), 1.71 (m, 3H), 1.52 (s, 9H).

Rf: 0.55 (heptane:EtOAc = 2:1).

These data are consistent with the previously reported characterization.¹²⁵

Preparation of (*S*)-2-((*R*)-(aminooxy)(phenyl)methyl)pyrrolidine-1-carbonitrile (**37**)



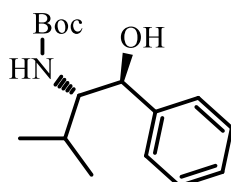
37

TEA (3 eq., 17.2 mg, 0.0236 mL, 0.17 mmol) was slowly added to a solution of **26b** (1 eq., 15 mg, 0.0566 mmol) in MeCN (1.25 mL) at 0 °C and stirred for 5 min. Then, a solution of BrCN (1.2 eq., 7.19 mg, 0.0679 mmol) in MeCN (0.25 mL) was added dropwise at 0 °C. The resulting mixture was stirred at 0 °C for 30 min and concentrated in vacuo. The crude was purified by reverse phase chromatography (MeOH/H₂O) to afford **37** as a white solid (8.4 mg, 68%).

¹H NMR (400 MHz, DMSO-*d*⁶): δ 7.41 – 7.31 (m, 5H), 6.05 (s, 2H), 4.54 (d, $J = 4.1$ Hz, 1H), 3.92 (m, 1H), 3.34 – 3.08 (m, 3H), 1.85 – 1.69 (m, 2H), 1.37 (m, 1H).

¹³C NMR (101 MHz, DMSO-*d*⁶): δ 138.66, 128.08, 127.64, 127.37, 117.01, 86.09, 64.24, 51.20, 26.23, 23.86.

Preparation of *tert*-butyl ((1*S*,2*S*)-1-hydroxy-3-methyl-1-phenylbutan-2-yl) carbamate (**38**)



38

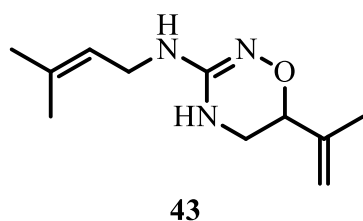
The reaction was performed with **17c** (1 eq., 1 g, 3.61 mmol) in MeOH (30 mL) with

NaBH₄ (2 eq., 0.273 g, 7.21 mmol) according to typical procedure **TP3** in 2 h. The crude was purified by reverse phase chromatography (MeOH/H₂O) to afford **38** as a white solid (201 mg, 20 %).

¹H NMR (400 MHz, CDCl₃): δ 7.35 – 7.33 (m, 4H), 7.28 – 7.26 (m, 1H), 4.83 – 4.75 (m, 2H), 3.50 – 3.42 (m, 1H), 1.89 – 1.79 (m, 1H), 1.36 (s, 9H), 1.19 (s, 1H), 1.01 (d, *J* = 6.7 Hz, 3H), 0.94 (d, *J* = 6.8 Hz, 3H).

These data are consistent with the previously reported characterization.¹²⁸

Preparation of *N*-(3-methylbut-2-en-1-yl)-6-(prop-1-en-2-yl)-5,6-dihydro-4*H*-1,2,4-oxadiazin-3-amine (**43**)



47 (1 eq., 6.5 mg, 0.021 mmol) was added to a solution of HCl in dioxane (4 M, 1 mL) and stirred at rt for 25h. The reaction mixture was concentrated in vacuo and basified by an aqueous solution of saturated NaHCO₃ until pH~8. After concentrated under reduced pressure, the residue was purified by reverse phase chromatography (ACN/H₂O) to afford **43** as a white solid (4.2 mg, 96%).

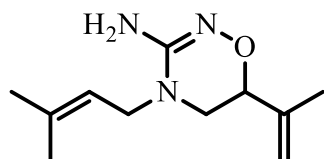
¹H NMR (400 MHz, DMSO-*d*⁶): δ 5.76 (s, 1H), 5.20 (t, *J* = 7.0 Hz, 1H), 4.95 (s, 1H), 4.89 (s, 1H), 4.63 – 4.59 (m, 1H), 3.72 (dd, *J* = 9.5, 3.0 Hz, 1H), 3.43 – 3.37 (m, 2H), 3.29 – 3.26 (m, 1H), 3.05 – 2.99 (m, 1H), 1.71 (s, 3H), 1.67 (s, 3H), 1.59 (s, 3H).

¹H NMR (400 MHz, MeOD-*d*⁴): δ 5.28 – 5.22 (m, 1H), 5.03 – 4.97 (m, 2H), 3.97 (dd, *J* = 9.6, 3.3 Hz, 1H), 3.54 (d, *J* = 6.8 Hz, 2H), 3.40 (dd, *J* = 11.2, 3.3 Hz, 1H), 3.27 – 3.21 (m, 1H), 1.80 – 1.66 (m, 9H).

¹³C NMR (101 MHz, DMSO-*d*⁶): δ 153.77, 142.46, 132.62, 122.75, 111.90, 74.47, 43.65, 38.81, 25.35, 19.04, 17.65.

Preparation of 4-(3-methylbut-2-en-1-yl)-6-(prop-1-en-2-yl)-5,6-dihydro-4*H*-

1,2,4-oxadiazin-3-amine (45)



45

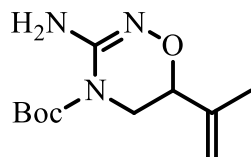
10d (1 eq., 10 mg, 0.0708 mmol) was dissolved in MeCN (0.6 mL), followed by the addition of 3,3-dimethylallyl bromide (1 eq., 8.3 μ L, 0.0708 mmol) and TEA (2 eq., 19.7 μ L, 0.142 mmol). The resulting mixture was stirred at rt for 16 h, then, concentrated in vacuo and purified by reverse phase chromatography (MeCN/H₂O) to afford **45** as a white solid (11 mg, 74 %).

¹H NMR (400 MHz, DMSO-*d*⁶): δ 7.50 (s, 2H), 5.32 – 5.23 (m, 1H), 5.02 – 4.96 (m, 2H), 4.21 (dd, *J* = 10.0, 3.3 Hz, 1H), 4.13 (dd, *J* = 15.8, 7.1 Hz, 1H), 4.00 (dd, *J* = 15.7, 7.0 Hz, 1H), 3.32 – 3.27 (m, 1H), 3.20 (dd, *J* = 13.7, 10.1 Hz, 1H), 1.73 – 1.71 (m, 6H), 1.66 (s, 3H).

¹H NMR (400 MHz, MeOD-*d*⁴): δ 5.37 – 5.30 (m, 1H), 5.14 – 5.12 (m, 1H), 5.09 (q, *J* = 1.1 Hz, 1H), 4.48 (dd, *J* = 10.0, 3.5 Hz, 1H), 4.34 (dd, *J* = 15.9, 7.0 Hz, 1H), 4.21 (dd, *J* = 15.9, 7.5 Hz, 1H), 3.54 (dd, *J* = 12.3, 3.5 Hz, 1H), 3.42 (dd, *J* = 12.4, 10.1 Hz, 1H), 1.82 – 1.79 (m, 6H), 1.76 (s, 3H).

¹³C NMR (101 MHz, DMSO-*d*⁶): δ 153.73, 140.15, 138.29, 117.88, 113.67, 75.95, 49.53, 44.57, 25.49, 18.87, 17.84.

Preparation of *tert*-butyl 3-amino-6-(prop-1-en-2-yl)-5,6-dihydro-4*H*-1,2,4-oxadiazine-4-carboxylate (46)



46

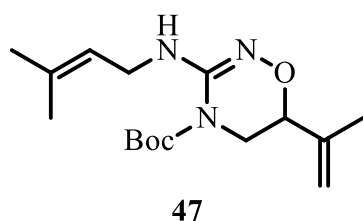
TEA (2 eq., 39.4 μ L, 0.283 mmol) was added to a solution of **10d** (1 eq., 20 mg, 0.142 mmol) and Boc₂O (1.1 eq., 34 mg, 0.156 mmol) in DCM (1 mL). The mixture was stirred at rt for 16 h, then, concentrated in vacuo and purified by reverse phase

chromatography (MeOH/H₂O) to afford **46** as a white solid (31 mg, 91 %).

¹H NMR (400 MHz, CDCl₃): δ 5.25 (s, 2H), 5.07 – 5.05 (m, 1H), 5.04 – 5.02 (m, 1H), 4.14 (dd, *J* = 10.3, 3.0 Hz, 1H), 3.84 (dd, *J* = 12.0, 3.1 Hz, 1H), 3.53 (dd, *J* = 12.0, 10.3 Hz, 1H), 1.81 (s, 3H), 1.52 (s, 9H).

¹³C NMR (101 MHz, CDCl₃): δ 151.81, 150.68, 140.65, 114.18, 84.06, 76.58, 48.39, 28.23, 19.18.

Preparation of *tert*-butyl 3-((3-methylbut-2-en-1-yl)amino)-6-(prop-1-en-2-yl)-5,6-dihydro-4*H*-1,2,4-oxadiazine-4-carboxylate (47**)**

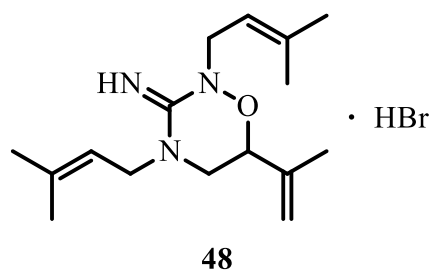


A solution of NaH (4 eq., 4.61 mg, 0.182 mmol) in THF (0.4 mL) was slowly added to a solution of **46** (1 eq., 11 mg, 0.0456 mmol) in THF (0.7 mL) under Ar at rt. The mixture was stirred at 60 °C for 1 h and then a solution of 3,3-dimethylallyl bromide (4 eq., 21.4 μL, 0.182 mmol) in THF (0.1 mL) was added and stirred at 60 °C for an additional 4h. The reaction mixture was concentrated in vacuo and purified by reverse phase chromatography (ACN/H₂O) to afford **47** as a white solid (10.7 mg, 76 %).

¹H NMR (400 MHz, CDCl₃): δ 6.65 (s, 1H), 5.34 – 5.24 (m, 1H), 5.07 – 4.93 (m, 2H), 4.11 (d, *J* = 10.6 Hz, 1H), 3.81 (dd, *J* = 11.9, 3.1 Hz, 1H), 3.70 – 3.60 (m, 2H), 3.54 (t, *J* = 11.3 Hz, 1H), 1.81 (s, 3H), 1.72 (s, 3H), 1.66 (s, 3H), 1.51 (s, 9H).

¹³C NMR (101 MHz, CDCl₃): δ 162.28, 150.53, 140.95, 138.85, 120.88, 113.69, 83.73, 76.54, 48.83, 39.86, 29.86, 28.25, 25.82, 19.19.

Preparation of *N*,4-bis(3-methylbut-2-en-1-yl)-6-(prop-1-en-2-yl)-5,6-dihydro-4*H*-1,2,4-oxadiazin-3-amine hydrobromide (48**)**



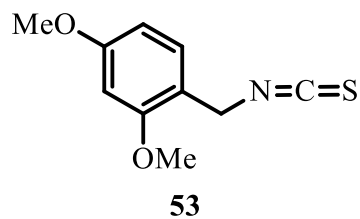
A solution of NaH (1.5 eq., 5.1 mg, 0.213 mmol) in THF (0.2 mL) was added to a solution of **10d** (1 eq., 20 mg, 0.142 mmol) in THF (0.4 mL) at 0 °C under Ar. The mixture was stirred at 0 °C for 2 h, followed by the addition of 3,3-dimethylallyl bromide (1.5 eq., 24.9 μ L, 0.213 mmol) at 0 °C and stirred at rt for 16 h. Two drops of water was added to quench the reaction. The mixture was concentrated in vacuo and purified by reverse phase chromatography (ACN/H₂O) to afford **48** as a white solid (21 mg, 53%).

¹H NMR (400 MHz, MeOD-*d*⁴): δ 5.38 – 5.32 (m, 1H), 5.29 – 5.23 (m, 1H), 5.14 – 5.12 (m, 1H), 5.09 (q, *J* = 1.1 Hz, 1H), 4.56 – 4.50 (m, 1H), 4.41 – 4.21 (m, 2H), 4.20 – 4.01 (m, 2H), 3.49 – 3.44 (m, 2H), 1.82 (d, *J* = 1.3 Hz, 3H), 1.80 (t, *J* = 1.2 Hz, 6H), 1.78 – 1.76 (m, 3H), 1.75 (d, *J* = 1.3 Hz, 3H).

¹H NMR (400 MHz, DMSO-*d*⁶): δ 8.07 (s, 2H), 5.34 – 5.20 (m, 2H), 5.10 (s, 1H), 5.04 (s, 1H), 4.56 (dd, *J* = 8.7, 5.2 Hz, 1H), 4.42 (dd, *J* = 15.7, 7.5 Hz, 1H), 4.27 – 4.14 (m, 2H), 3.98 (dd, *J* = 15.6, 6.3 Hz, 1H), 3.46 – 3.40 (m, 2H), 1.75 (s, 3H), 1.73 (s, 6H), 1.70 (s, 3H), 1.67 – 1.65 (m, 3H).

¹³C NMR (101 MHz, DMSO-*d*⁶): δ 153.59, 138.58, 138.56, 138.44, 116.91, 116.48, 115.25, 77.52, 50.21, 48.15, 47.38, 25.45, 18.63, 17.87.

Preparation of 1-(isothiocyanatomethyl)-2,4-dimethoxybenzene (**53**)



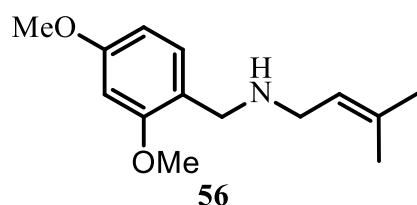
A solution of 2,4-dimethoxybenzylamine (1 eq., 0.45 mL, 2.99 mmol) in anhydrous DCM (3 mL) was added slowly to a solution of thiophosgene (3 eq., 1.03 g, 8.97

mmol) in anhydrous DCM (18 mL) at 0 °C under Ar. NaOH (3 eq., 0.36 g, 8.97 mmol) was then added at 0 °C. After stirred at rt for 2 h, the reaction mixture was filtered through a silica gel pad with DCM. The filtrate was concentrated in vacuo to afford **53** as a yellow oil (0.62 g, 99 %).

¹H NMR (400 MHz, CDCl₃): δ 7.18 (d, *J* = 8.8 Hz, 1H), 6.50 – 6.45 (m, 2H), 4.60 (s, 2H), 3.83 (s, 3H), 3.81 (s, 3H).

¹³C NMR (101 MHz, CDCl₃): δ 161.40, 158.01, 131.71, 129.53, 115.22, 104.34, 98.73, 55.60, 55.54, 44.19.

Preparation of *N*-(2,4-dimethoxybenzyl)-3-methylbut-2-en-1-amine (**56**)

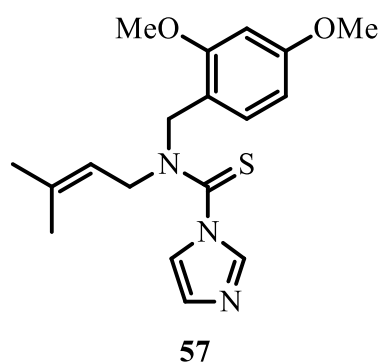


A solution of 3,3-dimethylallyl bromide (1 eq., 0.472 mL, 4.03 mmol) in THF (2.4 mL) was added dropwise to a solution of 2,4-dimethoxybenzylamine (1.5 eq., 0.91 mL, 6.04 mmol) and TEA (2 eq., 814 mg, 1.12 mL, 8.05 mmol) in THF (18 mL). The mixture was stirred at rt for 3h. The reaction was quenched by the addition of water and extracted with EtOAc thrice. The combined organic phases were concentrated in vacuo and purified by silica gel chromatography (DCM:MeOH = 20:1, contain 0.5% ammonia) to afford **56** as a yellow oil (0.72 g, 76 %).

¹H NMR (400 MHz, CDCl₃): δ 9.31 (s, 1H), 7.31 (d, *J* = 8.5 Hz, 1H), 6.44 – 6.39 (m, 2H), 5.42 (s, 1H), 3.96 (s, 2H), 3.86 (s, 3H), 3.75 – 3.72 (m, 3H), 3.39 (s, 2H), 1.74 (s, 3H), 1.54 (s, 3H).

¹³C NMR (101 MHz, CDCl₃): δ 162.11, 159.21, 141.36, 132.87, 114.72, 111.36, 104.65, 98.49, 55.79, 55.47, 44.15, 43.18, 25.92, 18.38.

Preparation of *N*-(2,4-dimethoxybenzyl)-*N*-(3-methylbut-2-en-1-yl)-1*H*-imidazole-1-carbothioamide (**57**)

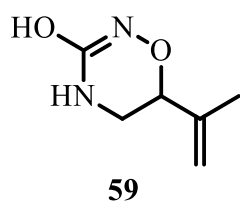


A solution of **56** (1 eq., 30 mg, 0.127 mmol) in MeCN (0.47 mL) was added dropwise to a solution of 1,1'-thiocarbonyldiimidazole (2 eq., 45.4 mg, 0.255 mmol) in MeCN (0.94 mL) and stirred at rt for 2h. The mixture was concentrated in vacuo and purified by reverse phase chromatography (MeOH/H₂O) to afford **57** as an orange solid (40 mg, 91 %).

¹H NMR (400 MHz, CDCl₃): δ 7.86 (s, 1H), 7.22 (s, 1H), 7.10 – 6.98 (m, 2H), 6.48 – 6.42 (m, 2H), 5.24 (s, 1H), 4.74 (s, 2H), 4.27 (s, 2H), 3.79 (s, 3H), 3.77 (s, 3H), 1.73 (s, 3H), 1.47 (s, 3H).

¹³C NMR (101 MHz, CDCl₃): δ 179.75, 161.21, 158.68, 138.55, 137.36, 129.94, 129.58, 119.47, 117.49, 115.04, 104.37, 98.80, 55.52, 55.46, 51.48, 50.84, 25.81, 18.16.

Preparation of 6-(prop-1-en-2-yl)-5,6-dihydro-4H-1,2,4-oxadiazin-3-ol (**59**)

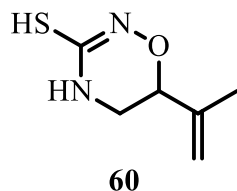


A mixture of **26d** (1 eq., 15 mg, 0.0793 mmol) and TEA (2 eq., 22.1 μL, 0.159 mmol) in DMF (1 mL) was stirred at rt for 1 min. Then, CDI (1.05 eq., 13.5 mg, 0.0833 mmol) was added to the mixture and stirred for another 2h. After completion, the reaction mixture was evaporated to dryness and the crude was purified by reverse phase chromatography (ACN/H₂O) to afford **59** as a white solid (10 mg, 89 %).

¹H NMR (400 MHz, DMSO-*d*⁶): δ 9.30 (s, 1H), 7.13 (s, 1H), 5.05 – 4.90 (m, 2H), 4.20 (dd, *J* = 9.6, 3.6 Hz, 1H), 3.31 – 3.26 (m, 1H), 3.20 – 3.13 (m, 1H), 1.72 (s, 3H).

^{13}C NMR (101 MHz, $\text{DMSO-}d^6$): δ 156.99, 140.36, 113.15, 77.11, 43.86, 18.86.

Preparation of 6-(prop-1-en-2-yl)-5,6-dihydro-4H-1,2,4-oxadiazine-3-thiol (**60**)

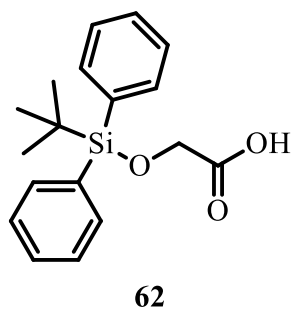


A mixture of **26d** (1 eq., 20 mg, 0.106 mmol) and TEA (2.2 eq., 32.3 μL , 0.233 mmol) in MeCN (0.67 mL) was stirred at rt for 1 min. Then, 1,1'-thiocarbonyldiimidazole (1.1 eq., 21.8 mg, 0.116 mmol) in MeCN (0.333 mL) was added dropwise to the mixture at 0°C and stirred at rt for 30 min. The mixture was concentrated in vacuo at 30°C and purified by reverse phase chromatography (MeCN/ H_2O) to afford **60** as a yellow solid (16 mg, 96 %).

^1H NMR (400 MHz, $\text{DMSO-}d^6$): δ 6.13 (s, 1H), 4.97 – 4.94 (m, 1H), 4.88 – 4.81 (m, 2H), 3.72 (dd, $J = 12.0, 9.4$ Hz, 1H), 3.42 – 3.25 (m, 2H), 1.65 (s, 3H).

^{13}C NMR (101 MHz, $\text{DMSO-}d^6$): δ 160.09, 143.70, 111.17, 81.11, 56.56, 16.52.

Preparation of 2-((*tert*-butyldiphenylsilyl)oxy)acetic acid (**62**)



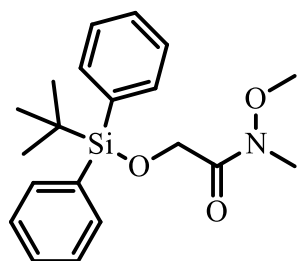
DMAP (3 %, 0.144 g, 1.18 mmol) and TEA (1.06 eq., 5.79 mL, 41.7 mmol) was added to a solution of glycolic acid (1 eq., 2.36 mL, 39.4 mmol) in THF (150 mL) and stirred at 0°C for five minutes. Then, chlorotrimethylsilane (1.05 eq., 5.28 mL, 41.3 mmol) was added dropwise over 15 minutes. After stirred at 0°C for 1 h and at rt for 2 h, a second portion of TEA (1.06 eq., 5.8 mL, 41.7 mmol) was added at rt followed by the addition of *tert*-butylchlorodiphenylsilane (1.05 eq., 10.7 mL, 41.3 mmol). The resulted mixture was stirred for at rt for 3 hours. Upon completion, the reaction was

quenched by the addition of an aqueous solution of AcOH (45 mL in 100 mL of H₂O). After stirred at rt for 2 hour, the mixture was poured into water, and extracted with Et₂O thrice. The combined organic phases were washed with brine, dried over anhydrous Na₂SO₄ and filtered. The filtrate was concentrated in vacuo and purified by silical gel chromatography (Et₂O/heptane =10:1 to 1:1) to afford **62** as a light yellow oil (11.4 g, 92%).

¹H NMR (400 MHz, CDCl₃): δ 10.07 (s, 1H), 7.70 – 7.67 (m, 4H), 7.49 – 7.40 (m, 6H), 4.28 (s, 2H), 1.12 (s, 9H).

These data are consistent with the previously reported characterization.¹⁸¹

Preparation of 2-((*tert*-butyldiphenylsilyl)oxy)-*N*-methoxy-*N*-methylacetamide (63)



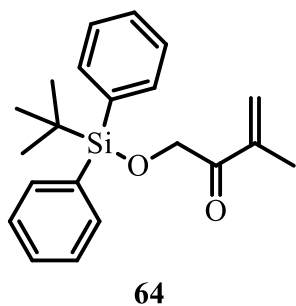
63

The reaction was performed with **62** (1 eq., 1.7 g, 5.41 mmol), CDI (1.3 eq., 1.14 g, 7.03 mmol) and *N,O*-dimethylhydroxylamine hydrochloride (1.3 eq., 0.686 g, 7.03 mmol) in DCM (15 mL) according to typical procedure **TP1**, affording **63** as a colorless oil (1.9 g, 98%).

¹H NMR (400 MHz, CDCl₃): δ 7.75 – 7.72 (m, 4H), 7.43 – 7.37 (m, 6H), 4.43 (s, 2H), 3.44 (s, 3H), 3.14 (s, 3H), 1.11 (s, 9H).

¹³C NMR (101 MHz, CDCl₃): δ 171.90, 135.82, 133.35, 129.89, 127.86, 62.17, 61.32, 32.59, 26.89, 19.49.

Preparation of 1-((*tert*-butyldiphenylsilyl)oxy)-3-methylbut-3-en-2-one (64)

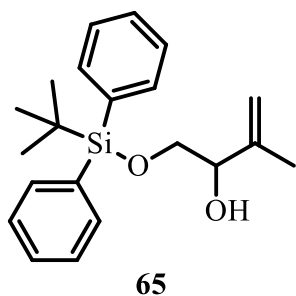


The reaction was performed with **63** (1 eq., 600 mg, 1.68 mmol) in THF (5.5 mL) and the THF solution of isopropenylmagnesium bromide (4 eq., 0.5 M, 13.4 mL, 6.71 mmol) according to typical procedure **TP2** without further purification to afford **64** as a yellow oil (557 mg, 98 %).

^1H NMR (400 MHz, CDCl_3): δ 7.71 – 7.66 (m, 4H), 7.43 – 7.37 (m, 6H), 5.74 (s, 1H), 5.66 (d, $J = 1.6$ Hz, 1H), 4.65 (s, 2H), 1.84 (dd, $J = 1.5, 0.9$ Hz, 3H), 1.12 – 1.09 (m, 9H).

^{13}C NMR (101 MHz, CDCl_3): δ 198.23, 142.47, 135.74, 133.20, 129.96, 127.89, 124.09, 66.82, 26.88, 19.47, 17.86.

Preparation of 1-((*tert*-butyldiphenylsilyl)oxy)-3-methylbut-3-en-2-ol (**65**)



Trichlorocerium heptahydrate (1.6 eq., 1041 mg, 2.79 mmol) was added to a solution of **64** (1 eq., 591 mg, 1.75 mmol) in MeOH (10 mL) and stirred at rt until the solution became clear. Then, the mixture was cooled to -70°C and NaBH_4 (1.3 eq., 85.9 mg, 2.27 mmol) was added portionwise. After stirred at -70°C for 20 min, the reaction was quenched by the addition of H_2O at -20°C and stirred for 5 min. MeOH was removed under reduced pressure. The resulting suspension was extracted with EtOAc thrice. The combined organic phases were washed with brine, dried over anhydrous Na_2SO_4 and filtered. The filtrate was concentrated in vacuo without further purification to

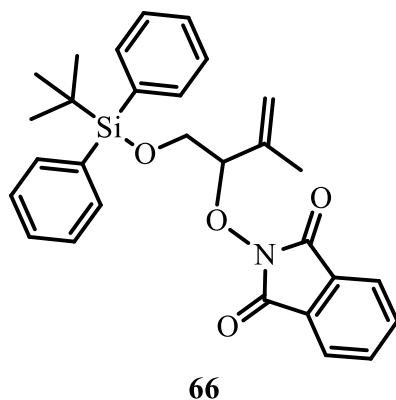
afford **65** as a colorless oil (571 mg, 96 %).

^1H NMR (400 MHz, CDCl_3): δ 7.69 – 7.66 (m, 4H), 7.45 – 7.38 (m, 6H), 5.02 (s, 1H), 4.89 (s, 1H), 4.20 – 4.14 (m, 1H), 3.73 (dd, $J = 10.2, 3.7$ Hz, 1H), 3.59 (dd, $J = 10.2, 7.7$ Hz, 1H), 2.72 (s, 1H), 1.64 (s, 3H), 1.08 (s, 9H).

^{13}C NMR (101 MHz, CDCl_3): δ 143.84, 135.71, 133.31, 130.00, 127.93, 112.08, 75.49, 67.08, 27.01, 19.41, 18.89.

Rf: 0.8 (heptane:EtOAc = 2:1).

Preparation of 2-((1-((*tert*-butyldiphenylsilyl)oxy)-3-methylbut-3-en-2-yl)oxy)isoindoline-1,3-dione (**66**)



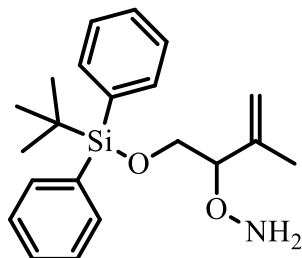
According to typical procedure **TP4**, the reaction was performed by the addition of DEAD (1.3 eq., 0.353 mL, 2.25 mmol) into a solution of **65** (1 eq., 590 mg, 1.73 mmol), NHPI (1.3 eq., 367 mg, 2.25 mmol) and PPh_3 (1.3 eq., 590 mg, 2.25 mmol) in THF (10 mL) under Ar at 0°C and stirred at rt for 2 h. The crude was purified by silica gel chromatography (heptane:EtOAc = 7:1) to afford **66** as a yellow oil (723 mg, 86 %).

^1H NMR (400 MHz, CDCl_3): δ 7.81 (dd, $J = 5.4, 3.1$ Hz, 2H), 7.72 (dd, $J = 5.5, 3.0$ Hz, 2H), 7.68 – 7.65 (m, 4H), 7.41 – 7.35 (m, 6H), 5.04 – 4.98 (m, 2H), 4.83 (dd, $J = 6.6, 5.0$ Hz, 1H), 4.12 (dd, $J = 11.4, 6.6$ Hz, 1H), 3.83 (dd, $J = 11.4, 5.0$ Hz, 1H), 1.78 (s, 3H), 1.00 (s, 9H).

^{13}C NMR (101 MHz, CDCl_3): δ 163.72, 140.48, 135.80, 134.36, 133.37, 129.89, 129.20, 127.84, 123.50, 118.18, 91.21, 64.07, 26.81, 19.27, 17.73.

Rf: 0.7 (heptane:EtOAc = 2:1).

Preparation of *O*-(1-((*tert*-butyldiphenylsilyl)oxy)-3-methylbut-3-en-2-yl)hydroxylamine (67)



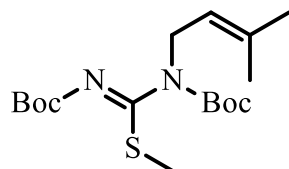
67

According to typical procedure **TP5**, the reaction was performed with **66** (1 eq., 250 mg, 0.515 mmol) and hydrazine hydrate (15 eq., 0.749 mL, 7.72 mmol) in EtOH (6.25 mL) in 20 min. The reaction mixture was concentrated in vacuo and filtered through a silica gel pad with EtOAc. The filtrate was concentrated in vacuo to afford **67** as a colorless oil (181 mg, 99 %).

^1H NMR (400 MHz, CDCl_3): δ 7.72 – 7.68 (m, 4H), 7.42 – 7.37 (m, 6H), 5.29 (s, 2H), 4.99 – 4.96 (m, 2H), 4.04 (dd, $J = 6.8, 4.5$ Hz, 1H), 3.74 (dd, $J = 11.1, 6.8$ Hz, 1H), 3.66 (dd, $J = 11.1, 4.5$ Hz, 1H), 1.64 – 1.62 (m, 3H), 1.06 (s, 9H).

^{13}C NMR (101 MHz, CDCl_3): δ 142.51, 135.79, 133.75, 129.79, 127.78, 113.93, 89.41, 64.82, 26.98, 19.40, 18.72.

Preparation of *tert*-butyl *N*-((1*Z*)-(((*tert*-butoxy)carbonyl)imino)(methylsulfanyl)methyl)-*N*'-(3-methylbut-2-en-1-yl)carbamate (68)



68

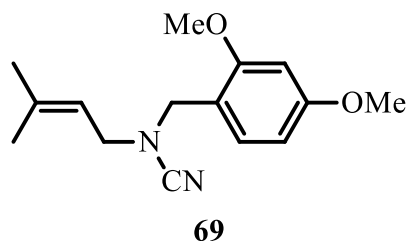
A solution of *N, N'*-bis-Boc-*S*-Methyl-thiourea (1 eq., 500 mg, 1.72 mmol) in DCM (8.14 mL)/MeCN (0.429 mL) was added dropwise to a stirred mixture of KOH (2.81 eq., 271 mg, 4.84 mmol) and TBAB (0.185 eq., 102 mg, 0.319 mmol) in DCM (8.14 mL)/MeCN (0.429 mL) at rt. After the resulting solution was stirred for 10 min, a

solution of 3,3-dimethylallyl bromide (2.39 eq., 0.484 mL, 4.12 mmol) in DCM (13.6 mL)/MeCN (0.714 mL) was slowly added over 10 min and stirred at rt for 3 h. The reaction mixture was diluted with water, and extracted with DCM thrice. The combine organic phases were washed with brine, dried over Na₂SO₄ and filtered. The filtrate was concentrated in vacuo to afford the residue, which was then filtered through a short silica gel pad with heptane/EtOAc (9:1). The filtrate was concentrated in vacuo to afford **68** as a colorless oil (592 mg, 96%).

¹H NMR (400 MHz, CDCl₃): δ 5.28 – 5.21 (m, 1H), 4.11 (d, *J* = 6.8 Hz, 2H), 2.34 (s, 3H), 1.70 (s, 3H), 1.65 (s, 3H), 1.48 (s, 9H), 1.44 (s, 9H).

¹³C NMR (101 MHz, CDCl₃): δ 163.34, 158.12, 152.02, 136.02, 119.79, 82.31, 81.81, 46.95, 28.25, 28.16, 25.85, 18.16, 15.74.

Preparation of *N*-(2,4-dimethoxybenzyl)-*N*-(3-methylbut-2-en-1-yl)cyanamide (**69**)

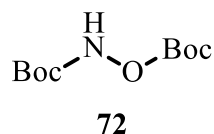


BrCN (1.1 eq., 32.7 mg, 0.309 mmol) was added to a solution of **56** (1 eq., 66 mg, 0.28 mmol) and TEA (1.1 eq., 42.9 μL, 0.309 mmol) in THF (1 mL) and stirred at rt for 20 min. The crude was washed with saturated NaHCO₃ aqueous solution and extracted with EtOAc. The organic phase was separated and filtered through a silica gel pad. The filtrate was concentrated in vacuo to afford **69** as a colorless oil (73 mg, 100 %).

¹H NMR (400 MHz, CDCl₃): δ 7.22 – 7.12 (m, 1H), 6.54 – 6.42 (m, 2H), 5.37 – 5.22 (m, 1H), 4.09 (s, 2H), 3.90 – 3.78 (m, 6H), 3.52 (d, *J* = 7.2 Hz, 2H), 1.76 (s, 3H), 1.62 (s, 3H).

¹³C NMR (101 MHz, CDCl₃): δ 161.39, 159.04, 139.33, 131.34, 118.64, 117.73, 115.85, 104.24, 98.76, 55.48, 49.50, 48.07, 25.88, 18.07.

Preparation of *tert*-butyl (*tert*-butoxycarbonyl)oxycarbamate (**72**)



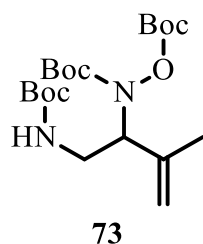
A solution of Boc₂O (2.1 eq., 27.9 g, 127 mmol) and TEA (2.1 eq., 17.8 mL, 127 mmol) in petroleum ether (20 mL)/methyl *tert*-butyl ether (7 mL) was added dropwise over 45 minutes to a solution of hydroxylamine hydrochloride (1 eq., 4.23 g, 60.9 mmol) in H₂O (40 mL) at 0 °C. The resulting biphasic reaction mixture was stirred at 0 °C for 6 hours, and then at rt for 16 hours. The reaction mixture was extracted with ether thrice. The combined organic phases were washed with brine, dried over Na₂SO₄ and filtered. The filtrate was concentrated in vacuo and purified by silica gel chromatography (Heptane:EtOAc=20:1 to 10:1) to **72** as a colorless oil (11.6 g, 82 %).

¹H NMR (400 MHz, CDCl₃): δ 7.58 (s, 1H), 1.51 (s, 9H), 1.48 (s, 9H).

Rf: 0.8 (heptane:EtOAc = 5:1).

These data are consistent with the previously reported characterization.¹⁸²

Preparation of *tert*-butyl (1-((*tert*-butoxycarbonyl)amino)-3-methylbut-3-en-2-yl) ((*tert*-butoxycarbonyl)oxy)carbamate (**73**)



To a solution of **20d** (1 eq., 600 mg, 2.98 mmol), PPh₃ (1.4 eq., 1094 mg, 4.17 mmol) and **72** (1.4 eq., 973 mg, 4.17 mmol) in THF (18 mL) was added dropwise DEAD (1.4 eq., 0.66 mL, 4.17 mmol) under Ar at 0 °C. The resulting mixture was stirred for an additional 1h at 0°C then at rt for 16 h. The reaction was quenched with the addition of water and extracted with EtOAc thrice. The combined organic phases were washed

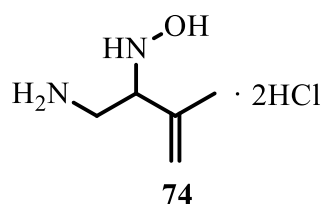
with brine, dried over Na₂SO₄ and filtered. The filtrate was concentrated in vacuo and purified by silica gel chromatography (Heptane:EtOAc = 15:1 to 10:1) to afford **73** as a colorless oil (1.2 g, 97 %).

¹H NMR (400 MHz, CDCl₃): δ 5.47 (s, 0.63H), 4.96 (s, 1H), 4.88 (s, 1H), 4.81 (s, 0.35H), 4.69 – 4.61 (m, 1H), 3.79 (t, *J* = 11.1 Hz, 0.66H), 3.58 (s, 0.34H), 3.40 (s, 0.3H), 2.89 (t, *J* = 12.0 Hz, 0.7H), 1.83 (s, 1H), 1.75 (s, 2H), 1.54 – 1.42 (m, 27H).

¹³C NMR (101 MHz, CDCl₃): δ 159.12, 156.18, 154.80, 140.70, 114.00, 85.42, 82.88, 79.41, 63.20, 39.39, 28.58, 28.27, 27.70, 21.15.

Rf: 0.55 (heptane:EtOAc = 3:1).

Preparation of 2-(hydroxyamino)-3-methylbut-3-en-1-amine dihydrochloride (**74**)

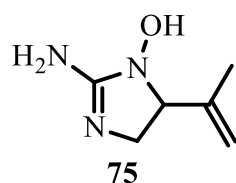


A solution of **73** (1 eq., 187 mg, 0.449 mmol) in HCl/dioxane (4M, 3 mL) was stirred at rt for 3 h. The reaction was concentrated in vacuo and dried under reduced pressure overnight to afford **74** as a hygroscopic white solid (84 mg, 99 %).

¹H NMR (400 MHz, DMSO-*d*⁶): δ 11.86 (s, 2H), 10.91 (s, 1H), 8.35 (s, 3H), 5.28 (s, 1H), 5.25 (t, *J* = 1.5 Hz, 1H), 4.10 (t, *J* = 6.6 Hz, 1H), 3.32 – 3.11 (m, 2H), 1.82 (s, 3H).

¹³C NMR (101 MHz, DMSO-*d*⁶): δ 135.48, 120.57, 62.94, 36.34, 19.34.

Preparation of 2-amino-5-(prop-1-en-2-yl)-4,5-dihydro-1H-imidazol-1-ol (**75**)



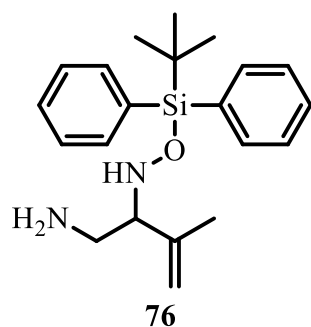
TEA (4 eq., 119 mg, 0.165 mL, 1.18 mmol) was added dropwise to a solution of **74** (1

eq., 56 mg, 0.296 mmol) in MeCN (12 mL) under at 0 °C and stirred for additional 15 min. Then a solution of BrCN (1.1 eq., 34.5 mg, 0.326 mmol) in MeCN (2 mL) was added slowly at 0 °C. After stirring at 0 °C for 4 h, the reaction mixture was concentrated in vacuo and purified by reverse phase chromatography (100% H₂O) to afford **75** as a white solid (34 mg, 81 %).

¹H NMR (400 MHz, DMSO-*d*⁶): δ 10.29 (s, 1H), 8.60 (s, 2H), 5.13 (s, 1H), 5.06 (t, *J* = 1.7 Hz, 1H), 4.31 (t, *J* = 9.3 Hz, 1H), 3.64 (t, *J* = 9.4 Hz, 1H), 3.25 (t, *J* = 9.9 Hz, 1H), 1.74 (s, 3H).

¹³C NMR (101 MHz, DMSO-*d*⁶): δ 161.96, 139.50, 116.68, 68.26, 43.84, 17.14.

Preparation of 2-(((*tert*-butyldiphenylsilyl)oxy)amino)-3-methylbut-3-en-1-amine (76)



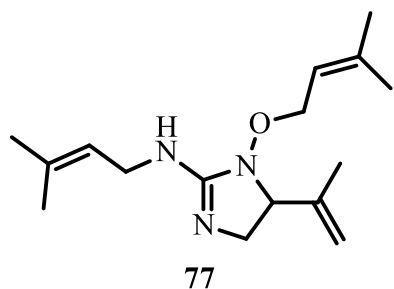
TEA (2 eq., 0.147 mL, 1.06 mmol) was slowly added to a suspension of **74** (1 eq., 100 mg, 0.529 mmol) in dry DMF (3 mL) at 0 °C and stirred for 10 min. Then TBDMSCl (3 eq., 0.411 mL, 1.59 mmol) and imidazole (3.5 eq., 126 mg, 1.85 mmol) was added and stirred at 60 °C for 4 h. The crude was purified by reverse phase chromatography (MeOH/H₂O) to afford **76** as a white solid (26 mg, 14 %).

¹H NMR (400 MHz, CDCl₃): δ 10.76 (s, 2H), 7.72 – 7.67 (m, 4H), 7.48 – 7.39 (m, 6H), 5.45 (d, *J* = 6.8 Hz, 1H), 5.01 – 4.93 (m, 1H), 4.78 (s, 1H), 3.69 – 3.59 (m, 2H), 3.38 (dd, *J* = 14.0, 7.7 Hz, 1H), 1.79 (s, 3H), 1.06 (s, 9H).

¹³C NMR (101 MHz, CDCl₃): δ 150.84, 143.11, 135.73, 130.24, 128.11, 119.89, 66.50, 37.42, 27.22, 20.44, 19.32.

Preparation of *N*-(3-methylbut-2-en-1-yl)-1-((3-methylbut-2-en-1-yl)oxy)-5-

(prop-1-en-2-yl)-4,5-dihydro-1H-imidazol-2-amine (77)



A solution of NaH (3 eq., 9.84 mg, 0.41 mmol) in THF (0.4 mL) was added slowly to a solution of **75** (1 eq., 19.3 mg, 0.137 mmol) in THF (0.2 mL) at 0 °C under Ar. The mixture was stirred at 0 °C for 2 h followed by the addition of 3,3-dimethylallyl bromide (3 eq., 48.1 μ L, 0.41 mmol) and then the resulting mixture was stirred at rt for additional 16 h. The reaction mixture was concentrated in vacuo and purified by reverse phase chromatography (MeOH/H₂O) to afford **77** as a white solid (29 mg, 76 %).

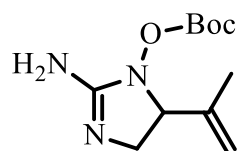
¹H NMR (400 MHz, MeOD-*d*⁴): δ 5.46 – 5.40 (m, 1H), 5.24 – 5.17 (m, 2H), 5.17 – 5.14 (m, 1H), 4.54 (dd, *J* = 8.7, 7.2 Hz, 1H), 4.51 – 4.40 (m, 2H), 4.02 (d, *J* = 7.3 Hz, 2H), 3.68 (dd, *J* = 10.0, 8.8 Hz, 1H), 3.40 (dd, *J* = 10.0, 7.2 Hz, 1H), 1.82 – 1.80 (m, 3H), 1.80 – 1.78 (m, 6H), 1.77 – 1.75 (m, 3H), 1.72 – 1.70 (m, 3H).

¹³C NMR (101 MHz, MeOD-*d*⁴): δ 161.57, 142.62, 142.23, 140.71, 119.69, 119.06, 116.07, 73.90, 68.46, 49.39, 44.00, 25.97, 25.81, 18.26, 18.05, 17.10.

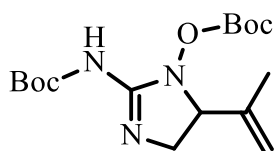
Preparation of 2-amino-5-(prop-1-en-2-yl)-4,5-dihydro-1H-imidazol-1-yl *tert*-butyl carbonate (79a),

***tert*-butyl(1-((*tert*-butoxycarbonyl)oxy)-5-(prop-1-en-2-yl)-4,5-dihydro-1H-imidazol-2-yl)carbamate (79b) and**

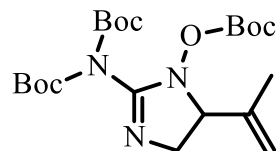
2-(bis((*tert*-butoxy)carbonyl)amino)-5-(prop-1-en-2-yl)-4,5-dihydro-1H-imidazol-1-yl *tert*-butyl carbonate (79c)



79a



79b



79c

75 (1 eq., 25 mg, 0.177 mmol) and TEA (2.1 eq., 51.7 μ L, 0.372 mmol) were dissolved in THF (2.45 mL), cooled to 0°C, and then a solution of Boc₂O (2.1 eq., 81.2 mg, 0.372 mmol) in THF (0.49 mL) was added. The mixture was stirred at 0 °C for an additional 12 h and concentrated in vacuo. The crude was purified by reverse phase chromatography (ACN/H₂O) to afford **79a** (15 mg, 35 %), **79b** (9 mg, 15 %) and **79c** (17 mg, 22 %) as white solids.

¹H NMR (400 MHz, DMSO-*d*⁶) of **79a**: δ 8.28 (s, 2H), 5.05 (s, 1H), 4.97 (t, *J* = 1.7 Hz, 1H), 3.90 (t, *J* = 9.0 Hz, 1H), 3.75 (dd, *J* = 10.0, 8.4 Hz, 1H), 3.23 (t, *J* = 9.8 Hz, 1H), 1.70 (s, 3H), 1.46 (s, 9H).

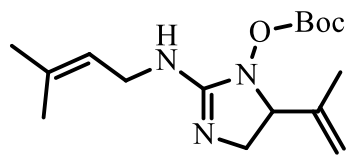
¹³C NMR (101 MHz, DMSO-*d*⁶) of **79a**: δ 155.73, 151.39, 141.28, 114.93, 82.15, 63.79, 44.68, 27.67, 17.00.

¹H NMR (400 MHz, DMSO-*d*⁶) of **79b**: δ 9.53 (s, 1H), 5.07 (s, 1H), 5.01 – 4.99 (m, 1H), 4.07 (t, *J* = 9.0 Hz, 1H), 3.83 (dd, *J* = 10.1, 8.8 Hz, 1H), 3.37 – 3.34 (m, 1H), 1.72 (s, 3H), 1.44 (s, 9H), 1.38 (s, 9H).

¹³C NMR (101 MHz, DMSO-*d*⁶) of **79b**: δ 158.18, 149.83, 148.90, 140.55, 115.88, 81.72, 78.14, 64.79, 45.35, 27.83, 27.58, 16.74.

¹H NMR (400 MHz, DMSO-*d*⁶) of **79c**: δ 5.13 (s, 1H), 5.06 – 5.03 (m, 1H), 4.35 (t, *J* = 8.8 Hz, 1H), 3.94 (dd, *J* = 10.2, 8.7 Hz, 1H), 3.59 (dd, *J* = 10.2, 9.1 Hz, 1H), 1.77 (s, 3H), 1.45 (s, 9H), 1.43 (s, 9H), 1.39 (s, 9H).

Preparation of *tert*-butyl (2-((3-methylbut-2-en-1-yl)amino)-5-(prop-1-en-2-yl)-4,5-dihydro-1*H*-imidazol-1-yl) carbonate (**80**)



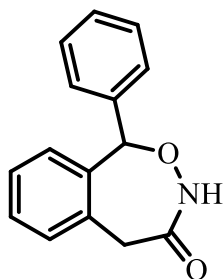
80

A suspension of NaH (1.2 eq., 1.55 mg, 0.0647 mmol) in THF (0.4 mL) was added slowly to a solution of **79a** (1 eq., 13 mg, 0.0539 mmol) in THF (1 mL) at 0 °C under Ar and stirred for an additional 2 h at 0 °C. Then, 3,3-dimethylallyl bromide (1.2 eq., 7.6 μ L, 0.0647 mmol) was added to the reaction mixture at 0 °C and the resulting mixture was stirred at rt for 16 h. The reaction mixture was then concentrated in vacuo and purified by reverse phase chromatography (ACN/H₂O) to afford **80** as a white solid (11 mg, 66 %).

¹H NMR (400 MHz, DMSO-*d*⁶): δ 7.50 (s, 1H), 5.30 (t, *J* = 7.0 Hz, 1H), 5.11 (s, 1H), 5.05 – 5.01 (m, 1H), 4.51 (t, *J* = 9.0 Hz, 1H), 4.30 (dd, *J* = 10.6, 7.3 Hz, 1H), 3.95 (t, *J* = 8.7 Hz, 1H), 3.69 (dd, *J* = 10.2, 8.3 Hz, 1H), 3.28 (t, *J* = 9.8 Hz, 1H), 1.74 (s, 3H), 1.69 (s, 3H), 1.65 – 1.62 (m, 3H), 1.47 (s, 9H).

¹³C NMR (101 MHz, DMSO-*d*⁶): δ 166.32, 161.96, 140.73, 140.36, 119.31, 116.41, 70.45, 65.15, 63.28, 44.25, 27.65, 25.39, 17.93, 16.86.

Preparation of 1-phenyl-3,5-dihydrobenzo[*e*][1,2]oxazepin-4(1*H*)-one (**81**)



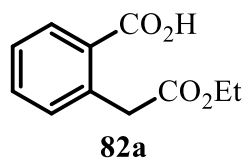
81

TEA (2.2 eq., 8.32 mg, 0.0114 mL, 0.0822 mmol) was added to solution of **105** (1 eq., 15 mg, 0.0374 mmol) and methylhydrazine sulphate (1.1 eq., 5.93 mg, 0.0411 mmol) in EtOH (0.97 mL). After stirred at 25 °C for 4 h, the mixture was concentrated in vacuo and purified by reverse phase chromatography (MeOH/H₂O) to **81** as a white solid (7.5 mg, 84 %).

¹H NMR (400 MHz, DMSO-*d*⁶): δ 11.01 (s, 1H), 7.38 – 7.34 (m, 5H), 7.30 – 7.27 (m, 1H), 7.21 – 7.15 (m, 2H), 6.90 – 6.85 (m, 1H), 6.18 (s, 1H), 4.63 (d, *J* = 13.5 Hz, 1H), 3.64 – 3.63 (m, 1H).

^{13}C NMR (101 MHz, $\text{DMSO-}d^6$): δ 176.48, 140.14, 137.99, 130.74, 130.53, 128.78, 128.60, 128.58, 128.52, 127.12, 127.06, 87.82, 41.60.

Preparation of 2-(2-ethoxy-2-oxoethyl)benzoic acid (**82a**)



Method 1: H_2SO_4 (0.5 eq., 0.71 mL, 13.3 mmol) was added to a solution of homophthalic acid (1 eq., 4.8 g, 26.6 mmol) in EtOH (12 mL) and the resulting mixture was refluxed at 85°C for 2 h. After completion, the reaction mixture was concentrated in vacuo, water was added and basified by Na_2CO_3 to pH~9. The aqueous layer was washed with EtOAc, then acidified by H_2SO_4 (1M) to pH~3 and extracted with EtOAc thrice. The organic phases were washed with brine, dried over anhydrous Na_2SO_4 and filtered. The filtrate was concentrated in vacuo to afford **82a** as a white solid (4.5 g, 81 %).

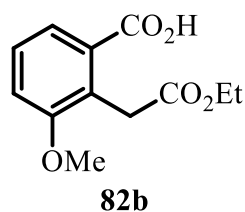
Method 2: The reaction was performed with 2-bromobenzoic acid (1 eq., 500 mg, 2.49 mmol), ethyl acetoacetate (2 eq., 0.629 mL, 4.97 mmol), NaOEt (3 eq., 507 mg, 7.46 mmol) and CuBr (0.1 eq., 35.7 mg, 0.249 mmol) in anhydrous ethanol (10 mL) in 1.5 h according to typical procedure method **TP8**, affording **82a** as a yellow solid (507 mg, 98 %).

^1H NMR (400 MHz, CDCl_3): δ 8.13 (d, $J = 7.8$ Hz, 1H), 7.54 (t, $J = 7.5$ Hz, 1H), 7.40 (t, $J = 7.6$ Hz, 1H), 7.28 (d, $J = 7.6$ Hz, 1H), 4.17 (q, $J = 7.0$ Hz, 2H), 4.05 (s, 2H), 1.26 (t, $J = 7.0$ Hz, 3H).

Rf: 0.5 (DCM:MeOH = 20:1, containing 0.5% AcOH).

These data are consistent with the previously reported characterization.¹⁸³

Preparation of 2-(2-ethoxy-2-oxoethyl)-3-methoxybenzoic acid (**82b**)

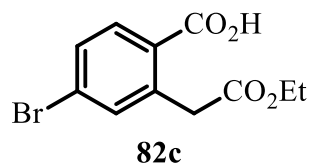


The reaction was performed with 2-bromo-3-methoxybenzoic acid (1 eq., 50 mg, 0.216 mmol), ethyl acetoacetate (2 eq., 0.0547 mL, 0.433 mmol), NaOEt (3 eq., 44.2 mg, 0.649 mmol) and CuBr (0.1 eq., 3.1 mg, 0.0216 mmol) in anhydrous ethanol (0.75 mL) in 16 h according to typical procedure **TP8**, affording **82b** as a white solid (48.5 mg, 94 %).

¹H NMR (400 MHz, CDCl₃): δ 7.69 (d, *J* = 7.8 Hz, 1H), 7.34 (t, *J* = 8.1 Hz, 1H), 7.11 (d, *J* = 8.2 Hz, 1H), 4.21 – 4.12 (m, 4H), 3.85 (s, 3H), 1.26 (t, *J* = 7.1 Hz, 3H).

These data are consistent with the previously reported characterization.¹⁷³

Preparation of 4-bromo-2-(2-ethoxy-2-oxoethyl)benzoic acid (**82c**)

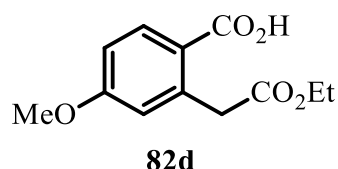


The reaction was performed with 2,4-dibromobenzoic acid (1 eq., 1.4 g, 5 mmol), ethyl acetoacetate (2 eq., 1.26 mL, 10 mmol), NaOEt (3 eq., 1.02 g, 15 mmol) and CuBr (0.1 eq., 71.7 mg, 0.5 mmol) in anhydrous ethanol (16 mL) in 3 h according to typical procedure **TP8**, affording **82c** as a white solid (1.4 g, 97 %).

¹H NMR (400 MHz, CDCl₃): δ 7.98 (d, *J* = 8.4 Hz, 1H), 7.54 (dd, *J* = 8.4, 2.0 Hz, 1H), 7.45 (d, *J* = 2.0 Hz, 1H), 4.17 (q, *J* = 7.1 Hz, 2H), 4.00 (s, 2H), 1.26 (t, *J* = 7.1 Hz, 3H).

¹³C NMR (101 MHz, CDCl₃): δ 171.81, 170.99, 138.97, 135.54, 133.42, 130.95, 128.29, 127.73, 61.18, 40.62, 14.29.

Preparation of 2-(2-ethoxy-2-oxoethyl)-4-methoxybenzoic acid (**82d**)

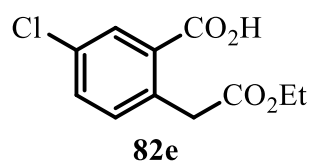


The reaction was performed with 2-bromo-4-methoxybenzoic acid (1 eq., 600 mg, 2.6 mmol), ethyl acetoacetate (2 eq., 0.656 mL, 5.19 mmol), NaOEt (3 eq., 530 mg 7.79 mmol) and CuBr (0.1 eq., 37.3 mg 0.26 mmol) in anhydrous ethanol (10 mL) in 3 h according to typical procedure **TP8**, affording **82d** as a white solid (602 mg, 97 %).

¹H NMR (400 MHz, CDCl₃): δ 8.13 (d, *J* = 8.8 Hz, 1H), 6.87 (dd, *J* = 8.8, 2.6 Hz, 1H), 6.77 (d, *J* = 2.6 Hz, 1H), 4.17 (q, *J* = 7.1 Hz, 2H), 4.01 (s, 2H), 3.86 (s, 3H), 1.26 (t, *J* = 7.1 Hz, 3H).

¹³C NMR (101 MHz, CDCl₃): δ 172.08, 171.50, 163.39, 139.71, 134.46, 120.85, 118.32, 112.44, 60.88, 55.58, 41.33, 14.32.

Preparation of 5-chloro-2-(2-ethoxy-2-oxoethyl)benzoic acid (**82e**)



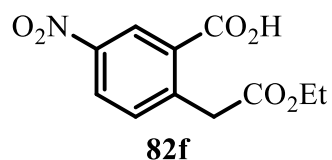
Method 1: The reaction was performed with 2-bromo-5-chlorobenzoic acid (1 eq., 1 g, 4.25 mmol), ethyl acetoacetate (2 eq., 1.07 mL, 8.49 mmol), NaOEt (3 eq., 1.01 g, 14.9 mmol) and CuBr (0.1 eq., 60.9 mg, 0.425 mmol) in anhydrous ethanol (12 mL) in 1 h according to typical procedure **TP8**, affording **82e** as a white solid (1 g, 97 %).

Method 2: The reaction was performed with 5-chloro-2-iodobenzoic acid (1 eq., 1.4 g, 4.96 mmol), ethyl acetoacetate (2 eq., 1.25 mL, 9.91 mmol), NaOEt (3 eq., 1.01 g, 14.9 mmol) and CuBr (0.1 eq., 71.1 mg, 0.496 mmol) in anhydrous ethanol (12 mL) in 3 h according to typical procedure **TP8**, affording **82e** as a white solid (1.1 g, 91 %).

¹H NMR (400 MHz, CDCl₃): δ 10.09 (s, 1H), 8.10 (d, *J* = 2.4 Hz, 1H), 7.50 (dd, *J* = 8.2, 2.3 Hz, 1H), 7.23 (d, *J* = 8.2 Hz, 1H), 4.17 (q, *J* = 7.1 Hz, 2H), 4.01 (s, 2H), 1.26 (t, *J* = 7.1 Hz, 3H).

^{13}C NMR (101 MHz, CDCl_3): δ 171.33, 171.25, 135.42, 133.83, 133.64, 133.27, 131.89, 130.33, 61.17, 40.29, 14.29.

Preparation of 2-(2-ethoxy-2-oxoethyl)-5-nitrobenzoic acid (**82f**)

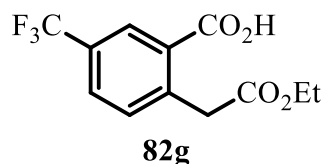


The reaction was performed with 2-bromo-5-nitrobenzoic acid (1 eq., 1 g, 4.06 mmol), ethyl acetoacetate (2 eq., 1.03 mL, 8.13 mmol), NaOEt (3 eq., 0.83 g, 12.2 mmol) and CuBr (0.1 eq., 58.3 mg, 0.406 mmol) in anhydrous ethanol (12 mL) in 3 h according to typical procedure **TP8**, affording **82f** as a white solid (0.96 g, 93 %).

^1H NMR (400 MHz, CDCl_3): δ 8.96 (d, $J = 2.5$ Hz, 1H), 8.38 (dd, $J = 8.4, 2.4$ Hz, 1H), 7.51 (d, $J = 8.4$ Hz, 1H), 4.23 – 4.15 (m, 4H), 1.27 (t, $J = 7.1$ Hz, 3H).

These data are consistent with the previously reported characterization.¹⁸³

Preparation of 2-(2-ethoxy-2-oxoethyl)-5-(trifluoromethyl)benzoic acid (**82g**)

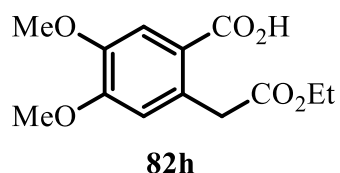


The reaction was performed with 2-bromo-5-(trifluoromethyl)benzoic acid (1 eq., 1.35 g, 5 mmol), ethyl acetoacetate (2 eq., 1.26 mL, 10 mmol), NaOEt (3 eq., 1.02 g, 15 mmol) and CuBr (0.1 eq., 71.7 mg, 0.5 mmol) in anhydrous ethanol (12 mL) in 1 h according to typical procedure **TP8**, affording **82g** as a white solid (1.35 g, 98 %).

^1H NMR (400 MHz, CDCl_3): δ 9.99 (s, 1H), 8.39 (d, $J = 2.0$ Hz, 1H), 7.78 (dd, $J = 8.1, 2.0$ Hz, 1H), 7.44 (d, $J = 8.0$ Hz, 1H), 4.18 (q, $J = 7.1$ Hz, 2H), 4.12 (s, 2H), 1.27 (t, $J = 7.1$ Hz, 3H).

^{13}C NMR (101 MHz, CDCl_3): δ 171.27, 170.91, 140.83, 133.25, 130.83, 130.50, 130.17, 129.83, 129.79, 129.75, 129.65, 129.01, 128.97, 128.93, 128.90, 127.68, 124.98, 122.27, 119.57, 61.36, 40.76, 14.25.

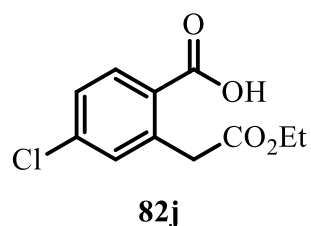
Preparation of 2-(2-ethoxy-2-oxoethyl)-4,5-dimethoxybenzoic acid (**82h**)



The reaction was performed with 2-bromo-4,5-dimethoxybenzoic acid (1 eq., 0.922 g, 3.53 mmol), ethyl acetoacetate (2 eq., 0.892 mL, 7.06 mmol), NaOEt (3 eq., 0.721 g, 10.6 mmol) and CuBr (0.1 eq., 50.7 mg, 0.353 mmol) in anhydrous ethanol (15 mL) in 3 h according to typical procedure **TP8**, affording **82h** as a white solid (0.94 g, 99 %).

¹H NMR (400 MHz, CDCl₃): δ 7.65 (s, 1H), 6.73 (s, 1H), 4.17 (q, *J* = 7.1 Hz, 2H), 3.99 (s, 2H), 3.94 (s, 3H), 3.93 (s, 3H), 1.26 (t, *J* = 7.0 Hz, 3H).

Preparation of 4-chloro-2-(ethoxycarbonyl)benzoic acid (**82j**)

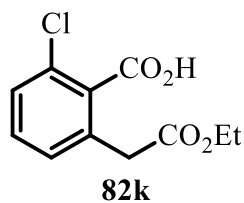


The reaction was performed with 2,4-dichlorobenzoic acid (1 eq., 0.96 g, 5.03 mmol), ethyl acetoacetate (2 eq., 1.27 mL, 10.1 mmol), NaOEt (3 eq., 1.03 g, 15.1 mmol) and CuBr (0.1 eq., 72.1 mg, 0.503 mmol) in anhydrous ethanol (12 mL) in 24 h according to typical procedure **TP8**, affording **82j** as a white solid (1.08 g, 89 %).

¹H NMR (400 MHz, CDCl₃): δ 8.07 (d, *J* = 8.4 Hz, 1H), 7.41 – 7.35 (m, 1H), 7.29 (d, *J* = 2.1 Hz, 1H), 4.17 (q, *J* = 7.1 Hz, 2H), 4.01 (s, 2H), 1.26 (t, *J* = 7.1 Hz, 3H).

¹³C NMR (101 MHz, CDCl₃): δ 171.00, 139.61, 139.00, 133.56, 133.48, 132.67, 127.95, 61.17, 40.70, 14.29.

Preparation of 2-chloro-6-(2-ethoxy-2-oxoethyl)benzoic acid (**82k**)

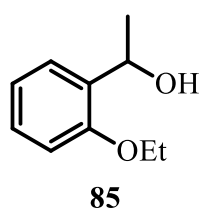


The reaction was performed with 2-chloro-6-iodobenzoic acid (1 eq., 1.41 g, 4.99 mmol), ethyl acetoacetate (2 eq., 1.26 mL, 9.98 mmol), NaOEt (3 eq., 1.02 g, 15 mmol) and CuBr (0.1 eq., 71.6 mg, 0.499 mmol) in anhydrous ethanol (12 mL) in 48 h according to typical procedure **TP8**, affording **82k** as a white solid (1.1 g, 91 %).

^1H NMR (400 MHz, CDCl_3): δ 9.59 (s, 1H), 7.41 – 7.31 (m, 2H), 7.24 (dd, $J = 7.4$, 1.2 Hz, 1H), 4.17 (q, $J = 7.1$ Hz, 2H), 3.80 (s, 2H), 1.25 (t, $J = 7.1$ Hz, 3H).

^{13}C NMR (101 MHz, CDCl_3): δ 171.12, 133.99, 131.97, 131.13, 129.40, 129.13, 61.69, 39.62, 14.16

Preparation of 1-(2-ethoxyphenyl)ethanol (**85**)



To a dry tube filled with Ar was added NaOEt (3 eq., 50.8 mg, 0.746 mmol) and anhydrous ethanol (1 mL). Then, ethyl acetoacetate (2 eq., 62.8 μL , 0.497 mmol) was added and stirred at rt for 2 min. CuBr (0.1 eq., 3.57 mg, 0.0249 mmol) and 2-bromo- α -methylbenzyl alcohol (1 eq., 50 mg, 0.249 mmol) were successively added. The reaction mixture was irradiated in microwaves under Ar at 150 $^\circ\text{C}$ for 15 min. The reaction mixture was concentrated in vacuo and acidified by H_2SO_4 (1M) to pH~3. The crude was extracted with EtOAc thrice. The combined organic phases were washed with brine and dried over anhydrous Na_2SO_4 and filtered. The filtrate was concentrated in vacuo and purified by silica gel chromatography (Heptane:EtOAc = 8:1) to afford **85** as a yellow oil (40 mg, 97 %).

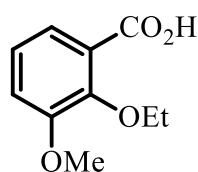
^1H NMR (400 MHz, CDCl_3): δ 7.27 (d, $J = 7.5$ Hz, 1H), 7.17 (t, $J = 7.8$ Hz, 1H), 6.89

(t, $J = 7.5$ Hz, 1H), 6.81 (d, $J = 8.2$ Hz, 1H), 5.04 (q, $J = 6.2$ Hz, 1H), 4.04 (q, $J = 6.9$ Hz, 2H), 2.80 (s, 1H), 1.47 (d, $J = 6.5$ Hz, 3H), 1.39 (t, $J = 6.9$ Hz, 3H).

^{13}C NMR (101 MHz, CDCl_3): δ 155.58, 133.58, 128.04, 125.79, 120.57, 111.24, 65.77, 63.53, 22.89, 14.72.

Rf: 0.3 (heptane:EtOAc = 2:1).

Preparation of 2-bromo-3-methoxybenzoic acid (**86**)



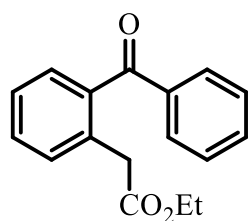
86

The reaction was performed with 2-bromo-3-methoxybenzoic acid (1 eq., 200 mg, 0.866 mmol), ethyl acetoacetate (2 eq., 0.219 mL, 1.73 mmol), NaOEt (4 eq., 235 mg, 3.46 mmol) and CuBr (0.1 eq., 12.4 mg, 0.0866 mmol) in anhydrous ethanol (3.5 mL) in 16 h according to typical procedure **TP8**, affording **86** as a brown solid (162 mg, 95 %).

^1H NMR (400 MHz, CDCl_3): δ 7.72 (dd, $J = 7.7, 1.9$ Hz, 1H), 7.21 – 7.12 (m, 2H), 4.36 (q, $J = 7.1$ Hz, 2H), 3.91 (s, 3H), 1.46 (t, $J = 7.1$ Hz, 3H).

^{13}C NMR (101 MHz, CDCl_3): δ 165.74, 152.25, 147.25, 124.93, 124.10, 122.75, 117.56, 71.44, 56.35, 15.51.

Preparation of ethyl 2-(2-benzoylphenyl)acetate (**87**)



87

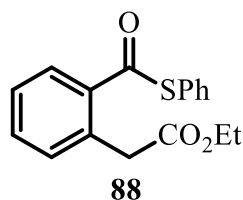
A solution of PhZnCl (2 eq., 0.5 M in THF, 6.66 mL, 3.33 mmol) was slowly added to a solution of **88** (1 eq., 500 mg, 1.66 mmol) and $\text{PdCl}_2(\text{PPh}_3)_2$ (1 %, 11.7 mg, 0.0166 mmol) in toluene (7 mL) under Ar at rt. After stirred at rt for 5 h, the reaction was

quenched by the addition of saturated NH_4Cl aqueous solution and extracted with EtOAc thrice. The combined organic phases were washed with brine, dried over anhydrous Na_2SO_4 , and filtered. The filtrate was concentrated in vacuo and purified by silica gel chromatography (Heptane:EtOAc = 6:1) to afford **87** as a yellow oil (424 mg, 95 %).

^1H NMR (400 MHz, CDCl_3): δ 7.82 (d, $J = 7.6$ Hz, 2H), 7.57 (t, $J = 7.4$ Hz, 1H), 7.51 – 7.42 (m, 3H), 7.42 – 7.30 (m, 3H), 4.02 (q, $J = 7.1$ Hz, 2H), 3.89 (s, 2H), 1.11 (t, $J = 7.1$ Hz, 3H).

These data are consistent with the previously reported characterization.¹⁷³

Preparation of ethyl 2-(2-((phenylthio)carbonyl)phenyl)acetate (**88**)



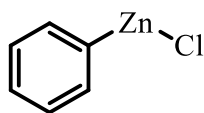
EDCI (1.3 eq., 5.5 g, 28.1 mmol) was added portionwise to a mixture of **82a** (1 eq., 4.5 g, 21.6 mmol) and HOBt (1.3 eq., 3.8 g, 28.1 mmol) in DCM (50 mL) at 0 °C. After stirred at 0 °C for 30 min, thiophenol (1.3 eq., 2.87 mL, 28.1 mmol) was added slowly and the mixture was stirred at rt for 15 h. The reaction was quenched with saturated NaHCO_3 aqueous solution and extracted with DCM thrice. The combined organic phases were washed with brine, dried over anhydrous Na_2SO_4 , and filtered. The filtrate was concentrated in vacuo and purified by silica gel chromatography (Heptane:EtOAc = 10:1) to afford **88** as a yellow solid (6.15 g, 95 %).

^1H NMR (400 MHz, CDCl_3): δ 8.08 (d, $J = 7.7$ Hz, 1H), 7.55 – 7.39 (m, 7H), 7.31 (d, $J = 7.5$ Hz, 1H), 4.13 (q, $J = 7.1$ Hz, 2H), 3.92 (s, 2H), 1.22 (t, $J = 7.1$ Hz, 3H).

Rf: 0.4 (heptane:EtOAc = 3:1).

These data are consistent with the previously reported characterization.¹⁷³

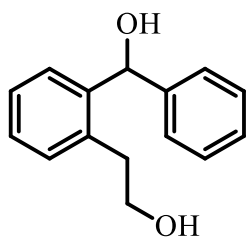
Preparation of phenylzinc(II) chloride (**89**)



89

To a dry flask was added ZnCl_2 (1.4 eq., 1.56 g, 11.2 mmol) and sealed. After heated (550 °C, 15 min) by a heating gun under reduced pressure, the flask was cooled to rt and backfilled with argon thrice. Then THF (8 mL) was added, the suspension was sonicated until it became clear. After cooled to 0 °C, PhMgBr (1 eq., 1 M in THF, 8 mL, 8 mmol) was slowly added and a white precipitation formed. The mixture was stirred at rt for 3 h to afford **89** in quantitative yield (0.5 M in THF).

Preparation of 2-(2-(hydroxy(phenyl)methyl)phenyl)ethanol (**91**)



91

Method 1: To a solution of **87** (1 eq., 200 mg, 0.745 mmol) in EtOH (4 mL) was added NaBH_4 (4 eq., 112 mg, 2.98 mmol) in small portions at rt. After stirred at rt for 1 h, the reaction was quenched with water and concentrated in vacuo. The suspension was extracted with EtOAc thrice. The combined organic phases were washed with brine, dried over anhydrous Na_2SO_4 and filtered. The filtrate was concentrated in vacuo to afford **91** as a white oil (160 mg, 94 %).

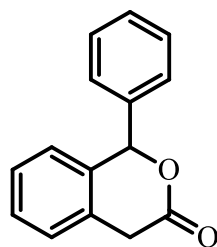
Method 2: The mixture of **87** (1 eq., 60 mg, 0.224 mmol), Zn (24 eq., 351 mg, 5.37 mmol) and NaOH (6.25 eq., 55.9 mg, 1.4 mmol) in H_2O (0.7 mL) was refluxed for 20 h. The suspension was extracted with EtOAc thrice. The combined organic phases were washed with brine, dried over anhydrous Na_2SO_4 and filtered. The filtrate was concentrated in vacuo to afford **91** as a white oil (51 mg, 100 %).

^1H NMR (400 MHz, CDCl_3): δ 7.30 – 7.08 (m, 9H), 6.00 (s, 1H), 3.82 – 3.64 (m, 2H),

3.42 (s, 1H), 2.98 – 2.72 (m, 2H), 2.00 (s, 1H).

These data are consistent with the previously reported characterization.¹⁸⁴

Preparation of 1-phenylisochroman-3-one (92)



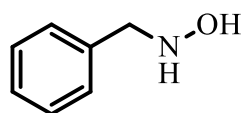
92

To a solution of **87** (1 eq., 2.5 g, 9.32 mmol) in THF (6 mL) was added a solution of LiOH (1.5 eq., 0.335 g, 14 mmol) in H₂O (6 mL). After stirred at rt for 2 h, the mixture was concentrated under reduced pressure until dryness. The crude was dissolved in MeOH (50 mL) followed by the addition of NaBH₄ (4 eq., 1.41 g, 37.4 mmol) in small portions at 25 °C. After stirred at rt for 16 h, HCl (1 M) was added dropwise to the mixture until pH~3 and stirred at rt for 1 h. The reaction mixture was concentrated in vacuo and extracted by EtOAc thrice. The combined organic phases were washed with brine, dried over anhydrous Na₂SO₄ and filtered. The filtrate was concentrated in vacuo to afford **92** as a white solid (2.1 g, 100 %).

¹H NMR (400 MHz, CDCl₃): δ 7.43 – 7.22 (m, 8H), 6.97 (d, J = 7.5 Hz, 1H), 6.39 (s, 1H), 3.74 (d, J = 18.2 Hz, 1H), 3.62 (d, J = 18.2 Hz, 1H).

These data are consistent with the previously reported characterization.¹⁸⁵

Preparation of *N*-benzylhydroxylamine (98)



98

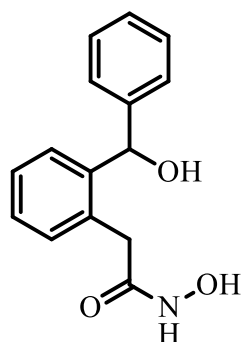
Na(CN)BH₃ (2.2 eq., 1.14 g, 18.2 mmol) was added in small portions to a solution of (*E*)-benzaldehyde oxime (1 eq., 1 g, 8.26 mmol) in MeOH (20 mL) at rt. During the course of addition, pH was maintained around 2 by adding H₂SO₄(2M). After stirred

at rt for 6 h, NaOH (1M) was added until pH ~ 9. The reaction mixture was concentrated in vacuo and extracted with EtOAc thrice. The combined organic phases were washed with brine, dried over anhydrous Na₂SO₄ and filtered. The filtrate was concentrated in vacuo to afford **98** as a yellow solid (0.98 g, 96 %).

¹H NMR (400 MHz, DMSO-*d*⁶): δ 7.36 – 7.21 (m, 5H), 6.07 (br, 1H), 3.87 (s, 2H).

These data are consistent with the previously reported characterization.¹⁸⁶

Preparation of *N*-hydroxy-2-(2-(hydroxy(phenyl)methyl)phenyl)acetamide (**101**)



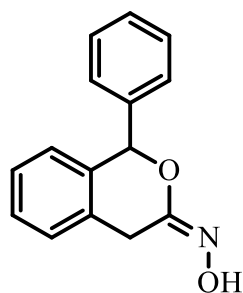
101

KOH (10 eq., 3.39 g, 60.4 mmol) was added to a cooled solution of hydroxylamine hydrochloride (10 eq., 4.2 g, 60.4 mmol) in MeOH (70.3 mL) at 0 °C. After stirred for 5 min, the suspension was filtered and filtrate was collected. **92** (1 eq., 1.36 g, 6.04 mmol) was then added to aforementioned filtrate and stirred at rt overnight. The mixture was concentrated in vacuo followed by the addition of THF and filtered through celite. The filtrate was concentrated in vacuo to afford **101** as a yellow oil (1.4 g, 90 %).

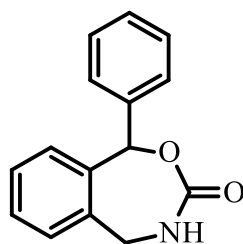
¹H NMR (400 MHz, DMSO-*d*⁶): δ 9.69 (s, 1H), 7.38 – 7.14 (m, 9H), 6.07 (s, 1H), 3.42 (s, 2H), 3.17 (s, 1H), 1.70 (s, 1H).

¹H NMR (400 MHz, MeOD-*d*⁴): δ 7.37 – 7.16 (m, 9H), 6.10 (s, 1H), 3.47 (s, 2H).

Preparation of (*E*)-1-phenylisochroman-3-one oxime (**102**) and 1-phenyl-4,5-dihydrobenzo[*e*][1,3]oxazepin-3(*1H*)-one (**103**)



102



103

Method 1: A solution of **101** (1 eq., 50 mg, 0.194 mmol) in THF (4 mL) was added dropwise to a solution of PPh₃ (1.3 eq., 66.3 mg, 0.253 mmol) and DIAD (1.3 eq., 50.1 μL, 0.253 mmol) in THF (4 mL) at 0 °C under Ar and stirred at rt over night. The reaction mixture was concentrated in vacuo and purified by reverse phase chromatography (ACN/H₂O) to afford **102** (8.2 mg, 18%) and **103** (19 mg, 41%) as white solids.

Method 2: To a solution of **101** (1 eq., 50 mg, 0.117 mmol) in THF (2 mL) was added CDI (2 eq., 37.8 mg, 0.233 mmol) and the resulting mixture was stirred at rt for 16h. The reaction mixture was then concentrated in vacuo and purified by reverse phase chromatography (ACN/H₂O) to afford **102** (15.6 mg, 56%) and **103** (7.5 mg, 27%) as white solids.

¹H NMR (400 MHz, DMSO-*d*⁶) of **102**: δ 9.35 (s, 1H), 7.49 – 7.33 (m, 7H), 7.26 (t, *J* = 7.1 Hz, 1H), 6.83 (d, *J* = 7.5 Hz, 1H), 6.37 (s, 1H), 3.69 (d, *J* = 17.2 Hz, 1H), 3.45 (d, *J* = 17.2 Hz, 1H).

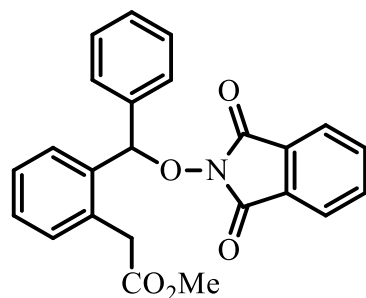
¹³C NMR (101 MHz, DMSO-*d*⁶) of **102**: δ 150.77, 137.83, 137.09, 132.46, 128.53, 128.40, 128.35, 127.35, 126.89, 126.60, 125.26, 78.98, 30.10.

¹H NMR (400 MHz, DMSO-*d*⁶) of **103**: δ 7.74 (s, 1H), 7.50 – 7.30 (m, 7H), 7.25 (t, *J* = 7.4 Hz, 1H), 6.80 (s, 1H), 6.70 (d, *J* = 7.5 Hz, 1H), 4.64 (d, *J* = 14.8 Hz, 1H), 4.06 (dd, *J* = 14.9, 6.0 Hz, 1H).

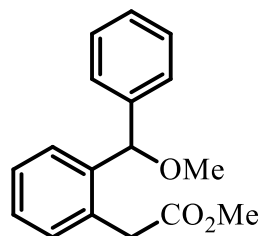
¹³C NMR (101 MHz, DMSO-*d*⁶) of **103**: δ 154.59, 139.22, 138.32, 137.39, 128.51, 128.38, 128.11, 127.85, 127.77, 127.16, 127.05, 77.61, 43.70.

Preparation of methyl 2-(2-(((1,3-dioxoisindolin-2-yl)oxy)(phenyl)methyl)

phenyl)acetate (**105**) and methyl 2-(2-(methoxy(phenyl)methyl)phenyl)acetate (**106**)



105



106

A solution of **92** (1 eq., 10 mg, 0.0446 mmol) and ZnCl₂ (0.1 eq., 0.608 mg, 0.00446 mmol) in SOCl₂ (0.2 mL) was stirred at 70 °C for 16h. After the solvent was removed under reduced pressure, DCM (0.4 mL) and MeOH (1.5 eq., 2.71 μL, 0.0669 mmol) were added and stirred at rt for 1h. The mixture was filtered through a silica gel pad with DCM/MeOH (10:1), the filtrate was concentrated in vacuo at rt to afford the crude. The crude was dissolved in DMF (0.2 mL), followed by the addition of TEA (1.5 eq., 9.3 μL, 0.0669 mmol) and NHPI (1.3 eq., 9.46 mg, 0.058 mmol). After stirred at rt for 4h, the reaction mixture was purified by reverse phase chromatography (ACN/H₂O) to afford **105** as a yellow solid (8.4 mg, 47 %) and **106** as a white solid (5.3 mg, 44 %).

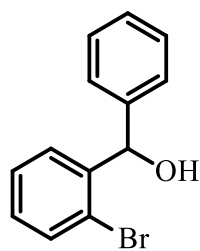
¹H NMR (400 MHz, CDCl₃) of **105**: δ 7.79 – 7.66 (m, 5H), 7.55 – 7.51 (m, 2H), 7.37 – 7.30 (m, 6H), 6.85 (s, 1H), 3.93 (d, *J* = 16.0 Hz, 1H), 3.71 (d, *J* = 16.0 Hz, 1H), 3.53 (s, 3H).

¹³C NMR (101 MHz, CDCl₃) of **105**: δ 171.74, 163.87, 137.01, 136.24, 134.45, 133.43, 131.20, 129.28, 129.07, 129.05, 128.96, 128.92, 128.49, 127.64, 123.52, 86.56, 52.11, 38.49.

¹H NMR (400 MHz, CDCl₃) of **106**: δ 7.36 – 7.32 (m, 1H), 7.28 – 7.17 (m, 8H), 5.42 (s, 1H), 3.60 (d, *J* = 3.2 Hz, 2H), 3.55 (s, 3H), 3.32 (s, 3H).

¹³C NMR (101 MHz, CDCl₃) of **106**: δ 171.95, 140.74, 139.83, 132.74, 131.50, 128.41, 128.28, 128.03, 127.64, 127.52, 127.50, 82.97, 57.24, 51.99, 38.41.

Preparation of (2-bromophenyl)(phenyl)methanol (**107**)



107

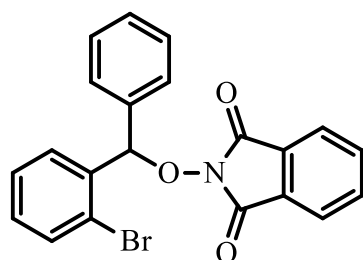
A solution of PhMgBr (1.2 eq., 1 M, 6.49 mL, 6.49 mmol) in THF was added dropwise to a vigorously stirred solution of 2-bromobenzaldehyde (1 eq., 1 g, 0.633 mL, 5.4 mmol) in Et₂O (15 mL) under Ar at -30 °C. After stirred at -30 °C for 12 h, the reaction was quenched with saturated NH₄Cl aqueous solution and extracted with EtOAc thrice. The combined organic phases were washed with brine, dried over anhydrous Na₂SO₄ and filtered. The filtrate was concentrated under reduced pressure and purified by silica gel chromatography (Heptane:EtOAc = 15:1) to afford **107** as a yellow oil (1.2 g, 84 %).

¹H NMR (400 MHz, CDCl₃): δ 7.58 (dd, *J* = 16.1, 7.9 Hz, 2H), 7.45 – 7.23 (m, 6H), 7.16 (t, *J* = 7.6 Hz, 1H), 6.19 (s, 1H), 2.63 (s, 1H).

Rf: 0.3 (heptane:EtOAc = 3:1).

These data are consistent with the previously reported characterization.¹⁸⁷

Preparation of 2-((2-bromophenyl)(phenyl)methoxy)isoindoline-1,3-dione (**108**)



108

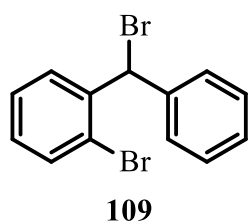
A mixture of **109** (1 eq., 120 mg, 0.368 mmol), NHPI (1.1 eq., 66 mg, 0.405 mmol) and TEA (2 eq., 0.102 mL, 0.736 mmol) in DMF (1 mL) was stirred at rt overnight. After completion, water was added to the reaction mixture and acidified to pH~3 with HCl (1M). The mixture was extracted with EtOAc thrice. The combined organic

phases were washed with brine, dried over anhydrous Na₂SO₄ and filtered. The filtrate was concentrated in vacuo and purified by silica gel chromatography (Heptane:EtOAc = 5:1) to afford **108** as a white solid (147 mg, 98 %).

¹H NMR (400 MHz, CDCl₃): δ 8.11 (dd, *J* = 7.8, 1.8 Hz, 1H), 7.79 – 7.73 (m, 2H), 7.73 – 7.67 (m, 2H), 7.54 – 7.45 (m, 4H), 7.38 – 7.27 (m, 4H), 7.20 (td, *J* = 7.7, 1.8 Hz, 1H), 6.91 (s, 1H).

Rf: 0.35 (heptane:EtOAc = 5:1).

Preparation of 1-bromo-2-(bromo(phenyl)methyl)benzene (**109**)



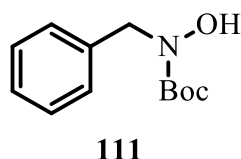
PBr₃ (2 eq., 2.5 mL, 26.6 mmol) was added dropwise to a solution of **107** (1 eq., 3.5 g, 13.3 mmol) in dry DCM (20 mL) at 0 °C and stirred at rt for 2h. The reaction mixture was added slowly into ice water under stirring and extracted with DCM thrice. The combined organic phases were washed with saturated NaHCO₃ aqueous solution, dried over anhydrous Na₂SO₄ and filtered. The filtrate was concentrated in vacuo to afford **109** as a yellow oil (4.3 g, 99 %).

¹H NMR (400 MHz, CDCl₃): δ 7.69 (dd, *J* = 7.9, 1.7 Hz, 1 H), 7.55 (dd, *J* = 8.0, 1.3 Hz, 1 H), 7.50 - 7.43 (m, 2 H), 7.39 - 7.27 (m, 4 H), 7.18 – 7.10 (m, 1 H), 6.70 (s, 1 H).

Rf: 0.7 (heptane:EtOAc = 3:1).

These data are consistent with the previously reported characterization.¹⁸⁸

Preparation of *tert*-butyl benzyl(hydroxy)carbamate (**111**)



A solution of Boc₂O (1.1 eq., 976 mg, 4.48 mmol) in THF (10 mL) was added

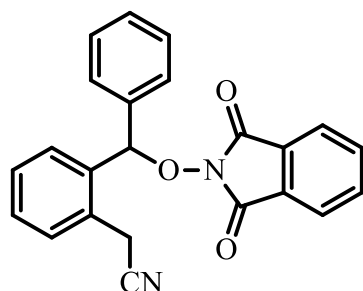
dropwise to a solution of **98** (1 eq., 500 mg, 4.06 mmol) in THF (5 mL) at 0 °C. After stirred at 0 °C for 1 h and at rt for 4h, water was added to the reaction mixture and extracted with DCM thrice. The combined organic phases were washed with brine, dried over anhydrous Na₂SO₄ and filtered. The filtrate was concentrated in vacuo and purified by silica gel chromatography (Heptane:EtOAc = 8:1) to afford **111** as a colorless oil (671 mg, 74 %).

¹H NMR (400 MHz, CDCl₃): δ 7.35 – 7.27 (m, 5H), 7.03 (s, 1H), 4.65 (s, 2H), 1.47 (s, 9H).

Rf: 0.5 (heptane:EtOAc = 2:1).

These data are consistent with the previously reported characterization.¹⁸⁹

Preparation of 2-(2-(((1,3-dioxoisindolin-2-yl)oxy)(phenyl)methyl)phenyl)acetonitrile (**113**)



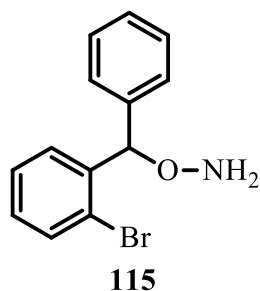
113

A mixture of **108** (1 eq., 15 mg, 0.0367 mmol), sodium 2-cyanoacetate (1.5 eq., 5.9 mg, 0.0551 mmol), [Pd(Cl)(C₃H₅)₂] (2 %, 0.274 mg, 0.000735 mmol) and SPhos (6 %, 0.933 mg, 0.0022 mmol) in toluene (1 mL) was stirred under Ar at rt for 10 min and then stirred at 120 °C for 16 h. The mixture was concentrated in vacuo and purified by reverse phase chromatography (ACN/H₂O) to afford **113** as a white solid (4.6 mg, 34 %).

¹H NMR (400 MHz, CDCl₃): δ 7.79 – 7.67 (m, 4H), 7.61 (d, *J* = 7.4 Hz, 1H), 7.51 – 7.29 (m, 8H), 6.62 (s, 1H), 4.29 (d, *J* = 19.0 Hz, 1H), 3.85 (d, *J* = 19.0 Hz, 1H).

¹³C NMR (400 MHz, CDCl₃): δ 163.86, 136.09, 134.98, 134.69, 130.74, 130.66, 130.07, 129.79, 129.29, 128.89, 128.86, 128.18, 128.14, 123.73, 118.15, 88.25, 21.77.

Preparation of *O*-((2-bromophenyl)(phenyl)methyl)hydroxylamine (**115**)

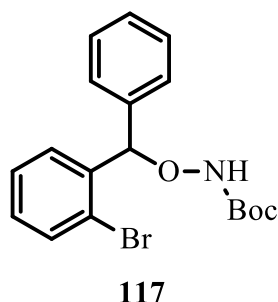


A solution of **108** (1 eq., 870 mg, 2.13 mmol) and hydrazine hydrate (15 eq., 3.1 mL, 32 mmol) in EtOH (20 mL) was refluxed for 1 h and concentrated in vacuo. The crude was basified with 10% Na₂CO₃ aqueous solution to pH ~ 10 and extracted with EtOAc thrice. The combined organic phases were washed brine, dried with anhydrous Na₂SO₄ and filtered. The filtrate was concentrated in vacuo to afford **115** as a yellow oil (586 mg, 99 %).

¹H NMR (400 MHz, CDCl₃): δ 7.45 (dd, *J* = 24.3, 7.8 Hz, 2H), 7.34 – 7.27 (m, 3H), 7.24 – 7.16 (m, 3H), 7.11 – 7.05 (m, 1H), 5.96 (s, 1H), 5.42 (s, 2H).

These data are consistent with the previously reported characterization.¹⁹⁰

Preparation of *tert*-butyl (2-bromophenyl)(phenyl)methoxycarbamate (**117**)



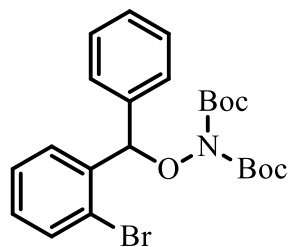
To a solution of **115** (1 eq., 268 mg, 0.964 mmol) and TEA (1.5 eq., 0.201 mL, 1.45 mmol) in DCM (10 mL) was added Boc₂O (1.1 eq., 231 mg, 1.06 mmol) and stirred at rt for 16 h. The reaction was concentrated in vacuo and purified by reverse phase chromatography (MeOH/H₂O) to afford **117** as a colorless oil (100 mg, 27 %).

¹H NMR (400 MHz, CDCl₃): δ 7.66 – 7.55 (m, 2H), 7.45 – 7.30 (m, 6H), 7.20 (td, *J* = 7.7, 1.7 Hz, 1H), 6.32 (s, 1H), 1.51 (s, 9H).

¹³C NMR (400 MHz, CDCl₃): δ 156.45, 139.03, 137.99, 133.11, 129.51, 128.53,

128.42, 128.39, 127.76, 123.82, 87.50, 82.00, 28.31.

Preparation of *tert*-butyl *N*-[(2-bromophenyl)(phenyl)methoxy]-*N*-[(*tert*-butoxy)carbonyl]carbamate (119**)**



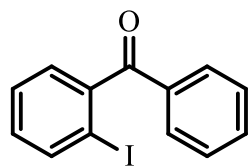
119

To a solution of **115** (1 eq., 187.5 mg, 0.67 mmol) and TEA (4 eq., 0.37 mL, 2.7 mmol) in DCM (7 mL) was added Boc₂O (4 eq., 588.49 mg, 2.7 mmol) and stirred at rt for 16 h. The reaction was concentrated in vacuo and purified by reverse phase chromatography (MeOH/H₂O) to afford **119** as a colorless oil (306 mg, 95 %).

¹H NMR (400 MHz, CDCl₃): δ 7.84 (dd, *J* = 7.8, 1.7 Hz, 1H), 7.52 (dd, *J* = 8.0, 1.3 Hz, 1H), 7.41 – 7.35 (m, 3H), 7.33 – 7.28 (m, 3H), 7.17 (td, *J* = 7.7, 1.8 Hz, 1H), 6.45 (s, 1H), 1.41 (s, 18H).

¹³C NMR (400 MHz, CDCl₃): δ 150.57, 138.59, 137.24, 132.77, 129.78, 129.56, 129.15, 128.55, 128.29, 127.47, 123.55, 87.05, 83.86, 28.00.

Preparation of (2-iodophenyl)(phenyl)methanone (121**)**



121

A mixture of 2-iodobenzoic acid (1 eq., 2 g, 8.06 mmol), SOCl₂ (15.4 eq., 9 mL, 124 mmol) and DMF (1.6 %, 0.01 mL, 0.129 mmol) was stirred at 70 °C for 0.5 h and then cooled to rt. After removal of SOCl₂ under reduced pressure, benzene (11.2 eq., 8 mL, 90.1 mmol) and AlCl₃ (1.1 eq., 1.18 g, 8.87 mmol) were added to the residue. The reaction mixture was stirred at 80 °C for 1.5 h, cooled to rt, poured into ice water.

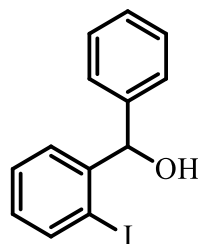
and extracted with EtOAc thrice. The combined organic phases were washed with saturated NaHCO₃ aqueous solution, dried over anhydrous Na₂SO₄ and filtered through a silica gel pad with EtOAc. The filtrate was concentrated in vacuo to afford **121** as a pale yellow oil (2.45 g, 99 %).

¹H NMR (400 MHz, CDCl₃): δ 7.93 (d, *J* = 7.9 Hz, 1H), 7.81 (d, *J* = 7.7 Hz, 2H), 7.61 (t, *J* = 7.4 Hz, 1H), 7.46 (q, *J* = 7.4 Hz, 3H), 7.30 (d, *J* = 7.5 Hz, 1H), 7.19 (t, *J* = 7.7 Hz, 1H).

Rf: 0.6 (heptane:EtOAc = 3:2).

These data are consistent with the previously reported characterization.¹⁹¹

Preparation of (2-iodophenyl)(phenyl)methanol (**122**)



122

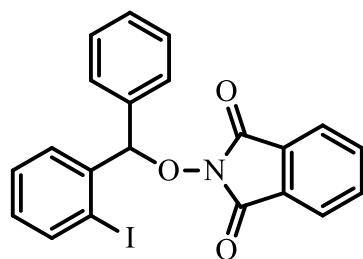
NaBH₄ (4 eq., 1.066 g, 28.17 mmol) was added in portions to a solution of **121** (1 eq., 2.17 g, 7.043 mmol) in MeOH (15 mL)/toluene (7.5 mL) at 0 °C. After stirred at rt for 1.5 h, the reaction mixture was quenched by H₂O and extracted with EtOAc thrice. The combined organic phases were washed with brine, dried over anhydrous Na₂SO₄ and filtered a silica gel pad with EtOAc. The filtrate was concentrated in vacuo to afford **121** as a colorless oil (2.18 g, 100%) .

¹H NMR (400 MHz, CDCl₃): δ 7.84 (d, *J* = 7.9 Hz, 1H), 7.53 (d, *J* = 7.7 Hz, 1H), 7.44 – 7.28 (m, 6H), 6.99 (t, *J* = 7.5 Hz, 1H), 6.07 (s, 1H), 2.33 (s, 1H).

Rf: 0.5 (heptane:EtOAc = 3:1).

These data are consistent with the previously reported characterization.¹⁹²

Preparation of 2-((2-iodophenyl)(phenyl)methoxy)isoindoline-1,3-dione (**123**)



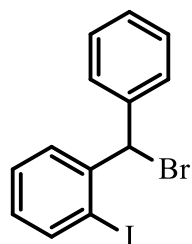
123

A mixture of **124** (1 eq., 700 mg, 1.88 mmol), TEA (2 eq., 0.522 mL, 3.75 mmol), NHPI (1.1 eq., 336 mg, 2.06 mmol) in DMF (5.1 mL) was stirred at 50 °C over night. After completion, water was added and acidified to pH~3 with HCl (1M). The mixture was extracted by EtOAc thrice. The combined organic phases were washed with brine, dried over anhydrous Na₂SO₄ and filtered. The filtrate was concentrated in vacuo and purified by silica gel chromatography (Heptane:EtOAc = 4:1) to **123** as a white solid (740 mg, 87 %).

¹H NMR (400 MHz, CDCl₃): δ 8.13 – 8.05 (m, 1H), 7.83 – 7.68 (m, 5H), 7.60 – 7.48 (m, 3H), 7.39 – 7.31 (m, 3H), 7.11 – 7.01 (m, 1H), 6.78 (s, 1H).

¹³C NMR (400 MHz, CDCl₃): δ 163.69, 140.46, 139.53, 136.71, 134.51, 130.37, 129.69, 129.07, 129.01, 128.56, 128.51, 123.61, 99.14, 92.52.

Preparation of 1-(bromo(phenyl)methyl)-2-iodobenzene (**124**)



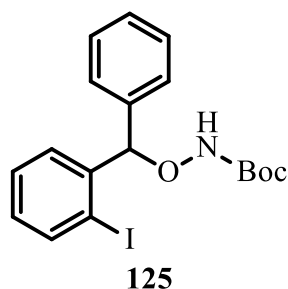
124

PBr₃ (2 eq., 1.28 mL, 13.67 mmol) was added slowly to a solution of **122** (1 eq., 2.12 g, 6.84 mmol) in dry DCM (10.28 mL) at 0 °C. After stirred at rt for 2h, the reaction mixture was slowly poured into ice water and extracted with DCM thrice. The combined organic phases were washed with saturated NaHCO₃ aqueous solution, dried over anhydrous Na₂SO₄, and filtered. The filtrate was concentration in vacuo to afford gave **124** as a yellow oil (2.4 g, 94%).

^1H NMR (400 MHz, CDCl_3): δ 7.85 (dd, $J = 7.9, 1.1$ Hz, 1H), 7.68 (dd, $J = 7.9, 1.6$ Hz, 1H), 7.51 – 7.45 (m, 2H), 7.39 – 7.28 (m, 4H), 6.97 (td, $J = 7.7, 1.7$ Hz, 1H), 6.58 (s, 1H).

^{13}C NMR (400 MHz, CDCl_3): δ 143.40, 140.06, 139.87, 131.24, 129.87, 128.95, 128.81, 128.72, 128.27, 99.35, 58.98.

Preparation of *tert*-butyl (2-iodophenyl)(phenyl)methoxycarbamate (**125**)



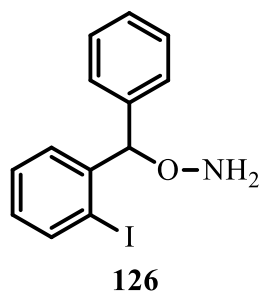
Method 1: A mixture of **127** (1 eq., 40 mg, 0.0761 mmol), ethyl acetoacetate (3 eq., 28.9 μL , 0.228 mmol), EtOH (3 eq., 13.3 μL , 0.228 mmol), K_3PO_4 (3 eq., 48.5 mg, 0.228 mmol) and CuI (10 %, 1.45 mg, 0.00761 mmol) in DMSO (0.5 mL) was stirred at 80 $^\circ\text{C}$ under Ar for 16h. The reaction mixture was directly purified by reverse phase chromatography (MeOH/ H_2O) to afford **125** as a colorless oil (15.8 mg, 54 %).

Method 2: A solution of (2-ethoxy-2-oxoethyl)zinc(II) bromide (1.5 eq., 0.51 M, 0.224 mL, 0.114 mmol) in THF was added slowly to a solution of **127** (1 eq., 40 mg, 0.0761 mmol) and $\text{PdCl}(\text{Ph})(\text{PPh}_3)_2$ (1 %, 0.566 mg, 0.000761 mmol) in THF (0.5 mL) under Ar at rt. The mixture was stirred at 60 $^\circ\text{C}$ for 15 h and concentrated in vacuo. The crude was purified by reverse phase chromatography (MeOH/ H_2O) to afford **125** as a colorless oil (32.4 mg, 100 %).

^1H NMR (400 MHz, CDCl_3): δ 7.86 (dd, $J = 7.9, 1.0$ Hz, 1H), 7.56 (dd, $J = 7.8, 1.6$ Hz, 1H), 7.46 – 7.38 (m, 3H), 7.36 – 7.29 (m, 3H), 7.10 (s, 1H), 7.04 (td, $J = 7.7, 1.7$ Hz, 1H), 6.16 (s, 1H), 1.50 (s, 9H).

^{13}C NMR (400 MHz, CDCl_3): δ 156.44, 141.91, 139.91, 137.94, 129.89, 128.67, 128.65, 128.51, 128.49, 128.43, 99.66, 91.84, 82.14, 28.40.

Preparation of *O*-((2-iodophenyl)(phenyl)methyl)hydroxylamine (**126**)

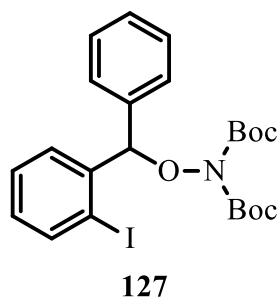


A solution of **123** (1 eq., 618 mg, 1.36 mmol) and hydrazine hydrate (15 eq., 1.98 mL, 20.4 mmol) in EtOH (15 mL) was refluxed for 1 h and concentrated in vacuo. The crude was basified with 10% Na₂CO₃ aqueous solution to pH ~ 10 and extracted with EtOAc thrice. The combined organic phases were washed brine, dried with anhydrous Na₂SO₄ and filtered. The filtrate was concentrated in vacuo to afford **126** as a yellow oil (436 mg, 99 %).

¹H NMR (400 MHz, CDCl₃): δ 7.78 (dd, *J* = 7.9, 1.0 Hz, 1H), 7.35 – 7.26 (m, 5H), 7.25 – 7.16 (m, 2H), 6.94 – 6.88 (m, 1H), 5.80 (s, 1H), 5.43 (s, 2H).

¹³C NMR (400 MHz, CDCl₃): δ 143.02, 139.93, 139.35, 129.62, 128.56, 128.29, 128.16, 128.06, 127.31, 99.90, 91.42.

Preparation of *tert*-butyl *N*-[(*tert*-butoxy)carbonyl]-*N*-[(2-iodophenyl)(phenyl)methoxy]carbamate (**127**)



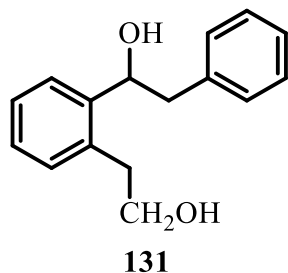
TEA (4 eq., 0.675 mL, 4.86 mmol) was added to a solution of **126** (1 eq., 395 mg, 1.21 mmol) and Boc₂O (4 eq., 1.06 g, 4.86 mmol) in DCM (15 mL) and stirred at rt for 16 h. The mixture was concentrated in vacuo and purified by reverse phase chromatography (MeOH/H₂O) to afford **127** as a colorless oil (485 mg, 76 %).

¹H NMR (400 MHz, CDCl₃): δ 7.81 (d, *J* = 8.0 Hz, 2H), 7.44 – 7.37 (m, 3H), 7.34 –

7.27 (m, 3H), 7.01 (td, $J = 7.7, 1.7$ Hz, 1H), 6.31 (s, 1H), 1.42 (s, 18H).

^{13}C NMR (400 MHz, CDCl_3): δ 150.48, 141.39, 139.40, 137.02, 129.82, 129.51, 129.38, 128.53, 128.25, 99.27, 91.41, 83.82, 27.99.

Preparation of 1-(2-(2-hydroxyethyl)phenyl)-2-phenylethanol (**131**)



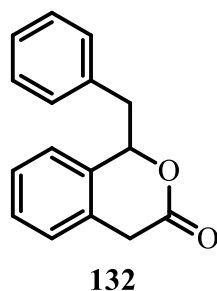
To a solution of **130** (1 eq., 170 mg, 0.602 mmol) in EtOH (5 mL) at 0 °C was added NaBH_4 (4 eq., 91.1 mg, 2.41 mmol) and the resulting mixture was stirred rt for 3 h. After quenched by H_2O and acidified by H_2SO_4 (1 M) to pH~6, the reaction mixture was extracted by EtOAc thrice. The combined organic phases were washed with brine, dried over anhydrous Na_2SO_4 and filtered. The filtrate was concentrated in vacuo and purified by silica gel chromatography (heptane:EtOAc = 5:1) to afford **131** as a yellow oil (120 mg, 82 %).

^1H NMR (400 MHz, CDCl_3): δ 7.49 (d, $J = 7.1$ Hz, 1H), 7.33 – 7.07 (m, 8H), 5.13 – 5.02 (m, 1H), 3.74 – 3.49 (m, 2H), 3.16 (s, 1H), 3.08 – 2.97 (m, 2H), 2.88 – 2.67 (m, 2H), 2.54 (s, 1H).

Rf: 0.25 (heptane:EtOAc = 2:1).

These data are consistent with the previously reported characterization.¹⁸⁴

Preparation of 1-benzylisochroman-3-one (**132**)



To a solution of **130** (1 eq., 34 mg, 0.12 mmol) in EtOH (1 mL) at 0 °C was added NaBH₄ (4 eq., 18.2 mg, 0.482 mmol) and stirred at 0 °C for 2 h. The reaction was quenched by H₂O and acidified by H₂SO₄ (2 M) to pH~1. After stirred at rt for 20 min, the mixture was extracted by EtOAc thrice. The combined organic phases were washed with brine, dried over anhydrous Na₂SO₄ and filtered. The filtrate was concentrated in vacuo to afford **132** as a white solid (27 mg, 94 %).

¹H NMR (400 MHz, CDCl₃): δ 7.34 – 6.98 (m, 9H), 5.70 (t, *J* = 5.7 Hz, 1H), 3.48 (d, *J* = 19.5 Hz, 1H), 3.37 (dd, *J* = 13.9, 5.6 Hz, 1H), 3.22 (dd, *J* = 13.9, 5.6 Hz, 1H), 2.94 (d, *J* = 19.4 Hz, 1H).

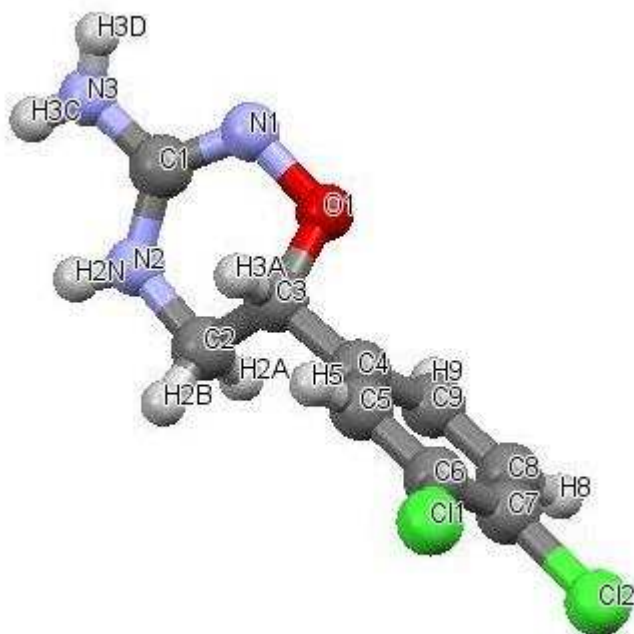
These data are consistent with the previously reported characterization.¹⁹³

IX. Appendix

IX. Appendix

Appendix I. Crystallographic data and structure refinement

parameters of cpd 10a



Formula: C₉H₉Cl₂N₃O

Space group: P 2₁/c (14)

Cell lengths: **a** 11.7566(10) **b** 9.7544(10) **c** 9.4306(8)

Cell Angles: **a** 90 **b** 110.976(4) **g** 90

Cell Volume: 1009.82

Z: 4 **Z'**: 0

R-factor (%): 5.01

Atoms

Number	Label	Charge	SybylType	Xfrac + ESD	Yfrac + ESD	Zfrac + ESD	Symm. op.
1	C1	0	C.2	0.9835(2)	0.4100(3)	0.2055(3)	x,y,z
2	C2	0	C.3	0.8579(3)	0.3695(3)	0.3589(3)	x,y,z
3	H2A	0	H	0.8935	0.4068	0.4632	x,y,z
4	H2B	0	H	0.8065	0.2895	0.3603	x,y,z
5	C3	0	C.3	0.7847(3)	0.4756(4)	0.2532(4)	x,y,z
6	H3A	0	H	0.7435	0.4331	0.1510	x,y,z
7	C4	0	C.2	0.6900(4)	0.5386(5)	0.3046(5)	x,y,z
8	C5	0	C.2	0.5677(4)	0.5138(5)	0.2272(5)	x,y,z
9	H5	0	H	0.5430	0.4601	0.1372	x,y,z
10	C6	0	C.3	0.4807(4)	0.5669(6)	0.2799(6)	x,y,z
11	C7	0	C.3	0.5161(4)	0.6468(6)	0.4091(6)	x,y,z

12	C8	0	C.2	0.6371(4)	0.6758(5)	0.4851(5)	x,y,z
13	H8	0	H	0.6611	0.7330	0.5724	x,y,z
14	C9	0	C.2	0.7242(4)	0.6207(5)	0.4333(6)	x,y,z
15	H9	0	H	0.8080	0.6396	0.4865	x,y,z
16	N1	0	N.2	0.9435(2)	0.5344(2)	0.1641(3)	x,y,z
17	N2	0	N.3	0.9539(2)	0.3296(3)	0.3031(3)	x,y,z
18	N3	0	N.3	1.0642(2)	0.3579(3)	0.1475(3)	x,y,z
19	C11	0	C1	0.32856(11)	0.52574(17)	0.17658(19)	x,y,z
20	C12	0	C1	0.4058(2)	0.7084(3)	0.4754(3)	x,y,z
21	O1	0	O.3	0.8640(3)	0.5841(5)	0.2397(5)	x,y,z
22	H2N	0	H	0.974(3)	0.251(4)	0.309(4)	x,y,z
23	H3C	0	H	1.093(4)	0.280(4)	0.179(4)	x,y,z
24	H3D	0	H	1.070(3)	0.398(4)	0.069(4)	x,y,z
25	H2C	0	H	0.8833	0.3479	0.4685	x,y,z
26	H2D	0	H	0.7828	0.3171	0.3044	x,y,z
27	C3B	0	C.3	0.8328(8)	0.5195(10)	0.3349(10)	x,y,z
28	H3B	0	H	0.9019	0.5690	0.4123	x,y,z
29	C4B	0	C.3	0.7167(6)	0.5671(9)	0.3538(10)	x,y,z
30	C5B	0	C.3	0.6043(8)	0.5242(9)	0.2524(9)	x,y,z
31	H5B	0	H	0.6000	0.4700	0.1669	x,y,z
32	C6B	0	C.3	0.4982(6)	0.5604(11)	0.2762(10)	x,y,z
33	C7B	0	C.3	0.5045(6)	0.6396(11)	0.4013(11)	x,y,z
34	C8B	0	C.3	0.6169(7)	0.6826(9)	0.5027(9)	x,y,z
35	H8B	0	H	0.6212	0.7367	0.5882	x,y,z
36	C9B	0	C.3	0.7230(5)	0.6464(9)	0.4789(9)	x,y,z
37	H9B	0	H	0.7999	0.6757	0.5481	x,y,z
38	C11B	0	C1	0.3622(3)	0.5090(5)	0.1644(5)	x,y,z
39	C12B	0	C1	0.3812(6)	0.6872(8)	0.4445(8)	x,y,z
40	O1B	0	O.3	0.8272(9)	0.5647(13)	0.1925(13)	x,y,z

Bonds

Number	Atom1	Atom2	Type	Polymeric	Cyclicity	Length	SybylType
1	C1	N1	Unknown	no	cyclic	1.309(3)	un
2	C1	N2	Unknown	no	cyclic	1.346(4)	1
3	C1	N3	Unknown	no	acyclic	1.352(4)	1
4	C2	H2A	Unknown	no	acyclic	0.990	1
5	C2	H2B	Unknown	no	acyclic	0.990	1
6	C2	C3	Unknown	no	cyclic	1.480(4)	1
7	C2	N2	Unknown	no	cyclic	1.459(5)	1
8	C3	H3A	Unknown	no	acyclic	1.001	1
9	C3	C4	Unknown	no	acyclic	1.496(7)	1
10	C3	O1	Unknown	no	cyclic	1.446(6)	1
11	C4	C5	Unknown	no	cyclic	1.381(6)	un
12	C4	C9	Unknown	no	cyclic	1.388(7)	un

13	C5	H5	Unknown	no	acyclic	0.950	1
14	C5	C6	Unknown	no	cyclic	1.388(8)	1
15	C6	C7	Unknown	no	cyclic	1.379(8)	1
16	C6	C11	Unknown	no	acyclic	1.750(4)	1
17	C7	C8	Unknown	no	cyclic	1.374(6)	1
18	C7	C12	Unknown	no	acyclic	1.736(6)	1
19	C8	H8	Unknown	no	acyclic	0.950	1
20	C8	C9	Unknown	no	cyclic	1.391(8)	un
21	C9	H9	Unknown	no	acyclic	0.950	1
22	N1	O1	Unknown	no	cyclic	1.447(6)	1
23	N2	H2N	Unknown	no	acyclic	0.80(4)	1
24	N3	H3C	Unknown	no	acyclic	0.84(4)	1
25	N3	H3D	Unknown	no	acyclic	0.86(4)	1

Symmetry

Number	Symm. Op.	Description	Detailed Description	Order	Type
1	x, y, z	Identity	Identity	1	1
2	-x, 1/2+y, 1/2-z	Screw axis (2-fold)	2-fold screw axis with direction [0, 1, 0] at 0, y, 1/4 with screw component [0, 1/2, 0]	2	2
3	-x, -y, -z	Inversion centre	Inversion at [0, 0, 0]	2	-1
4	x, 1/2-y, 1/2+z	Glide plane	Glide plane perpendicular to [0, 1, 0] with glide component [0, 0, 1/2]	2	-2

Angles

Number	Atom1	Atom2	Atom3	Angle
1	N1	C1	N2	126.2(3)
2	N1	C1	N3	117.2(3)
3	N2	C1	N3	116.6(3)
4	H2A	C2	H2B	108.6
5	H2A	C2	C3	110.4
6	H2A	C2	N2	110.5
7	H2B	C2	C3	110.5
8	H2B	C2	N2	110.4
9	C3	C2	N2	106.4(3)
10	C2	C3	H3A	108.9
11	C2	C3	C4	112.9(3)
12	C2	C3	O1	109.5(3)
13	H3A	C3	C4	108.8
14	H3A	C3	O1	108.9
15	C4	C3	O1	107.8(3)
16	C3	C4	C5	120.8(4)
17	C3	C4	C9	120.3(4)
18	C5	C4	C9	119.0(4)

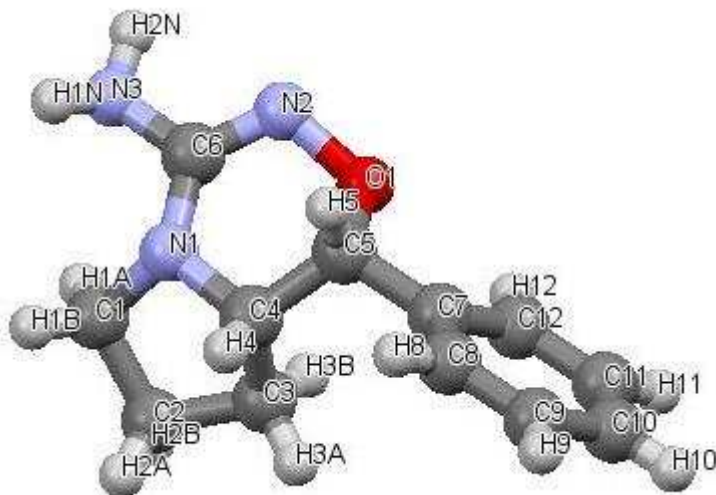
19	C4	C5	H5	119.7
20	C4	C5	C6	120.4(5)
21	H5	C5	C6	119.8
22	C5	C6	C7	120.0(5)
23	C5	C6	C11	116.9(4)
24	C7	C6	C11	123.1(4)
25	C6	C7	C8	120.4(5)
26	C6	C7	C12	119.1(4)
27	C8	C7	C12	120.5(4)
28	C7	C8	H8	120.3
29	C7	C8	C9	119.5(5)
30	H8	C8	C9	120.3
31	C4	C9	C8	120.7(5)
32	C4	C9	H9	119.7
33	C8	C9	H9	119.6
34	C1	N1	O1	112.9(3)
35	C1	N2	C2	120.9(3)
36	C1	N2	H2N	118(3)
37	C2	N2	H2N	119(3)
38	C1	N3	H3C	117(3)
39	C1	N3	H3D	117(2)
40	H3C	N3	H3D	125(4)
41	C3	O1	N1	110.4(3)

Torsions

Number	Atom1	Atom2	Atom3	Atom4	Torsion
1	N2	C1	N1	O1	2.3(4)
2	N3	C1	N1	O1	-176.2(3)
3	N1	C1	N2	C2	8.4(4)
4	N1	C1	N2	H2N	169(3)
5	N3	C1	N2	C2	-173.1(3)
6	N3	C1	N2	H2N	-12(3)
7	N1	C1	N3	H3C	176(3)
8	N1	C1	N3	H3D	-17(3)
9	N2	C1	N3	H3C	-3(3)
10	N2	C1	N3	H3D	165(3)
11	H2A	C2	C3	H3A	-174.7
12	H2A	C2	C3	C4	-53.8
13	H2A	C2	C3	O1	66.3
14	H2B	C2	C3	H3A	-54.6
15	H2B	C2	C3	C4	66.4
16	H2B	C2	C3	O1	-173.5
17	N2	C2	C3	H3A	65.3
18	N2	C2	C3	C4	-173.7(3)

19	N2	C2	C3	O1	-53.6(4)
20	H2A	C2	N2	C1	-101.8
21	H2A	C2	N2	H2N	97
22	H2B	C2	N2	C1	138.0
23	H2B	C2	N2	H2N	-23
24	C3	C2	N2	C1	18.1(4)
25	C3	C2	N2	H2N	-143(3)
26	C2	C3	C4	C5	-110.6(5)
27	C2	C3	C4	C9	68.0(5)
28	H3A	C3	C4	C5	10.4
29	H3A	C3	C4	C9	-171.0
30	O1	C3	C4	C5	128.3(5)
31	O1	C3	C4	C9	-53.1(5)
32	C2	C3	O1	N1	67.3(4)
33	H3A	C3	O1	N1	-51.6
34	C4	C3	O1	N1	-169.5(3)
35	C3	C4	C5	H5	-3.3
36	C3	C4	C5	C6	176.7(4)
37	C9	C4	C5	H5	178.1
38	C9	C4	C5	C6	-1.9(7)
39	C3	C4	C9	C8	-177.7(4)
40	C3	C4	C9	H9	2.4
41	C5	C4	C9	C8	0.9(7)
42	C5	C4	C9	H9	-179.0
43	C4	C5	C6	C7	1.0(8)
44	C4	C5	C6	C11	-178.3(4)
45	H5	C5	C6	C7	-178.9
46	H5	C5	C6	C11	1.8
47	C5	C6	C7	C8	0.9(8)
48	C5	C6	C7	C12	-178.4(4)
49	C11	C6	C7	C8	-179.8(4)
50	C11	C6	C7	C12	0.9(7)
51	C6	C7	C8	H8	178.2
52	C6	C7	C8	C9	-1.8(8)
53	C12	C7	C8	H8	-2.6
54	C12	C7	C8	C9	177.4(4)
55	C7	C8	C9	C4	1.0(8)
56	C7	C8	C9	H9	-179.1
57	H8	C8	C9	C4	-179.1
58	H8	C8	C9	H9	0.8
59	C1	N1	O1	C3	-39.4(4)

Appendix II. Crystallographic data and structure refinement parameters of cpd 10b



Formula: C₁₂ H₁₅ N₃ O

Space group: P 2₁ (4)

Cell lengths: **a** 8.2172(2) **b** 6.5985(2) **c** 11.2773(3)

Cell Angles: **a** 90 **b** 103.3510(10) **g** 90

Cell Volume: 594.943

Z: 2 **Z'**: 0

R-factor (%): 3.01

Atoms

Number	Label	Charge	SybylType	Xfrac + ESD	Yfrac + ESD	Zfrac + ESD	Symm. op.
1	C1	0	C.3	0.7032(2)	0.7257(4)	0.01324(18)	x,y,z
2	H1A	0	H	0.6489	0.6603	-0.0649	x,y,z
3	H1B	0	H	0.7625	0.8488	-0.0041	x,y,z
4	C2	0	C.3	0.5728(3)	0.7793(4)	0.0870(2)	x,y,z
5	H2A	0	H	0.5872	0.9210	0.1165	x,y,z
6	H2B	0	H	0.4578	0.7626	0.0365	x,y,z
7	C3	0	C.3	0.6057(3)	0.6306(4)	0.19424(19)	x,y,z
8	H3A	0	H	0.5770	0.6915	0.2670	x,y,z
9	H3B	0	H	0.5410	0.5039	0.1729	x,y,z
10	C4	0	C.3	0.7926(2)	0.5917(3)	0.21567(17)	x,y,z
11	H4	0	H	0.8539	0.7112	0.2590	x,y,z
12	C5	0	C.3	0.8610(2)	0.4003(3)	0.28438(16)	x,y,z
13	H5	0	H	0.9859	0.4054	0.3034	x,y,z
14	C6	0	C.2	0.8611(2)	0.4030(3)	0.04676(15)	x,y,z
15	C7	0	C.2	0.8047(2)	0.3744(3)	0.40216(17)	x,y,z
16	C8	0	C.2	0.8828(3)	0.4868(4)	0.50276(18)	x,y,z

17	H8	0	H	0.9689	0.5794	0.4963	x,y,z
18	C9	0	C.2	0.8369(3)	0.4656(4)	0.6127(2)	x,y,z
19	H9	0	H	0.8914	0.5439	0.6811	x,y,z
20	C10	0	C.2	0.7131(3)	0.3321(4)	0.62335(19)	x,y,z
21	H10	0	H	0.6822	0.3170	0.6990	x,y,z
22	C11	0	C.2	0.6338(3)	0.2200(5)	0.5235(2)	x,y,z
23	H11	0	H	0.5475	0.1278	0.5303	x,y,z
24	C12	0	C.2	0.6793(3)	0.2411(4)	0.41317(18)	x,y,z
25	H12	0	H	0.6240	0.1635	0.3447	x,y,z
26	N1	0	N.3	0.82045(18)	0.5841(2)	0.09168(14)	x,y,z
27	N2	0	N.2	0.87942(19)	0.2305(3)	0.10345(14)	x,y,z
28	N3	0	N.3	0.8875(2)	0.4081(3)	-0.06902(14)	x,y,z
29	O1	0	O.3	0.80620(16)	0.2293(2)	0.20873(11)	x,y,z
30	H1N	0	H	0.946(3)	0.512(5)	-0.087(2)	x,y,z
31	H2N	0	H	0.922(4)	0.287(5)	-0.090(2)	x,y,z

Bonds

Number	Atom1	Atom2	Type	Polymeric	Cyclic	Length	SybylType
1	C1	H1A	Unknown	no	acyclic	0.990	1
2	C1	H1B	Unknown	no	acyclic	0.990	1
3	C1	C2	Unknown	no	cyclic	1.542(3)	1
4	C1	N1	Unknown	no	cyclic	1.480(2)	1
5	C2	H2A	Unknown	no	acyclic	0.990	1
6	C2	H2B	Unknown	no	acyclic	0.990	1
7	C2	C3	Unknown	no	cyclic	1.532(3)	1
8	C3	H3A	Unknown	no	acyclic	0.990	1
9	C3	H3B	Unknown	no	acyclic	0.990	1
10	C3	C4	Unknown	no	cyclic	1.520(3)	1
11	C4	H4	Unknown	no	acyclic	1.000	1
12	C4	C5	Unknown	no	cyclic	1.520(3)	1
13	C4	N1	Unknown	no	cyclic	1.469(3)	1
14	C5	H5	Unknown	no	acyclic	0.999	1
15	C5	C7	Unknown	no	acyclic	1.514(3)	1
16	C5	O1	Unknown	no	cyclic	1.423(2)	1
17	C6	N1	Unknown	no	cyclic	1.369(2)	1
18	C6	N2	Unknown	no	cyclic	1.297(3)	un
19	C6	N3	Unknown	no	acyclic	1.373(2)	1
20	C7	C8	Unknown	no	cyclic	1.383(3)	un
21	C7	C12	Unknown	no	cyclic	1.382(3)	un
22	C8	H8	Unknown	no	acyclic	0.950	1
23	C8	C9	Unknown	no	cyclic	1.384(3)	un
24	C9	H9	Unknown	no	acyclic	0.950	1
25	C9	C10	Unknown	no	cyclic	1.372(4)	un
26	C10	H10	Unknown	no	acyclic	0.950	1

27	C10	C11	Unknown	no	cyclic	1.379(3)	un
28	C11	H11	Unknown	no	acyclic	0.951	1
29	C11	C12	Unknown	no	cyclic	1.386(3)	un
30	C12	H12	Unknown	no	acyclic	0.950	1
31	N2	O1	Unknown	no	cyclic	1.450(2)	1
32	N3	H1N	Unknown	no	acyclic	0.89(3)	1
33	N3	H2N	Unknown	no	acyclic	0.90(3)	1

Symmetry

Number	Symm. Op.	Description	Detailed Description	Order	Type
1	x, y, z	Identity	Identity	1	1
2	-x, 1/2+y, -z	Screw axis (2-fold)	2-fold screw axis with direction [0, 1, 0] at 0, y, 0 with screw component [0, 1/2, 0]	2	2

Angles

Number	Atom1	Atom2	Atom3	Angle
1	H1A	C1	H1B	108.9
2	H1A	C1	C2	110.7
3	H1A	C1	N1	110.7
4	H1B	C1	C2	110.7
5	H1B	C1	N1	110.7
6	C2	C1	N1	105.1(2)
7	C1	C2	H2A	110.7
8	C1	C2	H2B	110.7
9	C1	C2	C3	105.1(2)
10	H2A	C2	H2B	108.8
11	H2A	C2	C3	110.7
12	H2B	C2	C3	110.7
13	C2	C3	H3A	111.2
14	C2	C3	H3B	111.2
15	C2	C3	C4	102.8(2)
16	H3A	C3	H3B	109.1
17	H3A	C3	C4	111.2
18	H3B	C3	C4	111.2
19	C3	C4	H4	108.7
20	C3	C4	C5	117.5(2)
21	C3	C4	N1	103.2(2)
22	H4	C4	C5	108.7
23	H4	C4	N1	108.7
24	C5	C4	N1	109.7(1)
25	C4	C5	H5	108.8
26	C4	C5	C7	112.9(2)
27	C4	C5	O1	108.9(1)

28	H5	C5	C7	108.8
29	H5	C5	O1	108.8
30	C7	C5	O1	108.5(1)
31	N1	C6	N2	126.4(2)
32	N1	C6	N3	115.9(2)
33	N2	C6	N3	117.7(2)
34	C5	C7	C8	118.8(2)
35	C5	C7	C12	122.4(2)
36	C8	C7	C12	118.8(2)
37	C7	C8	H8	119.6
38	C7	C8	C9	120.7(2)
39	H8	C8	C9	119.7
40	C8	C9	H9	119.8
41	C8	C9	C10	120.3(2)
42	H9	C9	C10	119.9
43	C9	C10	H10	120.2
44	C9	C10	C11	119.6(2)
45	H10	C10	C11	120.2
46	C10	C11	H11	119.9
47	C10	C11	C12	120.3(2)
48	H11	C11	C12	119.8
49	C7	C12	C11	120.4(2)
50	C7	C12	H12	119.8
51	C11	C12	H12	119.8
52	C1	N1	C4	108.9(1)
53	C1	N1	C6	120.7(2)
54	C4	N1	C6	119.1(1)
55	C6	N2	O1	112.7(2)
56	C6	N3	H1N	117(2)
57	C6	N3	H2N	111(2)
58	H1N	N3	H2N	114(3)
59	C5	O1	N2	110.7(1)

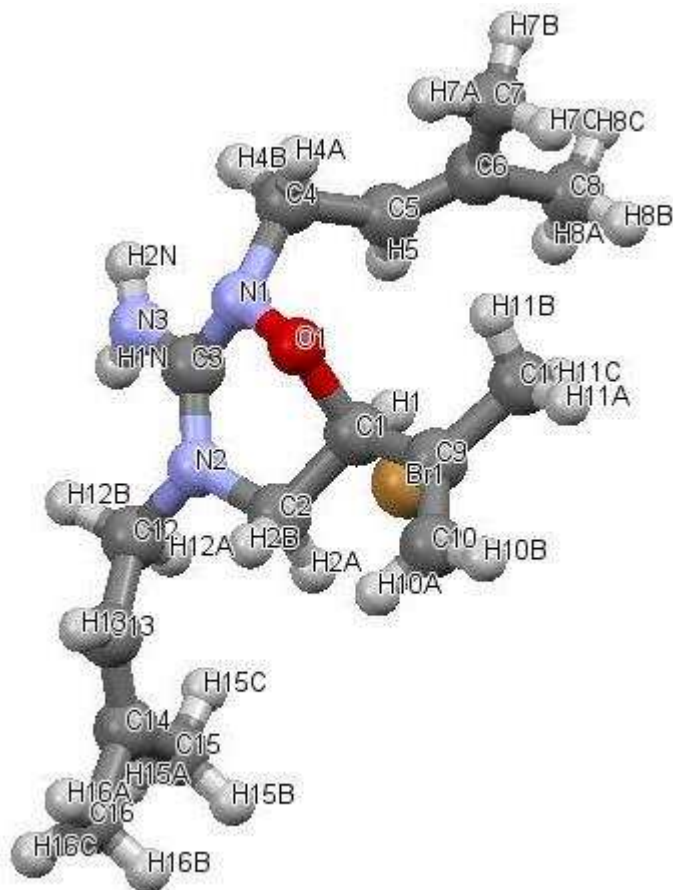
Torsions

Number	Atom1	Atom2	Atom3	Atom4	Torsion
1	H1A	C1	C2	H2A	-131.5
2	H1A	C1	C2	H2B	-10.7
3	H1A	C1	C2	C3	108.9
4	H1B	C1	C2	H2A	-10.7
5	H1B	C1	C2	H2B	110.1
6	H1B	C1	C2	C3	-130.3
7	N1	C1	C2	H2A	108.9
8	N1	C1	C2	H2B	-130.3
9	N1	C1	C2	C3	-10.7(2)

10	H1A	C1	N1	C4	-133.6
11	H1A	C1	N1	C6	9.8
12	H1B	C1	N1	C4	105.6
13	H1B	C1	N1	C6	-111.1
14	C2	C1	N1	C4	-14.0(2)
15	C2	C1	N1	C6	129.4(2)
16	C1	C2	C3	H3A	149.4
17	C1	C2	C3	H3B	-88.8
18	C1	C2	C3	C4	30.3(2)
19	H2A	C2	C3	H3A	29.7
20	H2A	C2	C3	H3B	151.5
21	H2A	C2	C3	C4	-89.4
22	H2B	C2	C3	H3A	-91.0
23	H2B	C2	C3	H3B	30.8
24	H2B	C2	C3	C4	149.9
25	C2	C3	C4	H4	76.7
26	C2	C3	C4	C5	-159.4(2)
27	C2	C3	C4	N1	-38.6(2)
28	H3A	C3	C4	H4	-42.4
29	H3A	C3	C4	C5	81.5
30	H3A	C3	C4	N1	-157.7
31	H3B	C3	C4	H4	-164.2
32	H3B	C3	C4	C5	-40.3
33	H3B	C3	C4	N1	80.5
34	C3	C4	C5	H5	-171.0
35	C3	C4	C5	C7	-50.1(2)
36	C3	C4	C5	O1	70.5(2)
37	H4	C4	C5	H5	-47.1
38	H4	C4	C5	C7	73.8
39	H4	C4	C5	O1	-165.5
40	N1	C4	C5	H5	71.6
41	N1	C4	C5	C7	-167.5(1)
42	N1	C4	C5	O1	-46.8(2)
43	C3	C4	N1	C1	33.3(2)
44	C3	C4	N1	C6	-110.7(2)
45	H4	C4	N1	C1	-82.0
46	H4	C4	N1	C6	134.0
47	C5	C4	N1	C1	159.3(1)
48	C5	C4	N1	C6	15.3(2)
49	C4	C5	C7	C8	-78.0(2)
50	C4	C5	C7	C12	102.7(2)
51	H5	C5	C7	C8	42.9
52	H5	C5	C7	C12	-136.5
53	O1	C5	C7	C8	161.1(2)

54	O1	C5	C7	C12	-18.2(2)
55	C4	C5	O1	N2	65.9(2)
56	H5	C5	O1	N2	-52.6
57	C7	C5	O1	N2	-170.8(1)
58	N2	C6	N1	C1	-140.1(2)
59	N2	C6	N1	C4	-0.4(3)
60	N3	C6	N1	C1	41.1(2)
61	N3	C6	N1	C4	-179.1(2)
62	N1	C6	N2	O1	16.9(3)
63	N3	C6	N2	O1	-164.3(2)
64	N1	C6	N3	H1N	42(2)
65	N1	C6	N3	H2N	175(2)
66	N2	C6	N3	H1N	-137(2)
67	N2	C6	N3	H2N	-4(2)
68	C5	C7	C8	H8	0.9
69	C5	C7	C8	C9	-179.0(2)
70	C12	C7	C8	H8	-179.7
71	C12	C7	C8	C9	0.3(3)
72	C5	C7	C12	C11	178.9(2)
73	C5	C7	C12	H12	-1.1
74	C8	C7	C12	C11	-0.4(3)
75	C8	C7	C12	H12	179.6
76	C7	C8	C9	H9	-179.9
77	C7	C8	C9	C10	0.1(4)
78	H8	C8	C9	H9	0.2
79	H8	C8	C9	C10	-179.8
80	C8	C9	C10	H10	179.6
81	C8	C9	C10	C11	-0.4(4)
82	H9	C9	C10	H10	-0.4
83	H9	C9	C10	C11	179.6
84	C9	C10	C11	H11	-179.7
85	C9	C10	C11	C12	0.3(4)
86	H10	C10	C11	H11	0.3
87	H10	C10	C11	C12	-179.7
88	C10	C11	C12	C7	0.1(4)
89	C10	C11	C12	H12	-179.9
90	H11	C11	C12	C7	-179.9
91	H11	C11	C12	H12	0.1
92	C6	N2	O1	C5	-50.3(2)

Appendix III. Crystallographic data and structure refinement parameters of cpd 48



Formula: C₁₆ H₂₈ N₃ O, Br

Space group: P 2₁/c (14)

Cell lengths: **a** 11.8270(4) **b** 6.8408(2) **c** 23.5402(9)

Cell Angles: **a** 90 **b** 102.434(2) **g** 90

Cell Volume: 1859.88

Z: 4 **Z'**: 0

R-factor (%): 3.41

Atoms

Number	Label	Charge	SybylType	Xfrac + ESD	Yfrac + ESD	Zfrac + ESD	Symm. op.
1	C1	0	C.3	0.35796(15)	0.6005(2)	0.41942(7)	x,y,z
2	H1	0	H	0.3105	0.6228	0.3794	x,y,z
3	C2	0	C.3	0.48331(15)	0.6279(3)	0.41841(7)	x,y,z
4	H2A	0	H	0.4946	0.7556	0.4006	x,y,z
5	H2B	0	H	0.5307	0.6261	0.4586	x,y,z
6	C3	0	C.2	0.44898(15)	0.3208(2)	0.36353(7)	x,y,z
7	C4	0	C.3	0.24872(16)	0.1927(3)	0.35780(9)	x,y,z

8	H4A	0	H	0.2086	0.1312	0.3860	x,y,z
9	H4B	0	H	0.2636	0.0896	0.3308	x,y,z
10	C5	0	C.2	0.17172(17)	0.3439(3)	0.32413(8)	x,y,z
11	H5	0	H	0.2025	0.4166	0.2965	x,y,z
12	C6	0	C.2	0.06413(18)	0.3882(3)	0.32861(10)	x,y,z
13	C7	0	C.3	-0.0012(2)	0.2921(4)	0.36867(13)	x,y,z
14	H7A	0	H	0.0504	0.2029	0.3948	x,y,z
15	H7B	0	H	-0.0664	0.2184	0.3458	x,y,z
16	H7C	0	H	-0.0303	0.3921	0.3917	x,y,z
17	C8	0	C.3	-0.0020(2)	0.5443(4)	0.29034(14)	x,y,z
18	H8A	0	H	0.0474	0.6019	0.2663	x,y,z
19	H8B	0	H	-0.0258	0.6461	0.3146	x,y,z
20	H8C	0	H	-0.0708	0.4866	0.2652	x,y,z
21	C9	0	C.2	0.30980(16)	0.7226(3)	0.46157(8)	x,y,z
22	C10	0	C.2	0.37529(19)	0.8323(3)	0.50217(9)	x,y,z
23	H10A	0	H	0.4568	0.8360	0.5055	x,y,z
24	H10B	0	H	0.3407	0.9072	0.5279	x,y,z
25	C11	0	C.3	0.18019(18)	0.7140(3)	0.45240(10)	x,y,z
26	H11A	0	H	0.1551	0.7913	0.4825	x,y,z
27	H11B	0	H	0.1558	0.5779	0.4547	x,y,z
28	H11C	0	H	0.1452	0.7672	0.4140	x,y,z
29	C12	0	C.3	0.62511(16)	0.5020(3)	0.36189(9)	x,y,z
30	H12A	0	H	0.6053	0.5804	0.3258	x,y,z
31	H12B	0	H	0.6558	0.3747	0.3521	x,y,z
32	C13	0	C.2	0.71619(17)	0.6054(3)	0.40474(8)	x,y,z
33	H13	0	H	0.7371	0.5508	0.4427	x,y,z
34	C14	0	C.2	0.77072(16)	0.7664(3)	0.39488(9)	x,y,z
35	C15	0	C.3	0.7450(3)	0.8794(5)	0.33971(16)	x,y,z
36	H15A	0	H	0.8101	0.8680	0.3203	x,y,z
37	H15B	0	H	0.7331	1.0172	0.3482	x,y,z
38	H15C	0	H	0.6748	0.8275	0.3143	x,y,z
39	C16	0	C.3	0.8687(2)	0.8471(5)	0.43993(13)	x,y,z
40	H16A	0	H	0.8738	0.7765	0.4766	x,y,z
41	H16B	0	H	0.8552	0.9862	0.4459	x,y,z
42	H16C	0	H	0.9414	0.8314	0.4268	x,y,z
43	N1	0	N.3	0.36011(13)	0.2728(2)	0.38938(6)	x,y,z
44	N2	0	N.3	0.51932(12)	0.4684(2)	0.38424(6)	x,y,z
45	N3	0	N.3	0.46773(15)	0.2092(3)	0.32060(7)	x,y,z
46	O1	0	O.3	0.34567(11)	0.39552(17)	0.43548(5)	x,y,z
47	H1N	0	H	0.5130(19)	0.248(3)	0.2997(9)	x,y,z
48	H2N	0	H	0.430(2)	0.106(4)	0.3118(10)	x,y,z
49	Br1	0	Br	0.35034(2)	0.77807(3)	0.27258(2)	x,y,z

Bonds

Number	Atom1	Atom2	Type	Polymeric	Cyclic	Length	SybylType
1	C1	H1	Unknown	no	acyclic	0.999	1
2	C1	C2	Unknown	no	cyclic	1.500(3)	1
3	C1	C9	Unknown	no	acyclic	1.500(3)	1
4	C1	O1	Unknown	no	cyclic	1.468(2)	1
5	C2	H2A	Unknown	no	acyclic	0.990	1
6	C2	H2B	Unknown	no	acyclic	0.990	1
7	C2	N2	Unknown	no	cyclic	1.472(2)	1
8	C3	N1	Unknown	no	cyclic	1.363(2)	1
9	C3	N2	Unknown	no	cyclic	1.332(2)	1
10	C3	N3	Unknown	no	acyclic	1.323(2)	1
11	C4	H4A	Unknown	no	acyclic	0.989	1
12	C4	H4B	Unknown	no	acyclic	0.990	1
13	C4	C5	Unknown	no	acyclic	1.489(3)	1
14	C4	N1	Unknown	no	acyclic	1.472(2)	1
15	C5	H5	Unknown	no	acyclic	0.951	1
16	C5	C6	Unknown	no	acyclic	1.334(3)	un
17	C6	C7	Unknown	no	acyclic	1.494(4)	1
18	C6	C8	Unknown	no	acyclic	1.503(3)	1
19	C7	H7A	Unknown	no	acyclic	0.981	1
20	C7	H7B	Unknown	no	acyclic	0.980	1
21	C7	H7C	Unknown	no	acyclic	0.980	1
22	C8	H8A	Unknown	no	acyclic	0.979	1
23	C8	H8B	Unknown	no	acyclic	0.980	1
24	C8	H8C	Unknown	no	acyclic	0.980	1
25	C9	C10	Unknown	no	acyclic	1.326(3)	un
26	C9	C11	Unknown	no	acyclic	1.502(3)	1
27	C10	H10A	Unknown	no	acyclic	0.951	1
28	C10	H10B	Unknown	no	acyclic	0.951	1
29	C11	H11A	Unknown	no	acyclic	0.980	1
30	C11	H11B	Unknown	no	acyclic	0.980	1
31	C11	H11C	Unknown	no	acyclic	0.980	1
32	C12	H12A	Unknown	no	acyclic	0.989	1
33	C12	H12B	Unknown	no	acyclic	0.990	1
34	C12	C13	Unknown	no	acyclic	1.487(3)	1
35	C12	N2	Unknown	no	acyclic	1.476(3)	1
36	C13	H13	Unknown	no	acyclic	0.951	1
37	C13	C14	Unknown	no	acyclic	1.322(3)	un
38	C14	C15	Unknown	no	acyclic	1.485(4)	1
39	C14	C16	Unknown	no	acyclic	1.498(3)	1
40	C15	H15A	Unknown	no	acyclic	0.979	1
41	C15	H15B	Unknown	no	acyclic	0.980	1
42	C15	H15C	Unknown	no	acyclic	0.979	1
43	C16	H16A	Unknown	no	acyclic	0.980	1

44	C16	H16B	Unknown	no	acyclic	0.980	1
45	C16	H16C	Unknown	no	acyclic	0.980	1
46	N1	O1	Unknown	no	cyclic	1.411(2)	1
47	N3	H1N	Unknown	no	acyclic	0.84(2)	1
48	N3	H2N	Unknown	no	acyclic	0.84(3)	1

Symmetry

Number	Symm. Op.	Description	Detailed Description	Order	Type
1	x, y, z	Identity	Identity	1	1
2	-x, 1/2+y, 1/2-z	Screw axis (2-fold)	2-fold screw axis with direction [0, 1, 0] at 0, y, 1/4 with screw component [0, 1/2, 0]	2	2
3	-x, -y, -z	Inversion centre	Inversion at [0, 0, 0]	2	-1
4	x, 1/2-y, 1/2+z	Glide plane	Glide plane perpendicular to [0, 1, 0] with glide component [0, 0, 1/2]	2	-2

Angles

Number	Atom1	Atom2	Atom3	Angle
1	H1	C1	C2	108.8
2	H1	C1	C9	108.8
3	H1	C1	O1	108.8
4	C2	C1	C9	117.3(1)
5	C2	C1	O1	106.1(1)
6	C9	C1	O1	106.8(1)
7	C1	C2	H2A	109.9
8	C1	C2	H2B	110.0
9	C1	C2	N2	108.6(1)
10	H2A	C2	H2B	108.4
11	H2A	C2	N2	110.0
12	H2B	C2	N2	110.0
13	N1	C3	N2	120.0(1)
14	N1	C3	N3	118.3(2)
15	N2	C3	N3	121.5(2)
16	H4A	C4	H4B	107.8
17	H4A	C4	C5	109.0
18	H4A	C4	N1	109.0
19	H4B	C4	C5	109.0
20	H4B	C4	N1	109.0
21	C5	C4	N1	112.9(2)
22	C4	C5	H5	116.5
23	C4	C5	C6	126.9(2)
24	H5	C5	C6	116.6
25	C5	C6	C7	125.6(2)
26	C5	C6	C8	119.7(2)

27	C7	C6	C8	114.7(2)
28	C6	C7	H7A	109.5
29	C6	C7	H7B	109.4
30	C6	C7	H7C	109.4
31	H7A	C7	H7B	109.5
32	H7A	C7	H7C	109.4
33	H7B	C7	H7C	109.5
34	C6	C8	H8A	109.5
35	C6	C8	H8B	109.5
36	C6	C8	H8C	109.4
37	H8A	C8	H8B	109.4
38	H8A	C8	H8C	109.5
39	H8B	C8	H8C	109.4
40	C1	C9	C10	123.1(2)
41	C1	C9	C11	113.8(2)
42	C10	C9	C11	123.0(2)
43	C9	C10	H10A	119.9
44	C9	C10	H10B	120.0
45	H10A	C10	H10B	120.1
46	C9	C11	H11A	109.5
47	C9	C11	H11B	109.4
48	C9	C11	H11C	109.5
49	H11A	C11	H11B	109.5
50	H11A	C11	H11C	109.5
51	H11B	C11	H11C	109.5
52	H12A	C12	H12B	107.9
53	H12A	C12	C13	109.1
54	H12A	C12	N2	109.2
55	H12B	C12	C13	109.2
56	H12B	C12	N2	109.1
57	C13	C12	N2	112.2(2)
58	C12	C13	H13	117.0
59	C12	C13	C14	125.9(2)
60	H13	C13	C14	117.0
61	C13	C14	C15	124.8(2)
62	C13	C14	C16	121.0(2)
63	C15	C14	C16	114.1(2)
64	C14	C15	H15A	109.4
65	C14	C15	H15B	109.5
66	C14	C15	H15C	109.4
67	H15A	C15	H15B	109.5
68	H15A	C15	H15C	109.5
69	H15B	C15	H15C	109.5
70	C14	C16	H16A	109.5

71	C14	C16	H16B	109.5
72	C14	C16	H16C	109.5
73	H16A	C16	H16B	109.5
74	H16A	C16	H16C	109.4
75	H16B	C16	H16C	109.4
76	C3	N1	C4	123.8(1)
77	C3	N1	O1	115.6(1)
78	C4	N1	O1	111.5(1)
79	C2	N2	C3	122.0(1)
80	C2	N2	C12	116.5(1)
81	C3	N2	C12	119.9(1)
82	C3	N3	H1N	120(1)
83	C3	N3	H2N	121(2)
84	H1N	N3	H2N	119(2)
85	C1	O1	N1	109.6(1)

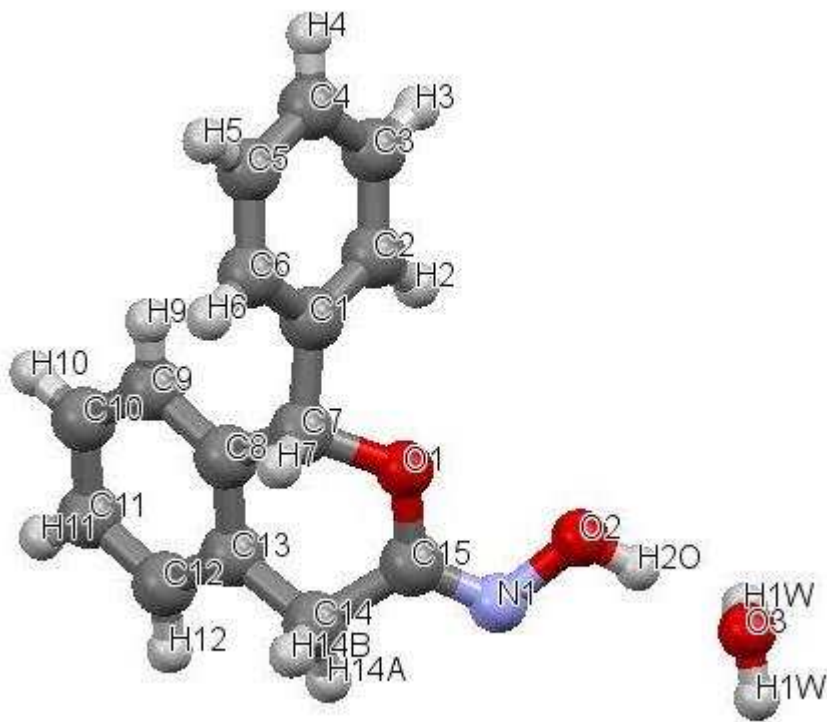
Torsions

Number	Atom1	Atom2	Atom3	Atom4	Torsion
1	H1	C1	C2	H2A	52.3
2	H1	C1	C2	H2B	171.5
3	H1	C1	C2	N2	-68.1
4	C9	C1	C2	H2A	-71.7
5	C9	C1	C2	H2B	47.5
6	C9	C1	C2	N2	168.0(1)
7	O1	C1	C2	H2A	169.2
8	O1	C1	C2	H2B	-71.6
9	O1	C1	C2	N2	48.8(2)
10	H1	C1	C9	C10	-132.9
11	H1	C1	C9	C11	45.3
12	C2	C1	C9	C10	-8.9(3)
13	C2	C1	C9	C11	169.3(2)
14	O1	C1	C9	C10	109.8(2)
15	O1	C1	C9	C11	-71.9(2)
16	H1	C1	O1	N1	47.2
17	C2	C1	O1	N1	-69.7(2)
18	C9	C1	O1	N1	164.5(1)
19	C1	C2	N2	C3	-5.2(2)
20	C1	C2	N2	C12	160.5(1)
21	H2A	C2	N2	C3	-125.5
22	H2A	C2	N2	C12	40.2
23	H2B	C2	N2	C3	115.2
24	H2B	C2	N2	C12	-79.1
25	N2	C3	N1	C4	147.9(2)
26	N2	C3	N1	O1	3.7(2)

27	N3	C3	N1	C4	-36.8(2)
28	N3	C3	N1	O1	179.0(1)
29	N1	C3	N2	C2	-23.7(2)
30	N1	C3	N2	C12	171.1(2)
31	N3	C3	N2	C2	161.1(2)
32	N3	C3	N2	C12	-4.1(2)
33	N1	C3	N3	H1N	168(2)
34	N1	C3	N3	H2N	-6(2)
35	N2	C3	N3	H1N	-17(2)
36	N2	C3	N3	H2N	169(2)
37	H4A	C4	C5	H5	177.7
38	H4A	C4	C5	C6	-2.3
39	H4B	C4	C5	H5	-64.9
40	H4B	C4	C5	C6	115.1
41	N1	C4	C5	H5	56.4
42	N1	C4	C5	C6	-123.6(2)
43	H4A	C4	N1	C3	162.2
44	H4A	C4	N1	O1	-52.3
45	H4B	C4	N1	C3	44.8
46	H4B	C4	N1	O1	-169.7
47	C5	C4	N1	C3	-76.5(2)
48	C5	C4	N1	O1	69.0(2)
49	C4	C5	C6	C7	-0.4(4)
50	C4	C5	C6	C8	-179.2(2)
51	H5	C5	C6	C7	179.6
52	H5	C5	C6	C8	0.8
53	C5	C6	C7	H7A	7.2
54	C5	C6	C7	H7B	-112.8
55	C5	C6	C7	H7C	127.1
56	C8	C6	C7	H7A	-174.0
57	C8	C6	C7	H7B	66.0
58	C8	C6	C7	H7C	-54.1
59	C5	C6	C8	H8A	-2.6
60	C5	C6	C8	H8B	-122.6
61	C5	C6	C8	H8C	117.5
62	C7	C6	C8	H8A	178.5
63	C7	C6	C8	H8B	58.5
64	C7	C6	C8	H8C	-61.4
65	C1	C9	C10	H10A	0.0
66	C1	C9	C10	H10B	-180.0
67	C11	C9	C10	H10A	-178.0
68	C11	C9	C10	H10B	1.9
69	C1	C9	C11	H11A	177.1
70	C1	C9	C11	H11B	57.1

71	C1	C9	C11	H11C	-62.9
72	C10	C9	C11	H11A	-4.6
73	C10	C9	C11	H11B	-124.7
74	C10	C9	C11	H11C	115.3
75	H12A	C12	C13	H13	173.9
76	H12A	C12	C13	C14	-6.1
77	H12B	C12	C13	H13	-68.4
78	H12B	C12	C13	C14	111.7
79	N2	C12	C13	H13	52.7
80	N2	C12	C13	C14	-127.2(2)
81	H12A	C12	N2	C2	-81.7
82	H12A	C12	N2	C3	84.3
83	H12B	C12	N2	C2	160.6
84	H12B	C12	N2	C3	-33.4
85	C13	C12	N2	C2	39.4(2)
86	C13	C12	N2	C3	-154.5(2)
87	C12	C13	C14	C15	3.9(4)
88	C12	C13	C14	C16	-174.3(2)
89	H13	C13	C14	C15	-176.1
90	H13	C13	C14	C16	5.7
91	C13	C14	C15	H15A	-111.8
92	C13	C14	C15	H15B	128.2
93	C13	C14	C15	H15C	8.2
94	C16	C14	C15	H15A	66.5
95	C16	C14	C15	H15B	-53.5
96	C16	C14	C15	H15C	-173.4
97	C13	C14	C16	H16A	-9.2
98	C13	C14	C16	H16B	-129.2
99	C13	C14	C16	H16C	110.8
100	C15	C14	C16	H16A	172.4
101	C15	C14	C16	H16B	52.3
102	C15	C14	C16	H16C	-67.7
103	C3	N1	O1	C1	43.2(2)
104	C4	N1	O1	C1	-105.2(1)

Appendix IV. Crystallographic data and structure refinement parameters of cpd 102



Formula: 2(C₁₅ H₁₃ N O₂),H₂ O
 Space group: P b c n (60)
 Cell lengths: **a** 16.1722(9) **b** 22.6903(13) **c** 6.9291(3)
 Cell Angles: **a** 90 **b** 90 **g** 90
 Cell Volume: 2542.65
Z: 4 **Z'**: 0
 R-factor (%): 8.36

Atoms

Number	Label	Charge	SybylType	Xfrac + ESD	Yfrac + ESD	Zfrac + ESD	Symm. op.
1	C1	0	C.2	0.17894(16)	0.29276(13)	0.3331(4)	x,y,z
2	C2	0	C.2	0.15250(17)	0.30886(13)	0.5164(4)	x,y,z
3	H2	0	H	0.1718	0.3445	0.5728	x,y,z
4	C3	0	C.2	0.09828(19)	0.27323(15)	0.6169(5)	x,y,z
5	H3	0	H	0.0811	0.2841	0.7431	x,y,z
6	C4	0	C.2	0.0690(2)	0.22198(15)	0.5350(5)	x,y,z
7	H4	0	H	0.0308	0.1979	0.6032	x,y,z
8	C5	0	C.2	0.09559(18)	0.20579(14)	0.3535(5)	x,y,z
9	H5	0	H	0.0755	0.1705	0.2967	x,y,z
10	C6	0	C.2	0.15113(17)	0.24049(13)	0.2537(5)	x,y,z

11	H6	0	H	0.1703	0.2284	0.1303	x,y,z
12	C7	0	C.3	0.23099(17)	0.33295(13)	0.2126(4)	x,y,z
13	H7	0	H	0.2616	0.3086	0.1159	x,y,z
14	C8	0	C.2	0.18213(19)	0.37932(13)	0.1059(4)	x,y,z
15	C9	0	C.2	0.0973(2)	0.37573(15)	0.0761(5)	x,y,z
16	H9	0	H	0.0668	0.3436	0.1274	x,y,z
17	C10	0	C.2	0.0575(2)	0.41903(17)	-0.0283(6)	x,y,z
18	H10	0	H	-0.0005	0.4165	-0.0494	x,y,z
19	C11	0	C.2	0.1012(3)	0.46589(17)	-0.1019(6)	x,y,z
20	H11	0	H	0.0735	0.4954	-0.1746	x,y,z
21	C12	0	C.2	0.1854(3)	0.47006(16)	-0.0700(5)	x,y,z
22	H12	0	H	0.2153	0.5029	-0.1184	x,y,z
23	C13	0	C.2	0.2262(2)	0.42654(14)	0.0319(4)	x,y,z
24	C14	0	C.3	0.3170(2)	0.42742(15)	0.0711(5)	x,y,z
25	H14A	0	H	0.3384	0.4680	0.0545	x,y,z
26	H14B	0	H	0.3457	0.4016	-0.0225	x,y,z
27	C15	0	C.2	0.33474(18)	0.40663(13)	0.2726(5)	x,y,z
28	N1	0	N.2	0.38840(16)	0.43299(12)	0.3736(4)	x,y,z
29	O1	0	O.3	0.29140(12)	0.36058(9)	0.3415(3)	x,y,z
30	O2	0	O.3	0.39803(15)	0.40761(11)	0.5558(4)	x,y,z
31	H2O	0	H	0.434(2)	0.4293(15)	0.623(5)	x,y,z
32	O3	0	O.3	0.5000	0.48223(14)	0.7500	x,y,z
33	H1W	0	H	0.463(2)	0.5076(15)	0.797(5)	x,y,z
34	H1W	0	H	0.537(2)	0.5076(15)	0.703(5)	1-x,y,1.5-z

Bonds

Number	Atom1	Atom2	Type	Polymeric	Cyclicity	Length	SybylType
1	C1	C2	Unknown	no	cyclic	1.389(4)	un
2	C1	C6	Unknown	no	cyclic	1.383(4)	un
3	C1	C7	Unknown	no	acyclic	1.496(4)	1
4	C2	H2	Unknown	no	acyclic	0.951	1
5	C2	C3	Unknown	no	cyclic	1.381(4)	un
6	C3	H3	Unknown	no	acyclic	0.950	1
7	C3	C4	Unknown	no	cyclic	1.378(5)	un
8	C4	H4	Unknown	no	acyclic	0.951	1
9	C4	C5	Unknown	no	cyclic	1.379(5)	un
10	C5	H5	Unknown	no	acyclic	0.950	1
11	C5	C6	Unknown	no	cyclic	1.380(4)	un
12	C6	H6	Unknown	no	acyclic	0.950	1
13	C7	H7	Unknown	no	acyclic	1.000	1
14	C7	C8	Unknown	no	cyclic	1.509(4)	1
15	C7	O1	Unknown	no	cyclic	1.465(3)	1
16	C8	C9	Unknown	no	cyclic	1.390(4)	un
17	C8	C13	Unknown	no	cyclic	1.385(4)	un

18	C9	H9	Unknown	no	acyclic	0.949	1
19	C9	C10	Unknown	no	cyclic	1.379(5)	un
20	C10	H10	Unknown	no	acyclic	0.951	1
21	C10	C11	Unknown	no	cyclic	1.375(6)	un
22	C11	H11	Unknown	no	acyclic	0.950	1
23	C11	C12	Unknown	no	cyclic	1.383(7)	un
24	C12	H12	Unknown	no	acyclic	0.949	1
25	C12	C13	Unknown	no	cyclic	1.382(5)	un
26	C13	C14	Unknown	no	cyclic	1.493(5)	1
27	C14	H14A	Unknown	no	acyclic	0.990	1
28	C14	H14B	Unknown	no	acyclic	0.990	1
29	C14	C15	Unknown	no	cyclic	1.501(5)	1
30	C15	N1	Unknown	no	acyclic	1.265(4)	un
31	C15	O1	Unknown	no	cyclic	1.346(4)	1
32	N1	O2	Unknown	no	acyclic	1.396(4)	1
33	O2	H2O	Unknown	no	acyclic	0.89(3)	1
34	O3	H1W	Unknown	no	acyclic	0.89	1
35	O3	H1W	Unknown	no	acyclic	0.89	1

Symmetry

Number	Symm. Op.	Description	Detailed Description	Order	Type
1	x,y,z	Identity	Identity	1	1
2	1/2+x, 1/2-y, -z	Screw axis (2-fold)	2-fold screw axis with direction [1, 0, 0] at x, 1/4, 0 with screw component [1/2, 0, 0]	2	2
3	-x, y, 1/2-z	Rotation axis (2-fold)	2-fold rotation axis with direction [0, 1, 0] at 0, y, 1/4	2	2
4	1/2-x, 1/2-y, 1/2+z	Screw axis (2-fold)	2-fold screw axis with direction [0, 0, 1] at 1/4, 1/4, z with screw component [0, 0, 1/2]	2	2
5	-x, -y, -z	Inversion centre	Inversion at [0, 0, 0]	2	-1
6	1/2-x, 1/2+y, z	Glide plane	Glide plane perpendicular to [1, 0, 0] with glide component [0, 1/2, 0]	2	-2
7	x, -y, 1/2+z	Glide plane	Glide plane perpendicular to [0, 1, 0] with glide component [0, 0, 1/2]	2	-2
8	1/2+x, 1/2+y, 1/2-z	Glide plane	Glide plane perpendicular to [0, 0, 1] with glide component [1/2, 1/2, 0]	2	-2

Angles

Number	Atom1	Atom2	Atom3	Angle
1	C2	C1	C6	119.3(3)
2	C2	C1	C7	121.6(2)
3	C6	C1	C7	118.9(3)
4	C1	C2	H2	119.9
5	C1	C2	C3	120.2(3)
6	H2	C2	C3	119.9

7	C2	C3	H3	119.9
8	C2	C3	C4	120.3(3)
9	H3	C3	C4	119.8
10	C3	C4	H4	120.2
11	C3	C4	C5	119.6(3)
12	H4	C4	C5	120.2
13	C4	C5	H5	119.7
14	C4	C5	C6	120.5(3)
15	H5	C5	C6	119.7
16	C1	C6	C5	120.1(3)
17	C1	C6	H6	120.0
18	C5	C6	H6	119.9
19	C1	C7	H7	108.4
20	C1	C7	C8	113.8(2)
21	C1	C7	O1	107.2(2)
22	H7	C7	C8	108.4
23	H7	C7	O1	108.4
24	C8	C7	O1	110.5(2)
25	C7	C8	C9	123.3(3)
26	C7	C8	C13	116.8(3)
27	C9	C8	C13	119.9(3)
28	C8	C9	H9	120.2
29	C8	C9	C10	119.8(3)
30	H9	C9	C10	120.1
31	C9	C10	H10	119.9
32	C9	C10	C11	120.4(4)
33	H10	C10	C11	119.8
34	C10	C11	H11	120.0
35	C10	C11	C12	120.0(4)
36	H11	C11	C12	120.1
37	C11	C12	H12	119.9
38	C11	C12	C13	120.2(4)
39	H12	C12	C13	119.9
40	C8	C13	C12	119.8(3)
41	C8	C13	C14	116.7(3)
42	C12	C13	C14	123.6(3)
43	C13	C14	H14A	109.6
44	C13	C14	H14B	109.5
45	C13	C14	C15	110.7(3)
46	H14A	C14	H14B	108.1
47	H14A	C14	C15	109.5
48	H14B	C14	C15	109.5
49	C14	C15	N1	119.8(3)
50	C14	C15	O1	118.3(3)

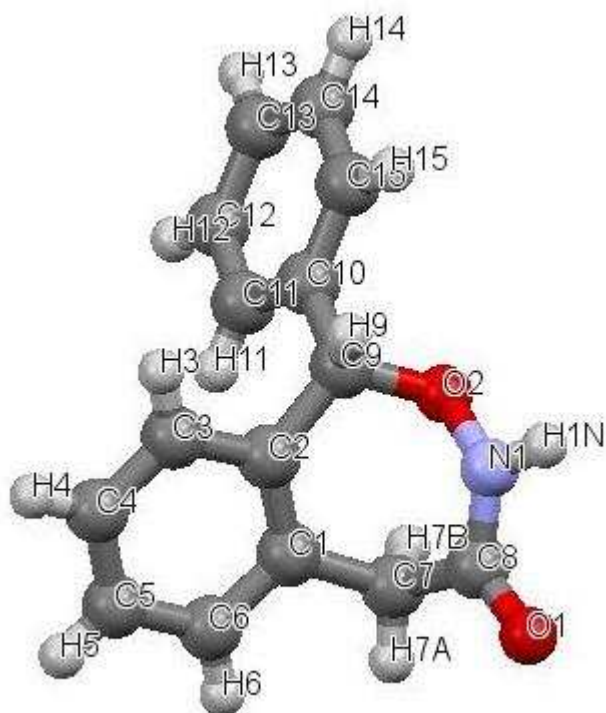
51	N1	C15	O1	121.9(3)
52	C15	N1	O2	112.4(3)
53	C7	O1	C15	117.6(2)
54	N1	O2	H2O	108(2)
55	H1W	O3	H1W	100

Torsions

Number	Atom1	Atom2	Atom3	Atom4	Torsion
1	C6	C1	C2	H2	179.3
2	C6	C1	C2	C3	-0.7(4)
3	C7	C1	C2	H2	-6.0
4	C7	C1	C2	C3	174.0(3)
5	C2	C1	C6	C5	2.1(4)
6	C2	C1	C6	H6	-177.8
7	C7	C1	C6	C5	-172.7(3)
8	C7	C1	C6	H6	7.3
9	C2	C1	C7	H7	157.2
10	C2	C1	C7	C8	-82.0(3)
11	C2	C1	C7	O1	40.4(3)
12	C6	C1	C7	H7	-28.1
13	C6	C1	C7	C8	92.7(3)
14	C6	C1	C7	O1	-144.9(3)
15	C1	C2	C3	H3	178.9
16	C1	C2	C3	C4	-1.0(5)
17	H2	C2	C3	H3	-1.0
18	H2	C2	C3	C4	179.0
19	C2	C3	C4	H4	-178.7
20	C2	C3	C4	C5	1.4(5)
21	H3	C3	C4	H4	1.3
22	H3	C3	C4	C5	-178.6
23	C3	C4	C5	H5	-180.0
24	C3	C4	C5	C6	-0.0(5)
25	H4	C4	C5	H5	0.1
26	H4	C4	C5	C6	-179.9
27	C4	C5	C6	C1	-1.7(5)
28	C4	C5	C6	H6	178.2
29	H5	C5	C6	C1	178.2
30	H5	C5	C6	H6	-1.8
31	C1	C7	C8	C9	-17.4(4)
32	C1	C7	C8	C13	164.2(3)
33	H7	C7	C8	C9	103.4
34	H7	C7	C8	C13	-75.1
35	O1	C7	C8	C9	-138.0(3)
36	O1	C7	C8	C13	43.5(3)

37	C1	C7	O1	C15	-167.8(2)
38	H7	C7	O1	C15	75.4
39	C8	C7	O1	C15	-43.3(3)
40	C7	C8	C9	H9	2.1
41	C7	C8	C9	C10	-177.9(3)
42	C13	C8	C9	H9	-179.5
43	C13	C8	C9	C10	0.5(5)
44	C7	C8	C13	C12	179.0(3)
45	C7	C8	C13	C14	-1.9(4)
46	C9	C8	C13	C12	0.5(5)
47	C9	C8	C13	C14	179.6(3)
48	C8	C9	C10	H10	179.6
49	C8	C9	C10	C11	-0.4(5)
50	H9	C9	C10	H10	-0.4
51	H9	C9	C10	C11	179.6
52	C9	C10	C11	H11	179.5
53	C9	C10	C11	C12	-0.6(6)
54	H10	C10	C11	H11	-0.6
55	H10	C10	C11	C12	179.4
56	C10	C11	C12	H12	-178.6
57	C10	C11	C12	C13	1.5(6)
58	H11	C11	C12	H12	1.4
59	H11	C11	C12	C13	-178.5
60	C11	C12	C13	C8	-1.5(5)
61	C11	C12	C13	C14	179.4(3)
62	H12	C12	C13	C8	178.6
63	H12	C12	C13	C14	-0.5
64	C8	C13	C14	H14A	-160.1
65	C8	C13	C14	H14B	81.5
66	C8	C13	C14	C15	-39.3(4)
67	C12	C13	C14	H14A	19.0
68	C12	C13	C14	H14B	-99.3
69	C12	C13	C14	C15	139.9(3)
70	C13	C14	C15	N1	-138.3(3)
71	C13	C14	C15	O1	40.6(4)
72	H14A	C14	C15	N1	-17.4
73	H14A	C14	C15	O1	161.5
74	H14B	C14	C15	N1	100.9
75	H14B	C14	C15	O1	-80.2
76	C14	C15	N1	O2	-179.2(3)
77	O1	C15	N1	O2	2.0(4)
78	C14	C15	O1	C7	1.4(4)
79	N1	C15	O1	C7	-179.7(3)
80	C15	N1	O2	H2O	-176(2)

Appendix V. Crystallographic data and structure refinement parameters of cpd 81



Formula: C₁₅ H₁₃ N O₂

Space group: P 2₁/c (14)

Cell lengths: **a** 5.6544(4) **b** 13.9616(9) **c** 15.2825(8)

Cell Angles: **a** 90 **b** 91.623(3) **g** 90

Cell Volume: 1205.98

Z: 4 **Z'**: 0

R-factor (%): 4.45

Atoms

Number	Label	Charge	SybylType	Xfrac + ESD	Yfrac + ESD	Zfrac + ESD	Symm. op.
1	C1	0	C.2	0.0901(2)	0.61428(9)	0.27821(7)	x,y,z
2	C2	0	C.2	0.2825(2)	0.58878(8)	0.22740(7)	x,y,z
3	C3	0	C.2	0.3534(2)	0.65005(9)	0.16084(8)	x,y,z
4	H3	0	H	0.4882	0.6341	0.1281	x,y,z
5	C4	0	C.2	0.2308(3)	0.73362(10)	0.14174(9)	x,y,z
6	H4	0	H	0.2811	0.7745	0.0962	x,y,z
7	C5	0	C.2	0.0353(3)	0.75715(10)	0.18922(9)	x,y,z
8	H5	0	H	-0.0530	0.8132	0.1751	x,y,z
9	C6	0	C.2	-0.0323(2)	0.69878(9)	0.25765(8)	x,y,z
10	H6	0	H	-0.1643	0.7165	0.2912	x,y,z

11	C7	0	C.3	0.0137(2)	0.55724(9)	0.35739(8)	x,y,z
12	H7A	0	H	-0.1140	0.5921	0.3869	x,y,z
13	H7B	0	H	-0.0499	0.4945	0.3378	x,y,z
14	C8	0	C.2	0.2183(2)	0.54141(8)	0.42157(7)	x,y,z
15	C9	0	C.3	0.4170(2)	0.49523(9)	0.23587(7)	x,y,z
16	H9	0	H	0.5902	0.5096	0.2397	x,y,z
17	C10	0	C.2	0.3699(2)	0.42640(9)	0.16056(8)	x,y,z
18	C11	0	C.2	0.1635(2)	0.42983(10)	0.10922(9)	x,y,z
19	H11	0	H	0.0496	0.4784	0.1192	x,y,z
20	C12	0	C.2	0.1222(3)	0.36257(11)	0.04328(9)	x,y,z
21	H12	0	H	-0.0194	0.3654	0.0084	x,y,z
22	C13	0	C.2	0.2871(3)	0.29165(11)	0.02850(9)	x,y,z
23	H13	0	H	0.2589	0.2457	-0.0165	x,y,z
24	C14	0	C.2	0.4921(3)	0.28771(11)	0.07909(9)	x,y,z
25	H14	0	H	0.6054	0.2390	0.0689	x,y,z
26	C15	0	C.2	0.5341(2)	0.35474(10)	0.14501(8)	x,y,z
27	H15	0	H	0.6760	0.3515	0.1797	x,y,z
28	N1	0	N.am	0.3990(2)	0.49119(8)	0.38976(7)	x,y,z
29	O1	0	O.2	0.22959(16)	0.57590(6)	0.49591(6)	x,y,z
30	O2	0	O.3	0.35434(17)	0.43952(6)	0.31206(5)	x,y,z
31	H1N	0	H	0.517(3)	0.4675(12)	0.4240(11)	x,y,z

Bonds

Number	Atom1	Atom2	Type	Polymeric	Cyclicity	Length	SybylType
1	C1	C2	Unknown	no	cyclic	1.400(2)	un
2	C1	C6	Unknown	no	cyclic	1.399(2)	un
3	C1	C7	Unknown	no	cyclic	1.521(2)	1
4	C2	C3	Unknown	no	cyclic	1.397(2)	un
5	C2	C9	Unknown	no	cyclic	1.515(2)	1
6	C3	H3	Unknown	no	acyclic	0.950	1
7	C3	C4	Unknown	no	cyclic	1.384(2)	un
8	C4	H4	Unknown	no	acyclic	0.950	1
9	C4	C5	Unknown	no	cyclic	1.379(2)	un
10	C5	H5	Unknown	no	acyclic	0.950	1
11	C5	C6	Unknown	no	cyclic	1.388(2)	un
12	C6	H6	Unknown	no	acyclic	0.950	1
13	C7	H7A	Unknown	no	acyclic	0.990	1
14	C7	H7B	Unknown	no	acyclic	0.990	1
15	C7	C8	Unknown	no	cyclic	1.512(2)	1
16	C8	N1	Unknown	no	cyclic	1.342(2)	un
17	C8	O1	Unknown	no	acyclic	1.234(1)	2
18	C9	H9	Unknown	no	acyclic	1.000	1
19	C9	C10	Unknown	no	acyclic	1.517(2)	1
20	C9	O2	Unknown	no	cyclic	1.452(1)	1

21	C10	C11	Unknown	no	cyclic	1.389(2)	un
22	C10	C15	Unknown	no	cyclic	1.390(2)	un
23	C11	H11	Unknown	no	acyclic	0.950	1
24	C11	C12	Unknown	no	cyclic	1.392(2)	un
25	C12	H12	Unknown	no	acyclic	0.950	1
26	C12	C13	Unknown	no	cyclic	1.383(2)	un
27	C13	H13	Unknown	no	acyclic	0.951	1
28	C13	C14	Unknown	no	cyclic	1.376(2)	un
29	C14	H14	Unknown	no	acyclic	0.950	1
30	C14	C15	Unknown	no	cyclic	1.391(2)	un
31	C15	H15	Unknown	no	acyclic	0.950	1
32	N1	O2	Unknown	no	cyclic	1.406(1)	1
33	N1	H1N	Unknown	no	acyclic	0.90(2)	1

Symmetry

Number	Symm. Op.	Description	Detailed Description	Order	Type
1	x ,y ,z	Identity	Identity	1	1
2	-x, 1/2+y, 1/2-z	Screw axis (2-fold)	2-fold screw axis with direction [0, 1, 0] at 0, y, 1/4 with screw component [0, 1/2, 0]	2	2
3	-x, -y, -z	Inversion centre	Inversion at [0, 0, 0]	2	-1
4	x, 1/2-y, 1/2+z	Glide plane	Glide plane perpendicular to [0, 1, 0] with glide component [0, 0, 1/2]	2	-2

Angles

Number	Atom1	Atom2	Atom3	Angle
1	C2	C1	C6	118.5(1)
2	C2	C1	C7	123.4(1)
3	C6	C1	C7	118.0(1)
4	C1	C2	C3	119.5(1)
5	C1	C2	C9	124.6(1)
6	C3	C2	C9	115.9(1)
7	C2	C3	H3	119.4
8	C2	C3	C4	121.2(1)
9	H3	C3	C4	119.4
10	C3	C4	H4	120.2
11	C3	C4	C5	119.6(1)
12	H4	C4	C5	120.2
13	C4	C5	H5	120.1
14	C4	C5	C6	119.9(1)
15	H5	C5	C6	120.0
16	C1	C6	C5	121.3(1)
17	C1	C6	H6	119.3
18	C5	C6	H6	119.4

19	C1	C7	H7A	109.4
20	C1	C7	H7B	109.4
21	C1	C7	C8	111.3(1)
22	H7A	C7	H7B	108.0
23	H7A	C7	C8	109.3
24	H7B	C7	C8	109.4
25	C7	C8	N1	114.7(1)
26	C7	C8	O1	124.0(1)
27	N1	C8	O1	121.2(1)
28	C2	C9	H9	108.7
29	C2	C9	C10	113.8(1)
30	C2	C9	O2	113.38(9)
31	H9	C9	C10	108.8
32	H9	C9	O2	108.7
33	C10	C9	O2	103.14(9)
34	C9	C10	C11	122.2(1)
35	C9	C10	C15	118.8(1)
36	C11	C10	C15	118.9(1)
37	C10	C11	H11	119.8
38	C10	C11	C12	120.4(1)
39	H11	C11	C12	119.8
40	C11	C12	H12	120.0
41	C11	C12	C13	120.1(1)
42	H12	C12	C13	120.0
43	C12	C13	H13	120.1
44	C12	C13	C14	119.9(1)
45	H13	C13	C14	120.1
46	C13	C14	H14	119.8
47	C13	C14	C15	120.3(1)
48	H14	C14	C15	119.9
49	C10	C15	C14	120.5(1)
50	C10	C15	H15	119.8
51	C14	C15	H15	119.8
52	C8	N1	O2	117.0(1)
53	C8	N1	H1N	123(1)
54	O2	N1	H1N	115(1)
55	C9	O2	N1	111.11(9)

Torsions

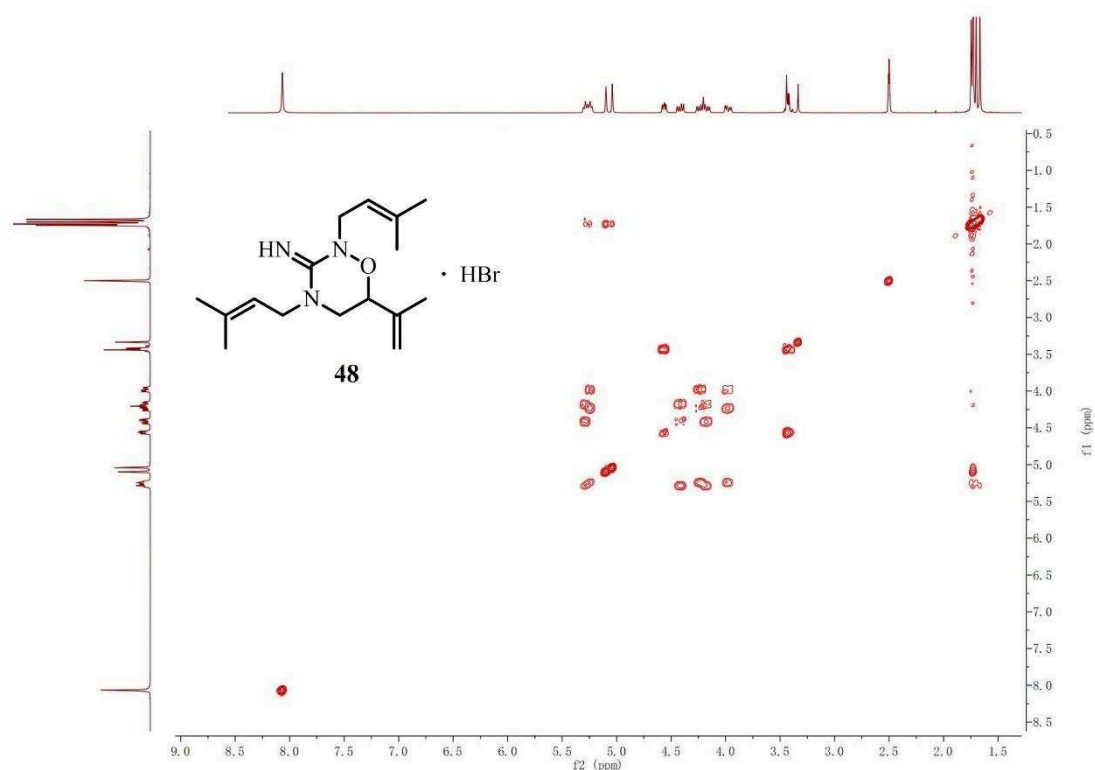
Number	Atom1	Atom2	Atom3	Atom4	Torsion
1	C6	C1	C2	C3	3.0(2)
2	C6	C1	C2	C9	-173.8(1)
3	C7	C1	C2	C3	-174.1(1)
4	C7	C1	C2	C9	9.1(2)

5	C2	C1	C6	C5	-0.7(2)
6	C2	C1	C6	H6	179.3
7	C7	C1	C6	C5	176.6(1)
8	C7	C1	C6	H6	-3.5
9	C2	C1	C7	H7A	173.8
10	C2	C1	C7	H7B	-68.1
11	C2	C1	C7	C8	52.9(1)
12	C6	C1	C7	H7A	-3.3
13	C6	C1	C7	H7B	114.8
14	C6	C1	C7	C8	-124.3(1)
15	C1	C2	C3	H3	177.2
16	C1	C2	C3	C4	-2.8(2)
17	C9	C2	C3	H3	-5.7
18	C9	C2	C3	C4	174.3(1)
19	C1	C2	C9	H9	-130.8
20	C1	C2	C9	C10	107.8(1)
21	C1	C2	C9	O2	-9.8(2)
22	C3	C2	C9	H9	52.3
23	C3	C2	C9	C10	-69.1(1)
24	C3	C2	C9	O2	173.4(1)
25	C2	C3	C4	H4	-179.9
26	C2	C3	C4	C5	0.1(2)
27	H3	C3	C4	H4	0.1
28	H3	C3	C4	C5	-179.9
29	C3	C4	C5	H5	-177.7
30	C3	C4	C5	C6	2.2(2)
31	H4	C4	C5	H5	2.3
32	H4	C4	C5	C6	-177.8
33	C4	C5	C6	C1	-1.9(2)
34	C4	C5	C6	H6	178.1
35	H5	C5	C6	C1	178.0
36	H5	C5	C6	H6	-1.9
37	C1	C7	C8	N1	-61.6(1)
38	C1	C7	C8	O1	114.2(1)
39	H7A	C7	C8	N1	177.4
40	H7A	C7	C8	O1	-6.8
41	H7B	C7	C8	N1	59.4
42	H7B	C7	C8	O1	-124.9
43	C7	C8	N1	O2	-15.9(1)
44	C7	C8	N1	H1N	-168(1)
45	O1	C8	N1	O2	168.2(1)
46	O1	C8	N1	H1N	16(1)
47	C2	C9	C10	C11	-24.2(2)
48	C2	C9	C10	C15	158.8(1)

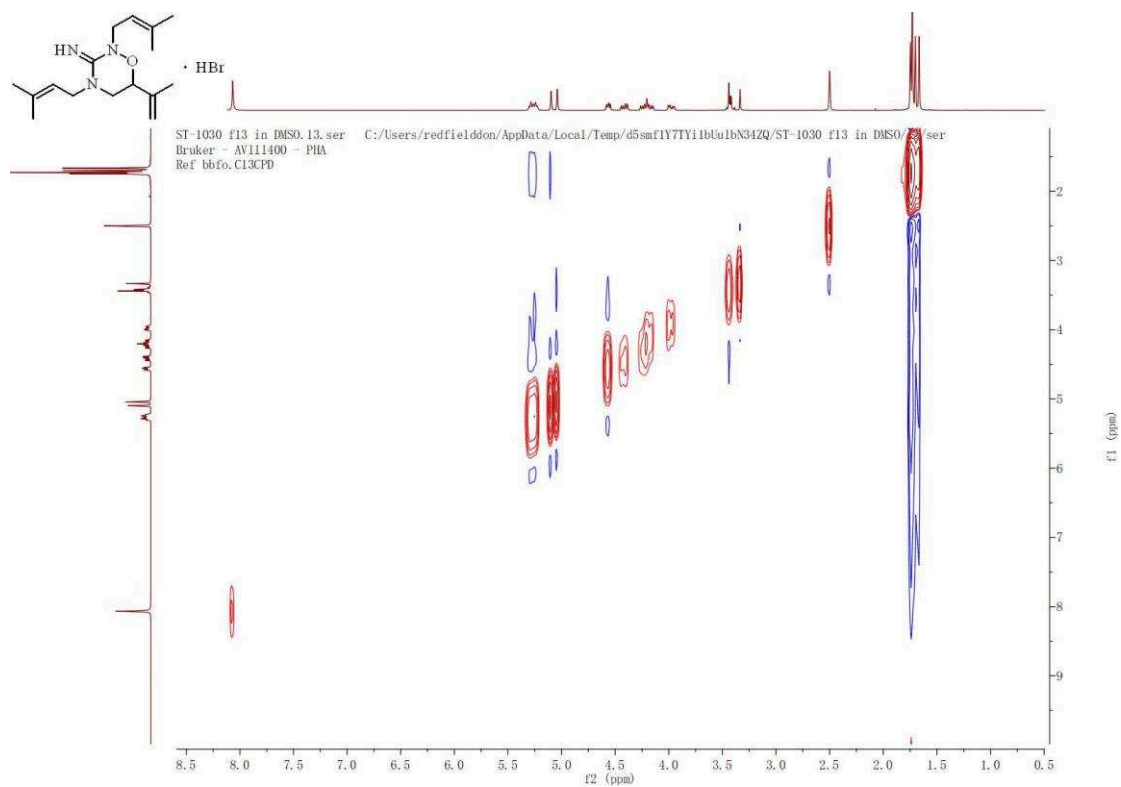
49	H9	C9	C10	C11	-145.6
50	H9	C9	C10	C15	37.4
51	O2	C9	C10	C11	99.1(1)
52	O2	C9	C10	C15	-77.9(1)
53	C2	C9	O2	N1	-59.4(1)
54	H9	C9	O2	N1	61.6
55	C10	C9	O2	N1	176.97(9)
56	C9	C10	C11	H11	2.9
57	C9	C10	C11	C12	-177.0(1)
58	C15	C10	C11	H11	179.9
59	C15	C10	C11	C12	-0.0(2)
60	C9	C10	C15	C14	177.1(1)
61	C9	C10	C15	H15	-2.8
62	C11	C10	C15	C14	0.0(2)
63	C11	C10	C15	H15	-179.9
64	C10	C11	C12	H12	-180.0
65	C10	C11	C12	C13	0.0(2)
66	H11	C11	C12	H12	0.1
67	H11	C11	C12	C13	-179.9
68	C11	C12	C13	H13	180.0
69	C11	C12	C13	C14	-0.0(2)
70	H12	C12	C13	H13	-0.0
71	H12	C12	C13	C14	180.0
72	C12	C13	C14	H14	-180.0
73	C12	C13	C14	C15	0.0(2)
74	H13	C13	C14	H14	0.1
75	H13	C13	C14	C15	-180.0
76	C13	C14	C15	C10	-0.0(2)
77	C13	C14	C15	H15	179.9
78	H14	C14	C15	C10	180.0
79	H14	C14	C15	H15	-0.1
80	C8	N1	O2	C9	93.6(1)
81	H1N	N1	O2	C9	-112(1)

Appendix VI. 2D NMRs of cpd 48

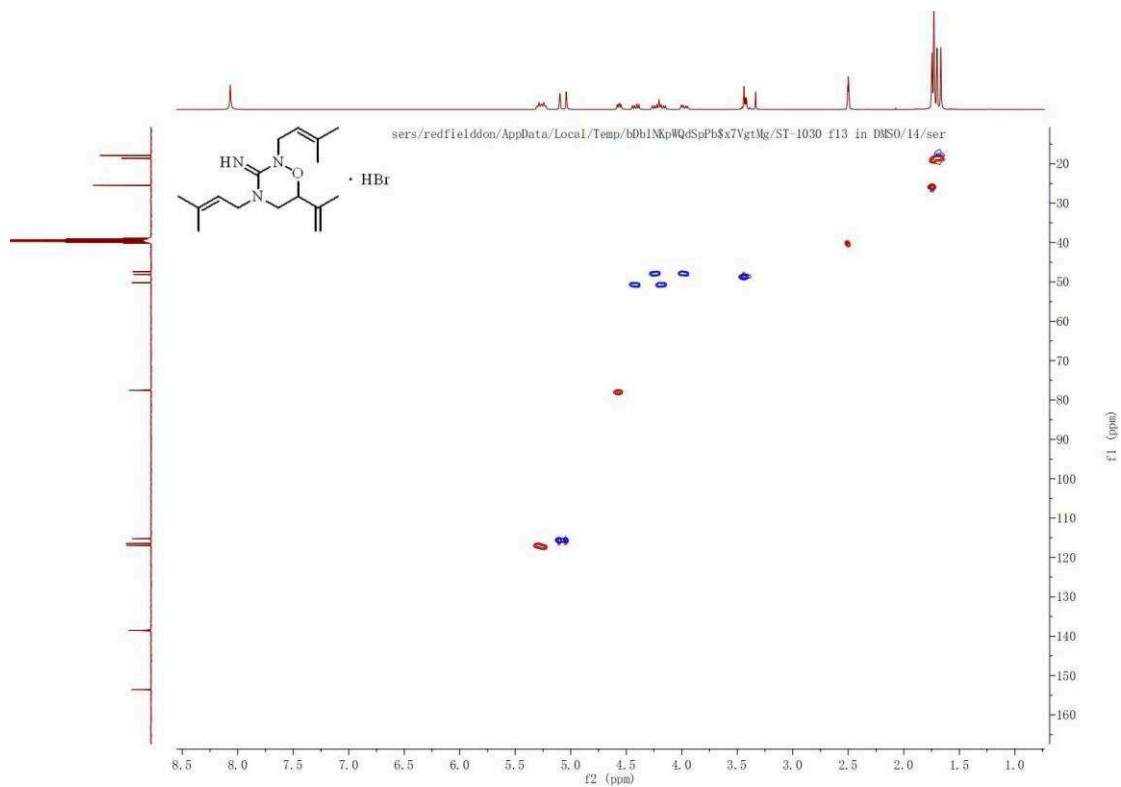
1. COSY in DMSO- d^6



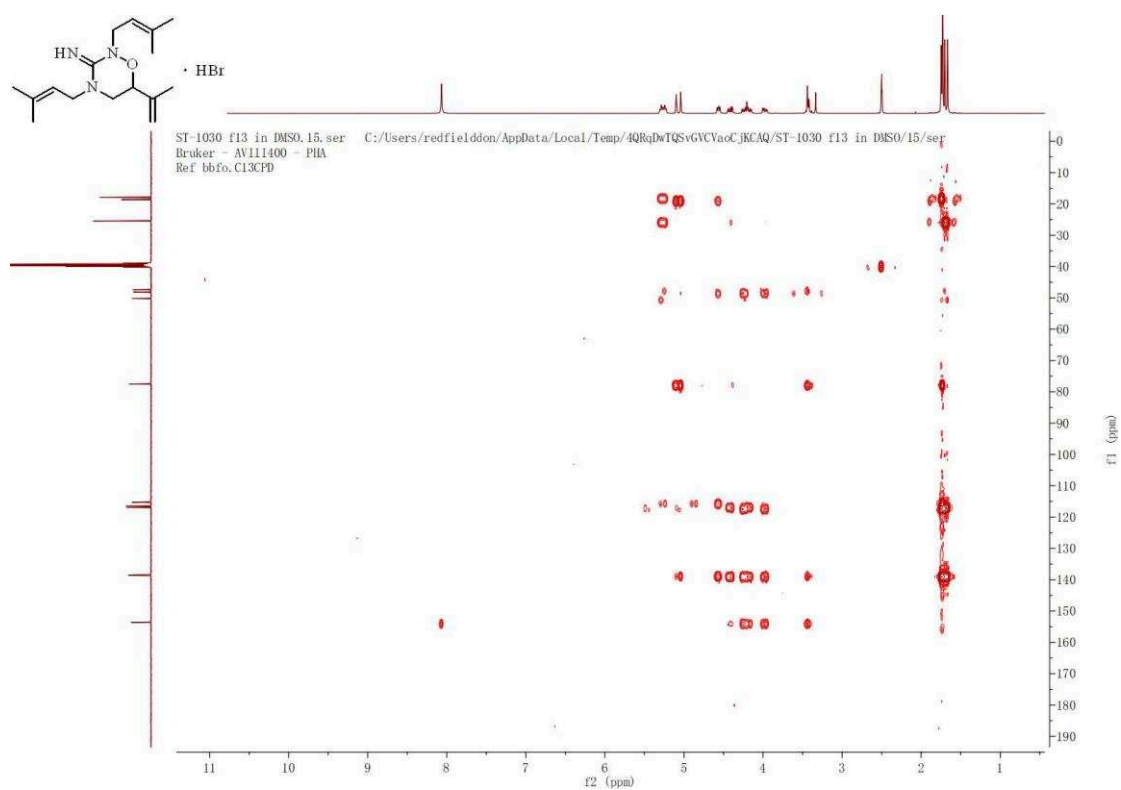
2. NOESY in DMSO- d^6



3. HSQC in DMSO- d^6

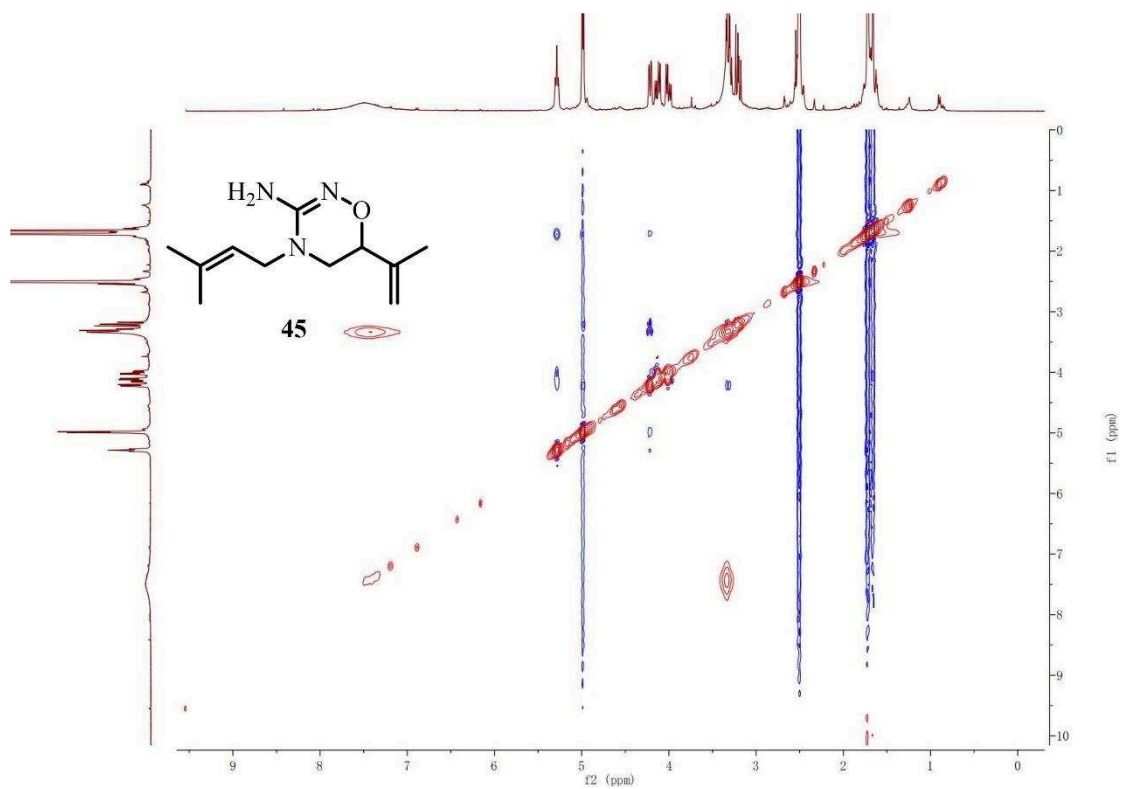


4. HMBC in DMSO- d^6

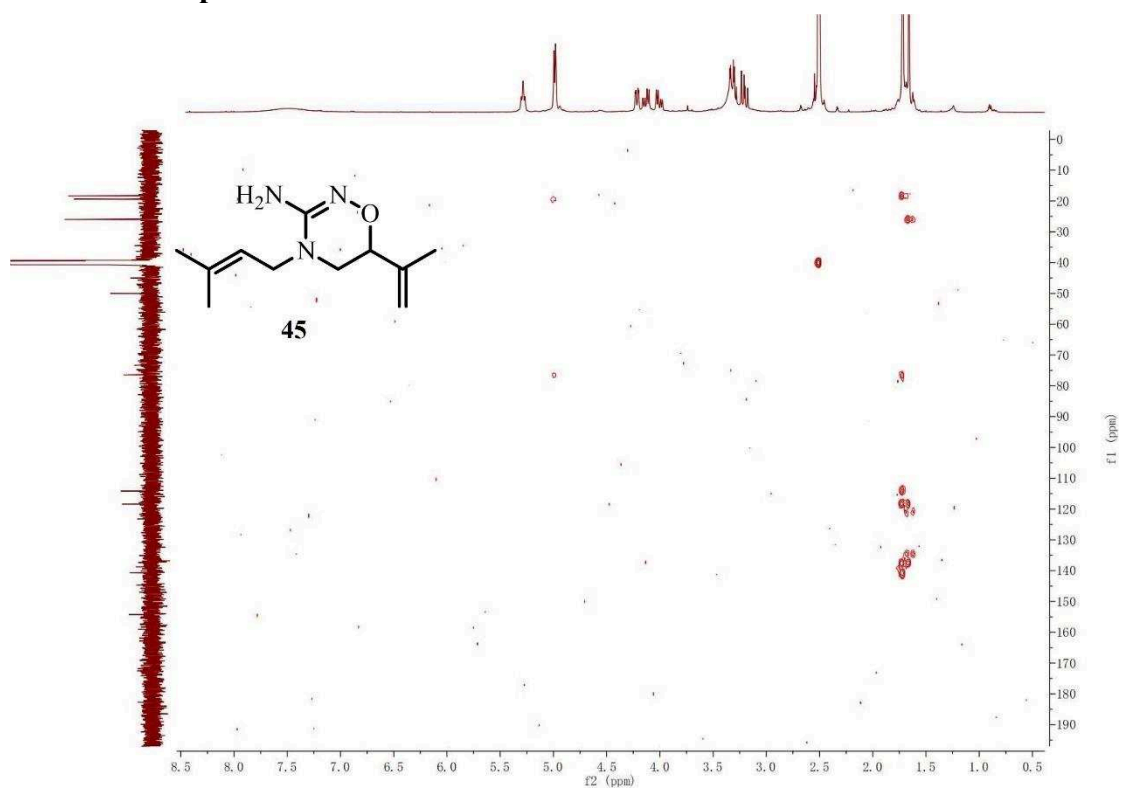


Appendix VII. NOESY and HMBC of cpd 45 and 43

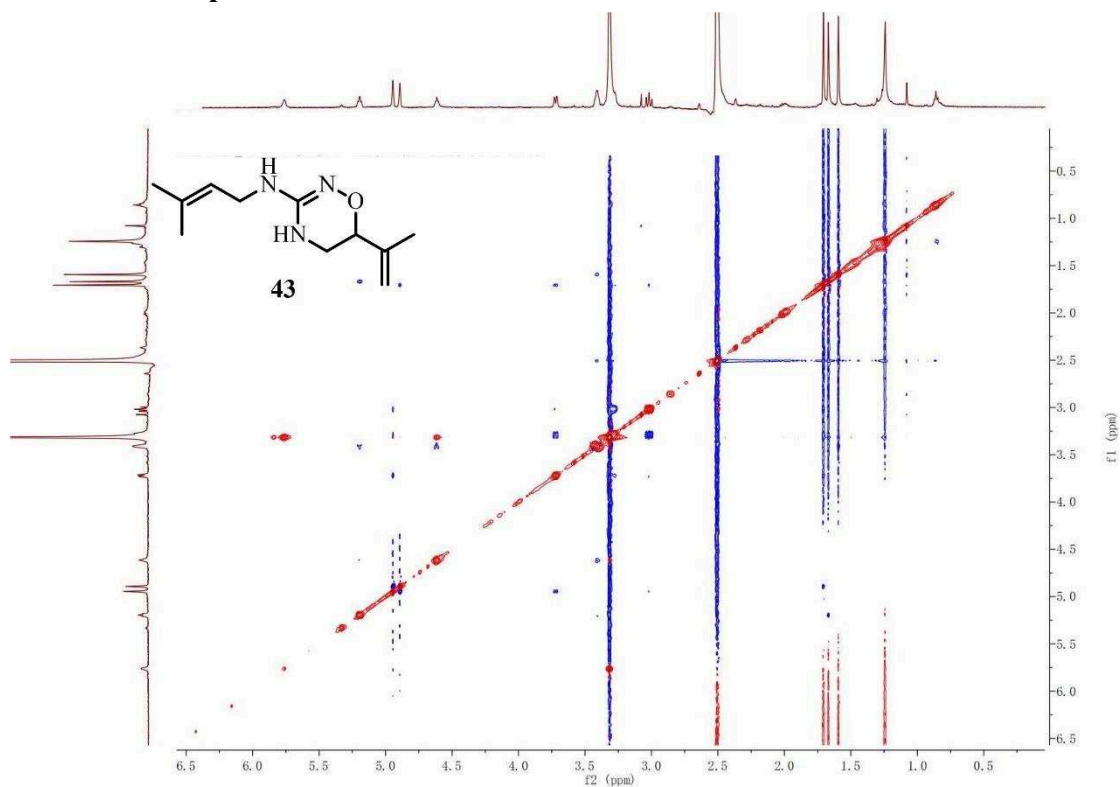
1. NOESY of cpd 45 in DMSO-*d*⁶



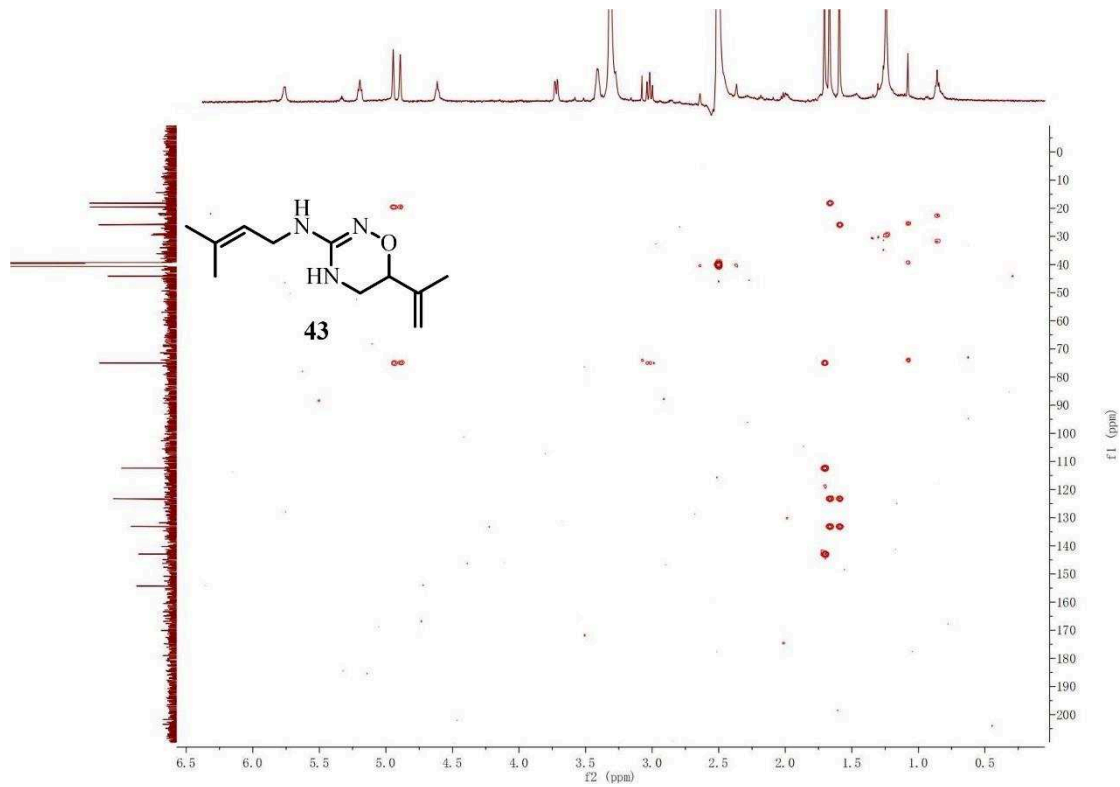
2. HMBC of cpd 45 in DMSO-*d*⁶



3. NOESY of cpd 43 in DMSO-*d*⁶



4. HMBC of cpd 43 in DMSO-*d*⁶



Appendix VIII. Dioxygenation of styrenes with molecular oxygen in water



Dioxygenation of styrenes with molecular oxygen in water

Shuang-Qi Tang, An-Ping Wang, Martine Schmitt, Frédéric Bihel*

Laboratoire d'Innovation thérapeutique, UMR 7200, CNRS, Université de Strasbourg, Faculté de Pharmacie, 74 route du Rhin, BP 60024, 67401 Illkirch, France

ARTICLE INFO

Article history:

Received 14 December 2017

Revised 23 February 2018

Accepted 2 March 2018

Available online 3 March 2018

Keywords:

Alkene

Oxidation

N-hydroxyphthalimide

Triton X-100

Water

ABSTRACT

Employing Triton X-100 as a surfactant, the *tert*-butyl hydroperoxide-mediated dioxygenation of styrene with molecular oxygen and *N*-hydroxyphthalimide was achieved in water at room temperature, providing the corresponding dioxygenated products in 9–93% yield. This facile method is eco-friendly, feasible on gram scale, and applicable to a wide range of styrene derivatives with a variety of functional groups.

© 2018 Elsevier Ltd. All rights reserved.

The environmental impact of the chemical industry is a major issue; approximately 80% of the chemical waste from a reaction mixture corresponds to organic solvents.¹ One of the main research fields is the development of alternatives to organic solvents, with expected outputs in terms of health, safety and environmental impacts. Solvent-free alternatives represent the best solution, however, most organic reactions require a medium to enable matter and heat transfer. Ionic liquids, supercritical media and other non-conventional media have been described as efficient alternatives to conventional organic solvents, but the use of water appears to be one of the best solutions in terms of safety and environmental impact.² Unfortunately, most organic reactants have poor solubility in water, leading to low yields and poor reaction rate. The development of organic synthesis in aqueous medium using surfactants represents an efficient ecofriendly strategy.³ Indeed, due to their amphiphilic nature, surfactants in water undergo spontaneous self-assembly into micelles, which act as nanoreactors, and their hydrophobic cores play the role of reaction vessels in which organic transformations involving water-insoluble reagents can occur. By using versatile nonionic surfactants, such as TPGS-750-M, a set of chemical transformations has been developed under micellar conditions, including nucleophilic substitution,⁴ oxidation,⁵ reduction,^{6,7} olefin metathesis,⁸ and Pd-catalyzed cross-coupling,⁹ as well as solution phase peptide synthesis in water.¹⁰ Recently, our group developed an efficient and versatile method for the Buchwald-Hartwig cross-coupling reaction and the Ullmann-type amination reaction in water with the assistance of

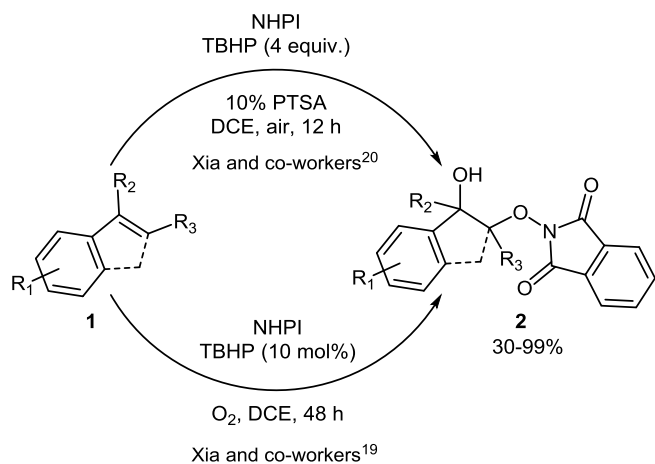
the non-ionic surfactant TPGS-750-M.^{11–14} The adoption of surfactants in these reactions resulted in significant benefits across the entire synthetic route, not just from an environment standpoint, but also from an economic and productivity perspective.¹⁵

1,2-Dioxygenated structures are present in many biologically active molecules.^{16–18} In view of the importance of such structures, Xia and co-workers have developed efficient radical methods for styrene 1,2-dioxygenation using *N*-hydroxyphthalimide (NHPI, Scheme 1).^{19,20} Although these methods furnished **2** in good to excellent yields, optimal yields were obtained in dichloroethane (DCE), a chlorinated organic solvent which is a known human carcinogen and highly hazardous for the environment. Accordingly, the development of an “*in water*” method is desirable to avoid the use of such a toxic solvent. Inspired by the work of Xia and co-workers, and in continuation of our efforts in the development of reactions in water,^{19,20} we considered whether it was possible to perform the radical dioxygenation of styrene with NHPI under micellar conditions in water. Herein, we disclose the radical dioxygenation of styrene derivatives in an aqueous solution including Triton X-100-based micelles.

Following Xia and co-workers conditions which were published in 2015,²⁰ we initiated our studies with styrene **1a** as a model substrate for the synthesis of 2-(2-hydroxy-2-phenylethoxy)-2,3-dihydro-1*H*-isoindoline-1,3-dione **2a** using commercially available NHPI, catalytic PTSA, and excess TBHP under air in an aqueous solution of TPGS-750-M (2 wt%) at room temperature (Table 1, entries 1 and 2). The reaction without surfactant was carried out in parallel as a control. Disappointedly, unsatisfactory yields were obtained (5% without surfactant and 9% in the TPGS-750-M solution), which prompted us to run subsequent reactions under O₂

* Corresponding author.

E-mail address: fbihel@unistra.fr (F. Bihel).



Scheme 1. Reported methods from Xia and co-workers.

with different types of surfactants (Table 1, entries 3–9). To our delight, the reaction proceeded well in the aqueous solution of Triton X-100 (2 wt%) and produced **2a** in 87% yield. Other surfactants did not produce better yields (58% TPGS-750-M, 73% Brij 30, 83% TPGS-1000, 14% SPGS-550-M, 57% Tween-80, 15% SDS). Interestingly, when the structures of these surfactants were compared (ESI, Fig. S1), it was noticeable that all the surfactants bearing one terminal hydroxyl group (Brij 30, TPGS-1000, Triton X-100) were favorable to the reaction except for Tween 80. In contrast with most of the reactions reported so far, surfactants bearing terminal ether groups such as TPGS-750-M or SPGS-550-M, appeared less efficient. Lipshutz and co-workers proposed that the size of the micelle may have an impact on the reaction.^{3–10} According to Lipshutz and co-workers, with a diameter of about 50 nm, micelles formed by TPGS-750-M are suitable for micellar chemistry.^{5,9} In

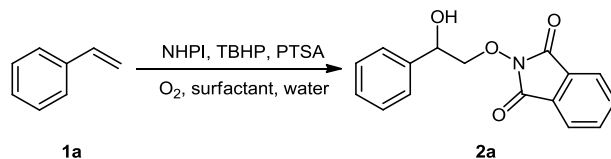
contrast, TPGS-1000 and Triton X-100 lead to micelles with a small diameter of 15 nm and 10 nm, respectively, while micelles resulting from Brij-30 have a diameter of 110 nm (ESI, Table S1).^{5,9,21,22} In this work, the good yields obtained with TPGS-1000, Triton X-100 and Brij-30 indicate that micelle diameter does not significantly influence the reaction. The common point of these three nonionic surfactants is the presence of a hydroxyl group at the terminus of the PEG moiety. Further work will be necessary to explain the role of this hydroxyl group in this reaction under micellar conditions. Triton X-100 and TPGS-1000 are both stable and biodegradable surfactants,²³ but since triton X-100 is much cheaper than TPGS-1000, it was preferred for the following reactions in water.

When the concentration of Triton X-100 was increased from 2 wt% to 5 wt% or decreased to 1 wt% (Table 1, entries 10 and 11), the yields decreased to 51% and 73%, respectively, suggesting the dependence of the reaction on the concentration of Triton X-100. Surprisingly, the absence of the PTSA catalyst did not have a significant impact on the reaction and produced **2a** in 88% yield (Table 1, entry 12). On another hand, decreasing **1a** or TBHP to 2 equivalents led to a significant decrease in yield (55% and 51%, respectively, Table 1, entries 13 and 14).

In an effort to accelerate the reaction, the temperature was raised to 50 °C (Table 1, entry 15), resulting in an exacerbation of side reactions and producing **2a** in only 62% yield. Several other catalyst/oxidant combinations also have been reported in the alkene 1,2-dioxygenation with NHPI.^{20,24–28} Herein, we tested several used combinations TBAI/TBHP, CuBr₂/DTBP, CuCl, Cu(OAc)₂/TBHP, FeCl₃ and PhI(OAc)₂. However, except for TBAI/TBHP which led to trace amounts of **2a**, most did not give the desired product.

To examine the scope of the established method, various styrene derivatives were investigated as substrates to react with NHPI under the optimized conditions (Table 1, entry 12). As shown in Scheme 2, the electronic properties and positions of the sub-

Table 1
Optimization of the reaction conditions.^a



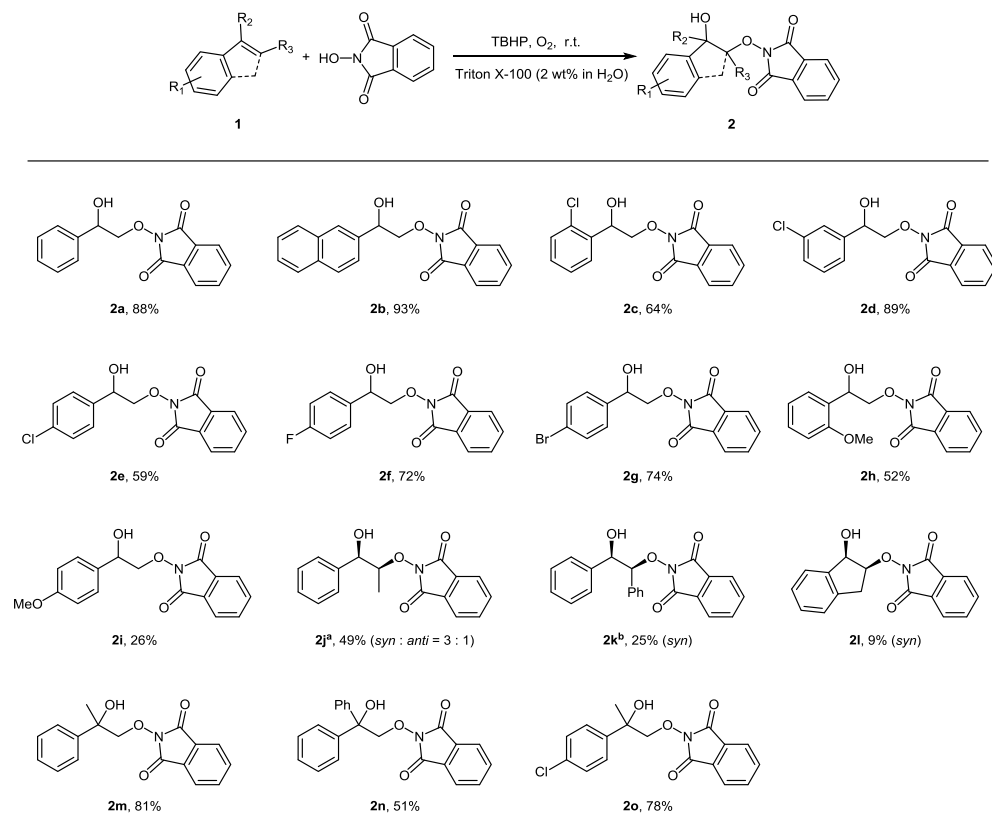
Entry	1a (equiv.)	TBHP (equiv.)	PTSA (mol%)	Surfactant (% w/w in H ₂ O)	Yield (%) ^c
1 ^b	3	4	10	–	5
2 ^b	3	4	10	TPGS-750-M (2)	9
3	3	4	10	TPGS-750-M (2)	58
4	3	4	10	Brij 30 (2)	73
5	3	4	10	TPGS-1000 (2)	83
6	3	4	10	Triton X-100 (2)	87
7	3	4	10	SPGS-550-M (2)	14
8	3	4	10	Tween 80 (2)	57
9	3	4	10	SDS (2)	15
10	3	4	10	Triton X-100 (5)	51
11	3	4	10	Triton X-100 (1)	73
12	3	4	–	Triton X-100 (2)	88
13	2	4	–	Triton X-100 (2)	55
14	3	2	–	Triton X-100 (2)	51
15 ^d	3	4	–	Triton X-100 (2)	62

^a Reactions were carried out in a vial on a bioshaker (1800 rpm) using NHPI (0.122 mmol, 1 equiv.), styrene (**1a**), PTSA, TBHP, and the surfactant in water (2 mL) under an O₂ balloon at r.t. for 19 h, unless otherwise noted.

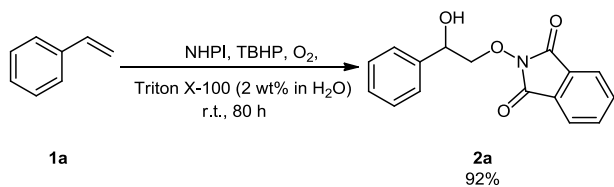
^b Reaction performed under air.

^c Yield of **2a** based on NHPI was determined by HPLC/UV using caffeine as an internal standard.

^d Reaction performed at 50 °C for 9 h.



Scheme 2. Scope of the reaction of styrene derivatives with NHPI in water. Reactions were carried out in a vial on a bioshaker (1800 rpm) using **1a** (0.366 mmol), NHPI (0.122 mmol) and TBHP (0.488 mmol) in a 2 wt% Triton X-100 aqueous solution (2 mL) under a O_2 balloon at r.t. for 20 h. Yields of the isolated compounds after flash chromatography are given. ^a*trans* configuration of the starting material. ^b*cis* configuration of the starting material.



Scheme 3. Gram-scale synthesis of **2a**.

stituents on styrene have a large influence on the reactivity. The dioxygenation reaction of 2-vinylnaphthalene proceeded in excellent yield (93% **2b**). The presence of a chlorine atom on the styrene moiety was well tolerated, producing moderate yields for the *ortho*-position (64% **2c**) and *para*-position (59% **2e**). However, a significant improvement in yield occurred when the chlorine atom was present at the *meta*-position (89% **2d**). Substrates with fluorine or bromine atom on the styrene moiety were also well tolerated (72% **2f**, 74% **2g**). Disappointingly, the introduction of electron-donating groups, such as a methoxy group, at the *ortho*- or *para*-position of the aromatic ring produced less satisfactory results (52% **2h**, 26% **2i**). The efficiency of the dioxygenation reaction was affected by the steric hindrance of a substituent at the β -position of the double bond. The methyl group significantly lowered the reactivity (49% **2j** compared to 88% **2a**). With a phenyl group at the β -position, the reaction proceeded sluggishly and compound **2k** was obtained in only 25% yield. Finally, starting from indene, compound **2l** was obtained in 9% yield after purification. The configuration of compound **2j**, **2k** and **2l** were deduced by comparing

the coupling constant of the α proton with the corresponding diols reported in the literature.^{19,20,29,30} Indeed, *syn*-diols show a coupling constant of about 4–5 Hz versus 7–8 Hz for *anti*-diols. In contrast, the presence of either a methyl or a phenyl group at the α -position of styrene did not alter the dioxygenation reaction, leading to **2m** (81%), **2n** (51%), and **2o** (78%).

Remarkably, this in water dioxygenation reaction could be performed on the gram scale with mechanical stirring. Treatment of **1a** (2.1 mL, 18.3 mmol) with NHPI (1.0 g, 6.1 mmol) and TBHP (2.3 mL, 24.4 mmol) in a 2 wt% Triton X-100 aqueous solution (100 mL) afforded product **2a** in excellent yield (92%, **Scheme 3**).

In summary, a convenient and eco-friendly protocol was developed for the dioxygenation of styrene derivatives with NHPI, resulting in the direct synthesis of substituted alcohols in moderate to good yields. This reaction is effective in water at room temperature; in the absence of any metal catalyst or organic solvent. Moreover, the reaction proceeded well on the gram scale and produced an excellent yield. The products **2** can be further transformed into β -hydroxy-*N*-alkoxyamines using hydrazine or diols using $Mo(CO)_6$, which are useful difunctionalized substrates in the synthesis of complex scaffolds.^{26,27,31} Further investigations will be carried out by replacing NHPI with *N*-hydroxybenzotriazole or *N*-hydroxysuccinimide.³²

Acknowledgment

We gratefully acknowledge the Ministry of Education of the P. R. China for financial support of this work.

A. Supplementary data

Supplementary data associated with this article can be found, in the online version, at <https://doi.org/10.1016/j.tetlet.2018.03.009>.

References

1. Chatterjee A, Ward TR. *Catal Lett*. 2016;146:820–840.
2. Karem S, Catharina N, Helmut S. *Curr Org Chem*. 2016;20:1576–1583.
3. Lipshutz BH, Aguinaldo GT, Ghorai S, Voigtritter K. *Org Lett*. 2008;10:1325–1328.
4. Lee NR, Gallou F, Lipshutz BH. *Org Process Res Dev*. 2017;21:218–221.
5. Lipshutz BH, Hageman M, Fennewald JC, Linstadt R, Slack E, Voigtritter K. *Chem Commun*. 2014;50:11378–11381.
6. Kelly SM, Lipshutz BH. *Org Lett*. 2014;16:98–101.
7. Fennewald JC, Landstrom EB, Lipshutz BH. *Tetrahedron Lett*. 2015;56:3608–3611.
8. Lipshutz BH, Ghorai S, Abela AR, et al. *J Org Chem*. 2011;76:4379–4391.
9. Klumphu P, Lipshutz BH. *J Org Chem*. 2014;79:888–900.
10. Cortes-Clerget M, Berthon J-Y, Krolikiewicz-Renimel I, Chaisemartin L, Lipshutz BH. *Green Chem*. 2017;19:4263–4267.
11. Wagner P, Bollenbach M, Doebelin C, et al. *Green Chem*. 2014;16:4170.
12. Salomé C, Wagner P, Bollenbach M, Bihel F, Bourguignon J-J, Schmitt M. *Tetrahedron*. 2014;70:3413–3421.
13. Bollenbach M, Wagner P, Aquino PGV, et al. *ChemSusChem*. 2016;9:3244–3249.
14. Bollenbach M, Aquino PGV, de Araujo-Junior JX, et al. *Chem Eur J*. 2017;23:13676–13683.
15. Gallou F, Isley NA, Ganic A, Onken U, Parmentier M. *Green Chem*. 2016;18:14–19.
16. Surivet JP, Zumbunn C, Rueedi G, et al. *J Med Chem*. 2015;58:927–942.
17. Kwon DY, Lee HE, Weitzel DH, et al. *J Med Chem*. 2015;58:7659–7671.
18. Chantigny YA, Murray JC, Kleinman EF, et al. *J Med Chem*. 2015;58:2658–2677.
19. Xia X-F, Zhu S-L, Hu Q-T, Chen C. *Tetrahedron*. 2016;72:8000–8003.
20. Xia XF, Zhu SL, Gu Z, et al. *J Org Chem*. 2015;80:5572–5580.
21. Paradies HH. *J Phys Chem*. 1980;84:599–607.
22. Deng LL, Taxipalati M, Que F, Zhang H. *Sci Rep*. 2016;6:38160.
23. Abu-Ghunmi L, Badawi M, Fayyad M. *J Surfactants Deterg*. 2014;17:833–838.
24. Zhang J-Z, Tang Y. *Adv Synth Catal*. 2016;358:752–764.
25. Samanta S, Donthiri RR, Ravi C, Adimurthy S. *J Org Chem*. 2016;81:3457–3463.
26. Bag R, Sar D, Punniyamurthy T. *Org Biomol Chem*. 2016;14:3246–3255.
27. Bag R, Sar D, Punniyamurthy T. *Org Lett*. 2015;17:2010–2013.
28. Andia AA, Miner MR, Woerpel KA. *Org Lett*. 2015;17:2704–2707.
29. Griffith JC, Jones KM, Picon S, et al. *J Am Chem Soc*. 2010;132:14409–14411.
30. Li X, Tanasova M, Vasileiou C, Borhan B. *J Am Chem Soc*. 2008;130:1885–1893.
31. Williams DR, Benbow JW, Sattleberg TR, Ihle DC. *Tetrahedron Lett*. 2001;42:8597–8601.
32. Lv Y, Wang X, Cui H, et al. *RSC Adv*. 2016;6:74917–74920.

Supporting Information

Dioxygenation of Styrenes with Molecular Oxygen in Water

Shuang-Qi Tang, An-Ping Wang, Martine Schmitt, and Frédéric Bihel *

Laboratoire d'Innovation thérapeutique, UMR 7200, CNRS, Université de Strasbourg, Faculté de Pharmacie, 74 route du Rhin, BP 60024, 67401 Illkirch, France

E-mail: fbihel@unistra.fr

Table of Contents

General information	S2
Typical experiment procedures	S3
Analytical data	S3
References	S4

General information

All reagents were purchased commercially without further purification. Compounds were purified using Armen spot flash chromatography on silica gel Merck 60 (particle size 0.040-0.063mm). The obtained compounds were characterized by ¹H-NMR and ¹³C-NMR spectra, which were recorded on a Bruker Advance III NMR spectrometer in CDCl₃ at 400 MHz/500MHz and 100 MHz, respectively. High resolution mass spectra (HRMS) were recorded on an Agilent Accurate Mass QToF 6520.

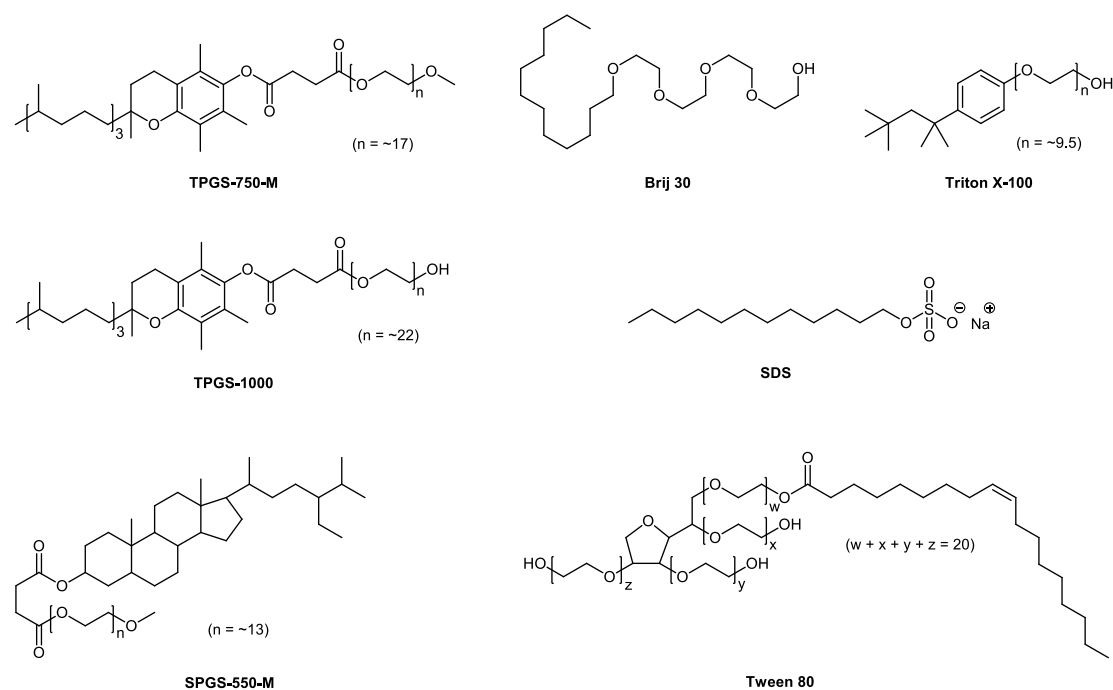


Fig. S1. Structures of the surfactants

Table S1. Size of micelle

Surfactant	Average diameter (nm)	Reference
TPGS-750-M	49	1
Brij 30	110	2
Triton X-100	10	3
TPGS-1000	15	1
SDS	17	2
SPGS-550-M	46	1
Tween 80	8	4

Typical experiment procedures

Synthesis of 2-(2-hydroxy-2-phenylethoxy)-2,3-dihydro-1H-isoindoline-1,3-dione (2a)

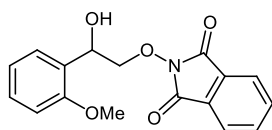
A solution of **1a** (42 μ L, 0.366 mmol, 3 equiv.), NHPI (20 mg, 0.122 mmol, 1 equiv.) and TBHP (46 μ L, 0.488 mmol, 4 equiv.) in an aqueous solution of 2 wt% Trion X-100 (2 mL) was vibrated (1800 rpm) under O₂ (balloon) on a bioshaker at room temperature for 20 h. Purification of the concentrated crude reaction mixture by flash chromatography (MeCN-H₂O, 10:90 to 50:50 in 40 min) afforded the product **2a** as a white solid (30.6 mg, 88%).

Gram scale synthesis of 2a

A solution of **1a** (2.1 mL, 18.3 mmol, 3 equiv.), NHPI (1 g, 6.1 mmol, 1 equiv.) and TBHP (2.3 mL, 24.4 mmol, 4 equiv.) in an aqueous solution of 2 wt% Trion X-100 (100 mL) was mechanically stirred (2000 rpm) under O₂ (balloon) at room temperature for 4 d. Purification of the concentrated crude reaction mixture by column chromatography (heptane-EtOAc, 4:1) afforded the product **2a** as a white solid (1.6 g, 92%).

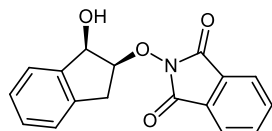
Analytical data

The NMR spectra of **2a-2o** except **2h** and **2l** were characterized according to the literatures.^{5,6}



2-(2-hydroxy-2-(2-methoxyphenyl)ethoxy)isoindoline-1,3-dione (2h)

White solid, ¹H NMR (400 MHz, CDCl₃): δ 9.61 (s, 1H), 7.88-7.84 (m, 2H), 7.79-7.76 (m, 2H), 7.45-7.43 (m, 1H), 7.31-7.26 (m, 1H), 6.96 (t, J = 7.5 Hz, 1H), 6.87 (d, J = 8.2 Hz, 1H), 5.80 (dd, J = 2.3, 8.4 Hz, 1H), 4.55-4.28 (m, 2H), 3.80 (s, 3H); ¹³C NMR (400 MHz, CDCl₃): δ 162.1, 154.6, 132.9, 127.8, 127.0, 125.7, 122.2, 121.9, 118.9, 108.7, 79.5, 76.8, 53.6; HRMS (ESI) m/z : calcd. for C₁₇H₁₅NO₅ [M + H₂O + H]⁺, 332.1056, found 332.1123.



2-((1-hydroxy-2,3-dihydro-1H-inden-2-yl)oxy)isoindoline-1,3-dione (2l)

White solid, ¹H NMR (500 MHz, CDCl₃): δ 7.88-7.86 (m, 2H), 7.79-7.77 (m, 2H), 7.39-7.38 (m, 1H), 7.29-7.26 (m, 2H), 7.21-7.19 (m, 1H), 5.53 (d, J = 5.8 Hz, 1H), 4.86-4.82 (m, 1H), 3.46-3.41 (m, 1H), 3.22-3.17 (m, 1H), 2.98 (s, 1H); ¹³C NMR (500 MHz, CDCl₃): δ 164.28, 140.65, 137.43, 134.77, 128.82, 127.63, 124.86, 124.18, 123.83, 96.91, 78.93, 34.4; HRMS (ESI) m/z : calcd. for C₁₇H₁₃NO₄ [M + H]⁺, 296.0845, found 296.0910.

References

1. Klumphu, P; Lipshutz, BH. *J. Org. Chem.* 2014; 79: 888-900.
2. Lipshutz, BH; Hageman, M; Fennewald, JC; Linstadt, R; Slack, E; Voigtritter, K. *Chem. Commun.* 2014; 50: 11378-11381.
3. Paradies, HH. *J. Phys. Chem.* 1980; 84: 599-607.
4. Deng, LL; Taxipalati, M; Que, F; Zhang, H. *Sci. Rep.* 2016; 6: 38160.
5. Xia, X-F; Zhu, S-L; Hu, Q-T; Chen, C. *Tetrahedron.* 2016; 72: 8000-8003.
6. Xia, XF; Zhu, SL; Gu, Z; Wang, H; Li, W; Liu, X; Liang, YM. *J. Org. Chem.* 2015; 80: 5572-5580.

Appendix IX. Fukuyama cross-coupling approach to isoprekinamycin: discovery of the highly active and bench-stable palladium precatalyst POxAP

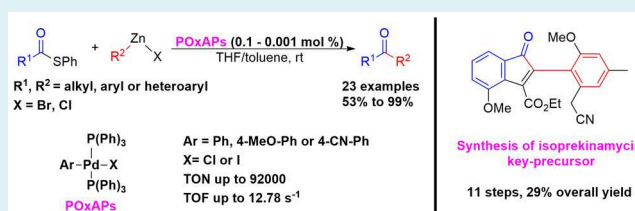
Fukuyama Cross-Coupling Approach to Isoprekinamycin: Discovery of the Highly Active and Bench-Stable Palladium Precatalyst POxAP

Shuang-Qi Tang, Jacques Bricard, Martine Schmitt,^{1b} and Frédéric Bihel*^{1b}

Laboratoire d'Innovation Thérapeutique, Labex MEDALIS, Faculté de Pharmacie, UMR7200 CNRS, Université de Strasbourg, 74 Route du Rhin, 67412 Illkirch, France

S Supporting Information

ABSTRACT: An efficient and user-friendly palladium(II) precatalyst, POxAP (post-oxidative-addition precatalyst), was identified for use in Fukuyama cross-coupling reactions. Suitable for storage under air, the POxAP precatalyst allowed reaction between thioesters and organozinc reagents with turnover numbers of ~90000. A series of 23 ketones were obtained with yields ranging from 53 to 99%. As proof of efficacy, an alternative approach was developed for the synthesis of a key precursor of the natural product isoprekinamycin.



Benzo[*a*]fluorenes, including isoprekinamycin (IPK) and fluostatins A–Q, represent an interesting class of natural products.¹ IPK is particularly noteworthy as it bears a diazo group at the 5-position, which plays a crucial role in its cytotoxicity against cancer cell lines.² To date, only one total synthesis of IPK has been reported (Figure 1),^{2c} where the key

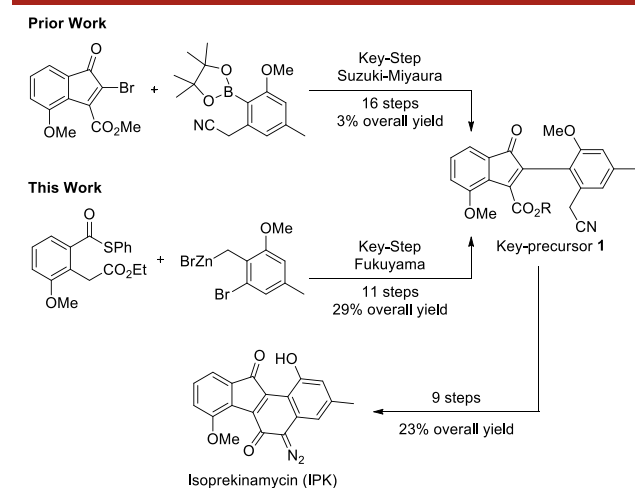


Figure 1. Synthetic strategies to the key IPK precursor.

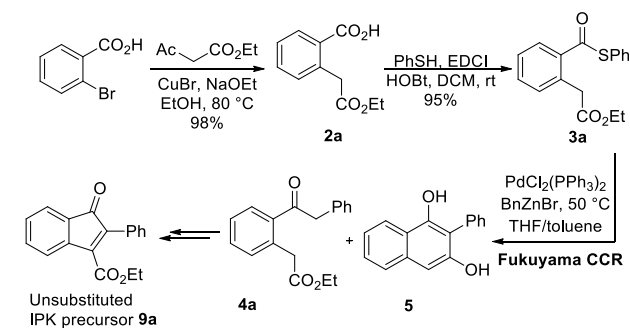
step involved formation of precursor 1 through a Suzuki–Miyaura cross-coupling reaction (CCR). While the transformation of 1 into IPK was efficiently achieved over nine steps and in a 23% overall yield, the synthesis of 1 appeared less efficient, with 16 steps being required to give an overall yield of 3%. Thus, we herein propose an alternative approach based on the Fukuyama cross-coupling reaction,³ where a palladium precatalyst POxAP, of generic formula PdX(Ar)(PPh₃)₂, is employed to efficiently generate ketones.

Initially, we investigated the preparation of an unsubstituted version of the key precursor of IPK, as outlined in Table 1. Starting from commercially available 2-bromobenzoic acid, a copper-mediated acetylation was easily performed to obtain 2a in 98% yield.⁴ A coupling reaction with EDCI/HOBt led to thioester 3a, a classical substrate of the Fukuyama reaction. Surprisingly, under standard conditions, the Fukuyama reaction between 3a and benzylzinc bromide afforded the expected compound 4a in a poor 8% yield (Table 1, entry 2), while naphthalenediol 5 was recovered as the main product (62% yield). A dropwise addition of benzylzinc bromide at 25 °C still gave a mixture of 4a and 5 in yields of 9% and 27%, respectively (Table 1, entry 1). It was therefore considered that the Fukuyama reaction was relatively slow, thereby allowing any unreacted BnZnBr to act as a base toward ketone 4a, speeding up the Dieckman condensation reaction and yielding compound 5. Consequently, other catalytic conditions described previously in the literature were investigated for the Fukuyama CCR, with palladium-, nickel-, and iron-based catalysts being employed in the presence of various ligands or additives (Table 1, entries 3–8).⁵ All conditions favored the formation of 5, which we expect may be due to the slow formation of Pd(0) from Pd(II). Indeed, during the past decade, significant effort has been focused on the development of stable Pd(II) precatalysts, which can be easily transformed *in situ* into Pd(0).⁶ In the Fukuyama CCR, fourth-generation palladacycles from Buchwald's group led to traces of 4a, while PEPPSI-IPr precatalyst from Organ's group afforded ketone 4a in a 15% yield (Table 1, entries 9 and 10). It is important to highlight that these two precatalysts have been optimized for the Negishi CCR⁷ and may require different ligands for Fukuyama CCR. We then examined an alternative palladium

Received: January 4, 2019

Published: January 18, 2019

Table 1. Fukuyama CCR on a Model System



entry ^a	cat.	temp (°C)	time (min)	yield ^b (%)	
				4a	5
1	PdCl ₂ (PPh ₃) ₂	25	15	9	27
2	PdCl ₂ (PPh ₃) ₂	50	15	8	62
3 ^c	Pd(dba) ₂ /P(Fu) ₃	50	45	19	14
4 ^d	Pd ₂ (dba) ₃ /PCy ₃ /ZnCl ₂	50	45	31	53
5 ^e	Ni(acac) ₂	50	45	0	0
6	NiCl ₂ (PPh ₃) ₂	50	45	19	44
7	Cu(TMHD) ₂	50	45	27	41
8	Fe(acac) ₃	50	45	15	22
9	XPhos-Pd-G4	50	30	trace	0
10	PEPPSI-IPr	50	30	15	51
11 ^f	PdCl(Ph)(PPh ₃) ₂ [POxAP]	50	5	95	0

^aReaction conditions: thioester **3a** (0.14 mmol), catalyst (1 mol %), BnZnBr (0.21 mmol, 0.82 M in THF), toluene (0.26 mL), rt. ^bIsolated yield. ^c1.4 mol % of P(Fu)₃. ^d2 mol % of PCy₃ and 1 equiv of ZnCl₂ were used. ^e10 mol % of Ni(acac)₂. ^f0.1 mol % of PdCl(Ph)(PPh₃)₂ (0.1 mL, 1.4 × 10⁻³ M in THF/toluene) was used.

precatalyst, PdCl(Ph)(PPh₃)₂, which we recently identified and referred to by a generic name, POxAP (i.e., a post-oxidative-addition precatalyst). Indeed, PdX(Ar)(PPh₃)₂ precatalysts respect the criteria of Pd-based OACs (oxidative addition complexes) recently described by Ingoglia and Buchwald.⁸ This palladium complex is well-known in the literature, as it is formed through the first oxidative addition between Pd(0)Ln and PhCl and is common in the majority of palladium-catalyzed CCRs.⁹ While this complex has been extensively cited in various mechanistic studies, it has been scarcely described *per se* as a catalyst. We have only found three papers published in the 1970s, at the very beginning of the palladium-catalyzed CCR era, in which PdI(Ph)(PPh₃)₂ was used in only one example of Heck CCR¹⁰ and Negishi CCR.¹¹ In 1976, Sekiya and Ishikawa reported that PdI(Ph)(PPh₃)₂ could be used as a catalyst in the Kumada CCR between ArI and ArMgX, with yields ranging from 32 to 82%.¹² Yet PdCl(Ph)(PPh₃)₂ complex is a bench-stable Pd(II) complex that can be both stored and manipulated under air and is easily obtained from Pd(PPh₃)₄.¹³ In the presence of an organozinc reagent R¹ZnX, this complex follows a Negishi-like initiation step and provides PhR¹ as well as a reactive Pd(0) entity, which is then available for a subsequent Fukuyama catalytic cycle (Figure 2).

Thus, using Fleming's procedure,¹³ PdCl(Ph)(PPh₃)₂ was obtained in a high yield, and was employed with a loading of 0.1 mol % in the Fukuyama CCR featured in Table 1. Pleasingly, ketone **4a** was obtained in a 95% yield after only 5 min, without any trace of naphthalenediol **5** being observed

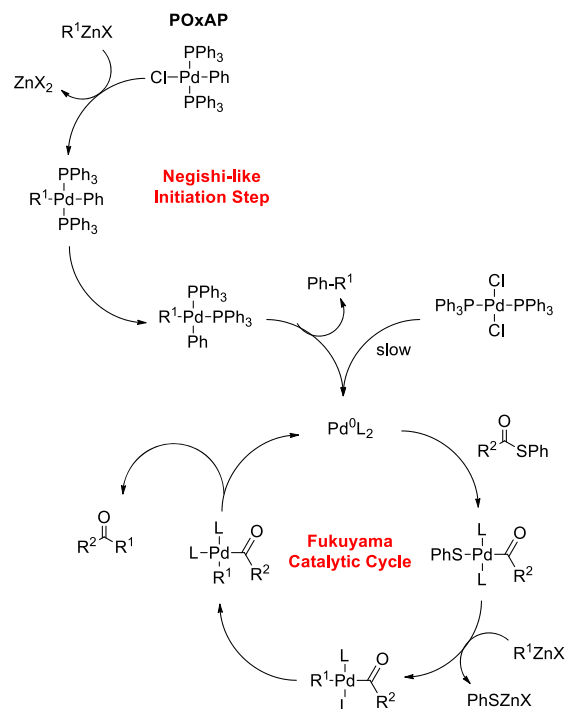


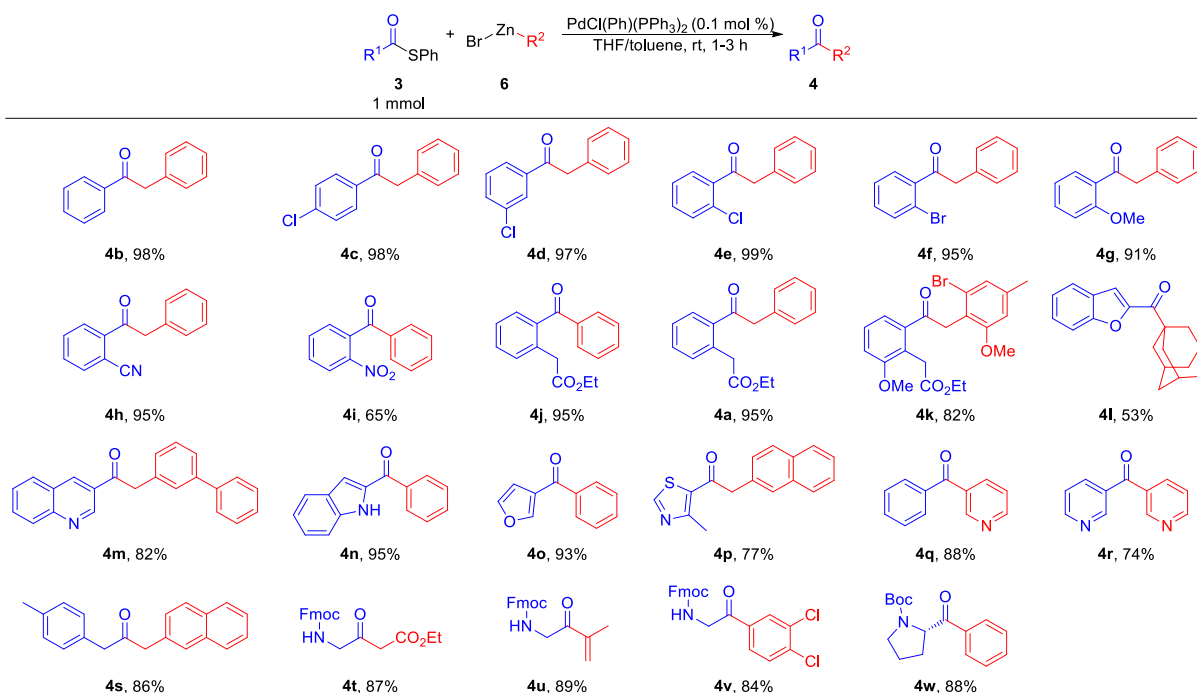
Figure 2. Comparison of the reaction mechanisms involved where PdCl₂(PPh₃)₂ and the POxAP PdCl(Ph)(PPh₃)₂ are employed.

(Table 1, entry 11). To better determine the reactivity of this new precatalyst, we synthesized three derivatives, namely PdCl(4-CN-Ph)(PPh₃)₂, PdCl(4-MeO-Ph)(PPh₃)₂, and PdI(4-MeO-Ph)(PPh₃)₂, in which electron-donating or -withdrawing groups were added to the phenyl ring or where chlorine was substituted with iodine. These potential POxAPs were compared in a kinetic study based on the Fukuyama CCR, as shown in Table 2. Interestingly, with a loading of only 0.001 mol %, PdCl(Ph)(PPh₃)₂ catalyzed the formation of ketone **4b** in a 92% yield with a turnover number (TON) of 92000 (Table 2, entry 2). In comparison, classical PdCl₂(PPh₃)₂ led to a poor yield of 12% (Table 2, entry 1), while other POxAPs gave similar yields and TONs to

Table 2. Kinetic Study^a into the Fukuyama CCR Using Various Precatalysts of Generic Formula PdX(Ar)(PPh₃)₂

entry	cat. or POxAP (0.001 mol %)	TON	TOF (s ⁻¹)		yield ^d (%)
			initial rate ^b	cruising rate ^c	
1	PdCl ₂ (PPh ₃) ₂	12000	0.55	0.21	12
2	PdCl(Ph)(PPh ₃) ₂	92000	5.55	1.46	92
3	PdCl(4-CN-Ph)(PPh ₃) ₂	83000	2.22	1.53	83
4	PdCl(4-MeO-Ph)(PPh ₃) ₂	89000	8.89	1.60	89
5	PdI(4-MeO-Ph)(PPh ₃) ₂	91000	12.78	1.53	91

^aReaction conditions: thioester **3b** (0.14 mmol), [Pd] (0.001 mol %), BnZnBr (0.21 mmol, 0.82 M in THF), toluene (0.26 mL), rt. ^bInitial rate was measured between 0 and 30 min. ^cCruising rate was measured between 4 and 8 h. ^dYield of **4b** was determined from the average of two independent experiments by HPLC/UV using caffeine as an internal standard.

Scheme 1. Scope of the Fukuyama CCR^a Using POxAP PdCl(Ph)(PPh₃)₂

^aReaction conditions: thioester **3** (1 mmol), PdCl(Ph)(PPh₃)₂ (0.1 mol %), R²ZnBr **6** (1.5 mmol in THF), toluene (2.5 mL), rt, 1–3 h.

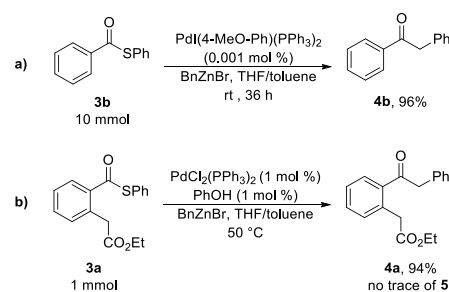
PdCl(Ph)(PPh₃)₂ (Table 2, entries 3–5). However, differences in reactivity appeared when measuring the turnover frequencies (TOF). Initial rates were determined for the first 30 min of the reaction, and it was found that the presence of an aryl moiety bearing an electron-withdrawing group (i.e., 4-CN-Ph, 2.22 vs 5.55 s⁻¹ for Ph) decreased the initial rate, while the presence of an electron-donating group (i.e., 4-OMe-Ph, 8.89 vs 5.55 s⁻¹ for Ph) increased this rate (Table 2, entries 3–5). This result is fully consistent with our proposed mechanism. Indeed, compared with electron-poor compounds, reductive elimination is favored by electron-rich compounds. Furthermore, the replacement of chlorine by iodine led also to an initial rate increase (i.e., 8.89 vs 12.8 s⁻¹) as iodine is more easily substituted by the organozinc reagent than chlorine (Table 2, entries 4 and 5). However, these differences in the initial rates disappeared between 4 and 8 h (i.e., the cruising rate), where rates ranging from 1.46 to 1.6 s⁻¹ were recorded. Indeed, following our concept, all four POxAPs led to the same catalytic entity Pd(0)Ln, which is consistent with observation of similar cruising rates following the initial stages of the reaction.

Further proof of the proposed mechanism shown in Figure 2 is the fact that 3-phenylpyridine (Ph-R¹) was detected by mass spectroscopy, which resulted from the Negishi-like initiation step in the presence of pyridin-3-ylzinc bromide. All POxAPs were bench-stable for several weeks, and could be both manipulated and stored under air.

Metal-catalyzed formation of ketones is still a very prolific area of scientific investigation,¹⁴ as ketone-containing products are numerous in many fields of chemistry.

Using PdCl(Ph)(PPh₃)₂, we then investigated the scope of the Fukuyama CCR at the 1 mmol scale, synthesizing 23 ketones in yields ranging from 53 to 99% (Scheme 1). As shown, aryl, heteroaryl, and alkyl thioesters were easily coupled to aryl or alkyl organozinc reagents in high yields. Even bulky

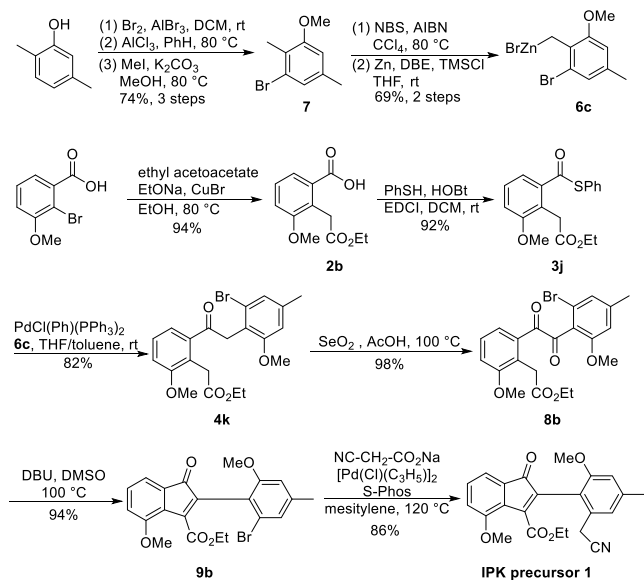
ketone **4k** was obtained in 82% yield despite the steric hindrance on both the thioester and the organozinc reagent. In addition, the use of 0.1 mol % of PdCl(Ph)(PPh₃)₂ produced a range of ketones over 1–3 h at room temperature. Furthermore, with a 0.001 mol % loading of PdI(4-MeO-Ph)(PPh₃)₂, an extended reaction time of 36 h transformed 10 mmol of thioester **3b** into the corresponding ketone **4b** in 96% yield (Scheme 2a).

Scheme 2. Scale-up (a) and in Situ Generation of PdCl(Ph)(PPh₃)₂ (b)

Interestingly, POxAP can also be generated in situ starting from PdCl₂(PPh₃)₂. Indeed, in 2006, Yasuda et al. reported that PdCl₂(PPh₃)₂ reacts with phenolate to afford PdCl(Ph)(PPh₃)₂ in a low yield (~10%).¹⁵ Moreover, through the use of equimolar amounts of PdCl₂(PPh₃)₂ and PhOH in the presence of organozinc reagents, the POxAP PdCl(Ph)(PPh₃)₂ was generated *in situ*, as confirmed by NMR spectroscopy (see the SI), and compound **4a** was obtained in 94% yield (Scheme 2b), without any trace of naphthalenediol **5**.

With the efficient precatalyst POxAP in hand, we attempted to complete the synthesis of the IPK precursor (Scheme 3) following the strategy proposed in Figure 1. Starting from 2,5-dimethylphenol, the perbromination of positions 3, 4, and 6,

Scheme 3. Total Synthesis of the IPK Precursor 1



followed by the debromination of positions 4 and 6 by AlCl₃, led to the desired 3-bromo-2,5-dimethylphenol. Following a subsequent O-methylation step, 7 was obtained in a 74% overall yield (three steps). Radical bromination of the methyl group at position 2 then gave organozinc 6c, which was stored in THF. Subsequently, 2-bromo-3-methoxybenzoic acid was coupled to ethyl acetoacetate in the presence of a catalytic amount of copper bromide. While sodium ethanolate is required for the copper-mediated coupling reaction, it also promoted an *in situ* deacetylation to afford 2b in a 94% yield. Following formation of the thioester 3j under standard conditions, a Fukuyama CCR was performed with organozinc 6c using POxAP PdCl(Ph)(PPh₃)₂ to give 4k in 82% yield, which was oxidized by SeO₂ in AcOH.¹⁶ Several conditions were then attempted for the subsequent cyclization. While TEA in hot ethanol produced 9a (Table 1), the unsubstituted analogue of 9b, the steric hindrance imparted by both aromatic rings of 8b prevented the formation of 9b itself. Several conditions were examined (see the SI), but only the use of DBU in hot DMSO led to indanone 9b in an excellent yield. Finally, a palladium-catalyzed cyanation reaction led to the desired IPK precursor 1. This compound was synthesized over 11 steps and in an overall yield of 29%. This compares to a 3% overall yield from 16 steps as reported previously.^{2e}

In conclusion, we demonstrated that the POxAPs of generic formula PdX(Ar)(PPh₃)₂, prepared from the oxidative addition of Pd(0) with ArX, constituted efficient Pd(II) precatalysts. Indeed, these bench stable POxAPs could be employed in particularly low quantities (0.001 mol %) to perform Fukuyama CCRs and generate a large diversity of ketones. This efficacy was demonstrated through the development of a convenient route to IPK. The use of these POxAP are not limited to the Fukuyama CCR, and their efficacies in other palladium-catalyzed CCRs are currently under investigation.

■ ASSOCIATED CONTENT

Supporting Information

The Supporting Information is available free of charge on the ACS Publications website at DOI: 10.1021/acs.orglett.9b00031.

Full experimental details; ¹H and ¹³C NMR spectra (PDF)

■ AUTHOR INFORMATION

Corresponding Author

*Tel: +33 (0)3 688 54 130. E-mail: fbihel@unistra.fr.

ORCID

Martine Schmitt: 0000-0002-8723-9502

Frédéric Bihel: 0000-0002-4122-0929

Notes

The authors declare no competing financial interest.

■ ACKNOWLEDGMENTS

We thank Dr. M. Gulea (UMR7200) and Dr. G. Blond (UMR7200) for assistance in the preparation of this manuscript. S.-Q.T. gratefully acknowledges the Ministry of Education of the P.R. China for financial support of this work (China Scholarship Council (201608310124)).

■ REFERENCES

- (1) (a) Ito, S.; Matsuya, T.; Omura, S.; Otani, M.; Nakagawa, A. *J. Antibiot.* **1970**, *23*, 315–317. (b) Seaton, P. J.; Gould, S. J. *J. Antibiot.* **1989**, *42*, 189–197. (c) Herzon, S. B.; Woo, C. M. *Nat. Prod. Rep.* **2012**, *29*, 87–118.
- (2) (a) Hauser, F. M.; Zhou, M. *J. Org. Chem.* **1996**, *61*, 5722–5722. (b) Proteau, P. J.; Li, Y.; Chen, J.; Williamson, R. T.; Gould, S. J.; Laufer, R. S.; Dmitrienko, G. I. *J. Am. Chem. Soc.* **2000**, *122*, 8325–8326. (c) Laufer, R. S.; Dmitrienko, G. I. *J. Am. Chem. Soc.* **2002**, *124*, 1854–1855. (d) Birman, V. B.; Zhao, Z.; Guo, L. *Org. Lett.* **2007**, *9*, 1223–1225. (e) Liu, W.; Buck, M.; Chen, N.; Shang, M.; Taylor, N. J.; Asoud, J.; Wu, X.; Hasinoff, B. B.; Dmitrienko, G. I. *Org. Lett.* **2007**, *9*, 2915–2918.
- (3) Tokuyama, H.; Yokoshima, S.; Yamashita, T.; Fukuyama, T. *Tetrahedron Lett.* **1998**, *39*, 3189–3192.
- (4) Velicky, J.; Bodendorf, U.; Rigollier, P.; Epple, R.; Beisner, D. R.; Guerini, D.; Smith, P.; Liu, B.; Feifel, R.; Wipfli, P.; Aichholz, R.; Couttet, P.; Dix, I.; Widmer, T.; Wen, B.; Brandl, T. *J. Med. Chem.* **2018**, *61*, 865–880.
- (5) (a) Kunchithapatham, K.; Eichman, C. C.; Stambuli, J. P. *Chem. Commun. (Cambridge, U. K.)* **2011**, *47*, 12679–12681. (b) Cherney, A. H.; Reisman, S. E. *Tetrahedron* **2014**, *70*, 3259–3265. (c) Shimizu, T.; Seki, M. *Tetrahedron Lett.* **2002**, *43*, 1039–1042. (d) Cardellicchio, C.; Fiandanese, V.; Marchese, G.; Ronzini, L. *Tetrahedron Lett.* **1985**, *26*, 3595–3598.
- (6) For reviews, see: (a) Valente, C.; Çalimsiz, S.; Hoi, K. H.; Mallik, D.; Sayah, M.; Organ, M. G. *Angew. Chem., Int. Ed.* **2012**, *51*, 3314–3332. (b) Bruno, N. C.; Tudge, M. T.; Buchwald, S. L. *Chem. Sci.* **2013**, *4*, 916–920.
- (7) (a) Organ, M. G.; Avola, S.; Dubovyk, I.; Hadei, N.; Kantchev, E. A. B.; O'Brien, C. J.; Valente, G. *Chem. - Eur. J.* **2006**, *12*, 4749–4755. (b) Valente, C.; Belowich, M. E.; Hadei, N.; Organ, M. G. *Eur. J. Org. Chem.* **2010**, *23*, 4343–4354. (c) Yang, Y.; Oldenhuis, N. J.; Buchwald, S. L. *Angew. Chem., Int. Ed.* **2013**, *52*, 615–619. (d) Haas, D.; Hammann, J. M.; Greiner, R.; Knochel, P. *ACS Catal.* **2016**, *6*, 1540–1552.
- (8) Ingoglia, B. T.; Buchwald, S. L. *Org. Lett.* **2017**, *19*, 2853–2856.
- (9) (a) Jutand, A.; Négri, S.; Principaud, A. *Eur. J. Inorg. Chem.* **2005**, *2005*, 631–635. (b) Carrow, B. P.; Hartwig, J. F. *J. Am. Chem. Soc.* **2011**, *133*, 2116–2119. (c) Grushin, V. V. *Organometallics* **2000**, *19*, 1888–1900.
- (10) Schoenberg, A.; Heck, R. F. *J. Org. Chem.* **1974**, *39*, 3327–3331.
- (11) Fauvarque, J. F.; Jutand, A. *J. Organomet. Chem.* **1979**, *177*, 273–281.

(12) Sekiya, A.; Ishikawa, N. *J. Organomet. Chem.* **1976**, *118*, 349–354.

(13) Flemming, J. P.; Pilon, M. C.; Borbulevitch, O. Y.; Antipin, M. Y.; Grushin, V. V. *Inorg. Chim. Acta* **1998**, *280*, 87–98.

(14) For recent examples of other recent strategies to form ketones, see: (a) Ben Halima, T.; Zhang, W.; Yalaoui, I.; Hong, X.; Yang, Y. F.; Houk, K. N.; Newman, S. G. *J. Am. Chem. Soc.* **2017**, *139*, 1311–1318. (b) Zhang, M.; Xie, J.; Zhu, C. *Nat. Commun.* **2018**, *9*, 1–10. (c) Xia, Y.; Wang, J.; Dong, G. *J. Am. Chem. Soc.* **2018**, *140*, 5347–5351. (d) Kinney, R. G.; Tjutrins, J.; Torres, G. M.; Liu, N. J.; Kulkarni, O.; Arndtsen, B. A. *Nat. Chem.* **2017**, *10*, 193–199. (e) Fujii, T.; Oki, Y.; Nakada, M. *Tetrahedron Lett.* **2018**, *59* (10), 882–886. (f) Carlson, A. S.; Calcanas, C.; Brunner, R. M.; Topczewski, J. J. *Org. Lett.* **2018**, *20* (6), 1604–1607.

(15) Yasuda, H.; Maki, N.; Choi, J. C.; Abla, M.; Sakakura, T. *J. Organomet. Chem.* **2006**, *691*, 1307–1310.

(16) Klein, D. J.; Modarelli, D. A.; Harris, F. W. *Macromolecules (Washington, DC, U. S.)* **2001**, *34*, 2427–2437.

Fukuyama Cross-Coupling Approach to Isoprekinamycin: Discovery of the Highly Active and Bench Stable Palladium Precatalyst POxAP

Shuang-Qi Tang, Jacques Bricard, Martine Schmitt, and Frédéric Bihel*

Laboratoire d'Innovation Thérapeutique, Faculté de Pharmacie, UMR7200 CNRS, Université de Strasbourg, 74 Route du Rhin, 67412 Illkirch, France

Supporting Information

Table of Contents

I. General Information	S2
II. Preparation of POxAPs	S3
III. Kinetic Study of POxAPs	S4
IV. POxAPs Catalyzed Fukuyama Cross-Coupling Reactions	S5
V. Generation of POxAPs with the Addition of PhOH	S24
VI. Synthesis of the Unsubstituted IPK Precursor 9a	S25
VII. Synthesis of IPK Precursor 1	S28
VIII. References	S32

I. General Information

All commercial reagents were used without additional purification. Analytical TLC was performed using silica gel plates Merck 60 F₂₅₄ and plates were visualized by exposure to ultraviolet light (254 nm). Compounds were purified on silica gel Merck 60 (particle size 0.040-0.063 nm).

¹H and ¹³C NMR spectra were recorded on Bruker Avance Spectrometer operating at 400 or 500 MHz and 100 or 125 MHz, respectively. All chemical shift values δ and coupling constants J are quoted in ppm and in Hz, respectively, multiplicity (s= singulet, d= doublet, t= triplet, q= quartet, quin = quintet, sex= sextet m= multiplet, br= broad).

Analytical RP-HPLC-MS was performed using a LC 1200 Agilent with quadrupole-time-of-flight (QTOF) (Agilent Accurate Mass QToF 6520) with a Zorbax Agilent C18-column (C18, 50 mm x 2.1 mm; 1.8 μ m) using the following parameters: 1) The solvent system: A (0.05% of formic acid in acetonitrile) and B (0.05% of formic acid in H₂O); 2) A linear gradient: t= 0 min, 98% B; t = 8 min, 0% B; t = 12.5 min, 0% B; t = 12.6 min, 98% B; t = 13 min, 98% B; 3) Flow rate of 0.5 mL/min; 4) Column temperature: 35 °C; 5) DAD scan from 190 nm to 700 nm; 6) Ionization mode : ESI⁺ or ESI⁻.

HPLC were performed using a Dionex UltiMate 3000 using the following parameters: Flow rate of 0.5 mL/min, column temperature: 30 °C, solvent system: A (MeOH) and B (0.05% of TFA in H₂O), t = 0 min to 1 min: 50 to 60% of B, then t = 1 min to t = 10 min: 60 to 100% of B and t = 10 min to t = 15 min: 100% of B.

II. Preparation of POxAPs

$\text{PdCl}(\text{Ph})(\text{PPh}_3)_2$, $\text{PdCl}(4\text{-CN-Ph})(\text{PPh}_3)_2$, $\text{PdCl}(4\text{-MeO-Ph})(\text{PPh}_3)_2$ and $\text{PdI}(4\text{-MeO-Ph})(\text{PPh}_3)_2$ were synthesized according to the previous reported methods.¹

1. Preparation of $\text{PdCl}(\text{Ph})(\text{PPh}_3)_2$: The mixture of $\text{Pd}(\text{PPh}_3)_4$ (1 equiv, 480 mg, 0.41 mmol) and PhBr (3.4 equiv, 146 μL , 1.39 mmol) in degassed benzene (3.2 mL) was stirred at 80 °C under Ar for 16 h. The reaction mixture was concentrated in vacuo, the residue was washed with ether and then dissolved into a vial charged with the mixture of CH_2Cl_2 (3 mL) and saturated KCl aqueous solution (3 mL), then capped and vibrated on a bioshaker (1800 rpm) for 30 min. The aqueous layer was separated and disposed of, the organic phase was treated with another 3 mL of saturated KCl aqueous solution and vibrated (1800 rpm) for another 30 min. After repeated this procedure for 8 times, the organic phase was separated, dried over anhydrous Na_2SO_4 and filtered through a 0.22 μm filter. Ether (10 mL) was added to the filtrate, the mixture was left overnight and then filtered to obtain $\text{PdCl}(\text{Ph})(\text{PPh}_3)_2$ as a yellow solid (287 mg, 94%).

2. Preparation of $\text{PdCl}(4\text{-CN-Ph})(\text{PPh}_3)_2$: The mixture of $\text{Pd}(\text{PPh}_3)_4$ (1 equiv, 260 mg, 0.22 mmol) and 4-chlorobenzonitrile (1.2 equiv, 36.8 mg, 0.27 mmol) in degassed benzene (3 mL) was stirred at 100 °C under Ar for 16 h. The reaction mixture was concentrated in vacuo and Et_2O (5 mL) was added. The suspension was filtered, the residue was washed with Et_2O (5 mL) thrice and dried under vacuum to afford $\text{PdCl}(4\text{-CN-Ph})(\text{PPh}_3)_2$ as a white solid (164 mg, 96%).

3. Preparation of $\text{PdI}(4\text{-MeO-Ph})(\text{PPh}_3)_2$: The mixture of $\text{Pd}(\text{PPh}_3)_4$ (1 equiv, 379 mg, 0.33 mmol) and 4-iodoanisole (1.2 equiv, 91 mg, 0.39 mmol) in degassed toluene (6 mL) was stirred at rt under Ar for 16 h. The reaction mixture was concentrated in vacuo and Et_2O (5 mL) was added. The suspension was filtered, the residue was washed with Et_2O (5 mL) thrice and dried under vacuum to afford $\text{PdI}(4\text{-MeO-Ph})(\text{PPh}_3)_2$ as a white solid (250 mg, 89%).

4. Preparation of $\text{PdCl}(4\text{-MeO-Ph})(\text{PPh}_3)_2$: To the solution of $\text{PdI}(4\text{-MeO-Ph})(\text{PPh}_3)_2$ (1 equiv, 150 mg, 0.17 mmol) in CH_2Cl_2 (2 mL) was added tetrabutylammonium chloride (7 equiv, 337 mg, 1.2 mmol) under Ar at 0 °C and stirred at rt for 30 min. The reaction mixture was concentrated in vacuo and then MeOH (3 mL) was added. The suspension was filtered, the residue was washed with MeOH (3 mL) thrice, dried under reduced pressure to afford $\text{PdCl}(4\text{-MeO-Ph})(\text{PPh}_3)_2$ as a white solid (130 mg, 97%).

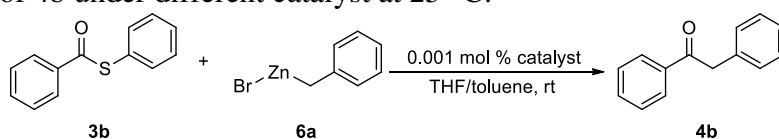
III. Kinetic Study of POxAPs

1.4×10^{-2} mmol POxAPs was added to a 20 mL microwave tube charged with 10 mL THF/toluene (1:1) and sonicated until the solution became clear (1.4×10^{-3} M). From this solution, 100 μ L were taken to a second 20 mL microwave tube and diluted with 900 μ L THF/toluene (1:1) (1.4×10^{-4} M). Then, 100 μ L from this last solution were taken and diluted with 900 μ L THF/toluene (1:1) in a third 20 mL microwave tube (1.4×10^{-5} M). The microwave tubes were sealed, degassed and backfilled with Ar thrice.

To the solution of **3b** (1 equiv, 30 mg, 0.14 mmol) in toluene (0.26 mL) was added the corresponding catalyst solution (10^{-3} mol %, 100 μ L, 1.4×10^{-6} mmol, 1.4×10^{-5} M in THF/toluene), degassed and backfilled with argon thrice. Then, the solution of the organozinc reagent **6a** (1.5 equiv, 0.26 mL, 0.21 mmol, 0.82 M in THF) was added and stirred at 25 °C for the given time. Yields of **4b** were determined from the average of two independent experiments by HPLC/UV using caffeine as an internal standard (Table S1).

TON and TOF were calculated with the formulas in Figure S1.

Table S1. Yield (%) of **4b** under different catalyst at 25 °C.



Time (h)	PdCl ₂ (PPh ₃) ₂	PdCl(Ph)(PPh ₃) ₂	PdCl(4-CN-Ph)(PPh ₃) ₂	PdCl(4-MeO-Ph)(PPh ₃) ₂	PdI(4-MeO-Ph)(PPh ₃) ₂
0.5	1	10	4	16	23
4	3	35	27	44	56
8	6	56	49	67	78
16	10	81	77	86	88
40	12	92	83	89	91

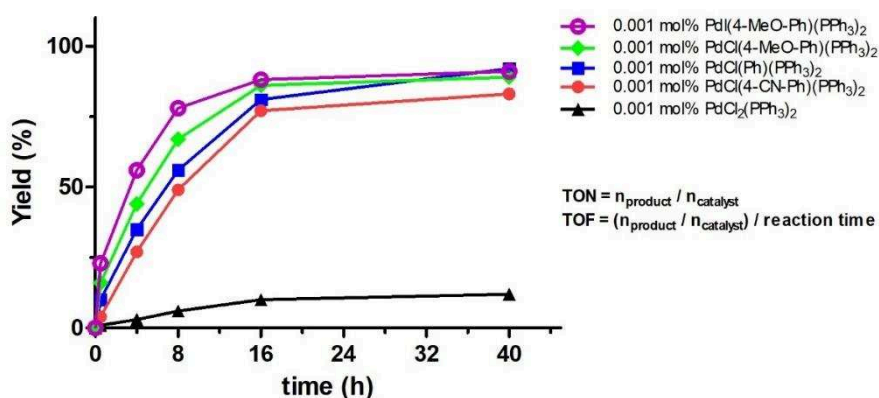


Figure S1. Calculation of TON and TOF (See Table 2, article).

IV. POxAPs Catalyzed Fukuyama Cross-Coupling Reactions

1. Typical procedure for the synthesis of thioester (TP1)

To an ice-cooled solution of carboxylic acid (1 equiv, 5.0 mmol) and EDCI (1.3 eq., 1.27 mg, 6.5 mmol) in DCM (15 mL) was added HOBt (1.3 eq., 0.88 g, 6.5 mmol). The mixture was stirred at 0 °C for 10 min and then thiophenol (1.1 equiv, 562 μ L, 5.5 mmol) was added. The ice bath was removed and the resulting solution was stirred at room temperature for 5 h. After completion (HPLC or TLC monitoring), water (30 mL) was added and the mixture was extracted with DCM (20 mL) thrice. The combined organic phases were washed with brine, dried over anhydrous Na₂SO₄ and concentrated in vacuo. The crude was purified by silica gel chromatography (heptane/EtOAc) to afford corresponding thioester.

2. Typical procedures for the synthesis of organozinc reagents

(1) Typical procedure 2 (TP2):

An oven-dried 20 mL microwave vial equipped with a magnetic stirrer was charged with zinc (1.5 equiv, 392 mg, 6 mmol). The vial was properly capped and the vessel was heated using a heat gun (350 °C, 10 min) under reduced pressure, the tube was cooled to room temperature, degassed and backfilled with argon thrice. Then THF (4.0 mL) was added followed by 1,2-dibromoethane (5 %, 17.3 μ L, 0.2 mmol) and chlorotrimethylsilane (5 %, 25.6 μ L, 0.2 mmol). The suspension was heated (50 °C, 1 min) until the suspension became clear and grey precipitates formed. After cooling to room temperature, the corresponding bromide (1 equiv, 4 mmol) was added dropwise at 0 °C (solid bromides were dissolved in 1 mL THF before adding). The resulted solution was stirred at room temperature overnight to afford the corresponding organozinc reagent. The concentration and yield of the organozinc reagent were determined by iodometric titration of the supernatant solution.²

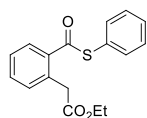
(2) Typical procedure 3 (TP3):

An oven-dried 20 mL microwave vial equipped with a magnetic stirrer was charged with ZnCl₂ (1.4 equiv, 779 mg, 5.6 mmol). The vial was properly capped and the vessel was heated using a heat gun (550 °C, 15 min) under reduced pressure, the tube was cooled to room temperature, degassed and backfilled with argon thrice. Then THF (4 mL) was added and the mixture was ultrasonicated until it became a clear solution. The corresponding organomagnesium bromide (1 equiv, 4 mmol) was added to the forementioned solution slowly at 0 °C and a white precipitate was observed. The resulting mixture was stirred at room temperature for additional 3 h to afford the corresponding organozinc reagent, which was used directly without titration.

3. Typical procedure for the synthesis of ketone (TP4):

A solution of thioester (1 equiv, 1 mmol) and PdCl(Ph)(PPh₃)₂ (0.1 mol %, 0.74 mg, 0.001 mmol) in toluene (2.5 mL) was degassed and backfilled with argon thrice. Then, the solution of organozinc reagent (1.5 equiv, 1.5 mmol) in THF was added dropwise at the given temperature. After stirring for the given time, the reaction mixture was quenched with saturated NH₄Cl solution (10 mL) and extracted with EtOAc (10 mL) thrice. The combined organic phases were dried over Na₂SO₄ and concentrated in vacuo. The crude was purified by silica gel chromatography to afford the corresponding ketone.

Preparation of ethyl 2-(2-((phenylthio)carbonyl)phenyl)acetate (**3a**)



3a

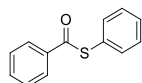
The reaction was performed with **2a** (1 equiv, 1.04 g, 5 mmol) according to **TP1**, the crude was purified silica gel chromatography (heptane:EtOAc = 10:1) to afford **3a** as a yellow solid (1.43 g, 95%).

¹H NMR (400 MHz, CDCl₃): δ 8.08 (d, J = 7.7 Hz, 1H), 7.56 – 7.38 (m, 7H), 7.31 (d, J = 7.5 Hz, 1H), 4.14 (q, J = 7.0 Hz, 2H), 3.93 (s, 2H), 1.23 (t, J = 7.1 Hz, 3H).

¹³C NMR (101 MHz, CDCl₃): δ 192.09, 170.98, 136.87, 135.00, 133.47, 132.41, 132.33, 129.53, 129.28, 129.23, 128.11, 127.55, 60.88, 39.51, 14.26.

HRMS (ESI): m/z calcd. for C₁₇H₁₆O₃S [M]⁺: 300.0820, found: 300.0805.

Preparation of S-phenyl benzothioate (**3b**)



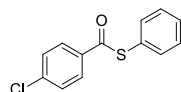
3b

The reaction was performed with benzoic acid (1 equiv 611 mg, 5 mmol) according to **TP1**, the crude was purified silica gel chromatography (heptane:EtOAc = 4:1) to afford **4c** as a yellow solid (1.05 g, 98%).

¹H NMR (400 MHz, CDCl₃): δ 8.04 (d, J = 7.9 Hz, 2H), 7.62 (t, J = 7.3 Hz, 1H), 7.56 – 7.43 (m, 7H).

These data are consistent with the previously reported characterization.³

Preparation of S-phenyl 4-chlorobenzothioate (**3c**)



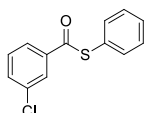
3c

The reaction was performed with 4-chlorobenzoic acid (1 equiv, 0.78 g, 5 mmol) according to **TP1**, the crude was purified silica gel chromatography (heptane:EtOAc = 18:1) to afford **3c** as a white solid (1.16 g, 93%).

$^1\text{H NMR}$ (400 MHz, CDCl_3): δ 8.02 – 7.94 (m, 2H), 7.57 – 7.43 (m, 7H).

These data are consistent with the previously reported characterization.⁴

Preparation of S-phenyl 3-chlorobenzothioate (**3d**)



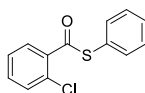
3d

The reaction was performed with 3-chlorobenzoic acid (1 equiv, 0.78 g, 5 mmol) according to **TP1**, the crude was purified silica gel chromatography (heptane:EtOAc = 18:1) to afford **3d** as a colorless oil (1.22 g, 98%).

$^1\text{H NMR}$ (400 MHz, CDCl_3): δ 8.02 (t, J = 2.0 Hz, 1H), 7.93 (dt, J = 7.8, 1.4 Hz, 1H), 7.60 – 7.46 (m, 6H), 7.42 (t, J = 7.9 Hz, 1H).

These data are consistent with the previously reported characterization.⁴

Preparation of S-phenyl 2-chlorobenzothioate (**3e**)



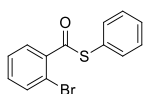
3e

The reaction was performed with 2-chlorobenzoic acid (1 equiv, 0.78 g, 5 mmol) according to **TP1**, the crude was purified silica gel chromatography (heptane:EtOAc = 18:1) to afford **3e** as a yellow solid (1.19 g, 96%).

$^1\text{H NMR}$ (400 MHz, CDCl_3): δ 7.77 (d, J = 7.5 Hz, 1H), 7.59 – 7.53 (m, 2H), 7.51 - 7.40 (m, 5H), 7.36 (t, J = 7.3 Hz, 1H).

These data are consistent with the previously reported characterization.⁵

Preparation of S-phenyl 2-bromobenzothioate (**3f**)



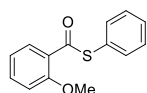
3f

The reaction was performed with 2-bromobenzoic acid (1 equiv, 1.01 g, 5 mmol) according to TP1, the crude was purified silica gel chromatography (heptane:EtOAc = 18:1) to afford **3f** as a yellow solid (1.31 g, 89%).

$^1\text{H NMR}$ (400 MHz, CDCl_3): δ 7.73 (d, $J = 7.5$ Hz, 1H), 7.67 (d, $J = 7.8$ Hz, 1H), 7.60 - 7.53 (m, 2H), 7.52 - 7.44 (m, 3H), 7.43 - 7.31 (m, 2H).

These data are consistent with the previously reported characterization.⁶

Preparation of S-phenyl 2-methoxybenzothioate (**3g**)



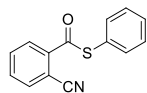
3g

The reaction was performed with 2-methoxybenzoic acid (1 equiv, 0.76 g, 5 mmol) according to TP1, the crude was purified silica gel chromatography (heptane:EtOAc = 18:1) to afford **3g** as a colorless oil (1.05 g, 86%).

$^1\text{H NMR}$ (400 MHz, CDCl_3): δ 7.87 (d, $J = 7.6$ Hz, 1H), 7.64 - 7.38 (m, 6H), 7.11 - 6.94 (m, 2H), 3.96 (s, 3H).

These data are consistent with the previously reported characterization.⁴

Preparation of S-phenyl 2-cyanobenzothioate (**3h**)



3h

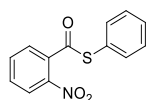
The reaction was performed with 2-cyanobenzoic acid (1 equiv, 0.74 g, 5 mmol) according to TP1, the crude was purified silica gel chromatography (heptane:EtOAc = 15:1) to afford **3h** as a white solid (1.06 g, 89%).

$^1\text{H NMR}$ (400 MHz, CDCl_3): δ 8.18 (dd, $J = 7.7, 1.5$ Hz, 1H), 7.84 (dd, $J = 7.3, 1.7$ Hz, 1H), 7.79 - 7.66 (m, 2H), 7.63 - 7.40 (m, 5H).

$^{13}\text{C NMR}$ (101 MHz, CDCl_3): δ 188.29, 139.19, 135.25, 135.02, 132.98, 132.79, 130.12, 129.57, 129.27, 126.35, 117.23, 110.58.

HRMS (ESI): m/z calcd. for $\text{C}_{14}\text{H}_9\text{NOS}$ $[\text{M}]^+$: 239.0405, found: 239.0393.

Preparation of S-phenyl 2-nitrobenzothioate (**3i**)



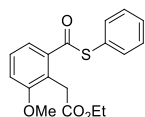
3i

The reaction was performed with 2-nitrobenzoic acid (1 equiv, 0.84 g, 5 mmol) according to **TP1**, the crude was purified silica gel chromatography (heptane:EtOAc = 6:1) to afford **3i** as a yellow solid (1.21 g, 93%).

¹H NMR (400 MHz, CDCl₃): δ 8.08 (d, J = 8.0 Hz, 1H), 7.78 - 7.62 (m, 3H), 7.61 - 7.54 (m, 2H), 7.51 - 7.42 (m, 3H).

¹³C NMR (101 MHz, CDCl₃): δ 190.20, 146.26, 134.83, 133.72, 131.79, 131.73, 130.15, 129.64, 128.54, 126.81, 124.86.

HRMS (ESI): m/z calcd. for C₁₃H₉NO₃S [M]⁺: 259.0303, found: 259.0288.

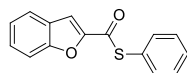
Preparation of ethyl 2-(2-methoxy-6-((phenylthio)carbonyl)phenyl)acetate (3j)**3j**

The reaction was performed with **2b** (1 equiv, 1.19 g, 5 mmol) according to **TP1**, the crude was purified silica gel chromatography (heptane:EtOAc = 14:1) to afford **3j** as a yellow solid (1.52 g, 92%).

¹H NMR (400 MHz, CDCl₃): δ 7.61 (dd, J = 7.8, 1.0 Hz, 1H), 7.53 - 7.43 (m, 5H), 7.38 (t, J = 8.1 Hz, 1H), 7.09 (d, J = 8.2 Hz, 1H), 4.12 (q, J = 7.1 Hz, 2H), 3.94 (s, 2H), 3.85 (s, 3H), 1.22 (t, J = 7.1 Hz, 3H).

¹³C NMR (101 MHz, CDCl₃): δ 192.44, 171.32, 158.40, 138.50, 134.97, 129.60, 129.35, 128.31, 128.26, 122.37, 120.91, 114.41, 60.71, 56.18, 31.87, 14.35.

HRMS (ESI): m/z calcd. for C₁₇H₁₈O₄S [M]⁺: 330.0926, found: 330.0909.

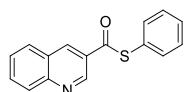
Preparation of S-phenyl benzofuran-2-carbothioate (3k)**3k**

The reaction was performed with benzofuran-2-carboxylic acid (1 equiv, 0.81 g, 5 mmol) according to **TP1**, the crude was purified silica gel chromatography (heptane:EtOAc = 6:1) to afford **3k** as a white solid (1.26 g, 99%).

¹H NMR (400 MHz, CDCl₃): δ 7.72 (dt, J = 7.8, 1.0 Hz, 1H), 7.65 - 7.59 (m, 2H), 7.58 - 7.53 (m, 2H), 7.53 - 7.46 (m, 4H), 7.37 - 7.31 (m, 1H).

¹³C NMR (101 MHz, CDCl₃): δ 180.55, 155.77, 150.87, 135.17, 129.91, 129.47, 128.40, 127.08, 126.25, 124.23, 123.35, 112.61, 111.94.

HRMS (ESI): m/z calcd. for C₁₅H₁₀O₂S [M]⁺: 254.0402, found: 254.0385.

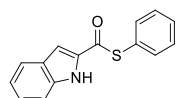
Preparation of S-phenyl quinoline-3-carbothioate (3l)**3l**

The reaction was performed with quinoline-3-carboxylic acid (1 equiv, 0.87 g, 5 mmol) according to TP1, the crude was purified silica gel chromatography (heptane:EtOAc = 3:1) to afford **3l** as a white solid (1.31 g, 99%).

¹H NMR (400 MHz, CDCl₃): δ 9.44 (d, J = 2.2 Hz, 1H), 8.83 (d, J = 2.0 Hz, 1H), 8.22 - 8.14 (m, 1H), 8.02 - 7.94 (m, 1H), 7.92 - 7.83 (m, 1H), 7.70 - 7.62 (m, 1H), 7.60 - 7.53 (m, 2H), 7.52 - 7.46 (m, 3H).

¹³C NMR (101 MHz, CDCl₃): δ 188.79, 150.35, 148.03, 136.49, 135.18, 132.31, 129.99, 129.73, 129.54, 129.47, 129.41, 127.91, 126.93, 126.63.

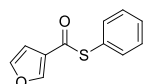
HRMS (ESI): m/z calcd. for C₁₆H₁₁NOS [M]⁺: 265.0561, found: 265.0549.

Preparation of S-phenyl 1H-indole-2-carbothioate (3m)**3m**

The reaction was performed with 1H-indole-2-carboxylic acid (1 equiv, 0.81 g, 5 mmol) according to TP1, the crude was purified silica gel chromatography (heptane:EtOAc = 3:1) to afford **3m** as a white solid (1.23 g, 97%).

¹H NMR (400 MHz, DMSO-d₆): δ 12.06 (s, 1H), 7.78 - 7.71 (m, 1H), 7.59 - 7.45 (m, 7H), 7.35 - 7.29 (m, 1H), 7.16 - 7.10 (m, 1H).

These data are consistent with the previously reported characterization.⁷

Preparation of S-phenyl furan-3-carbothioate (3n)**3n**

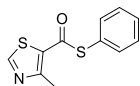
The reaction was performed with furan-3-carboxylic acid (1 equiv, 0.56 g, 5 mmol) according to TP1, the crude was purified silica gel chromatography (heptane:EtOAc = 15:1) to afford **3n** as a colorless oil (1.01 g, 99%).

¹H NMR (400 MHz, CDCl₃): δ 8.17 (dd, J = 1.6, 0.8 Hz, 1H), 7.53 - 7.43 (m, 6H), 6.82 (dd, J = 1.9, 0.9 Hz, 1H).

¹³C NMR (101 MHz, CDCl₃): δ 183.08, 146.26, 144.31, 135.00, 129.65, 129.33, 126.86, 126.55, 108.52.

HRMS (ESI): m/z calcd. for $C_{11}H_8O_2S$ $[M]^+$: 204.0245, found: 204.0231.

Preparation of S-phenyl 4-methylthiazole-5-carbothioate (**3o**)



3o

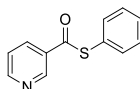
The reaction was performed with 4-methylthiazole-5-carboxylic acid (1 equiv, 0.72 g, 5 mmol) according to **TP1**, the crude was purified silica gel chromatography (heptane:EtOAc = 3:1) to afford **3o** as a white solid (1.15 g, 98%).

1H NMR (400 MHz, $CDCl_3$): δ 8.78 (s, 1H), 7.53 – 7.43 (m, 5H), 2.78 (s, 3H).

^{13}C NMR (101 MHz, $CDCl_3$): δ 181.97, 158.95, 154.90, 135.00, 130.03, 129.47, 129.43, 127.12, 18.22.

HRMS (ESI): m/z calcd. for $C_{11}H_9NOS_2$ $[M]^+$: 235.0126, found: 235.0110.

Preparation of S-phenyl pyridine-3-carbothioate (**3p**)



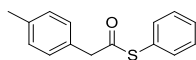
3p

The reaction was performed with nicotinic acid (1 equiv, 0.62 g, 5 mmol) according to **TP1**, the crude was purified silica gel chromatography (heptane:EtOAc = 3:1) to afford **3p** as a colorless oil (1.02 g, 95%).

1H NMR (400 MHz, $CDCl_3$): δ 9.23 (s, 1H), 8.80 (d, J = 3.9 Hz, 1H), 8.27 - 8.21 (m, 1H), 7.54 - 7.37 (m, 6H).

These data are consistent with the previously reported characterization.⁸

Preparation of S-phenyl 2-(p-tolyl)ethanethioate (**3q**)



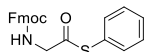
3q

The reaction was performed with 2-(p-tolyl)acetic acid (1 equiv, 0.75 g, 5 mmol) according to **TP1**, the crude was purified silica gel chromatography (heptane:EtOAc = 10:1) to afford **3q** as a colorless oil (1.16 g, 96%).

1H NMR (400 MHz, $CDCl_3$): δ 7.39 (s, 5H), 7.28 – 7.15 (m, 4H), 3.89 (s, 2H), 2.37 (s, 3H).

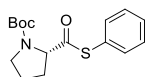
^{13}C NMR (101 MHz, $CDCl_3$): δ 195.61, 137.37, 134.54, 130.36, 129.67, 129.54, 129.43, 129.23, 128.07, 49.92, 21.26.

HRMS (ESI): m/z calcd. for $C_{15}H_{14}OS$ $[M]^+$: 242.0765, found: 242.0761.

Preparation of S-phenyl 2-(((9H-fluoren-9-yl)methoxy)carbonyl)amino)ethanethioate (3r)**3r**

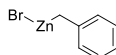
The reaction was performed with Fmoc-glycine (1 equiv, 1.49 g, 5 mmol) according to **TP1**, the crude was purified silica gel chromatography (heptane:EtOAc = 3:1) to afford **3r** as a white solid (1.79 g, 92%). ¹H NMR (400 MHz, CDCl₃): δ 7.78 (d, J = 7.5 Hz, 2H), 7.63 (d, J = 7.4 Hz, 2H), 7.48 - 7.36 (m, 7H), 7.32 (t, J = 7.9 Hz, 2H), 5.48 (s, 1H), 4.48 (d, J = 7.0 Hz, 2H), 4.27 (t, J = 7.0 Hz, 1H), 4.22 (d, J = 6.1 Hz, 2H).

These data are consistent with the previously reported characterization.⁹

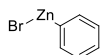
Preparation of (S)-tert-butyl 2-((phenylthio)carbonyl)pyrrolidine-1-carboxylate (3s)**3s**

The reaction was performed with N-Boc-L-proline (1 equiv, 1.08 g, 5 mmol) according to **TP1**, the crude was purified silica gel chromatography (heptane:EtOAc = 6:1) to afford **3s** as a white solid (1.48 g, 96%). ¹H NMR (400 MHz, CDCl₃): δ 7.42 - 7.37 (dd, J = 6.0, 3.5 Hz, 5H), 4.61 - 4.39 (m, 1H), 3.72 - 3.40 (m, 2H), 2.34 - 1.84 (m, 4H), 1.51 (s, 3H), 1.49 (s, 6H).

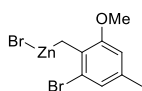
These data are consistent with the previously reported characterization.¹⁰

Preparation of benzylzinc(II) bromide (6a)**6a**

According to **TP2**, **6a** was prepared from (bromomethyl)benzene (1 equiv, 0.48 mL, 4 mmol). Titration against iodine indicates a concentration of 0.82 M (92 %).

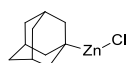
Preparation of phenylzinc(II) bromide (6b)**6b**

According to **TP3**, **6b** was prepared from phenylmagnesium bromide (1 equiv, 4 mL, 4 mmol, 1 M in THF). The concentration of **6b** was 0.5 M.

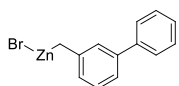
Preparation of (2-bromo-6-methoxy-4-methylbenzyl)zinc(II) bromide (6c)**6c**

The corresponding bromide was prepared from 2,5-dimethylphenol according to the previous reported methods (4 overall steps, 59%).¹¹

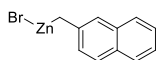
According to **TP2**, **6c** was prepared from the corresponding bromide (1 equiv, 1.18 g, 4 mmol) in THF (1 mL). Titration against iodine indicates a concentration of 0.57 M (86 %).

Preparation of adamantan-1-ylzinc(II) chloride (6d)**6d**

6d was prepared according to a previous reported method.¹² An oven-dried 20 mL microwave vial equipped with a magnetic stirrer was charged with LiCl (1.1 equiv, 163 mg, 3.85 mmol). The vial was capped and heated (450 °C, 5 min) by an heat gun under reduced pressure. The vial was then cooled to room temperature and backfilled with argon. Mg (2 equiv, 170 mg, 7 mmol) was added, the tube was properly sealed and heated under reduced pressure (90 °C, 3 min). After cooling to room temperature, the tube was backfilled with argon thrice. THF (5 mL) was added, followed by DBE (0.05 equiv, 15.1 μL, 0.19 mmol) and TMSCl (0.03 equiv, 13.4 μL, 0.11 mmol). Then, a solution of ZnCl₂ (1.1 equiv, 525 mg, 3.85 mmol) in THF (3.85 mL) was added followed by a solution of 1-bromoadamantane (1 equiv, 753 mg, 3.5 mmol) in THF (1 mL). The reaction mixture was stirred at room temperature overnight to afford adamantan-1-ylzinc(II) chloride. Titration against iodine indicates a concentration of 0.23 M (73%).

Preparation of ([1,1'-biphenyl]-3-ylmethyl)zinc(II) bromide (6e)**6e**

According to **TP2**, **6e** was prepared from the solution of 3-(bromomethyl)-1,1'-biphenyl (1 equiv, 0.99 g, 4 mmol) in THF (1 mL). Titration against iodine indicates a concentration of 0.55 M (83%).

Preparation of (naphthalen-2-ylmethyl)zinc(II) bromide (6f)**6f**

According to **TP2**, **6f** was prepared from the solution of 2-(bromomethyl)naphthalene (1 equiv, 0.88 g, 4 mmol) in THF (1 mL). Titration against iodine indicates a concentration of 0.59 M (89%).

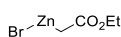
Preparation of pyridin-3-ylzinc(II) bromide (**6g**)



6g

6g was prepared according to a previous reported method.¹³ An oven-dried 20 mL microwave tube equipped with a magnetic stirrer was charged with LiCl (1.5 equiv, 191 mg, 4.5 mmol), ZnCl₂ (1.1 equiv, 450 mg, 3.3 mmol). The vial was capped and heated (550 °C, 15 min) by an heat gun under reduced pressure, the tube was cooled to room temperature and backfilled with argon. Mg (2.47 equiv, 180 mg, 7.41 mmol) was added, the tube was sealed and heated under reduced pressure (90 °C, 3 min). After cooling to room temperature, the tube was backfilled with argon thrice. THF (6 mL) was added, and the mixture was stirred for 30 min at room temperature. Then, 3-bromopyridine (1 equiv, 0.29 mL, 3 mmol) was added in one portion at 25 °C. The reaction mixture was stirred for at room temperature overnight to afford pyridin-3-ylzinc(II) bromide. Titration against iodine indicates a concentration of 0.3 M (64%).

Preparation of (2-ethoxy-2-oxoethyl)zinc(II) bromide (**6h**)



6h

According to **TP2**, **6h** was prepared from ethyl 2-bromoacetate (1 equiv, 0.44 mL, 4 mmol). Titration against iodine indicates a concentration of 0.74 M (83 %).

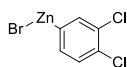
Preparation of prop-1-en-2-ylzinc(II) bromide (**6i**)



6i

According to **TP3**, **6i** was prepared from prop-1-en-2-ylmagnesium bromide (1 equiv, 8 mL, 4 mmol, 0.5 M in THF). The concentration of **6i** was 0.33 M.

Preparation of (3,4-dichlorophenyl)zinc(II) bromide (**6j**)

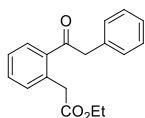


6j

(3,4-dichlorophenyl)magnesium bromide was prepared according to a previous reported method (0.74 M, 92%).¹⁴

According to **TP3**, **6j** was prepared from (3,4-dichlorophenyl)magnesium bromide (1 equiv, 5.4 mL, 4 mmol, 0.74 M in THF). The concentration of **6j** was 0.43 M.

Preparation of ethyl 2-(2-(2-phenylacetyl)phenyl)acetate (**4a**)



4a

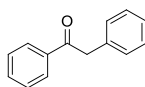
The cross-coupling reaction of **3a** (1 equiv, 300 mg, 1 mmol) with **6a** (1.5 equiv, 1.83 mL, 1.5 mmol, 0.82 M in THF) was performed according to **TP4** at room temperature in 1 h. the crude was purified by silica gel chromatography (heptane:EtOAc = 9:1) to afford **4a** as a yellow solid (268 mg, 95%).

Synthesis of 4a with PdCl₂(PPh₃)₂ with the addition of PhOH: A solution of **3a** (1 equiv, 300 mg, 1 mmol), PhOH (1 mol %, 0.94 mg, 0.01 mmol) and PdCl₂(PPh₃)₂ (1 mol %, 7.02 mg, 0.01 mmol) in toluene (2.5 mL) was degassed and backfilled with argon thrice. Then, **6a** (1.5 equiv, 1.83 mL, 1.5 mmol, 0.82 M in THF) was added slowly at room temperature. After stirring at 50°C for 25 min, the reaction mixture was quenched with saturated NH₄Cl solution (10 mL) and extracted with EtOAc (10 mL) thrice. The combined organic phases were dried over Na₂SO₄ and concentrated in vacuo. The crude was purified by silica gel chromatography (heptane:EtOAc = 9:1) to afford **4a** as a yellow solid (265 mg, 94%).

¹H NMR (400 MHz, CDCl₃): δ 7.86 (d, J = 7.7 Hz, 1H), 7.48 – 7.27 (m, 8H), 4.28 (s, 2H), 4.14 (q, J = 7.1 Hz, 2H), 3.92 (s, 2H), 1.25 (t, J = 7.2 Hz, 3H).

These data are consistent with the previously reported characterization.¹⁵

Preparation of 1,2-diphenylethanone (**4b**)



4b

The cross-coupling reaction of **3b** (1 equiv, 214 mg, 1 mmol) with **6a** (1.5 equiv, 1.83 mL, 1.5 mmol, 0.82 M in THF) was performed according to **TP4** at room temperature in 1 h. The crude was purified silica gel chromatography (heptane:EtOAc = 15:1) to afford **4b** as a white solid (192 mg, 98%).

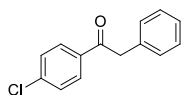
Synthesis of 4b in 10 mmol scale: To the solution of **3b** (1 equiv, 2.14g, 10 mmol) in toluene (18.3 mL) was added PdI(4-MeO-Ph)(PPh₃)₂ (0.001 mol %, 71.4 μL, 10⁻⁴ mmol, 1.4 × 10⁻³ M in THF/toluene). The resulting mixture was then degassed and backfilled with argon thrice. **6a** (1.5 equiv, 18.3 mL, 15 mmol, 0.82 M in THF) was added dropwise at room temperature. After stirring for 36 h, the reaction mixture was quenched with saturated NH₄Cl solution (40 mL) and extracted with EtOAc (40 mL) thrice. The

combined organic phases were dried over Na_2SO_4 and concentrated in vacuo. The crude was purified by silica gel chromatography (heptane:EtOAc = 15:1) to afford **4b** as a white solid (1.88 g, 96 %).

^1H NMR (400 MHz, CDCl_3): δ 8.09 – 8.02 (m, 2H), 7.55 (t, $J = 7.3$ Hz, 1H), 7.45 (t, $J = 7.7$ Hz, 2H), 7.38 – 7.26 (m, 5H), 4.29 (s, 2H).

These data are consistent with the previously reported characterization.¹⁶

Preparation of 1-(4-chlorophenyl)-2-phenylethanone (**4c**)



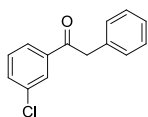
4c

The cross-coupling reaction of **3c** (1 equiv, 249 mg, 1 mmol) with **6a** (1.5 equiv, 1.83 mL, 1.5 mmol, 0.82 M in THF) was performed according to **TP4** at room temperature in 1 h. The crude was purified silica gel chromatography (heptane:EtOAc = 40:1) to afford **4c** as a colorless oil (226 mg, 98%).

^1H NMR (400 MHz, CDCl_3): δ 8.13 – 7.84 (m, 2H), 7.52 – 7.39 (m, 2H), 7.39 – 7.21 (m, 5H), 4.25 (s, 2H).

These data are consistent with the previously reported characterization.¹⁷

Preparation of 1-(3-chlorophenyl)-2-phenylethanone (**4d**)



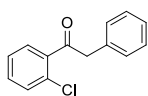
4d

The cross-coupling reaction of **3d** (1 equiv, 249 mg, 1 mmol) with **6a** (1.5 equiv, 1.83 mL, 1.5 mmol, 0.82 M in THF) was performed according to **TP4** at room temperature in 1 h. The crude was purified silica gel chromatography (heptane:EtOAc = 40:1) to afford **4d** as a white solid (224 mg, 97%).

^1H NMR (400 MHz, CDCl_3): δ 7.96 (t, $J = 2.0$ Hz, 1H), 7.86 (dt, $J = 7.8, 1.4$ Hz, 1H), 7.54 – 7.47 (m, 1H), 7.41 – 7.19 (m, 7H), 4.24 (s, 2H).

These data are consistent with the previously reported characterization.¹⁸

Preparation of 1-(2-chlorophenyl)-2-phenylethanone (**4e**)



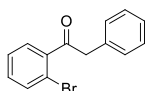
4e

The cross-coupling reaction of **3e** (1 equiv, 249 mg, 1 mmol) with **6a** (1.5 equiv, 1.83 mL, 1.5 mmol, 0.82 M in THF) was performed according to **TP4** at room temperature in 1 h. The crude was purified silica gel chromatography (heptane:EtOAc = 25:1) to afford **4e** as a colorless oil (229 mg, 99%).

¹H NMR (400 MHz, CDCl₃): δ 7.45 – 7.21 (m, 9H), 4.26 (s, 2H).

These data are consistent with the previously reported characterization.¹⁹

Preparation of 1-(2-bromophenyl)-2-phenylethanone (**4f**)



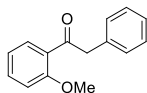
4f

The cross-coupling reaction of **3f** (1 equiv, 293 mg, 1 mmol) with **6a** (1.5 equiv, 1.83 mL, 1.5 mmol, 0.82 M in THF) was performed according to **TP4** at room temperature in 1 h. The crude was purified silica gel chromatography (heptane:EtOAc = 25:1) to afford **4f** as a colorless oil (261 mg, 95%).

¹H NMR (400 MHz, CDCl₃): δ 7.54 (d, J = 7.8 Hz, 1H), 7.29 - 7.19 (m, 8H), 4.19 (s, 2H).

These data are consistent with the previously reported characterization.²⁰

Preparation of 1-(2-methoxyphenyl)-2-phenylethanone (**4g**)



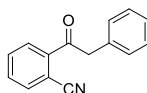
4g

The cross-coupling reaction of **3g** (1 equiv, 244 mg, 1 mmol) with **6a** (1.5 equiv, 1.83 mL, 1.5 mmol, 0.82 M in THF) was performed according to **TP4** at room temperature in 1 h. The crude was purified silica gel chromatography (heptane:EtOAc = 15:1) to afford **4g** as a white solid (205 mg, 91%).

¹H NMR (400 MHz, CDCl₃): δ 7.68 (dd, J = 7.7, 1.8 Hz, 1H), 7.46 (td, J = 8.7, 7.4, 1.9 Hz, 1H), 7.34 – 7.21 (m, 5H), 7.02 – 6.94 (m, 2H), 4.32 (s, 2H), 3.92 (s, 3H).

These data are consistent with the previously reported characterization.²¹

Preparation of 2-(2-phenylacetyl)benzonitrile (**4h**)



4h

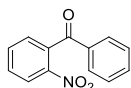
The cross-coupling reaction of **3h** (1 equiv, 239 mg, 1 mmol) with **6a** (1.5 equiv, 1.83 mL, 1.5 mmol, 0.82 M in THF) was performed according to **TP4** at room temperature in 1 h. The crude was purified silica gel chromatography (heptane:EtOAc = 40:1) to afford **4h** as a yellow solid (210 mg, 95%).

^1H NMR (500 MHz, CDCl_3): δ 7.97 – 7.93 (m, 1H), 7.83 – 7.79 (m, 1H), 7.67 (td, $J = 7.7, 1.5$ Hz, 1H), 7.62 (td, $J = 7.5, 1.4$ Hz, 1H), 7.36 – 7.31 (m, 2H), 7.29 – 7.25 (m, 3H), 4.34 (s, 2H).

^{13}C NMR (126 MHz, CDCl_3): δ 196.31, 139.73, 135.49, 133.33, 132.65, 132.49, 129.83, 129.61, 129.01, 127.44, 118.10, 111.53, 46.91.

HRMS (ESI): m/z calcd. for $\text{C}_{15}\text{H}_{11}\text{NO}$ $[\text{M}]^+$: 221.0841, found: 221.0829.

Preparation of (2-nitrophenyl)(phenyl)methanone (**4i**)



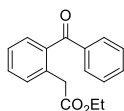
4i

The cross-coupling reaction of **3i** (1 equiv, 259 mg, 1 mmol) with **6b** (1.5 equiv, 3 mL, 1.5 mmol, 0.5 M in THF) was performed according to **TP4** at -10 °C in 3 h. The crude was purified silica gel chromatography (heptane:EtOAc = 7:1) to afford **4i** as a yellow solid (148 mg, 65%).

^1H NMR (400 MHz, CDCl_3): δ 8.22 (d, $J = 8.3$ Hz, 1H), 7.83 – 7.72 (m, 3H), 7.67 (t, $J = 7.9$ Hz, 1H), 7.58 (t, $J = 7.4$ Hz, 1H), 7.50 – 7.41 (m, 3H).

These data are consistent with the previously reported characterization.²²

Preparation of ethyl 2-(2-benzoylphenyl)acetate (**4j**)



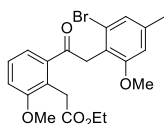
4j

The cross-coupling reaction of **3a** (1 equiv, 300 mg, 1 mmol) with **6b** (1.5 equiv, 3 mL, 1.5 mmol, 0.5 M in THF) was performed according to **TP4** at room temperature in 1 h. The crude was purified silica gel chromatography (heptane:EtOAc = 6:1) to afford **4j** as a yellow oil (255 mg, 95%).

^1H NMR (400 MHz, CDCl_3): δ 7.82 (d, $J = 7.8$ Hz, 2H), 7.61 – 7.54 (m, 1H), 7.51 – 7.42 (m, 3H), 7.41 – 7.30 (m, 3H), 4.02 (q, $J = 7.1$ Hz, 2H), 3.89 (s, 2H), 1.11 (t, $J = 7.1$ Hz, 3H).

These data are consistent with the previously reported characterization.²³

Preparation of ethyl 2-(2-(2-(2-bromo-6-methoxy-4-methylphenyl)acetyl)-6-methoxyphenyl)acetate (**4k**)



4k

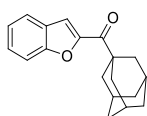
The cross-coupling reaction of **3j** (1 equiv, 330 mg, 1 mmol) with **6c** (1.5 equiv, 2.63 mL, 1.5 mmol, 0.57 M in THF) was performed according to **TP4** at room temperature in 1 h. the crude was purified silica gel chromatography (heptane:EtOAc = 5:1) to afford **4k** as a white solid (357 mg, 82%).

¹H NMR (400 MHz, CDCl₃): δ 7.35 – 7.33 (m, 2H), 7.07 – 7.01 (m, 2H), 6.66 (d, J = 1.4 Hz, 1H), 4.15 (s, 2H), 4.13 (q, J = 7.1 Hz, 2H), 3.95 (s, 2H), 3.83 (s, 3H), 3.79 (s, 3H), 2.27 (s, 3H), 1.24 (t, J = 7.1 Hz, 3H).

¹³C NMR (101 MHz, CDCl₃): δ 201.27, 171.89, 158.34, 139.44, 133.90, 128.04, 125.77, 125.65, 125.56, 123.11, 120.62, 113.93, 110.76, 60.70, 56.11, 55.91, 47.91, 31.40, 15.57, 14.37.

HRMS (ESI): m/z calcd. for C₂₁H₂₃BrO₅ [M]⁺: 434.0729, found: 434.0709.

Preparation of adamantan-1-yl(benzofuran-2-yl)methanone (**4l**)



4l

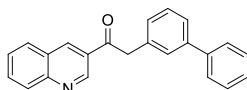
The cross-coupling reaction of **3k** (1 equiv, 254 mg, 1 mmol) with **6d** (1.5 equiv, 6.5 mL, 1.5 mmol, 0.23 M in THF) was performed according to **TP4** at room temperature in 3 h. The crude was purified silica gel chromatography (heptane:EtOAc = 8:1) to afford **4l** as a white solid (149 mg, 53%).

¹H NMR (500 MHz, CDCl₃): δ 7.29 – 7.14 (m, 4H), 6.94 – 6.85 (m, 1H), 1.97 – 1.30 (m, 15H).

¹³C NMR (126 MHz, CDCl₃): δ 202.32, 134.74, 129.46, 129.23, 128.92, 127.11, 121.16, 110.11, 86.48, 58.76, 43.75, 39.78, 39.19, 36.90, 36.30, 36.11, 30.11, 28.64, 28.40.

HRMS (ESI): m/z calcd. for C₁₉H₂₀O₂ [M]⁺: 280.1463, found: 280.1472.

Preparation of 2-([1,1'-biphenyl]-3-yl)-1-(quinolin-3-yl)ethanone (**4m**)



4m

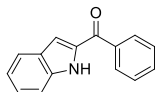
The cross-coupling reaction of **3l** (1 equiv, 265 mg, 1 mmol) with **6e** (1.5 equiv, 2.73 mL, 1.5 mmol, 0.55 M in THF) was performed according to **TP4** at room temperature in 3 h. The crude was purified silica gel chromatography (heptane:EtOAc = 2:1) to afford **4m** as a yellow solid (265 mg, 82%).

¹H NMR (400 MHz, CDCl₃): δ 9.50 (d, J = 2.3 Hz, 1H), 8.80 (d, J = 1.8 Hz, 1H), 8.19 – 8.13 (m, 1H), 7.94 (dd, J = 8.2, 1.4 Hz, 1H), 7.84 (dtd, J = 8.5, 6.9, 1.5 Hz, 1H), 7.63 (dtd, J = 8.1, 6.9, 1.2 Hz, 1H), 7.59 – 7.54 (m, 3H), 7.51 (dt, J = 7.7, 1.5 Hz, 1H), 7.45 – 7.40 (m, 3H), 7.37 – 7.29 (m, 2H), 4.48 (s, 2H).

¹³C NMR (101 MHz, CDCl₃): δ 196.40, 149.98, 149.56, 142.11, 140.94, 137.80, 134.38, 132.23, 129.64, 129.55, 129.43, 129.03, 128.89, 128.45, 128.44, 127.73, 127.57, 127.35, 127.03, 126.26, 46.15.

HRMS (ESI): m/z calcd. for $C_{23}H_{17}NO$ $[M]^+$: 323.1310, found: 323.1295.

Preparation of (1H-indol-2-yl)(phenyl)methanone (4n)



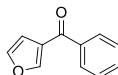
4n

The cross-coupling reaction of **3m** (1 equiv, 259 mg, 1 mmol) with **6b** (1.5 equiv, 3 mL, 1.5 mmol, 0.5 M in THF) was performed according to **TP4** at room temperature in 1 h. The crude was purified silica gel chromatography (heptane:EtOAc = 6:1) to afford **4n** as a white solid (210 mg, 95%).

1H NMR (400 MHz, DMSO- d_6): δ 11.99 (s, 1H), 7.98 – 7.90 (m, 2H), 7.74 – 7.64 (m, 2H), 7.62 – 7.50 (m, 3H), 7.32 (dtd, J = 8.3, 6.9, 1.2 Hz, 1H), 7.16 – 7.07 (m, 2H).

These data are consistent with the previously reported characterization.²⁴

Preparation of furan-3-yl(phenyl)methanone (4o)



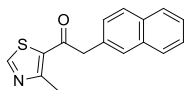
4o

The cross-coupling reaction of **3n** (1 equiv, 204 mg, 1 mmol) with **6b** (1.5 equiv, 3 mL, 1.5 mmol, 0.5 M in THF) was performed according to **TP4** at room temperature in 1 h. The crude was purified silica gel chromatography (heptane:EtOAc = 8:1) to afford **4o** as a colorless oil (160 mg, 93%).

1H NMR (400 MHz, $CDCl_3$): δ 7.91 (dd, J = 1.4, 0.9 Hz, 1H), 7.87 – 7.81 (m, 2H), 7.61 – 7.53 (m, 1H), 7.50 – 7.44 (m, 3H), 6.90 (dd, J = 1.9, 0.8 Hz, 1H).

These data are consistent with the previously reported characterization.²⁵

Preparation of 1-(4-methylthiazol-5-yl)-2-(naphthalen-2-yl)ethanone (4p)



4p

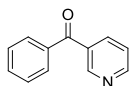
The cross-coupling reaction of **3o** (1 equiv, 235 mg, 1 mmol) with **6f** (1.5 equiv, 2.54 mL, 1.5 mmol, 0.59 M in THF) was performed according to **TP4** at room temperature in 1 h. The crude was purified silica gel chromatography (heptane:EtOAc = 4:1) to afford **4p** as a white solid (205 mg, 77%).

1H NMR (400 MHz, $CDCl_3$): δ 8.93 (s, 1H), 7.90 – 7.71 (m, 4H), 7.52 – 7.46 (m, 2H), 7.38 (dd, J = 8.4, 1.8 Hz, 1H), 4.31 (s, 2H), 2.80 (s, 3H).

^{13}C NMR (101 MHz, CDCl_3): δ 190.53, 135.05, 133.67, 132.78, 130.83, 129.61, 128.75, 128.57, 127.87, 127.84, 127.42, 126.53, 126.26, 125.94, 50.47, 17.93.

HRMS (ESI): m/z calcd. for $\text{C}_{16}\text{H}_{13}\text{NOS}$ $[\text{M}]^+$: 267.0718, found: 267.0702.

Preparation of phenyl(pyridin-3-yl)methanone (**4q**)



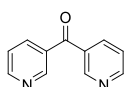
4q

The cross-coupling reaction of **3b** (1 equiv, 214 mg, 1 mmol) with **6g** (1.5 equiv, 5 mL, 1.5 mmol, 0.3 M in THF) was performed according to **TP4** at room temperature in 3 h. The crude was purified silica gel chromatography (heptane:EtOAc = 2:1) to afford **4q** as a colorless oil (161 mg, 88%).

^1H NMR (400 MHz, CDCl_3): δ 8.99 (s, 1H), 8.87 – 8.76 (m, 1H), 8.11 (dt, J = 7.9, 2.0 Hz, 1H), 7.85 – 7.78 (m, 2H), 7.66 – 7.60 (m, 1H), 7.56 – 7.48 (m, 2H), 7.44 (dd, J = 7.7, 4.9 Hz, 1H).

These data are consistent with the previously reported characterization.²⁶

Preparation of di(pyridin-3-yl)methanone (**4r**)



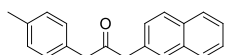
4r

The cross-coupling reaction of **3p** (1 equiv, 215 mg, 1 mmol) with **6g** (1.5 equiv, 5 mL, 1.5 mmol, 0.3 M in THF) was performed according to **TP4** at room temperature in 3 h. The crude was purified silica gel chromatography (DCM:MeOH = 30:1) to afford **4r** as a white solid (136 mg, 74%).

^1H NMR (400 MHz, Methanol- d_4): δ 8.96 (dd, J = 2.2, 0.9 Hz, 2H), 8.82 (dd, J = 5.0, 1.7 Hz, 2H), 8.29 – 8.22 (m, 2H), 7.68 - 7.61 (m, 2H).

These data are consistent with the previously reported characterization.²⁷

Preparation of 1-(naphthalen-2-yl)-3-(p-tolyl)propan-2-one (**4s**)



4s

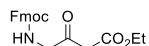
The cross-coupling reaction of **3q** (1 equiv, 242 mg, 1 mmol) with **6f** (1.5 equiv, 2.54 mL, 1.5 mmol, 0.59 M in THF) was performed according to **TP4** at room temperature in 1 h. The crude was purified silica gel chromatography (heptane:EtOAc = 10:1) to afford **4s** as a yellow solid (236 mg, 86%).

^1H NMR (400 MHz, CDCl_3): δ 7.88 – 7.76 (m, 3H), 7.65 – 7.59 (m, 1H), 7.54 – 7.43 (m, 2H), 7.29 (dd, J = 8.4, 1.8 Hz, 1H), 7.19 – 7.04 (m, 4H), 3.89 (s, 2H), 3.73 (s, 2H), 2.36 (s, 3H).

^{13}C NMR (101 MHz, CDCl_3): δ 205.97, 136.86, 133.70, 132.59, 131.79, 131.06, 129.58, 129.54, 128.48, 128.40, 127.81, 127.75, 127.65, 126.32, 125.94, 49.24, 49.01, 21.20.

HRMS (ESI): m/z calcd. for $\text{C}_{20}\text{H}_{18}\text{O}$ $[\text{M}]^+$: 274.1358, found: 274.135.

Preparation of ethyl 4-(((9H-fluoren-9-yl)methoxy)carbonyl)amino)-3-oxobutanoate (**4t**)



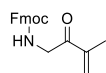
4t

The cross-coupling reaction of **3r** (1 equiv, 390 mg, 1 mmol) with **6h** (1.5 equiv, 2.03 mL, 1.5 mmol, 0.74 M in THF) was performed according to **TP4** at room temperature for 2h. The crude was purified silica gel chromatography (heptane:EtOAc = 3:1) to afford **4t** as a yellow solid (320 mg, 87%).

^1H NMR (400 MHz, CDCl_3): δ 7.77 (d, J = 7.5 Hz, 2H), 7.60 (d, J = 7.4 Hz, 2H), 7.40 (t, J = 7.3 Hz, 2H), 7.34 – 7.29 (m, 2H), 5.47 (s, 1H), 4.41 (d, J = 7.0 Hz, 2H), 4.25 – 4.18 (m, 5H), 3.49 (s, 2H), 1.30 (d, J = 7.1 Hz, 3H).

These data are consistent with the previously reported characterization.²⁸

Preparation of (9H-fluoren-9-yl)methyl (3-methyl-2-oxobut-3-en-1-yl)carbamate (**4u**)



4u

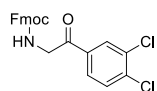
The cross-coupling reaction of **3r** (1 equiv, 390 mg, 1 mmol) with **6i** (1.5 equiv, 4.55 mL, 1.5 mmol, 0.33 M in THF) was performed according to **TP4** at room temperature for 1h. The crude was purified silica gel chromatography (heptane:EtOAc = 6:1) to afford **4u** as a yellow solid (286 mg, 89%).

^1H NMR (400 MHz, CDCl_3): δ 7.77 (d, J = 7.5 Hz, 2H), 7.62 (d, J = 7.5 Hz, 2H), 7.43 - 7.38 (m, 2H), 7.35 - 7.29 (m, 2H), 6.03 (s, 1H), 5.87 (s, 1H), 5.69 (s, 1H), 4.45 (d, J = 4.5 Hz, 2H), 4.40 (d, J = 7.2 Hz, 2H), 4.25 (t, J = 7.2 Hz, 1H), 1.94 (s, 3H).

^{13}C NMR (101 MHz, CDCl_3): δ 195.66, 156.34, 144.01, 142.38, 141.43, 127.82, 127.19, 125.83, 125.23, 120.09, 77.48, 77.16, 76.84, 67.28, 47.31, 47.07, 17.48.

HRMS (ESI): m/z calcd. for $\text{C}_{20}\text{H}_{19}\text{NO}_3$ $[\text{M}]^+$: 321.1365, found: 321.1361.

Preparation of (9H-fluoren-9-yl)methyl (2-(3,4-dichlorophenyl)-2-oxoethyl)carbamate (**4v**)



4v

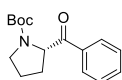
The cross-coupling reaction of **3r** (1 equiv, 390 mg, 1 mmol) with **6j** (1.5 equiv, 3.49 mL, 1.5 mmol, 0.43 M in THF) was performed according to **TP4** at room temperature in 1 h. The crude was purified silica gel chromatography (heptane:EtOAc = 5:1) to afford **4v** as a white solid (358 mg, 84%).

¹H NMR (400 MHz, CDCl₃): δ 8.06 (d, J = 2.0 Hz, 1H), 7.81 - 7.75 (m, 3H), 7.65 - 7.59 (m, 3H), 7.41 (t, J = 7.3 Hz, 2H), 7.33 (t, J = 7.3 Hz, 2H), 5.75 (s, 1H), 4.69 (d, J = 4.6 Hz, 2H), 4.44 (d, J = 7.1 Hz, 2H), 4.26 (t, J = 7.0 Hz, 1H).

¹³C NMR (101 MHz, CDCl₃): δ 192.29, 156.35, 143.97, 141.51, 138.99, 134.06, 134.03, 131.26, 130.06, 127.91, 127.26, 126.94, 125.23, 120.16, 67.48, 48.06, 47.36.

HRMS (ESI): m/z calcd. for C₂₃H₁₇Cl₂NO₃ [M]⁺: 425.0585, found: 425.0564.

Preparation of (S)-tert-butyl 2-benzoylpyrrolidine-1-carboxylate (**4w**)



4w

The cross-coupling reaction of **3s** (1 equiv, 307 mg, 1 mmol) with **6b** (1.5 equiv, 3 mL, 1.5 mmol, 0.5 M in THF) was performed according to **TP4** at room temperature in 1 h. The crude was purified silica gel chromatography (heptane:EtOAc = 15:1) to afford **4w** as a white solid (242 mg, 88%).

¹H NMR (400 MHz, CDCl₃): δ 8.01 - 7.90 (m, 2H), 7.60 - 7.51 (m, 1H), 7.50 - 7.39 (m, 2H), 5.32 (dd, J = 9.3, 2.9 Hz, 0.4 H), 5.18 (dd, J = 8.7, 3.7 Hz, 0.6 H), 3.73 - 3.41 (m, 2H), 2.42 - 2.19 (m, 1H), 2.01 - 1.85 (m, 3H), 1.45 (s, 3.5H), 1.25 (s, 5.5H).

These data are consistent with the previously reported characterization.²⁹

V. Generation of POxAPs with the Addition of PhOH

(A) An oven-dried 20 mL microwave vial equipped with a magnetic stirrer was charged with phenol (1 equiv, 13.4 mg, 0.14 mmol), PdCl₂(PPh₃)₂ (1 equiv, 100 mg, 0.14 mmol), THF (2 mL) and toluene (2 mL). The vial was properly sealed and the mixture vessel was evacuated and backfilled with argon thrice. After stirring for 1 h, 0.5 mL of the reaction mixture was transferred into an argon-prefilled NMR tube by syringe and the solvent was removed under high vacuum. The NMR tube was then backfilled with argon and 0.5 mL CDCl₃ was added. ¹H NMR of this crude showed phenol did not react with PdCl₂(PPh₃)₂ in the absence of organozinc reagent (**Figure S2 A**).

(B) An oven-dried 20 mL microwave tube equipped with a magnetic stirrer was charged with phenol (1 equiv, 13.4 mg, 0.14 mmol), PdCl₂(PPh₃)₂ (1 equiv, 100 mg, 0.14 mmol), THF (2 mL), toluene (2 mL) and sealed. The vial was properly sealed and the mixture vessel was evacuated and backfilled with argon thrice. **6a** (1 equiv 0.17 mL, 0.14 mmol, 0.82 M in THF) was added dropwise to the mixture at room temperature. After stirring for 1 h, 0.5 mL of the reaction mixture was transferred into an argon-prefilled NMR tube by syringe and the solvent was removed under high vacuum. The NMR tube was then backfilled with argon and 0.5 mL CDCl₃ was added. ¹H NMR of this crude showed the formation of a new compound compared to the control group (**Figure S2 B**).

(C) The rest of the forementioned reaction mixture was concentrated in vacuo. Toluene (5 mL) was added to the crude and cooled to 0 °C. The suspension was filtered. The filtrate was evaporated to dryness, the resulting product was washed with ether (2×5 mL) and dried under reduced pressure. Recrystallization from a CHCl₃–Et₂O solution at room temperature gave yellow crystals (11.5 mg, 11%). The ¹H NMR and X-ray crystallography results were consistent with the previously reported data, indicating that the identity of these crystals was PdCl(Ph)(PPh₃)₂ (**Figure S2 C**).

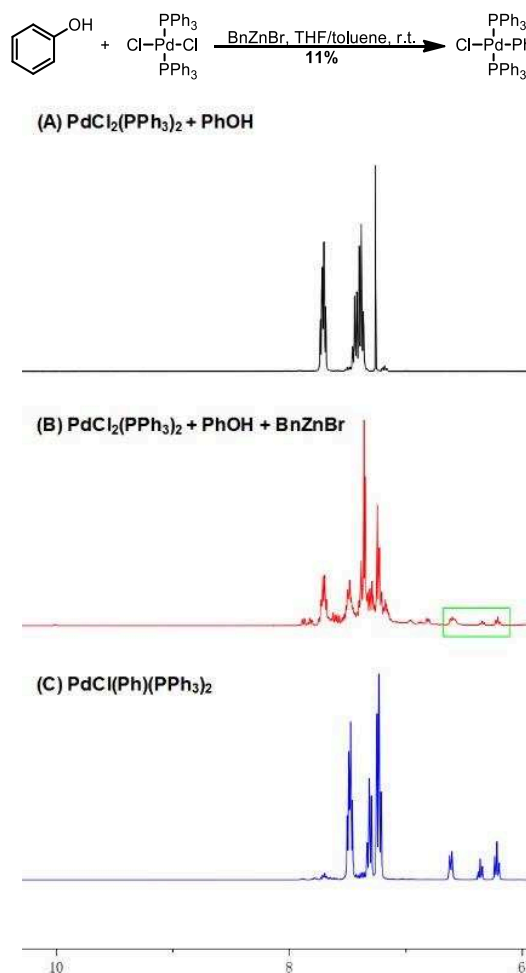
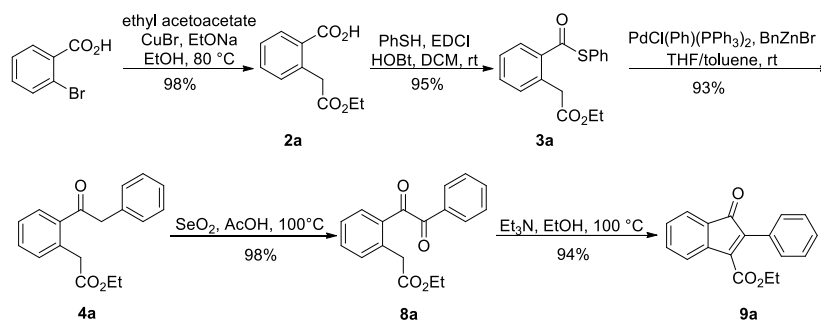
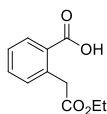


Figure S2. Generation of POxAPs with PhOH and BnZnBr

VI. Synthesis of the unsubstituted IPK precursor **9a**



Preparation of 2-(2-ethoxy-2-oxoethyl)benzoic acid (**2a**)



2a

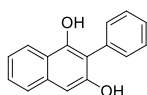
To a dry flask filled with Ar was added EtONa (3 equiv, 1.52 g, 22.4 mmol) and anhydrous EtOH (30 mL). The suspension was sonicated until it became a clear solution. Ethyl acetoacetate (2 equiv, 1.89 mL, 14.9 mmol) was added and the mixture was stirred at room temperature for 10 min. Then, CuBr (0.1 eq., 107 mg, 0.75 mmol) and 2-bromo-3-methoxybenzoic acid (1 equiv, 1.5 g, 7.46 mmol) were added and the reaction mixture was reflux under Ar at 80 °C for 16h. After completion, the reaction mixture was concentrated in vacuo, then acidified by 1N HCl (50 mL) and extracted with EtOAc (3 × 20 mL). The combined organic phase was washed with brine, dried over anhydrous Na₂SO₄ and filtered through a celite pad. The filtrate was concentrated in vacuo to afford **2a** as a white solid (1.52 g, 98 %).

¹H NMR (400 MHz, CDCl₃): δ 8.13 (d, J = 7.8 Hz, 1H), 7.54 (t, J = 7.5 Hz, 1H), 7.40 (t, J = 7.6 Hz, 1H), 7.28 (d, J = 7.6 Hz, 1H), 4.17 (q, J = 7.1 Hz, 2H), 4.04 (s, 2H), 1.26 (t, J = 7.1 Hz, 3H).

These data are consistent with the previously reported characterization.³⁰

Preparation of **3a**, BnZnBr and **4a** see Part IV. POxAPs Catalyzed Fuyayama Cross-Coupling Reactions.

Preparation of 2-phenylnaphthalene-1,3-diol (**5a**)



5a

The solution of **3a** (1 equiv, 50 mg, 0.17 mmol) and PdCl₂(PPh₃)₂ (1 mol %, 1.2 mg, 1.7×10⁻³ mmol) in toluene (0.3 mL) was degassed and backfilled with argon thrice. Then, a solution of benzyl zinc bromide **6a** (1.5 equiv, 0.3 mL, 0.25 mmol, 0.82 M in THF) in THF was added dropwise at room temperature.

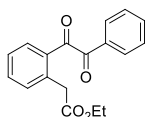
After stirring at 50 °C for 15 min, the reaction mixture was quenched with saturated NH₄Cl solution (5 mL) and extracted with EtOAc (5 mL) thrice. The combined organic phases were dried over anhydrous Na₂SO₄ and concentrated in vacuo. The crude was purified by silica gel column (heptane:EtOAc = 3:1) to afford **5a** as a yellow solid (24.9 mg, 62%), along with 8.1 mg **3a** and 10.7 mg **4a**.

¹H NMR (400 MHz, CDCl₃): δ 8.14 (d, J = 8.3 Hz, 1H), 7.70 – 7.60 (m, 3H), 7.55 – 7.43 (m, 4H), 7.34 (t, J = 7.6 Hz, 1H), 6.96 (s, 1H), 5.45 (s, 1H), 4.89 (s, 1H).

¹³C NMR (101 MHz, CDCl₃): δ 151.08, 149.29, 134.74, 131.29, 131.06, 130.57, 129.59, 127.39, 126.30, 123.19, 122.62, 119.82, 113.43, 102.34.

HRMS (ESI): m/z calcd. for C₁₆H₁₂O₂ [M]⁺: 236.0837, found: 236.0839

Preparation of ethyl 2-(2-(2-oxo-2-phenylacetyl)phenyl)acetate (**8a**)



8a

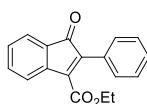
A solution of **4a** (1 equiv, 200 mg, 0.71 mmol) and SeO₂ (2 equiv, 157 mg, 1.42 mmol) in acetic acid (5 mL) was stirred at 100 °C for 2h. The reaction mixture was filtered through a silica gel pad with EtOAc, the filtrate was concentrated in vacuo to afford **8a** as a yellow solid (206 mg, 98%).

¹H NMR (400 MHz, CDCl₃): δ 8.03 – 7.90 (m, 2H), 7.70 (d, J = 7.8 Hz, 1H), 7.64 (t, J = 7.4 Hz, 1H), 7.61 – 7.55 (m, 1H), 7.51 (t, J = 7.7 Hz, 2H), 7.38 (t, J = 6.9 Hz, 2H), 4.21 (q, J = 7.1 Hz, 2H), 4.13 (s, 2H), 1.29 (t, J = 7.1 Hz, 3H).

¹³C NMR (101 MHz, CDCl₃): δ 196.87, 194.50, 171.19, 136.99, 134.89, 134.29, 133.97, 133.42, 133.27, 131.66, 130.19, 129.12, 127.78, 61.07, 40.72, 14.38.

HRMS (ESI): m/z calcd. for C₁₈H₁₆O₄ [M]⁺: 296.1049, found: 296.1044.

Preparation of ethyl 1-oxo-2-phenyl-1H-indene-3-carboxylate (**9a**)



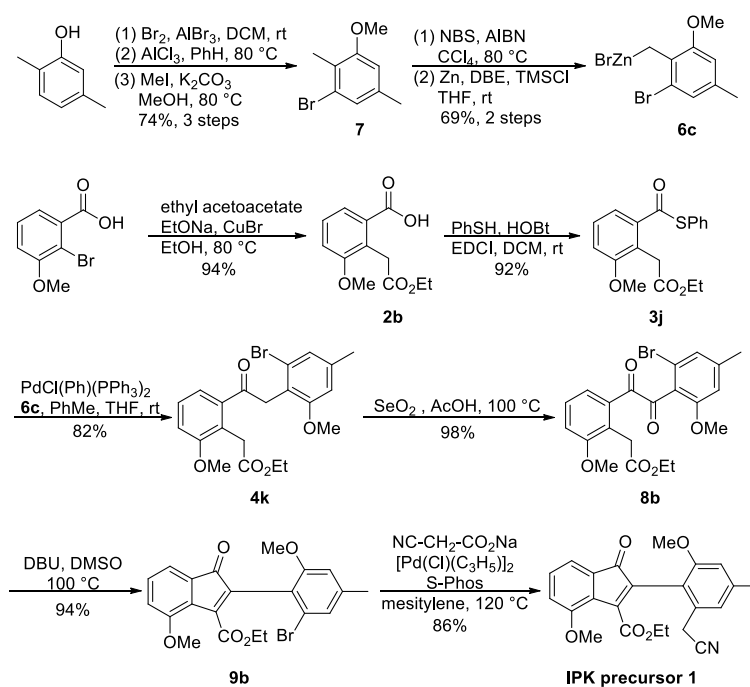
9a

A solution of **8a** (1 equiv, 200 mg, 0.68 mmol) and TEA (5 equiv, 0.47 mL, 3.37 mmol) in anhydrous EtOH (5 mL) was stirred at 100 °C for 5 h. The mixture was concentrated in vacuo and purified by silica gel column (Heptane:EtOAc=15:1) to afford **9a** as an orange solid (179 mg, 95 %).

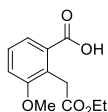
¹H NMR (400 MHz, CDCl₃): δ 7.56 (dd, J = 12.6, 7.3 Hz, 2H), 7.49 – 7.38 (m, 6H), 7.29 (t, J = 7.4 Hz, 1H), 4.32 (q, J = 7.1 Hz, 2H), 1.23 (t, J = 7.1 Hz, 3H).

These data are consistent with the previously reported characterization.³¹

VII. Synthesis of IPK precursor 1



Preparation of 2-(2-ethoxy-2-oxoethyl)-3-methoxybenzoic acid (2b)



2b

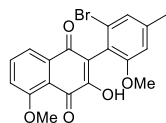
To an oven-dried flask filled with Argon was added EtONa (3 equiv, 1.33 g, 19.5 mmol) and anhydrous EtOH (25 mL). The suspension was sonicated until it became a clear solution. Ethyl acetoacetate (2 equiv, 1.64 mL, 13 mmol) was added and the mixture was stirred at room temperature for 10 min. Then, CuBr (0.1 eq., 93.1 mg, 0.65 mmol) and 2-bromo-3-methoxybenzoic acid (1 equiv, 1.5 g, 6.49 mmol) were added and the reaction mixture was reflux under Ar at 80°C for 16h. After completion, the reaction mixture was concentrated in vacuo, then acidified by 1N HCl (50 mL) and extracted with EtOAc (3×20 mL). The combined organic phase was washed with brine, dried over anhydrous Na_2SO_4 and filtered through a celite pad. The filtrate was concentrated in vacuo to afford **2b** as a white solid (1.45 g, 94 %).

$^1\text{H NMR}$ (400 MHz, CDCl_3): δ 7.69 (d, $J = 7.8$ Hz, 1H), 7.34 (t, $J = 8.1$ Hz, 1H), 7.11 (d, $J = 8.2$ Hz, 1H), 4.20 - 4.13 (d, $J = 6.9$ Hz, 4H), 3.85 (s, 3H), 1.26 (t, $J = 7.1$ Hz, 3H).

These data are consistent with the previously reported characterization.³²

Preparation of 3j, 6c and 4k see Part IV. POxAPs Catalyzed Fuyayama Cross-Coupling Reactions.

Preparation of 2-(2-bromo-6-methoxy-4-methylphenyl)-3-hydroxy-5-methoxynaphthalene-1,4-dione (**5b**)



5b

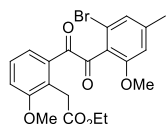
The solution of **3j** (1 equiv, 50 mg, 0.15 mmol) and PdCl₂(PPh₃)₂ (1 mol %, 1.1 mg, 1.5 × 10⁻³ mmol) in toluene (0.4 mL) was degassed and backfilled with argon thrice. Then, a solution of **6c** (1.5 equiv, 0.4 mL, 0.23 mmol, 0.57 M in THF) in THF was added dropwise at room temperature. After stirring at 50 °C for 25 min, the reaction mixture was quenched with saturated NH₄Cl solution (5 mL) and extracted with EtOAc (5 mL) thrice. The combined organic phases were dried over anhydrous Na₂SO₄ and concentrated in vacuo. The crude was purified by silica gel column (heptane:EtOAc = 1:1) to afford **5b** as a red solid (44 mg, 72%), along with 9.2 mg **3j** and 5.2 mg **4k**.

¹H NMR (400 MHz, CDCl₃): δ 7.86 (d, J = 7.1 Hz, 1H), 7.73 (t, J = 8.1 Hz, 1H), 7.28 (d, J = 8.4 Hz, 1H), 7.12 (s, 1H), 6.73 (s, 1H), 4.06 (s, 3H), 3.72 (s, 3H), 2.36 (s, 3H).

¹³C NMR (101 MHz, CDCl₃): δ 182.40, 179.99, 160.46, 158.11, 153.74, 141.36, 136.68, 135.54, 125.40, 124.57, 120.27, 118.66, 118.19, 117.40, 116.89, 111.20, 56.70, 56.23, 21.65.

HRMS (ESI): m/z calcd. for C₁₉H₁₅BrO₅ [M]⁺: 402.0103, found: 402.0086

Preparation of ethyl 2-(2-(2-(2-bromo-6-methoxy-4-methylphenyl)-2-oxoacetyl)-6-methoxyphenyl)acetate (**8b**)



8b

A solution of **4k** (1 equiv, 300 mg, 0.69 mmol) and SeO₂ (2 equiv, 152 mg, 1.38 mmol) in acetic acid (5 mL) was stirred at 100 °C for 2h. The reaction mixture was filtered through a silica gel pad with EtOAc, the filtrate was concentrated in vacuo to afford **8b** as a yellow solid (304 mg, 98%).

¹H NMR (400 MHz, CDCl₃): δ 7.45 (dd, J = 7.9, 1.1 Hz, 1H), 7.37 (t, J = 8.0 Hz, 1H), 7.18 – 7.09 (m, 2H), 6.68

(s, 1H), 4.13 (q, J = 7.1 Hz, 2H), 4.07 (s, 2H), 3.87 (s, 3H), 3.61 (s, 3H), 2.36 (s, 3H), 1.23 (t, J = 7.1 Hz, 3H).

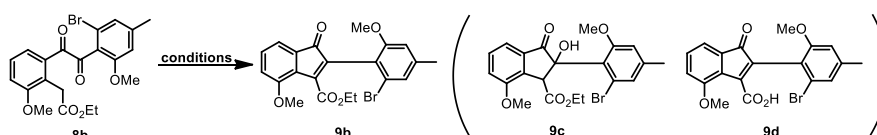
¹³C NMR (101 MHz, CDCl₃): δ 192.14, 171.45, 160.42, 158.49, 145.31, 132.68, 127.71, 127.70, 125.95, 125.16, 123.52, 122.66, 115.37, 111.81, 60.63, 56.23, 56.21, 32.08, 21.86, 14.38.

HRMS (ESI): m/z calcd. for C₂₁H₂₁BrO₆ [M]⁺: 448.0522, found: 448.0495.

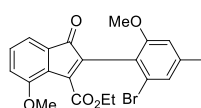
Preparation of ethyl 2-(2-bromo-6-methoxy-4-methylphenyl)-4-methoxy-1-oxo-1H-indene-3-carboxylate (**9b**)

Several conditions were tried for the preparation of **9b** from **8b** (Table S2). With TEA/EtOH, which was used in the synthesis of **9a**, we did not obtain **9b**, but **9c** in 94% yield (Table S2, entry 1). With the addition of PTSA or DBU to **9c** no formation of **9b** was observed (Table S2, entries 2 and 3). Strong bases such as EtONa or NaH produced a mixture of **9c** and **9d** (Table S2, entries 4 and 5). Finally, DBU in hot DMSO were tried and furnished **9b** in 94% yield.

Table S2. Cyclization of **8b**



Entry	Conditions	9b (%)	9c (%)	9d (%)
1	TEA, EtOH, 100 °C	0	94	0
2	(1) TEA, EtOH, 100 °C; (2) PTSA, toluene or EtOH, 100 °C	0	92	0
3	(1) TEA, EtOH, 100 °C; (2) DBU, toluene, 80 °C	0	96	0
4	EtONa, EtOH, 100 °C	0	73	13
5	NaH, THF, rt	0	65	9
6	DBU, DMSO, 100 °C	94	0	0



9b

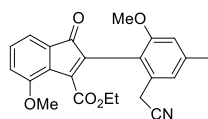
A solution of **8b** (1 equiv, 300 mg, 0.67 mmol) and DBU (1.2 equiv, 0.12 mL, 0.8 mmol) in anhydrous DMSO (5 mL) was stirred at 100 °C for 8 h. The mixture was concentrated under high vacuum and purified by silica gel column (Heptane:EtOAc = 4:1) to afford **9b** as a yellow solid (271 mg, 94 %).

¹H NMR (400 MHz, MeOD) δ 7.37 (dd, J = 8.5, 7.0 Hz, 1H), 7.23 (dd, J = 8.5, 0.8 Hz, 1H), 7.16 (dd, J = 7.0, 0.8 Hz, 1H), 7.07 (dd, J = 1.5, 0.8 Hz, 1H), 6.84 (s, 1H), 4.19 (q, J = 7.1 Hz, 2H), 3.88 (s, 3H), 3.73 (s, 3H), 2.36 (s, 3H), 1.15 (t, J = 7.1 Hz, 3H).

¹³C NMR (101 MHz, MeOD) δ 196.12, 166.70, 160.14, 154.59, 149.63, 143.06, 133.89, 133.00, 132.28, 129.10, 125.81, 125.28, 120.80, 119.09, 117.48, 111.84, 62.33, 56.63, 56.49, 21.44, 14.28.

HRMS (ESI): m/z calcd. for C₂₁H₁₉BrO₅ [M]⁺: 430.0416, found: 430.0428.

Preparation of ethyl 2-(2-(cyanomethyl)-6-methoxy-4-methylphenyl)-4-methoxy-1-oxo-1H-indene-3-carboxylate (**1**)



1

A mixture of **9b** (1 equiv, 180 mg, 0.417 mmol), sodium 2-cyanoacetate (1.5 equiv, 67 mg, 0.626 mmol), allylpalladium(II) chloride dimer (2 mol %, 3.12 mg, 0.00835 mmol) and SPhos (6 mol %, 10.6 mg, 0.025 mmol) in mesitylene (3 mL) was stirred under Argon at room temperature for 10 min and then stirred in a preheated heating plate at 120 °C for 16 h. The reaction mixture was loaded to the silica gel column and flushed with heptane (300 mL) to remove mesitylene, then eluted with heptane:EtOAc = 3:1 to afford **1** as an orange solid (140 mg, 0.358 mmol, 86 %).

¹H NMR (400 MHz, CDCl₃): δ 7.30 (dd, J = 8.4, 7.1 Hz, 1H), 7.20 (dd, J = 7.0, 0.8 Hz, 1H), 7.06 – 7.01 (m, 1H), 6.97 (s, 1H), 6.69 (s, 1H), 4.28 – 4.18 (m, 2H), 3.86 (s, 3H), 3.78 – 3.61 (m, 5H), 2.38 (s, 3H), 1.19 (t, J = 7.1 Hz, 3H).

¹³C NMR (101 MHz, CDCl₃): δ 195.36, 165.56, 158.33, 153.06, 148.97, 141.12, 131.87, 131.39, 131.02, 130.56, 128.22, 121.24, 119.13, 118.05, 117.14, 115.39, 111.51, 61.60, 56.07, 55.98, 22.12, 21.92, 14.11.
HRMS (ESI): m/z calcd. for C₂₃H₂₁NO₅ [M]⁺: 391.1420, found: 391.1416.

VIII. References

- (1) (a) Flemming, J. P.; Pilon, M. C.; Borbulevitch, O. Y.; Antipin, M. Y.; Grushin, V. V. *Inorg. Chim. Acta* **1998**, 280, 87-98. (b) Herrmann, W. A.; Broßmer, C.; Priermeier, T.; Öfele, K. *J. Organomet. Chem.* **1994**, 481, 97-108.
- (2) Krasovskiy, A.; Knochel, P. *Synthesis* **2006**, 2006, 0890-0891.
- (3) Pan, X.; Curran, D. P. *Org. Lett.* **2014**, 16, 2728-2731.
- (4) Zhu, X.; Shi, Y.; Mao, H.; Cheng, Y.; Zhu, C. *Adv. Synth. Catal.* **2013**, 355, 3558-3562.
- (5) Narayanaperumal, S.; Alberto, E. E.; Gul, K.; Kawasoko, C. Y.; Dornelles, L.; Rodrigues, O. E. D.; Braga, A. L. *Tetrahedron* **2011**, 67, 4723-4730.
- (6) Sancineto, L.; Tidei, C.; Bagnoli, L.; Marini, F.; Lippolis, V.; Arca, M.; Lenardão Eder, J.; Santi, C. *Eur. J. Org. Chem.* **2016**, 2016, 2999-3005.
- (7) Katritzky, A. R.; Shestopalov, A. A.; Suzuki, K. *Synthesis* **2004**, 2004, 1806-1813.
- (8) Ichiishi, N.; Malapit, C. A.; Woźniak, Ł.; Sanford, M. S. *Org. Lett.* **2018**, 20, 44-47.
- (9) Du, J.-J.; Gao, X.-F.; Xin, L.-M.; Lei, Z.; Liu, Z.; Guo, J. *Org. Lett.* **2016**, 18, 4828-4831.
- (10) Park, C.-M.; Niu, W.; Liu, C.; Biggs, T. D.; Guo, J.; Xian, M. *Org. Lett.* **2012**, 14, 4694-4697.
- (11) (a) Lin, H.; Xiao, L.-J.; Zhou, M.-J.; Yu, H.-M.; Xie, J.-H.; Zhou, Q.-L. *Org. Lett.* **2016**, 18, 1434-1437. (b) Hirano, Y.; Tokudome, K.; Takikawa, H.; Suzuki, K. *Synlett* **2017**, 28, 214-220.
- (12) Sämann, C.; Dhayalan, V.; Schreiner, P. R.; Knochel, P. *Org. Lett.* **2014**, 16, 2418-2421.
- (13) Peng, Z.; Yu, Z.; Chen, D.-H.; Liang, S.; Zhang, L.; Zhao, D.; Song, L.; Jiang, C. *Synlett* **2017**, 28, 1835-1839.
- (14) Reddy, M. R.; Aidhen, I. S.; Shruthi, K.; Reddy, G. B. *Eur. J. Org. Chem.* **2017**, 2017, 7283-7294.
- (15) Tambar, U. K.; Stoltz, B. M. *J. Am. Chem. Soc.* **2005**, 127, 5340-5341.
- (16) Liang, S.; Hammond, G. B.; Xu, B. *Chem. Commun. (London)* **2015**, 51, 903-906.
- (17) Speckmeier, E.; Padié, C.; Zeitler, K. *Org. Lett.* **2015**, 17, 4818-4821.
- (18) Wong, Y.-C.; Parthasarathy, K.; Cheng, C.-H. *Org. Lett.* **2010**, 12, 1736-1739.
- (19) Wommack, A. J.; Moebius, D. C.; Travis, A. L.; Kingsbury, J. S. *Org. Lett.* **2009**, 11, 3202-3205.
- (20) Mahendar, L.; Satyanarayana, G. J. *Org. Chem.* **2014**, 79, 2059-2074.
- (21) Le Bras, G.; Provot, O.; Peyrat, J.-F.; Alami, M.; Brion, J.-D. *Tetrahedron Lett.* **2006**, 47, 5497-5501.
- (22) Barroso, S.; Blay, G.; Cardona, L.; Fernández, I.; García, B.; Pedro, J. R. *J. Org. Chem.* **2004**, 69, 6821-6829.
- (23) Kovács, S.; Csincsi, Á. I.; Nagy, T. Z.; Boros, S.; Timári, G.; Novák, Z. *Org. Lett.* **2012**, 14, 2022-2025.
- (24) Kamlah, A.; Lirk, F.; Bracher, F. *Tetrahedron* **2016**, 72, 837-845.

- (25) Meng, G.; Lalancette, R.; Szostak, R.; Szostak, M. *Org. Lett.* **2017**, 19, 4656-4659.
- (26) Boudreau, J.; Doucette, M.; Ajjou, A. N. *Tetrahedron Lett.* **2006**, 47, 1695-1698.
- (27) Chen, X.-D.; Mak, T. C. W. *J. Mol. Struct.* **2005**, 743, 1-6.
- (28) Fan, W.; Li, W.; Ma, X.; Tao, X.; Li, X.; Yao, Y.; Xie, X.; Zhang, Z. *J. Org. Chem.* **2011**, 76, 9444-9451.
- (29) Kong, C.; Jana, N.; Driver, T. G. *Org. Lett.* **2013**, 15, 824-827.
- (30) Gopinath, P.; Nilaya, S.; Muraleedharan, K. M. *Org. Lett.* **2011**, 13, 1932-1935.
- (31) Qi, Z.; Wang, M.; Li, X. *Org. Lett.* **2013**, 15, 5440-5443.
- (32) Payne, S. L.; Rodriguez-Aristegui, S.; Bardos, J.; Cano, C.; Golding, B. T.; Hardcastle, I. R.; Peacock, M.; Parveen, N.; Griffin, R. J. *Bioorg. Med. Chem. Lett.* **2010**, 20, 3649-3653.

X. Reference

X. Reference

1. Tadesse, S.; Caldon, E.; Tilley, W.; Wang, S., Cyclin Dependent Kinase 2 Inhibitors in Cancer Therapy: an Update. *Journal of medicinal chemistry* **2018**.
2. Namasivayam, V.; Vanangamudi, M.; Kramer, V. G.; Kurup, S.; Zhan, P.; Liu, X.; Kongsted, J.; Byraredy, S. N., The journey of HIV-1 non-nucleoside reverse transcriptase inhibitors (NNRTIs) from lab to clinic. *Journal of medicinal chemistry* **2018**.
3. Li, Y.; Geng, J.; Liu, Y.; Yu, S.; Zhao, G., Thiadiazole-a promising structure in medicinal chemistry. *ChemMedChem* **2013**, *8*, 27-41.
4. Lesnikowski, Z. J., Challenges and Opportunities for the Application of Boron Clusters in Drug Design. *Journal of medicinal chemistry* **2016**, *59*, 7738-58.
5. Reis, J.; Gaspar, A.; Milhazes, N.; Borges, F., Chromone as a Privileged Scaffold in Drug Discovery: Recent Advances. *Journal of medicinal chemistry* **2017**, *60*, 7941-7957.
6. Yu, L. F.; Zhang, H. K.; Caldarone, B. J.; Eaton, J. B.; Lukas, R. J.; Kozikowski, A. P., Recent developments in novel antidepressants targeting alpha4beta2-nicotinic acetylcholine receptors. *Journal of medicinal chemistry* **2014**, *57*, 8204-23.
7. Vitaku, E.; Smith, D. T.; Njardarson, J. T., Analysis of the structural diversity, substitution patterns, and frequency of nitrogen heterocycles among U.S. FDA approved pharmaceuticals. *Journal of medicinal chemistry* **2014**, *57*, 10257-74.
8. Delost, M. D.; Smith, D. T.; Anderson, B. J.; Njardarson, J. T., From Oxiranes to Oligomers: Architectures of U.S. FDA Approved Pharmaceuticals Containing Oxygen Heterocycles. *Journal of medicinal chemistry* **2018**.
9. Polanski, J.; Kurczyk, A.; Bak, A.; Musiol, R., Privileged Structures - Dream or Reality: Preferential Organization of Azanaphthalene Scaffold. *Current Medicinal Chemistry* **2012**, *19*, 1921-1945.
10. Cho, S.; Kim, S. H.; Shin, D., Recent applications of hydantoin and thiohydantoin in medicinal chemistry. *European journal of medicinal chemistry* **2019**, *164*, 517-545.
11. Gita, C., 1,2,4-Oxadiazole as a Privileged Scaffold for Anti-inflammatory and Analgesic Activities: A Review. *Mini-Reviews in Medicinal Chemistry* **2018**, *18*, 1536-1547.
12. Berthet, M.; Cheviet, T.; Dujardin, G.; Parrot, I.; Martinez, J., Isoxazolidine: A Privileged Scaffold for Organic and Medicinal Chemistry. *Chemical Reviews* **2016**, *116*, 15235-15283.
13. Peng, Z.; Dongyue, L.; Junyi, L.; Xuwang, C.; Xinyong, L., Benzimidazole Heterocycle as a Privileged Scaffold in Antiviral Agents. *Mini-Reviews in Organic Chemistry* **2012**, *9*, 397-410.
14. Rajasekhar, S.; Maiti, B.; Chanda, K., A Decade Update on Benzoxazoles, a Privileged Scaffold in -Synthetic Organic Chemistry. *Synlett* **2017**, *28*, 521-541.
15. Rakesh, K. P.; Shantharam, C. S.; Sridhara, M. B.; Manukumar, H. M.; Qin, H.-L., Benzisoxazole: a privileged scaffold for medicinal chemistry. *MedChemComm* **2017**, *8*, 2023-2039.
16. Yu, J.-S.; Zhou, F.; Liu, Y.-L.; Zhou, J., A Journey in the Catalytic Synthesis of 3-Substituted 3-Amino-oxindoles. *Synlett* **2015**, *26*, 2491-2504.
17. Satyamaheshwar, P., 3-Substituted-3-hydroxy-2-oxindole, an Emerging New Scaffold for Drug Discovery with Potential Anti-Cancer and other Biological Activities. *Current Bioactive Compounds* **2009**, *5*, 20-38.
18. Jacques, P.; Pascal, C.; Evelina, C., 2(3H)-Benzoxazolone and Bioisosters as a Privileged Scaffold in the Design of Pharmacological Probes. *Current Medicinal Chemistry* **2005**, *12*,

877-885.

19. Poonam, T.; Sandeep, C.; Kapil, K.; Ravindra, K. R., Chemical and Medicinal Versatility of Substituted 1,4-Dihydropyridines. *Current Bioactive Compounds* **2017**, *13*, 109-120.
20. Ioan, P.; Carosati, E.; Micucci, M.; Cruciani, G.; Broccatelli, F.; Zhorov, B. S.; Chiarini, A.; Budriesi, R., 1,4-Dihydropyridine Scaffold in Medicinal Chemistry, The Story so Far And Perspectives (Part 1): Action in Ion Channels and GPCRs. *Current Medicinal Chemistry* **2011**, *18*, 4901-4922.
21. Goel, P.; Alam, O.; Naim, M. J.; Nawaz, F.; Iqbal, M.; Alam, M. I., Recent advancement of piperidine moiety in treatment of cancer- A review. *European journal of medicinal chemistry* **2018**, *157*, 480-502.
22. Wijdeven, M. A.; Willemsen, J.; Rutjes, F. P. J. T., The 3-Hydroxypiperidine Skeleton: Key Element in Natural Product Synthesis. *European Journal of Organic Chemistry* **2010**, *2010*, 2831-2844.
23. Musiol, R., An overview of quinoline as a privileged scaffold in cancer drug discovery. *Expert Opinion on Drug Discovery* **2017**, *12*, 583-597.
24. Solomon, V. R.; Lee, H., Quinoline as a Privileged Scaffold in Cancer Drug Discovery. *Current Medicinal Chemistry* **2011**, *18*, 1488-1508.
25. Perlíková, P.; Hocek, M., Pyrrolo[2,3-d]pyrimidine (7-deazapurine) as a privileged scaffold in design of antitumor and antiviral nucleosides. *Medicinal Research Reviews* **2017**, *37*, 1429-1460.
26. Cherukupalli, S.; Karpoomath, R.; Chandrasekaran, B.; Hampannavar, G. A.; Thapliyal, N.; Palakollu, V. N., An insight on synthetic and medicinal aspects of pyrazolo[1,5-a]pyrimidine scaffold. *European journal of medicinal chemistry* **2017**, *126*, 298-352.
27. Goel, R.; Luxami, V.; Paul, K., Synthetic approaches and functionalizations of imidazo[1,2-a]pyrimidines: an overview of the decade. *RSC Advances* **2015**, *5*, 81608-81637.
28. Yu; apos; ning, S.; Peng, Z.; Qingzhu, Z.; Xinyong, L., Privileged Scaffolds or Promiscuous Binders: A Glance of Pyrrolo[2,1-f][1,2,4]triazines and Related Bridgehead Nitrogen Heterocycles in Medicinal Chemistry. *Current Pharmaceutical Design* **2013**, *19*, 1528-1548.
29. Badolato, M.; Aiello, F.; Neamati, N., 2,3-Dihydroquinazolin-4(1H)-one as a privileged scaffold in drug design. *RSC Advances* **2018**, *8*, 20894-20921.
30. THOMAS, N.; ZACHARIAH, S. M., Pharmacological activities of chromene derivatives: an overview. *Asian J Pharm Clin res* **2013**, *6*, 11-15.
31. Ankita, C.; Jitender, M. K., Advances in the Synthesis of Xanthenes: An Overview. *Current Organic Synthesis* **2018**, *15*, 341-369.
32. Stefanachi, A.; Leonetti, F.; Pisani, L.; Catto, M.; Carotti, A., Coumarin: A Natural, Privileged and Versatile Scaffold for Bioactive Compounds. *Molecules* **2018**, *23*, 250.
33. Jameel, E.; Umar, T.; Kumar, J.; Hoda, N., Coumarin: A Privileged Scaffold for the Design and Development of Antineurodegenerative Agents. *Chemical Biology & Drug Design* **2016**, *87*, 21-38.
34. Grover, J.; Jachak, S. M., Coumarins as privileged scaffold for anti-inflammatory drug development. *RSC Advances* **2015**, *5*, 38892-38905.
35. Silva, C. F. M.; Pinto, D. C. G. A.; Silva, A. M. S., Chromones: A Promising Ring System for New Anti-inflammatory Drugs. *ChemMedChem* **2016**, *11*, 2252-2260.
36. Keri, R. S.; Budagumpi, S.; Pai, R. K.; Balakrishna, R. G., Chromones as a privileged scaffold in drug discovery: A review. *European journal of medicinal chemistry* **2014**, *78*, 340-374.
37. Isabelle, T.; Daniela, G., Bispidine as a Privileged Scaffold. *Current Topics in Medicinal Chemistry* **2016**, *16*, 1314-1342.

38. Smith, S. G.; Sanchez, R.; Zhou, M. M., Privileged diazepine compounds and their emergence as bromodomain inhibitors. *Chemistry & biology* **2014**, *21*, 573-83.
39. Butler, M. S.; Robertson, A. A. B.; Cooper, M. A., Natural product and natural product derived drugs in clinical trials. *Natural Product Reports* **2014**, *31*, 1612-1661.
40. Bansode, A. H.; Chimala, P.; Patil, N. T., Catalytic Branching Cascades in Diversity Oriented Synthesis. *ChemCatChem* **2017**, *9*, 30-40.
41. Garcia-Castro, M.; Zimmermann, S.; Sankar, M. G.; Kumar, K., Scaffold Diversity Synthesis and Its Application in Probe and Drug Discovery. *Angewandte Chemie International Edition* **2016**, *55*, 7586-7605.
42. Lenci, E.; Guarna, A.; Trabocchi, A., Diversity-oriented synthesis as a tool for chemical genetics. *Molecules* **2014**, *19*, 16506-28.
43. Collins, I.; Jones, A. M., Diversity-oriented synthetic strategies applied to cancer chemical biology and drug discovery. *Molecules* **2014**, *19*, 17221-55.
44. Kim, J.; Kim, H.; Park, S. B., Privileged structures: efficient chemical "navigators" toward unexplored biologically relevant chemical spaces. *Journal of the American Chemical Society* **2014**, *136*, 14629-38.
45. Mendez-Lucio, O.; Medina-Franco, J. L., The many roles of molecular complexity in drug discovery. *Drug discovery today* **2017**, *22*, 120-126.
46. Lipinski, C. A.; Lombardo, F.; Dominy, B. W.; Feeney, P. J., Experimental and computational approaches to estimate solubility and permeability in drug discovery and development settings. *advanced drug delivery reviews* **1997**, *23*, 3-25.
47. Veber, D. F.; Johnson, S. R.; Cheng, H.-Y.; Smith, B. R.; Ward, K. W.; Kopple, K. D., Molecular Properties That Influence the Oral Bioavailability of Drug Candidates. *Journal of medicinal chemistry* **2002**, *45*, 2615-2623.
48. Bertz, S. H., The first general index of molecular complexity. *J. Am. Chem. Soc.* **1981**, *103*, 3599-3601.
49. Whitlock, H. W., On the Structure of Total Synthesis of Complex Natural Products. *The Journal of Organic Chemistry* **1998**, *63*, 7982-7989.
50. Barone, R.; Chanon, M., A New and Simple Approach to Chemical Complexity. Application to the Synthesis of Natural Products. *Journal of Chemical Information and Computer Sciences* **2001**, *41*, 269-272.
51. Allu, T. K.; Oprea, T. I., Rapid Evaluation of Synthetic and Molecular Complexity for in Silico Chemistry. *Journal of Chemical Information and Modeling* **2005**, *45*, 1237-1243.
52. Lovering, F.; Bikker, J.; Humblet, C., Escape from flatland: increasing saturation as an approach to improving clinical success. *Journal of medicinal chemistry* **2009**, *52*, 6752-6.
53. McGaughey, G. B.; Gagné, M.; Rappé, A. K., π -Stacking Interactions: ALIVE AND WELL IN PROTEINS. *Journal of Biological Chemistry* **1998**, *273*, 15458-15463.
54. Dougherty, D. A., Cation- π Interactions in Chemistry and Biology: A New View of Benzene, Phe, Tyr, and Trp. *Science* **1996**, *271*, 163.
55. Thomas, V. H.; Bhattachar, S.; Hitchingham, L.; Zocharski, P.; Naath, M.; Surendran, N.; Stoner, C. L.; El-Kattan, A., The road map to oral bioavailability: an industrial perspective. *Expert Opinion on Drug Metabolism & Toxicology* **2006**, *2*, 591-608.
56. Lovering, F., Escape from Flatland 2: complexity and promiscuity. *MedChemComm* **2013**, *4*, 515.
57. Küçükgülzel, Ş. G.; Şenkardeş, S., Recent advances in bioactive pyrazoles. *European journal of*

medicinal chemistry **2015**, *97*, 786-815.

58. Asif, M., Some Recent Approaches of Biologically Active Substituted Pyridazine and Phthalazine Drugs. *Current Medicinal Chemistry* **2012**, *19*, 2984-2991.

59. Rajeev, K.; Sirohi, T. S.; Hariram, S.; Ramji, Y.; Roy, R. K.; Chaudhary, A.; Pandeya, S. N., 1,2,4-Triazine Analogs as Novel Class of Therapeutic Agents. *Mini-Reviews in Medicinal Chemistry* **2014**, *14*, 168-207.

60. Thoma, G.; Smith, A. B.; van Eis, M. J.; Vangrevelinghe, E.; Blanz, J.; Aichholz, R.; Littlewood-Evans, A.; Lee, C. C.; Liu, H.; Zerwes, H. G., Discovery and profiling of a selective and efficacious Syk inhibitor. *Journal of medicinal chemistry* **2015**, *58*, 1950-63.

61. Atamanyuk, D.; Faivre, F.; Oxoby, M.; Ledoussal, B.; Drocourt, E.; Moreau, F.; Gerusz, V., Vectorization efforts to increase Gram-negative intracellular drug concentration: a case study on HIdE-K inhibitors. *Journal of medicinal chemistry* **2013**, *56*, 1908-21.

62. Dao, P.; Lietha, D.; Etheve-Quellejeu, M.; Garbay, C.; Chen, H., Synthesis of novel 1,2,4-triazine scaffold as FAK inhibitors with antitumor activity. *Bioorganic & medicinal chemistry letters* **2017**, *27*, 1727-1730.

63. Mojzych, M.; Subertova, V.; Bielawska, A.; Bielawski, K.; Bazgier, V.; Berka, K.; Gucky, T.; Fornal, E.; Krystof, V., Synthesis and kinase inhibitory activity of new sulfonamide derivatives of pyrazolo[4,3-e][1,2,4]triazines. *European journal of medicinal chemistry* **2014**, *78*, 217-24.

64. Congreve, M.; Andrews, S. P.; Dore, A. S.; Hollenstein, K.; Hurrell, E.; Langmead, C. J.; Mason, J. S.; Ng, I. W.; Tehan, B.; Zhukov, A.; Weir, M.; Marshall, F. H., Discovery of 1,2,4-triazine derivatives as adenosine A(2A) antagonists using structure based drug design. *Journal of medicinal chemistry* **2012**, *55*, 1898-903.

65. Hammoud, H.; Elhabazi, K.; Quillet, R.; Bertin, I.; Utard, V.; Laboureyras, E.; Bourguignon, J. J.; Bihel, F.; Simonnet, G.; Simonin, F.; Schmitt, M., Aminoguanidine Hydrazone Derivatives as Nonpeptide NPPF1 Receptor Antagonists Reverse Opioid Induced Hyperalgesia. *ACS chemical neuroscience* **2018**, *9*, 2599-2609.

66. Espahbodinia, M.; Ettari, R.; Wen, W.; Wu, A.; Shen, Y. C.; Niu, L.; Grasso, S.; Zappala, M., Development of novel N-3-bromoisoxazolin-5-yl substituted 2,3-benzodiazepines as noncompetitive AMPAR antagonists. *Bioorganic & medicinal chemistry* **2017**, *25*, 3631-3637.

67. Xie, Z.; Zhou, Y.; Zhao, W.; Jiao, H.; Chen, Y.; Yang, Y.; Li, Z., Identification of novel PARP-1 inhibitors: Drug design, synthesis and biological evaluation. *Bioorganic & medicinal chemistry letters* **2015**, *25*, 4557-4561.

68. Prasad, C. V. C.; Zheng, M.; Vig, S.; Bergstrom, C.; Smith, D. W.; Gao, Q.; Yeola, S.; Polson, C. T.; Corsa, J. A.; Guss, V. L.; Loo, A.; Wang, J.; Slecza, B. G.; Dangler, C.; Robertson, B. J.; Hendrick, J. P.; Roberts, S. B.; Barten, D. M., Discovery of (S)-2-((S)-2-(3,5-difluorophenyl)-2-hydroxyacetamido)-N-((S,Z)-3-methyl-4-oxo-4,5-dihydro-3H-benzofuro[2,3-b]diazepin-5-yl)propanamide (BMS-433796): A γ -secretase inhibitor with A β lowering activity in a transgenic mouse model of Alzheimer's disease. *Bioorganic & medicinal chemistry letters* **2007**, *17*, 4006-4011.

69. Bihel, F. J.; Justiniano, H.; Schmitt, M.; Hellal, M.; Ibrahim, M. A.; Lugnier, C.; Bourguignon, J. J., New PDE4 inhibitors based on pharmacophoric similarity between papaverine and tofisopam. *Bioorganic & medicinal chemistry letters* **2011**, *21*, 6567-72.

70. Daouda, B.; Bihel, F.; Doumbia, M. L.; Essassi el, M.; Ng, S. W., 1-Phenyl-3H-2,3-benzodiazepin-4(5H)-one. *Acta crystallographica. Section E, Structure reports online*

2012, 68, o2443.

71. Audran, G.; Brémond, P.; Marque, S. R. A., Labile alkoxyamines: past, present, and future. *Chemical Communications* **2014**, 50, 7921-7928.
72. Tebben, L.; Studer, A., Nitroxides: Applications in Synthesis and in Polymer Chemistry. *Angewandte Chemie International Edition* **2011**, 50, 5034-5068.
73. Yusuf, M.; Shehneela; Singh, B., Synthesis and Antimicrobial Evaluation of New Pyrrolo-isoxazolidine Derivatives. *Asian Journal of Chemistry* **2019**, 31, 220-228.
74. Yépes, A. F.; Bahsas, A.; Escobar, P.; Cobo, J.; Palma, A.; Garro Martínez, J. C.; Enriz, R., Synthesis, anti-parasitic activity and QSAR study of a new library of polysubstituted tetrahydronaphtho[1,2-b]azepines. *Medicinal Chemistry Research* **2018**, 27, 2239-2264.
75. Malatinský, T.; Puhová, Z.; Babjak, M.; Doháňošová, J.; Moncol, J.; Marchalín, Š.; Fischer, R., Influence of the side chain protecting group on the stereoselectivity of the 1,3-dipolar cycloaddition of d-talo-configured nitrones. *Tetrahedron Letters* **2018**, 59, 3867-3871.
76. Sahani, R. L.; Patil, M. D.; Wagh, S. B.; Liu, R.-S., Catalytic Transformations of Alkynes into either α -Alkoxy or α -Aryl Enolates: Mannich Reactions by Cooperative Catalysis and Evidence for Nucleophile-Directed Chemoselectivity. *Angewandte Chemie International Edition* **2018**, 57, 14878-14882.
77. Tong, M.; Zhang, Y.; Qin, C.; Fu, Y.; Liu, Y.; Li, H.; Wang, W., Alkenylazaarenes as dipolarophiles in 1,3-dipolar cycloaddition of nitrones: regioselectivity-switchable and highly diastereoselective synthesis of multisubstituted isoxazolidines. *Organic Chemistry Frontiers* **2018**, 5, 2945-2949.
78. Afanaseva, K. K.; Efremova, M. M.; Kuznetsova, S. V.; Ivanov, A. V.; Starova, G. L.; Molchanov, A. P., The (3+2)- and formal (3+3)-cycloadditions of N-vinylpyrroles with cyclic nitrones and C,N-cyclic azomethine imines. *Tetrahedron* **2018**, 74, 5665-5673.
79. Sağırlı, A.; Dürüst, Y., Regioselective synthesis of some isoxazolines and isoxazolidines bearing caprolactam moiety. *Synthetic Communications* **2018**, 48, 1413-1424.
80. Dmitriev, V. A.; Efremova, M. M.; Novikov, A. S.; Zarubaev, V. V.; Slita, A. V.; Galochkina, A. V.; Starova, G. L.; Ivanov, A. V.; Molchanov, A. P., Highly efficient and stereoselective cycloaddition of nitrones to indolyl- and pyrrolylacrylates. *Tetrahedron Letters* **2018**, 59, 2327-2331.
81. Chakraborty, B.; Chettri, E., Synthesis of Some Novel Class of Regioselective Spiro Isoxazolidine Derivatives via 1,3-Dipolar Cycloaddition Reaction of N-Benzyl-C-fluoro-substituted Phenyl Nitrones in Ionic Liquid. *Journal of Heterocyclic Chemistry* **2018**, 55, 1157-1165.
82. Abbiati, G.; Arcadi, A.; Marinelli, F.; Rossi, E.; Verdecchia, M., Sequential 1,3-Dipolar Cycloaddition of Nitrones to β -(2-Aminophenyl) α,β -Ynones and Cyclocondensation: A New Entry to the Isoxazolino[4,5-c]quinoline Ring. *European Journal of Organic Chemistry* **2009**, 2009, 1027-1031.
83. Chen, J.; Guo, H.-M.; Zhao, Q.-Q.; Chen, J.-R.; Xiao, W.-J., Visible light-driven photocatalytic generation of sulfonamidyl radicals for alkene hydroamination of unsaturated sulfonamides. *Chemical Communications* **2018**, 54, 6780-6783.
84. Janza, B.; Studer, A., Stereoselective Cyclization Reactions of IBX-Generated Alkoxyamidyl Radicals. *The Journal of Organic Chemistry* **2005**, 70, 6991-6994.
85. Bates, R. W.; Lim, C. J.; Collier, S. J.; Sukumaran, J., Synthesis of (-)-Deoxynupharidine by Allenic Hydroxylamine Cyclisation. *Asian Journal of Organic Chemistry* **2015**, 4, 652-658.
86. Scholz, S.; Plietker, B., Fe-Catalyzed reductive NO-bond cleavage – a route to the diastereoselective 1,4-aminohydroxylation of 1,3-dienes. *Organic Chemistry Frontiers* **2016**, 3,

1295-1298.

87. McClure, K., F.; Danishefsky, S., J., Cycloaddition Reactions of Aromatic Nitroso Compounds with Oxygenated Dienes. An Approach to the Synthesis of the FR-900482 Family of Antibiotics. *J. Org. Chem.* **1991**, *56*, 850-853.
88. Yamamoto, Y.; Momiyama, N.; Yamamoto, H., Enantioselective Tandem O-Nitroso Aldol/Michael Reaction. *Journal of the American Chemical Society* **2004**, *126*, 5962-5963.
89. Yang, D.; Wan, C.; He, M.; Che, C.; Xiao, Y.; Fu, B.; Qin, Z., Design, synthesis, crystal structure and fungicidal activity of (E)-5-(methoxyimino)-3,5-dihydrobenzo[e][1,2]oxazepin-4(1H)-one analogues. *MedChemComm* **2017**, *8*, 1007-1014.
90. Numajiri, Y.; Jiménez-Osés, G.; Wang, B.; Houk, K. N.; Stoltz, B. M., Enantioselective Synthesis of Dialkylated N-Heterocycles by Palladium-Catalyzed Allylic Alkylation. *Organic letters* **2015**, *17*, 1082-1085.
91. Tabarki, M. A.; Besbes, R., Regioselective ring opening of β -phenylglycidate and aziridine-2-carboxylates with N-alkylhydroxylamines: synthesis of isoxazolidinones. *Tetrahedron* **2014**, *70*, 1060-1064.
92. Kim, H.-K.; Park, K.-J. J., Simple and efficient synthetic routes to d-cycloserine. *Tetrahedron Letters* **2012**, *53*, 1668-1670.
93. Padmaja, A.; Payani, T.; Muralikrishna, A.; Mahesh, K., E-1,2-diarylsulfonylene—Source for new class of heterocycles. *Journal of Heterocyclic Chemistry* **2011**, *48*, 199-204.
94. Shen, M.-H.; Ren, X.-T.; Pan, Y.-P.; Xu, H.-D., Iridium catalyzed fragmentation/cyclization of N-butynyl 4,4-dimethylisoxazolidine-3,5-diones: a unique access to multiply substituted pyrroles. *Organic Chemistry Frontiers* **2018**, *5*, 46-50.
95. Krishna, V., C.; Raja, S., DESIGN AND SYNTHESIS OF NOVEL SUBSTITUTED BENZIMIDAZOLE ANALOGS AS POTENT ANTICONVULSANT AGENTS. *Eur J Bio Pharm Sci* **2017**, *4*, 749-758.
96. Ibrar, A.; Shehzadi, S. A.; Saeed, F.; Khan, I., Developing hybrid molecule therapeutics for diverse enzyme inhibitory action: Active role of coumarin-based structural leads in drug discovery. *Bioorganic & medicinal chemistry* **2018**, *26*, 3731-3762.
97. Waring, M. J., Lipophilicity in drug discovery. *Expert Opinion on Drug Discovery* **2010**, *5*, 235-248.
98. Ishikawa, M.; Hashimoto, Y., Improvement in Aqueous Solubility in Small Molecule Drug Discovery Programs by Disruption of Molecular Planarity and Symmetry. *Journal of medicinal chemistry* **2011**, *54*, 1539-1554.
99. Wang, A.; Tomczuk, B. E.; Lu, T.; Soll, R. M.; Spurlino, J. C.; Bone, R. F., Preparation of cyclic oxyguanidine pyrazinones as protease inhibitors. *WO 2002006248 A2* **20020124**.
100. Kumarn, S.; Chimnoi, N.; Ruchirawat, S., Synthesis of integerrimide A by an on-resin tandem Fmoc-deprotection–macrocyclisation approach. *Organic & biomolecular chemistry* **2013**, *11*, 7760-7767.
101. Palandoken, H.; Bocian, C. M.; McCombs, M. R.; Nantz, M. H., A facile synthesis of (tert-alkoxy)amines. *Tetrahedron Letters* **2005**, *46*, 6667-6669.
102. Ewan, H. S.; Muli, C. S.; Toubas, S.; Bellinghiere, A. T.; Veitschegger, A. M.; Smith, T. B.; Pistel, W. L.; Jewell, W. T.; Rowe, R. K.; Hagen, J. P.; Palandoken, H., Synthesis of sugar oxime ether surfactants. *Tetrahedron Letters* **2014**, *55*, 4962-4965.
103. Williams, I.; Kariuki, B. M.; Reeves, K.; Cox, L. R., Stereoselective Synthesis of

- 2-Dienyl-Substituted Pyrrolidines Using an η^4 -Dienetricarbonyliron Complex as the Stereodirecting Element: Elaboration to the Pyrrolizidine Skeleton. *Organic letters* **2006**, *8*, 4389-4392.
104. Bélanger, É.; Pouliot, M.-F.; Paquin, J.-F., Use of 5,5-(Dimethyl)-i-Pr-PHOX as a Practical Equivalent to t-Bu-PHOX in Asymmetric Catalysis. *Organic letters* **2009**, *11*, 2201-2204.
105. Nowak, M., Weinreb Amides. *Synlett* **2015**, *26*, 561-562.
106. Yun, J. I.; Kim, H. R.; Kim, S. K.; Kim, D.; Lee, J., Cross-metathesis of allyl halides with olefins bearing amide and ester groups. *Tetrahedron* **2012**, *68*, 1177-1184.
107. Davies, J.; Sheikh, N. S.; Leonori, D., Photoredox Imino Functionalizations of Olefins. *Angewandte Chemie International Edition* **2017**, *56*, 13361-13365.
108. He, C.; Gaunt, M. J., Ligand-assisted palladium-catalyzed C–H alkenylation of aliphatic amines for the synthesis of functionalized pyrrolidines. *Chemical Science* **2017**, *8*, 3586-3592.
109. Reddy, M. R.; Aidhen, I. S.; Shruthi, K.; Reddy, G. B., Synthesis of C-Analogues of β -Glucogallin and Aldose Reductase Inhibition Studies. *European Journal of Organic Chemistry* **2017**, *2017*, 7283-7294.
110. Nahm, S.; Weinreb, S. M., N-methoxy-n-methylamides as effective acylating agents. *Tetrahedron Letters* **1981**, *22*, 3815-3818.
111. Vadim, K. K.; Dmitrii, G. M., Recent Advances in the Application of N,O-Dialkylhydroxylamines in Organic Chemistry. *Current Organic Chemistry* **2003**, *7*, 967-993.
112. Singh, J.; Satyamurthi, N.; Aidhen, I. S., The Growing Synthetic Utility of Weinreb's Amide. *Journal für praktische Chemie* **2000**, *342*, 340-347.
113. Hodgkinson, J. T.; Galloway, W. R. J. D.; Saraf, S.; Baxendale, I. R.; Ley, S. V.; Ladlow, M.; Welch, M.; Spring, D. R., Microwave and flow syntheses of Pseudomonas quinolone signal (PQS) and analogues. *Organic & biomolecular chemistry* **2011**, *9*, 57-61.
114. Swamy, K. C. K.; Kumar, N. N. B.; Balaraman, E.; Kumar, K. V. P. P., Mitsunobu and Related Reactions: Advances and Applications. *Chemical Reviews* **2009**, *109*, 2551-2651.
115. Beddoe, R. H.; Sneddon, H. F.; Denton, R. M., The catalytic Mitsunobu reaction: a critical analysis of the current state-of-the-art. *Organic & biomolecular chemistry* **2018**, *16*, 7774-7781.
116. Heravi, M. M.; Ghalavand, N.; Ghanbarian, M.; Mohammadkhani, L., Applications of Mitsunobu Reaction in total synthesis of natural products. *Applied Organometallic Chemistry* **2018**, *32*, e4464.
117. Fletcher, S., The Mitsunobu reaction in the 21st century. *Organic Chemistry Frontiers* **2015**, *2*, 739-752.
118. Reynolds, A. J.; Kassiou, M., Recent Advances in the Mitsunobu Reaction: Modifications and Applications to Biologically Active Molecules. *Current Organic Chemistry* **2009**, *13*, 1610-1632.
119. Wiczorek, P., Stereoisomers Separation. In *Electromigration Techniques: Theory and Practice*, Buszewski, B.; Dziubakiewicz, E.; Szumski, M., Eds. Springer Berlin Heidelberg: Berlin, Heidelberg, 2013; pp 237-252.
120. D' Orazio, G.; Asensio-Ramos, M.; Fanali, C., Enantiomers separation by capillary electrochromatography using polysaccharide-based stationary phases. *Journal of Separation Science* **2019**, *42*, 360-384.
121. Ilisz, I.; Bajtai, A.; Lindner, W.; Péter, A., Liquid chromatographic enantiomer separations applying chiral ion-exchangers based on Cinchona alkaloids. *Journal of Pharmaceutical and Biomedical Analysis* **2018**, *159*, 127-152.
122. Yang, J.; Ke, C.; Zhang, D.; Liu, X.; Feng, X., Enantioselective Synthesis of 2,2,3-Trisubstituted Indolines via Bimetallic Relay Catalysis of α -Diazoketones with Enones. *Organic letters* **2018**, *20*,

4536-4539.

123. Sathish Reddy, A.; Srihari, P., A facile approach to the synthesis of securinega alkaloids: stereoselective total synthesis of (-)-allonorsecurinine. *Tetrahedron Letters* **2012**, *53*, 5926-5928.

124. Kong, C.; Jana, N.; Driver, T. G., Rh₂(II)-Catalyzed Selective Aminomethylene Migration from Styryl Azides. *Organic letters* **2013**, *15*, 824-827.

125. Bilke, J. L.; Moore, S. P.; O'Brien, P.; Gilday, J., Catalytic Asymmetric Synthesis of Piperidines from Pyrrolidine: Concise Synthesis of L-733,060. *Organic letters* **2009**, *11*, 1935-1938.

126. Swamy, K. C.; Kumar, N. N.; Balaraman, E.; Kumar, K. V., Mitsunobu and related reactions: advances and applications. *Chem Rev* **2009**, *109*, 2551-651.

127. Deng, C., Preparation of difluoromethylmethyloxodihydropyridinylindazolyloxyphenylbutanylpropanamide for use as a SGR modulator. *WO 2017162747 A1* **20170928**.

128. Schmidt, F.; Keller, F.; Vedrenne, E.; Aggarwal, V. K., Stereocontrolled Synthesis of β -Amino Alcohols from Lithiated Aziridines and Boronic Esters. *Angewandte Chemie International Edition* **2009**, *48*, 1149-1152.

129. Morgenthaler, M.; Schweizer, E.; Hoffmann-Roder, A.; Benini, F.; Martin, R. E.; Jaeschke, G.; Wagner, B.; Fischer, H.; Bendels, S.; Zimmerli, D.; Schneider, J.; Diederich, F.; Kansy, M.; Muller, K., Predicting and tuning physicochemical properties in lead optimization: amine basicities. *ChemMedChem* **2007**, *2*, 1100-15.

130. Alex, A., Physicochemical Profiling (Solubility, Permeability and Charge State). *Current Topics in Medicinal Chemistry* **2001**, *1*, 277-351.

131. Manallack, D. T.; Prankerd, R. J.; Yuriev, E.; Oprea, T. I.; Chalmers, D. K., The significance of acid/base properties in drug discovery. *Chemical Society reviews* **2013**, *42*, 485-496.

132. Ruiz, R.; Ràfols, C.; Rosés, M.; Bosch, E., A potentially simpler approach to measure aqueous pK_a of insoluble basic drugs containing amino groups. *Journal of Pharmaceutical Sciences* **2003**, *92*, 1473-1481.

133. Barrosa, K. H.; Pinto, E. G.; Tempone, A. G.; Martins, E. G.; Lago, J. H., Alchornedine, a new anti-trypanosomal guanidine alkaloid from *Alchornea glandulosa*. *Planta medica* **2014**, *80*, 1310-4.

134. Wang, Z.; Zhao, Q.; Hou, J.; Yu, W.; Chang, J., Iodine-mediated direct synthesis of multifunctional 2-aminobenzimidazoles from N-substituted o-diaminoarenes and isothiocyanates. *Tetrahedron* **2018**, *74*, 2324-2329.

135. Chatterjee, A.; Ward, T. R., Recent Advances in the Palladium Catalyzed Suzuki–Miyaura Cross-Coupling Reaction in Water. *Catalysis Letters* **2016**, *146*, 820-840.

136. Lipshutz, B. H.; Aguinaldo, G. T.; Ghorai, S.; Voigtritter, K., Olefin Cross-Metathesis Reactions at Room Temperature Using the Nonionic Amphiphile “PTS”: Just Add Water. *Organic letters* **2008**, *10*, 1325-1328.

137. Wagner, P.; Bollenbach, M.; Doebelin, C.; Bihel, F.; Bourguignon, J.-J.; Salomé, C.; Schmitt, M., t-BuXPhos: a highly efficient ligand for Buchwald–Hartwig coupling in water. *Green Chemistry* **2014**, *16*, 4170.

138. Tang, S.-Q.; Wang, A.-P.; Schmitt, M.; Bihel, F., Dioxygenation of styrenes with molecular oxygen in water. *Tetrahedron Letters* **2018**, *59*, 1465-1468.

139. Kaur, N.; Kishore, D., Synthetic Strategies Applicable in the Synthesis of Privileged Scaffold: 1,4-Benzodiazepine. *Synthetic Communications* **2014**, *44*, 1375-1413.

140. Rahman, Y.; Afrin, S.; Husain, M. A.; Sarwar, T.; Ali, A.; Shamsuzzaman; Tabish, M., Unravelling

- the interaction of pirenzepine, a gastrointestinal disorder drug, with calf thymus DNA: An in vitro and molecular modelling study. *Archives of Biochemistry and Biophysics* **2017**, *625-626*, 1-12.
141. Darnag, R.; Mostapha Mazouz, E. L.; Schmitzer, A.; Villemin, D.; Jarid, A.; Cherqaoui, D., Support vector machines: Development of QSAR models for predicting anti-HIV-1 activity of TIBO derivatives. *European journal of medicinal chemistry* **2010**, *45*, 1590-1597.
142. Stechmann, B.; Bai, S.-K.; Gobbo, E.; Lopez, R.; Merer, G.; Pinchard, S.; Panigai, L.; Tenza, D.; Raposo, G.; Beaumelle, B.; Sauvaire, D.; Gillet, D.; Johannes, L.; Barbier, J., Inhibition of Retrograde Transport Protects Mice from Lethal Ricin Challenge. *Cell* **2010**, *141*, 231-242.
143. Pavlovsky, V. I.; Tsybalyuk, O. V.; Martynyuk, V. S.; Kabanova, T. A.; Semenishyna, E. A.; Khalimova, E. I.; Andronati, S. A., Analgesic Effects of 3-Substituted Derivatives of 1,4-Benzodiazepines and their Possible Mechanisms. *Neurophysiology* **2013**, *45*, 427-432.
144. Rupinder Kaur, G.; Shiv Om, K.; Jasreen, C.; Sumit, B.; Anamik, S.; Jitender, B., Recent Development in [1,4]Benzodiazepines as Potent Anticancer Agents: A Review. *Mini-Reviews in Medicinal Chemistry* **2014**, *14*, 229-256.
145. Hurley, L. H., Elucidation and formulation of novel biosynthetic pathways leading to the pyrrolo[1,4]benzodiazepine antibiotics anthramycin, tomaymycin, and sibiromycin. *Accounts of Chemical Research* **2002**, *13*, 263-269.
146. Sandor, S.; Istvan, T., Non-competitive AMPA Antagonists of 2,3-Benzodiazepine Type. *Current Pharmaceutical Design* **2002**, *8*, 913-939.
147. Rundfeldt, C.; Socała, K.; Wlaź, P., The atypical anxiolytic drug, tofisopam, selectively blocks phosphodiesterase isoenzymes and is active in the mouse model of negative symptoms of psychosis. *J Neural Transm (Vienna)* **2010**, *117*, 1319-1325.
148. Bond, A.; Lader, M., A comparison of the psychotropic profiles of tofisopam and diazepam. *European Journal of Clinical Pharmacology* **1982**, *22*, 137-142.
149. De Sarro, G.; Chimirri, A.; De Sarro, A.; Gitto, R.; Grasso, S.; Giusti, P.; Chapman, A. G., GYKI 52466 and related 2,3-benzodiazepines as anticonvulsant agents in DBA/2 mice. *European Journal of Pharmacology* **1995**, *294*, 411-422.
150. Chimirri, A.; De Sarro, G.; De Sarro, A.; Gitto, R.; Grasso, S.; Quartarone, S.; Giusti, P.; Libri, V.; Constanti, A.; Chapman, A. G., 1-Aryl-3,5-dihydro-4H-2,3-benzodiazepin-4-ones: Novel AMPA Receptor Antagonists. *Journal of medicinal chemistry* **1997**, *40*, 1258-1269.
151. Wang, Y.; Konkoy, C. S.; Ilyin, V. I.; Vanover, K. E.; Carter, R. B.; Weber, E.; Keana, J. F. W.; Woodward, R. M.; Cai, S. X., Synthesis of 7,8-(Methylenedioxy)-1-phenyl-3,5-dihydro-4H-2,3-benzodiazepin-4-ones as Novel and Potent Noncompetitive AMPA Receptor Antagonists. *Journal of medicinal chemistry* **1998**, *41*, 2621-2625.
152. Chimirri, A.; De Sarro, G.; De Sarro, A.; Gitto, R.; Quartarone, S.; Zappalà, M.; Constanti, A.; Libri, V., 3,5-Dihydro-4H-2,3-benzodiazepine-4-thiones: A New Class of AMPA Receptor Antagonists. *Journal of medicinal chemistry* **1998**, *41*, 3409-3416.
153. De Sarro, G.; Di Paola, E. D.; Gareri, P.; Gallelli, L.; Scotto, G.; De Sarro, A., Effects of some AMPA receptor antagonists on the development of tolerance in epilepsy-prone rats and in pentylenetetrazole kindled rats. *European Journal of Pharmacology* **1999**, *368*, 149-159.
154. Grasso, S.; De Sarro, G.; De Sarro, A.; Micale, N.; Polimeni, S.; Zappalà, M.; Puia, G.; Baraldi, M.; De Micheli, C., Synthesis and anticonvulsant activity of novel and potent 1-aryl-7,8-methylenedioxy-1,2,3,5-tetrahydro-4H-2,3-benzodiazepin-4-ones. *Bioorganic & medicinal chemistry letters* **2001**, *11*, 463-466.

155. Zappalà, M.; Postorino, G.; Micale, N.; Caccamese, S.; Parrinello, N.; Grazioso, G.; Roda, G.; Menniti, F. S.; De Sarro, G.; Grasso, S., Synthesis, Chiral Resolution, and Enantiopharmacology of a Potent 2,3-Benzodiazepine Derivative as Noncompetitive AMPA Receptor Antagonist. *Journal of medicinal chemistry* **2006**, *49*, 575-581.
156. Zappalà, M.; Pellicanò, A.; Micale, N.; Menniti, F. S.; Ferreri, G.; De Sarro, G.; Grasso, S.; De Micheli, C., New 7,8-ethylenedioxy-2,3-benzodiazepines as noncompetitive AMPA receptor antagonists. *Bioorganic & medicinal chemistry letters* **2006**, *16*, 167-170.
157. Micale, N.; Colleoni, S.; Postorino, G.; Pellicanò, A.; Zappalà, M.; Lazzaro, J.; Diana, V.; Cagnotto, A.; Mennini, T.; Grasso, S., Structure–activity study of 2,3-benzodiazepin-4-ones noncompetitive AMPAR antagonists: Identification of the 1-(4-amino-3-methylphenyl)-3,5-dihydro-7,8-ethylenedioxy-4H-2,3-benzodiazepin-4-one as neuroprotective agent. *Bioorganic & medicinal chemistry* **2008**, *16*, 2200-2211.
158. Calabrò, M. L.; Raneri, D.; Ficarra, P.; Mennini, T.; Colleoni, S.; Grazioso, G.; Micale, N.; Zappalà, M.; Grasso, S., Synthesis, Chiral Resolution and Pharmacological Evaluation of a 2,3-Benzodiazepine-Derived Noncompetitive AMPA Receptor Antagonist. *ChemMedChem* **2009**, *4*, 415-420.
159. Parenti, S.; Casagrande, G.; Montanari, M.; Espahbodinia, M.; Ettari, R.; Grande, A.; Corsi, L., A novel 2,3-benzodiazepine-4-one derivative AMPA antagonist inhibits G2/M transition and induces apoptosis in human leukemia Jurkat T cell line. *Life Sciences* **2016**, *152*, 117-125.
160. Li, Y.; Zhang, H.-Q.; Liu, J.; Yang, X.-P.; Liu, Z.-J., Stereoselective Synthesis and Antifungal Activities of (E)- α -(Methoxyimino)benzeneacetate Derivatives Containing 1,3,5-Substituted Pyrazole Ring. *Journal of Agricultural and Food Chemistry* **2006**, *54*, 3636-3640.
161. Hurltley, W. R. H., CCXLIV.—Replacement of halogen in orthobromo-benzoic acid. *Journal of the Chemical Society (Resumed)* **1929**, 1870-1873.
162. Goldberg, A. A., 837. Hydrolysis of substituted o-chlorobenzoic acids. The mechanism of the reaction between o-halogenobenzoic acids and nucleophilic reagents. *Journal of the Chemical Society (Resumed)* **1952**, 4368-4373.
163. Mayer, W.; Fikentscher, R., Über die nucleophile Substitution des Halogens in o-Brom-benzoesäuren. *Chemische Berichte* **1958**, *91*, 1536-1541.
164. Cirigottis, K.; Ritchie, E.; Taylor, W., Studies on the Hurltley reaction. *Australian Journal of Chemistry* **1974**, *27*, 2209-2228.
165. Alcaraz, L.; Furber, M.; Purdie, M.; Springthorpe, B., Preparation of piperidinyl alcohols as chemokine receptor modulators for treatment of diseases such as asthma. *WO 2003068743 A1* **20030821**.
166. Geneste, H.; Ochse, M.; Drescher, K.; Dinges, J.; Jakob, C., Dihydroisoquinolines and related as phosphodiesterase type 10a and their preparation and use in the treatment of neurological and psychiatric disorders. *US 20130116229 A1* **20130509**.
167. Bizet, V.; Bolm, C., Sulfur Imidations by Light-Induced Ruthenium-Catalyzed Nitrene Transfer Reactions. *European Journal of Organic Chemistry* **2015**, *2015*, 2854-2860.
168. Verbraeken, B.; Hullaert, J.; van Guyse, J.; Van Hecke, K.; Winne, J.; Hoogenboom, R., The Elusive Seven-Membered Cyclic Imino Ether Tetrahydrooxazepine. *Journal of the American Chemical Society* **2018**, *140*, 17404-17408.
169. Shang, R.; Ji, D.-S.; Chu, L.; Fu, Y.; Liu, L., Synthesis of α -Aryl Nitriles through Palladium-Catalyzed Decarboxylative Coupling of Cyanoacetate Salts with Aryl Halides and Triflates.

Angewandte Chemie International Edition **2011**, *50*, 4470-4474.

170. Luo, F.-T.; Jeevanandam, A., Simple transformation of nitrile into ester by the use of chlorotrimethylsilane. *Tetrahedron Letters* **1998**, *39*, 9455-9456.

171. Ke, J.; He, C.; Liu, H.; Xu, H.; Lei, A., Alcohol assisted C–C bond breaking: copper-catalyzed deacetylative α -arylation of β -keto esters and amides. *Chemical Communications* **2013**, *49*, 6767-6769.

172. Reddy, C. R.; Radhika, L.; Kumar, T. P.; Chandrasekhar, S., First Acid-Catalyzed Entry to O-Alkylated Hydroximides from Benzylic Alcohols. *European Journal of Organic Chemistry* **2011**, *2011*, 5967-5970.

173. Tang, S. Q.; Bricard, J.; Schmitt, M.; Bihel, F., Fukuyama Cross-Coupling Approach to Isoprekinamycin: Discovery of the Highly Active and Bench-Stable Palladium Precatalyst POxAP. *Organic letters* **2019**, *21*, 844-848.

174. Gulyaeva, N.; Zaslavsky, A.; Lechner, P.; Chlenov, M.; McConnell, O.; Chait, A.; Kipnis, V.; Zaslavsky, B., Relative hydrophobicity and lipophilicity of drugs measured by aqueous two-phase partitioning, octanol-buffer partitioning and HPLC. A simple model for predicting blood–brain distribution. *European journal of medicinal chemistry* **2003**, *38*, 391-396.

175. Wang, G.; Mahesh, U.; Chen, G. Y. J.; Yao, S. Q., Solid-Phase Synthesis of Peptide Vinyl Sulfones as Potential Inhibitors and Activity-Based Probes of Cysteine Proteases. *Organic letters* **2003**, *5*, 737-740.

176. Patel, B. H.; Mason, A. M.; Patel, H.; Coombes, R. C.; Ali, S.; Barrett, A. G. M., Conversion of α -Amino Acids into Bioactive o-Aminoalkyl Resorcyates and Related Dihydroxyisoindolinones. *The Journal of Organic Chemistry* **2011**, *76*, 6209-6217.

177. Ko, E.; Burgess, K., Pyrrole-Based Scaffolds for Turn Mimics. *Organic letters* **2011**, *13*, 980-983.

178. Hirayama, T.; Ishikawa, T.; Okaniwa, M.; Kakei, H.; Banno, H.; Yokota, A., Preparation of N,N-dialkylimidazo[1,2-a]pyridine-2-carboxamide derivatives as anticancer agents. *WO 2012008508 A1* **20120119**, *21*, 844-848.

179. Garcia, J.; Mata, E. G.; Tice, C. M.; Hormann, R. E.; Nicolas, E.; Albericio, F.; Michelotti, E. L., Evaluation of Solution and Solid-Phase Approaches to the Synthesis of Libraries of α,α -Disubstituted- α -acylaminoketones. *Journal of Combinatorial Chemistry* **2005**, *7*, 843-863.

180. Huy, P.; Neudörfl, J.-M.; Schmalz, H.-G., A Practical Synthesis of Trans-3-Substituted Proline Derivatives through 1,4-Addition. *Organic letters* **2011**, *13*, 216-219.

181. Fanjul, S.; Hulme, A. N., Anti and Syn Glycolate Aldol Reactions with a Readily Displaced Thiol Auxiliary. *The Journal of Organic Chemistry* **2008**, *73*, 9788-9791.

182. Staszak, M. A.; Doecke, C. W., A facile synthesis of N,O-bis(tert-butoxycarbonyl)-hydroxylamine. *Tetrahedron Letters* **1993**, *34*, 7043-7044.

183. Gopinath, P.; Nilaya, S.; Muraleedharan, K. M., Highly Chemoselective Esterification Reactions and Boc/THP/TBDMS Discriminating Deprotections under Samarium(III) Catalysis. *Organic letters* **2011**, *13*, 1932-1935.

184. Yus, M.; Foubelo, F.; Ferrández, J. V.; Bachki, A., Reductive lithiation of cyclic benzofused ethers: a source of oxygen-functionalised organolithium compounds. *Tetrahedron* **2002**, *58*, 4907-4915.

185. Terenin, V. I.; Volkov, A. A.; Ivanov, A. S.; Kabanova, E. V., Unusual recyclization of 2-methyl-1-phenyliso-quinolinium iodide to 1-phenyl-1,4-dihydro-3h-isochroman-3-one. *Chemistry of Heterocyclic Compounds* **2010**, *46*, 361-362.

186. Audubert, C.; Bouchard, A.; Mathieu, G.; Lebel, H., Chemoselective Synthesis of Amines from Ammonium Hydroxide and Hydroxylamine in Continuous Flow. *The Journal of Organic Chemistry*

2018, 83, 14203-14209.

187. Lee, C.-T.; Lipshutz, B. H., Nonracemic Diarylmethanols From CuH-Catalyzed Hydrosilylation of Diaryl Ketones. *Organic letters* **2008**, *10*, 4187-4190.

188. Zhang, W.; Mo, J. Y.; He, W.; Kennepohl, P.; Sammis, G. M., Regiocontrolled and Stereoselective Syntheses of Tetrahydrophthalazine Derivatives using Radical Cyclizations. *Chemistry – A European Journal* **2019**, *25*, 976-980.

189. Cló, E.; Blixt, O.; Jensen, K. J., Chemoselective Reagents for Covalent Capture and Display of Glycans in Microarrays. *European Journal of Organic Chemistry* **2010**, *2010*, 540-554.

190. Winters, M.; DuHadaway, J. B.; Pham, K. N.; Lewis-Ballester, A.; Badir, S.; Wai, J.; Sheikh, E.; Yeh, S.-R.; Prendergast, G. C.; Muller, A. J.; Malachowski, W. P., Diaryl hydroxylamines as pan or dual inhibitors of indoleamine 2,3-dioxygenase-1, indoleamine 2,3-dioxygenase-2 and tryptophan dioxygenase. *European journal of medicinal chemistry* **2019**, *162*, 455-464.

191. Hu, X.; Dong, Y.; Liu, G., Copper-catalyzed ligand-free amidation of aryl iodides and amino acid amides to synthesize C3-(Z)-1H-benzo[e][1,4]diazepin-2(3H)-ones. *Molecular Diversity* **2015**, *19*, 695-701.

192. Cvenroš, J.; Stolz, D.; Togni, A., A Concise Synthesis of ortho-Iodobenzyl Alcohols via Addition of ortho-Iodophenyl Grignard Reagent to Aldehydes and Ketones. *Synthesis* **2009**, *2009*, 2818-2824.

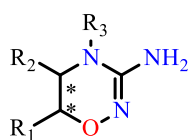
193. Chouhan, G.; Alper, H., Palladium-Catalyzed Carboxamidation Reaction and Aldol Condensation Reaction Cascade: A Facile Approach to Ring-Fused Isoquinolinones. *Organic letters* **2008**, *10*, 4987-4990.

Abstract

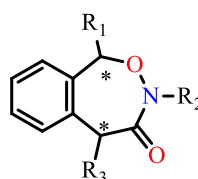
Keywords : 3-amino-1,2,4-oxadiazine ; benzo-2,3-oxazepin-4-one ; alchornedine ; green chemsitry ; POxAP

Heterocycles including two adjacent nitrogen atoms were very popular in medicinal chemistry. More particularly, the five-membered ring pyrazole, as well as both six-membered rings pyridazine and 1,2,4-triazine, were extensively used in drug design. Indeed, thanks to the nitrogen atoms, these three aromatic scaffolds exhibit 2 to 3 H-bond acceptors, capable to interact with target proteins. Moreover, these nitrogen atoms allow to decrease the lipophilicity of these heterocycles in comparison with benzene. However, due to their aromatic character, these scaffolds have still a planar geometry, which constitutes a significant limitation in the search for complex molecular structures. In 2009, Franck Lovering from Wyeth proposed the concept “Escape from Flatland”, which means to avoid aromatics, in favour of saturated carbon bonds and chiral sp^3 carbon atoms. The rational of this approach is that these non-planar molecules will be more natural product-like, and more amenable to explore additional areas of chemical space. Moreover, significant gains are expected in terms of ADME properties (solubility, biological selectivity, lipophilicity, etc). Despite the five-membered N-O heterocycles such as isoxazole or isooxazoline are well known, the corresponding six and seven-membered non-aromatic heterocycles exhibiting a N-O moiety are pretty rare in the literature. Besides the interesting non-planar geometry, the presence of the oxygen atom will strongly decrease the basicity of the adjacent nitrogen atom, endowing these N-O heterocycles particular physicochemical properties. Furthermore, the oximes ethers ($=N-O-$) possess a good resistance to protonation, which gives them better intrinsic stabilities towards hydrolysis than hydrazones or imines. Untill now, several alkoxyamides are under clinic trails.

In this project, new non-planar N-O heterocycles, 3-amino-1,2,4-oxadiazine and benzo-2,3-oxazepin-4-one would be synthesized and their physicochemical properties would be measured. During this course, a radical reaction in water was established to introduce N-O moiety and a novel precatalyst was developed for Fukuyama cross-coupling reaction. Futhermore, we also attempted to synthesize the natural product alchornedine with the established synthetic methods for 3-amino-1,2,4-oxadiazine scaffold.



3-amino-1,2,4-oxadiazine



benzo-2,3-oxazepin-4-one

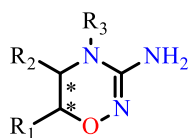
Synthèse d'hétérocycles non planaires à 6 ou 7 chaînons présentant une liaison N-O

Résumé

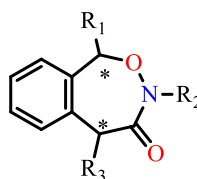
Mots-clés: 3-amino-1,2,4-oxadiazine ; benzo-2,3-oxazepin-4-one ; alchornedine ; chimie verte; POxAP

Les hétérocycles présentant 2 atomes d'azote adjacents sont très populaires en chimie médicinale. Ainsi, le cycle à 5 de type pyrazole, ainsi que les cycles à 6 de type pyridazine et 1,2,4-triazine ont été intensivement étudiés en drug design. En effet, la présence des atomes d'azote permet à ces systèmes hétérocycliques aromatiques de présenter 2 à 3 sites potentiels d'interactions de type accepteur de liaison hydrogène avec une cible protéique. De plus, la présence d'atomes d'azote permet de diminuer la lipophilie de ces systèmes aromatiques en comparaison avec le benzène. Toutefois, le caractère aromatique de ces hétérocycles leur confère une géométrie plane, ce qui constitue une limitation importante dans la recherche de structures moléculaires complexes. En 2009, Franck Lovering de Wyeth a proposé le concept "Escape from flatland", dans lequel il présente l'intérêt d'éviter les structures aromatiques pour privilégier des cycles saturés présentant des carbones sp^3 . Le rationnel de cette approche repose sur le fait que ces molécules non aromatiques sont plus proches des produits naturels, et que leur géométrie non-plane permet une plus grande exploration de l'espace chimique tridimensionnel, tout en améliorant les propriétés d'ADME (solubilité, sélectivité, lipophilie, etc). Dans ce projet de thèse, nous proposons de développer de nouveaux hétérocycles non aromatiques et non planaires présentant une liaison N-O. Si les cycles à 5 (isoxazole ou isoxazoline) sont bien connus, les cycles à 6 ou 7 chaînons présentant un motif N-O sont particulièrement rares ou inexistant dans la littérature. Outre l'intérêt géométrique de ces hétérocycles, la présence de l'oxygène en alpha de l'azote permet de fortement diminuer la basicité de ce dernier, conférant à l'hétérocycles des propriétés physico-chimiques particulières. Par ailleurs, les oximes ethers (=N-O-) présentent une bonne résistance à la protonation, ce qui leur confère une stabilité intrinsèque à l'hydrolyse bien meilleure que celle observée avec les hydrazones ou les imines. Enfin, plusieurs alkoxyamides sont actuellement en essai clinique.

Durant cette thèse, nous avons focaliser nos travaux sur la synthèse et propriétés physicochimiques de 3-amino-1,2,4-oxadiazine et benzo-2,3-oxazepin-4-one. Pendant ce cours, une réaction radicalaire dans l'eau a été établie pour introduire un fragment N-O et un nouveau précatalyseur a été développé pour la réaction de couplage croisé de Fukuyama. De plus, nous avons également tenté de synthétiser le produit naturel alchornédine avec les méthodes de synthèse établies pour l'échafaudage 3-amino-1,2,4-oxadiazine.



3-amino-1,2,4-oxadiazine



benzo-2,3-oxazepin-4-one